THE ANTI-TUMOUR EFFECTS AND MECHANISMS OF CURCUMIN IN HUMAN RETINOBLASTOMA CELL LINES

THESIS

Submitted in partial fulfillment

of the requirements for the degree of

DOCTOR OF PHILOSOPHY

By

T. SEETHALAKSHMI

2007 PHXF425

Under the supervision of

Dr. S. KRISHNAKUMAR

BIRLA INSTITUTE OF TECHNOLOGY AND SCIENCE

PILANI (RAJASTHAN) INDIA

2012

BIRLA INSTITUTE OF TECHNOLOGY & SCIENCE
PILANI - RAJASTHAN

CERTIFICATE

This is to certify that the thesis entitled "The Anti-tumour Effects and Mechanism of Curcumin in Human Retinoblastoma Cell Lines" submitted by Ms. T.Seethalakshmi, ID. No. 2007PHXF425 for award of Ph.D. Degree of the Institute embodies original work done by her under my supervision.

Signature of the Supervisor:

Name : **Dr. S.KRISHNAKUMAR, MD**

Designation : **Incharge Nanobiotechnology Department**
& Stem Cell Laboratory
Head of the Department of Ocular Pathology
Vision Research Foundation
Sankara Nethralaya,
41, College road, Nungambakkam
Chennai 600 006.
Tamil Nadu, India

Date:

ACKNOWLEDGEMENT

The most expected pleasant time has come now for me to express my gratitude to all of them who guided, supported and encouraged me throughout my PhD tenure.

First, I wish to give thanks to God, who is the source of my strength and abilities.

Next my sincere thanks to my supervisor, **Dr. S. Krishnakumar**, Reader and Head, Department of Ocular Pathology and Nanotechnology. I thank him for giving me the fellowship to work in his project and for his supervision, guidance, contributing with good ideas and valuable comments to complete my work.

I would like to thank **Prof. H.N. Madhavan,** President, Vision Research Foundation, Director of VIBS for his support and encouragement.

I would like to thank Padmabhushan **Dr.S.S Badrinath**, Chairman Emeritus, and **Dr. S.B. Vasanthi Badrinath**, Director, Laboratory Services, and **Dr. S. Baskaran,** Chairman, Sankara Nethralaya, Chennai, India for providing me the opportunity to work in this esteemed institution and to pursue my doctoral programme.

I thank **Dr. Ronnie George,** Director of Research, Vision Research Foundation, **Dr. Tarun Sharma**, Honorary Secretary and Treasurer, Vision Research Foundation, **Dr. T.S Surendran**, Vice-Chairman, Medical Research Foundation for their support.

I sincerely thank the Department of Indian council of medical research for funding my project and granting me the fellowship for my research.

I thank **Dr. Nivedita Chatterjee** for helping me in trouble shooting for some of the techniques during my fellowship. I thank **Dr.V. Uma Shankar,** Head, Bioinformatics Department and his team members **Ms. M. Sathyabaarathi and Mr. S. Muthukumar** for their help in bioinformatics.

My sincere thanks to **Prof. J. Biswas**, Director, Ocular Pathology Department, **Prof. Angayarkanni and Prof. K.N. Sulochana**, Biochemistry and Cell Biology Department, **Prof. Lily Therese**, Head, L&T Microbiology Research Centre, **Dr. K. Pandian,** Head, ONGC Department of Genetics and Molecular Biology, **Dr.B.Mahalakshmi**, Lecturer, **Dr. J. Malathi,** Reader, L&T Microbiology Research Centre, Vision Research Foundation, **Dr. Doreen Gracious**, consultant,

clinical lab for their kind words, support and encouragement during my research work.

I sincerely thank **Prof. L. K. Maheswari**, Vice Chancellor and Director, BITS, Pilani for giving me the great opportunity to do my thesis under the esteemed university. I thank **Dr. Ashish Kumar Das**, Dean, Research and Consultancy Division, BITS, Pilani, **Dr. Ravi Prakash**, Past Dean, Research and Consultancy Division, BITS, Pilani, **Prof Sundar**, Dean Distance Learning Programme division, **Dr Sanjay D.Pohekar**, **Dr. Deshmukh** and **Dr. Dinesh Kumar,** Convenor, PhD Monitoring, BITS, Pilani

I extend my sincere thanks to **Mr.S.Narayan**, Manager, Vision Research foundation and **Mr.N.Sivakumar**, Academic Officer for their support.

I thank **Mr.Thiyagarajan** HOD, Medical records Department and all his colleagues for their support in giving me patient's files.

I would like to thank IIT, Madras for allowing us to use the FT-IR instrument.

I acknowledge the help and support given by my wonderful department colleagues. I begin with **Mrs. S.Vandhana**, for her friendship during the years as students from UG and until now, sharing the tough parts, as well as good times, also for her moral support and encouragement throughout my work. I thank all my colleagues in the lab **Ms. Vanitha, Mr. Purushothaman, Ms. Charanya, Ms. Nithya, Ms. Vaishnavi, Mr. Job, Mr.Gopinath, Mr. Ravikanth, Mr. Madhu Beta, Ms. Vidhya, Ms. Jaisy Samuel, Ms. Nalini, Ms. Deepa, Ms. Sushma, Ms. Sangeetha and Mr. Narayan** for their loving words and encouragement**. I thank Mrs. Uma** for her tremendous help in formatting my thesis. All of them gave me the feeling of being at home at work.

I also thank **Mrs. Preethi Mehta**, Senior Scientist for her kindly help in correcting and formatting my thesis.

I also like to thank my friends **Ms. Abhirami, Ms. Barathi, Ms. Karthiyayini** and **Ms. Vinitha** for their timely help, moral support and encouragement through out my Ph.D.

I wish to extend my thanks to all the colleagues from the Departments of Microbiology, Biochemistry, Genetics and Molecular Biology and Clinical Laboratory for their support.

My special thanks to **Mr.Anadurai**, Lab Attendant for helping me in getting products from the communication department and for giving the required things for my research work on time.

I would like to express my gratitude to my mother **Mrs. T.Lalitha** and my father **Mr. A. Thiyagarajan**, they not only gave life and a much cherished childhood, but also taught me to love and instilled great values that I live by today. Their unfailing support and encouragement in the most desperate circumstances and constant emphasis on good education were drivers that got me this far.

I would like to express my greatfulness to my dearest sister **Ms. T.Dharani** for her constant love and support.

I would like to express my greatfulness and my love to my mother-in-law **Mrs. M. Pattammal** and my father-in-law **Mr S.Muthukrishnan** for being always with me patiently and for their understanding and any kind of support. If they were not with me during this study, I would not stand against many difficulties.

My special thanks to my sister in law **Mrs. K. Lakshmi**, her husband **Mr. Kirthivasan** and their daughters **Ms. K. Swathi and Ms. K. Janani** for their love, support, motivation.

I would like to thank my husband **Mr.M.Sreenivasan** for his priceless unconditional love, support, concern, great encouragement and understanding, without him, this accomplishment could not have been possible.

S.Abhirami is my precious 2 year old baby; keeping up with her incessant energy that gave me the energy to sail through with sanity.

I also want to thank all my other relatives and extended families for their any kind of help and support during my study.

T. SEETHALAKSHMI

ABSTRACT

RB is one of the most common intraocular pediatric tumors, which is rapidly gaining importance in Asia. Although treatments for RB cancer have improved over the recent years, the side effects which accompany current cancer treatments are still devastating, even potentially life threatening, to the patient. Natural compounds or dietary agents have historically played an important tool to treat cancer because of its low cytotoxicity and less adverse effects. Curcumin, a naturally occurring dietary compound with chemopreventive properties has been reported to trigger a variety of cancer cell types to apoptosis. Whether curcumin shows any activity on human retinoblastoma (RB) cells remained to be determined. The aim of this study was to investigate the effect and mechanism of curcumin on human RB cells. Treatment of curcumin resulted in significant decrease in cell proliferation and also induced apoptosis of RB cell lines in a dose- and time-dependent manner. Multiple molecular effects were observed during curcumin treatment including a significant loss of mitochondrial membrane potential, release of cytochrome c, activation of caspases-3 and -9. In addition up-regulation of pro-apoptotic (Bax, Bak) and anti-apoptotic proteins (Bcl-2) were also observed. Taken together, curcumin induces apoptosis in human RB cells through intrinsic pathway relying on mitochondria.

The GeneChip microarray data revealed several genes that were differentially expressed when treated with curcumin. Among those, the expression of genes involved in cell cycle signaling pathway which includes CDKN1A, CDKN2B, CCNL2, MCM7, CDC2, CCNH, CCNF and MAD2L1 were significantly regulated upon curcumin treatment. This shows that curcumin inhibits the cell proliferation of RB cells by deregulating genes involved in cell cycle check points and cell cycle progression. Apart from this, we also found that curcumin regulated the expression of genes that are involved in the regulation of apoptosis, tumor suppressor, cell cycle arrest, transcription factor and angiogenesis. The specific regulatory mechanism behind how these polyphenols affect gene expression and cancer cell survival has yet to be identified but current data suggests, that small non-coding miRNAs may be responsible. So, in the present study, the effect of curcumin on RB cancer cell miRNA expression was also investigated. Our result showed that curcumin regulated the expression of certain

miRNAs which have a tumor suppressor property. These include miR-22, miR-200c, let-7g* and miR-923 (tumour suppressor). Among the four miRNAs, miR-22 showed inhibition in cell proliferation after transfection. Over-expression of miR-22 inhibited the expression of its target protein Erbb3, which play an important role in cancer development and progression.

We were also interested to study the modulating effect of curcumin on the expression of multi-drug resistance (MDR) protein in RB cell lines, since MDR protein play an important role in drug resistance in RB tumours. The *in vitro* and *in silico* studies conducted showed that curcumin inhibited the expression of P-glycoprotein (P-gp), multi-drug resistance associated protein (MRP1) and lung resistance protein (LRP) in RB cell lines and molecular docking studies also showed that the binding of curcumin into the nucleotide binding domain (NBD) of P-gp, MRP1 and to the major vault repeats of LRP functional domain. Since we found that curcumin was able to modulate the expression of MDR, we further studied the chemosensitizing effect of curcumin in combination with the standard chemotherapy drugs (carboplatin, etoposide and vincristine) which has been routinely used for the treatment of RB. We found that the combination of curcumin with these drugs showed marked synergistic inhibitory effects on cell proliferation, cell cycle and induction of apoptosis on the RB cell lines.

In spite of various functional properties, curcumin has the disadvantage of poor solubility and bioavailability. So we also tried to conjugate curcumin with folic acid and polyethylene glycol, thereby increasing its solubility and stability in aqueous solution. In our preliminary data we found that conjugation of curcumin-PEG and curcumin-folic acid showed increased solubility and stability in aqueous solutions than their individual counterparts. We also tested the efficacy of nanoparticle (NP) curcumin and our result showed that NP curcumin was comparatively more effective than the native curcumin under *in vitro* conditions with time due to greater cellular uptake and enhanced anti-proliferative effect in RB cell lines.

The findings presented in this thesis clearly show that curcumin may exert its anti-tumor effects by regulating various cell signaling molecules, which indicates curcumin’s potential for chemotherapeutic activity in the treatment of RB cancer.

TABLE OF CONTENT

LIST OF FIGURES	
Figure No	**Figure title**
1.1	Incidence of different pediatric malignancies
1.2	Leukocoria in child with advanced unilateral sporadic RB
1.3	Retinoblastoma patterns
1.4	Enucleated globe with large RB filling the vitreous cavity
1.5	Flexner-Wintersteiner rosette with clear lumen at the centre
1.6	Carcinogenesis is initiated with the transformation of normal cell
2.1	Turmeric plant with rhizome
2.2	Biological activities of curcumin
2.3	No. of publications on curcumin has increased markedly over years
2.4	Chemical structure of curcumin
2.5	Absorption and metabolism of curcumin
2.6	Molecular targets shown to be regulated by curcumin
2.7	Chemical structure of naturally occurring curcumin and its novel synthetic analogs
3.1	Cellular uptake of curcumin in normal and RB cell lines
3.2a	Absorption spectra of curcumin
3.2b	Fluorescence spectra of
3.3	Absorption spectra of curcumin extracted from different sub-cellular fractions
3.4	Effect of curcumin on cell survival and therapeutic index
3.5	Cell morphology of normal and cancer cell line after curcumin treatment
3.6	DNA fragmentation in normal and cancer cell line after curcumin treatment
4.1	Effect of curcumin on cell viability in RB cell line
4.2	Effect of curcumin on cell nuclear morphology
4.3	Annexin V fluos staining
4.4	Effect of curcumin on mitochondrial membrane potential
4.5A	Effect of curcumin on apoptosis related protein by RT-PCR

4.5B	Effect of curcumin on apoptosis related protein by western blot
4.6	Effect of curcumin on cytochrome c release
4.7	Effect of curcumin on capase 3 and 9 activity in RB cells
4.8	Schematic representation of curcumin inducing apoptosis in RB cells
5.1	Change in gene expression profiling of Y79 RB cells by microarray
5.2	Functional grouping of up and down-regulated genes in Y79 cells
5.3	Schematic representation of differentially regulated genes on curcumin treatment
5.4	Validation of gene expression on curcumin treatment by real-time PCR
5.5	Cell cycle distribution in Y79 RB cells
5.6	DNA fragmentation by agarose gel electrophoresis
6.1	Change in miRNA expression profiling on curcumin treated Y79 RB cells
6.2	Fold change in the expression of altered miRNA after curcumin treatment
6.3	Validation of miRNA microarray data by real-time PCR
6.4	Over-expression of miR-22 in Y79 RB cells by transient transfection
6.5	Over-expression of miR-22 in RB cells and its effect on cell proliferation
6.6	Effect of miR-22 on cell migration
6.7	miR-22 controls Erbb3 expression in Y79 RB cells
6.8	Effect of curcumin on miRNA expression in RB cells
7.1	pMDR1-EGFP map
7.2	LRP expression by western blot and RT-PCR in RB cell line
7..3	MRP1 expression by western blot and RT-PCR in RB cell line
7.4	P-gp expression by western blot and RT-PCR in RB cell line
7.5	Expression of P-gp in transfected RB cell line and effect of curcumin treatment on MDR1 expression
7.6	Functional study of P-gp using Rhodmaine 123
7.7	ATPase activity of P-gp
7.8	Photoaffinity labeling study of P-gp
7.9	Homology based three dimensional structure of P-gp
7.10	Overall quality of the model assessed based on Z-score

LIST OF TABLES

LIST OF ABBREVIATIONS	
WHO	World Health Organization
RB	Retinoblastoma
RE	Reese-Ellsworth
EBRT	Exterenal Beam Radiation Therapy
FDA	Food and Drug Administration
SERM	Selective estrogen receptor modulators
AKT	Protein kinase B
ATP	Adenosine triphosphate
MAPK	Mitogen activated protein kinase
NF-κB	Nuclear factor kappa
STAT3	Signal transducer and activator of transcription
CDC25A	Cell division cycle homolog 25A
AP-1	Activator protein 1
CEV	Carboplatin- etoposide-vincristine
EGFR	Epidermal growth factor receptor
COX	Cyclooxygenase
Bcl-2	B-cell lymphoma 2
Bcl-xl	B-cell lymphoma extra large
HER2	Human epidermal receptor 2
THC	Tetrahydrocurcumin
PGE2	Prostaglandin metabolizing enzymes
PARP	Poly ADP-ribose polymerase
IKK	IκB kinase
DMSO	Dimethyl sulfoxide
DNA	Deoxy ribonucleic acid
EpRE	Electrophile response element
EDTA	Ethylene diamine tetra acetate
EGCG	Epigallocatechin 3 gallate
ATF3	Activating transcription factor 3
PPAR- γ	Peroxisome proliferators-activated receptor-gamma
EGR	Early growth response
ICN	Intracellular notch
CDF	3,4-difluoro-benzo-curcumin
DHT	Dihydrotestosterone
PAC	5-bis (4-hydroxy-3-methoxybenzylidene)-N-methyl-4-piperidine
FACS	Fluorescence-activated cell sorter
HO	Hemeoxygenase
FSC	Forward Scatter
GAPDH	Glyceraldehyde 3-phosphate dehydrogenase
cIAP	Apoptosis inhibiting protein
GST	Glutathione S-transferase
GSH	Glutathione
H	hour (s)
H & E	Hematoxylin and eosin

H_2O_2	Hydrogen peroxide
TGF	Transforming growth factor
CDK	Cyclin dependent kinase
CDC25	Cell division cycle 25
CYP3A	Cytochrome P450 family 3
IC_{50}	50% inhibitory concentration
ICRB	International classification of retinoblastoma
ICMR	Indian council of medical research
PDGF	Platelet derived growth factor
CHOP	C/EBP homology protein
AhR	Aryhydrocarbon receptor
IL	Interleukins
kDa	Kilodalton
CXCL	C-X-C motif chemokine 10
PLA2	Phospholipase A2
IMPH	Inosine monophosphate dehydrogenase
CAM	Cell adhesion molecules
ELAM	Endothelial leukocyte adhesion molecule
PCNA	Proliferative cell nuclear antigen
TIMP	Tissue inhibitor of metalloproteinase
MDA	Malondialdehyde
Min	minute(s)
HPV	Human papillomaviruses
CREB	Camp response element binding
IRAK	Interleukin receptor associated kinase
MRP1	Multi drug resistant protein -1
CDF	Difluorinated curcumin
mTOR	Mammalian target of rapamycin
MTT	[3-(4,5-dimethylthiazol-2-yl)-2,5-diphenyltetrazolium bromide
MW	Molecular weight
MePEG-b-PCL	methoxy poly (ethylene glycol)-block-polycaprolactone diblock polymers
NP-40	Nonidet P-40
PCD	Programmed cell death
MTP	Mitochondrial transition pore
ICAD	Inihibitor of caspase activated DNase
DISC	Death inducing signaling complex
PIG	p53 inducible gene
ALPS	Autoimmune lymphoproliferative syndrome
PEG	Poly ethylene glycol
HTLV	Human T-cell lymphoma virus
P-gp	P-glycoprotein
TMD	Transmembrane domain
NBD	Nucleotide binding domain
PDF	Probability Density Function
DOPE	Discrete Optimized potential Energy
LGA	Lamarckian genetic algorithms

PDB	Protein Data Bank
CI	Combination Index
PTEN	Phosphatase and tensin homolog
DRI	Dose Reduction Index
DCC	Dicyclohexylcadbodiimide
RIPA buffer	Radio immunoprecipitation buffer
DMAP	Dimethylaminopyridine
RNA	Ribonucleic acid
FT-IR	Fourier Transform Infra Red
NP	Nanoparticle
RT-PCR	Reverse transcriptase polymerase chain reaction
SDS-PAGE	Sodium Dodecyl Sulphate- Polyacrylamide gel electrophoresis
Sec	second(s)
TEMED	Tetra ethylene methylene diamine
TI	Therapeutic index
TNF-α	Tumor necrosis factor – alpha
TRAIL	Tumor necrosis factor–related apoptosis-inducing
VEGF	Vascular endothelial growth factor
MMP 9	Matrixmetalloproteases 9
FAB-MS	Fast Atom Bombardment Mass Spectrometry
MALDI-MS	Matrix Assisted Laser Desorption ionization time of Flight Mass Spectrometry
MIP-1	Monocyte inflammatory protein 1
ICN	Co-activator intracellular notch
MCP-1	Monocyte chemotactic protein-1
Symbols	
A	Alpha
B	Beta
Γ	Gamma
Δ	Delta
E	Epsilon
K	Kappa

CHAPTER 1: INTRODUCTION

1.0 PEDIATRIC CANCER

Thirteen percent of the annual deaths worldwide are cancer-related and 70% of these are mostly from the low and middle-income countries. The pediatric population (0-14 years of age) constitutes 32.4% of the total population of India. Malignant neoplasms are rare in children, yet it is an important cause of childhood mortality in many of the economically developed nations of the world. It is the third commonest cause of deaths in the 1 to 4 years of age group and second commonest cause of death in the 5-14 years of age group. In developing countries like India, the mortality is due to malnutrition and infections, but paediatric tumours are also rising in number.

Childhood cancers are unique in the sense that they arise from embryonic cells, respond to treatment rapidly and the survival have improved dramatically over the last two decades due to aggressive combine modality management. The most common malignancy seen in children are leukaemia, lymphomas, retinoblastoma (RB), germ cell tumours, squamous cell carcinoma, neuroblastoma and hepatoblastoma (**Figure 1.1**) (Arora et al. 2009).

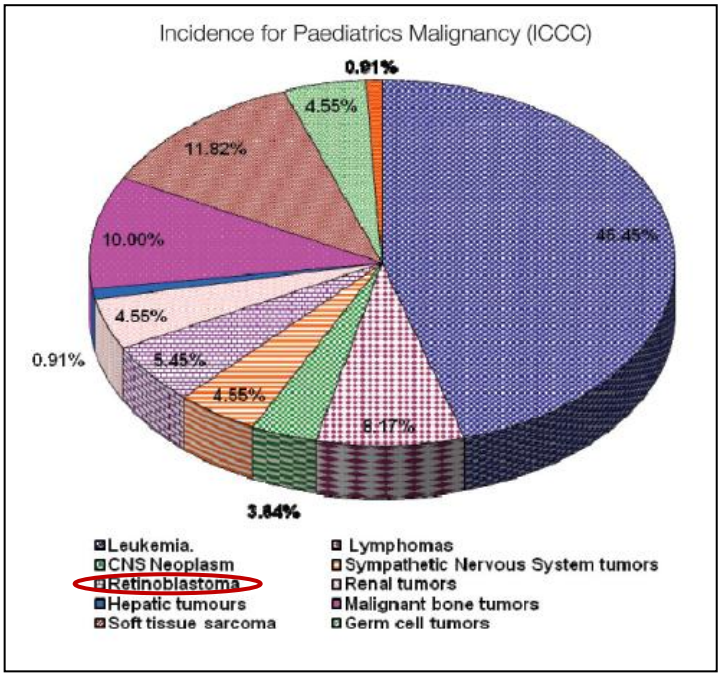

Figure 1.1: Incidence of different paediatric malignancies (Pattnaik et al. 2012**)**

Overall cancer in childhood is more common among males than females and the male to female ratio in the most resource-rich countries is around 1.2:1. However,

some cancers like retinoblastoma (RB), Wilm's tumour, osteosarcoma and germ cell tumour actually show a slight female predominance. In all the paediatric age groups, leukaemia was found to be the most common type of cancer, RB and lymphoma was the second most common malignancies in the 0-4 years and the 5-9 years age group respectively (Pattnaik et al. 2012).

Table 1.1: Comparison of incidence of paediatric malignancies with studies outside India (Pattnaik et al. 2012).

Cancer type (International childhood classification)	India	USA
Leukaemia	45.45	29.6
Lymphoma	8.18	11.2
Retinoblastoma	**5.45**	**1.8**
Neuroblastoma	4.55	6
CNS tumours	3.64	23.6
Germ cell tumour	4.55	2.8
Soft tissue sarcoma	11.82	7.4
Renal tumour	4.55	6.6

1.1 Background information of Retinoblastoma (RB) cancer

Retinoblastoma (RB), the most common malignant intraocular tumour of childhood. It affects approximately 1 in 15,000 to 20,000 live births, independent of race and sex. Almost, 80% of the cases occur before age group of 4 while 40% of cases occur during infancy. It can be inherited as a familial tumour in which the affected child has a history of RB or can be sporadic (non-familial) tumour in which the family history is negative for RB. Approximately, 94% of newly diagnosed cases are sporadic and 6% are familial. The highest mortality rate (40-70%) is recorded in large population of children in Asia and Africa (Dimaras et al. 2012).

1.1.1 Genetics of RB

RB is caused by germ line mutation in RB1 gene which is located on the chromosome 13 (13q14.2 deletion). A two-hit model proposed by Knudson, was based on the finding that children with bilateral RB developed multi-focal, bilateral tumours at an earlier stage than with children having unilateral, unifocal

tumours. Two events are necessary for retinal cells to develop into a tumour. First a mutational event can be inherited and would be present in all cells of the body and other events will result in the loss of the remaining allele. This occurs within a particular retinal cell or cells with deregulation of the cell cycle and inappropriate entry into S phases.

In the sporadic RB, both mutational events occur within single retinal cells after fertilization resulting in unilateral RB. Overall, 85% of children with unilateral RB represent somatic events, but 15% of the hereditary form has constitutional mutations in the RB1 gene. In cases of bilateral RB, children without a family history of the disease, develop RB1 mutations that primarily occur during spermatogenesis. This suggests that mutations in the RB1 gene occur more commonly during spermatogenesis or the parental chromosome in the early embryo is at higher risk for mutation. Genetic testing of the RB1 mutations is available in all diagnostic laboratories which detect mutations in 90% of the patients with bilateral disease. Therefore, genetic analysis often includes complete sequencing of coding region, analysis for deletions and rearrangements, methylation and RNA analysis. RB1 mutation identified in the tumour specimen is further processed with the peripheral blood to screen hereditary or non-hereditary RB (Chintagumpala et al. 2007)**.**

1.1.2 Clinical features of RB:

The clinical features of RB vary with the stage of the disease and also at the time of recognition. In the earlier stage, RB appears as less than 2mm dimension opthalmoscopically as a subtle, transparent or slightly translucent lesion in the sensory retina. In case of large tumours, there will be foci of chalk like calcification that resemble cottage cheese and often present with leukocoria (**Figure 1.2**). This white papillary reflex is a result of reflection of light from the white mass in the retrolental area.

Figure 1.2: Leukocoria in a child with advanced unilateral sporadic RB (photo taken at ocular pathology department, Sankara Nethralaya)

RB growth patterns are divided into endophytic and exophytic RB (**Figure 1.3**).

1) Endophytic RB: tumour that grows from the retina inward towards the vitreous cavity, which is characterized by a white, hazy mass with obscuration of the retinal blood vessels.
2) Exophytic RB: tumour that grows from the retina outward into the sub-retinal space, which produce a retinal detachment with a retinal displaced anteriorly behind a clear lens (**Figure 1.4**).

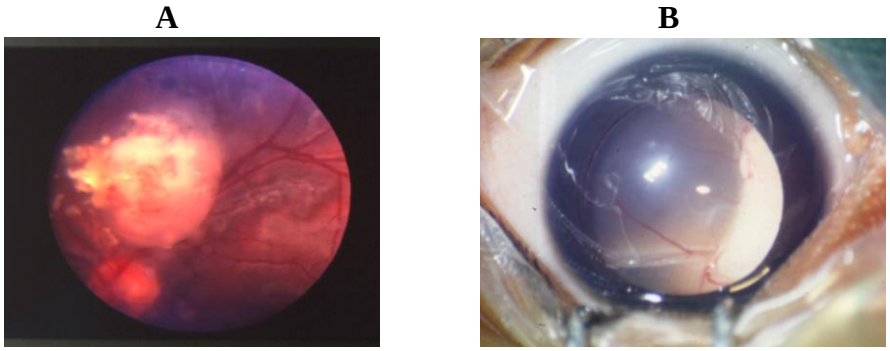

Figure 1.3: A) Endophytic RB. B) Exophytic RB (taken at ocular pathology department, Sankara Nethralaya**)**

Figure 1.4: Enucleated globe with large RB filling the vitreous cavity (taken at Ocular Pathology Department, Sankara Nethralaya)

1.1.3 Pathology of RB:

RB is composed of small, densely packed round cells with basophilic cytoplasm having large hyperchromic nuclei. There may be vast areas of necrosis and calcification due to the rapid tumour growth and insufficient blood supply. Flexner-Wintersteiner rosettes are aggregates of columnar or cuboidal cells around a central lumen, considered as an aborted attempt to form photoreceptors. A more advanced step towards photoreceptor formation is the fleurette type

rosettes (**Figure 1.5**). These are formed by tumour cells arranged in a semicircular fashion with bulb-like endings and eosinophilic cellular extensions.

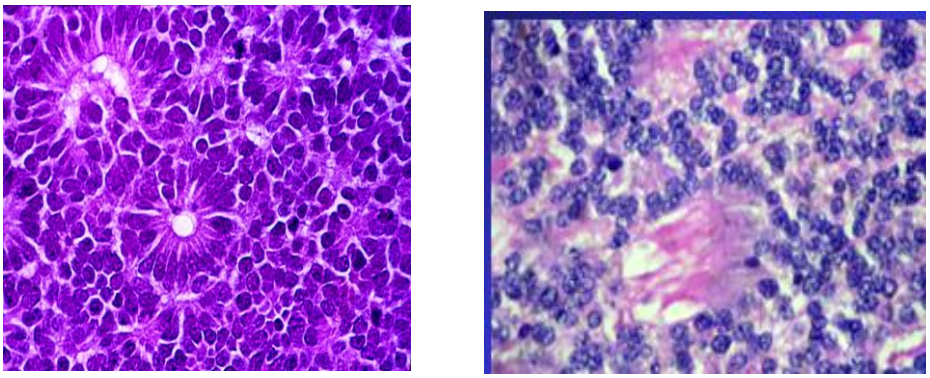

Figure 1.5: A Flexner-Wintersteiner rosette with a clear lumen at the centre of the figure and Fleurettes rosette arranged as flower bouquet like aggregates (taken at Ocular Pathology Department, Sankara Nethralaya)

1.1.4 Classification of RB:

The classification of tumour helps us to generate a roadmap for initial therapy, allows prediction of treatment morbidity and creates an environment for generating successful multicenter clinical trials. The parameters studies were the type of growth, presence or absence of vitreous seeds, differentiation of tumour and invasion of anterior chamber, iris, choroids and optic nerve.

1) The criteria to diagnose significant choroids invasion is when the maximum diameter (thickness) of invasive tumour measures 3mm or more in any diameter and, additionally, as helpful landmark, when most of these tumours reach atleast the inner fibres of the scleral tissue.
2) The focal choroids invasion are defines as a tumour focus of <3mm in any diameter and not reaching the sclera.
3) Artificial seeding should not be confused with the true tumour cells, where in artificial seeding it is composed of small groups of tumour cells, usually with many necrotic cells present inside natural spaces of the eye. In true tumour invasion, it is composed of solid nests of tumour that have usually pushed or infiltrating borders, expanding and replacing the area of invasion. They lack necrosis, unless the tumour is extremely large.

4) The optic nerve invasion includes classification as prelaminar, laminar, retrolaminar, or tumour at surgical margin. The maximum depth of invasion into the optic nerve should be measured from the level of the limiting membrane of the optic disc, the exit of the large central vessels, or, if none of these structures are preserved, from the level of the Bruch membrane to the deepest site of invasion (Sastre et al. 2009).

1.1.5 Modes of therapy in RB:

The aim of treatment in RB is to cure patients with preservation of vision and also to minimize the long term effects of therapy. Due to the advances in therapy, the survival of RB has been increased from 30 to 95% from 1930s to 1990s for non-metastatic RB. Enucleation and external beam radiation therapy (EBRT), both of which are associated with significant morbidity, which now have been resulted in improved survival rate.

1) **Enucleation**: Enucleation is a frequently used and important method for managing RB. If there is an advanced disease or invasion of tumour to optic nerve, choroid, orbit, then enucleation is appropriate. The percentage of enucleation has been decreased from 96% to 75% from the year 1974-1988.

The technique of enucleation is to gently remove the eye intact without seeding the malignancy into the orbit. Once enucleation is done, artificial orbital implant is placed to the patient that provides a more natural cosmetic appearance to the patient's artificial eye, minimizing sinking of the prosthesis and enabling motility to the prosthesis (Shields et al. 1992).

2) **External beam radiation therapy (EBRT):** RB is generally a radiosensitive tumour. EBRT is used to treat advanced RB, particularly when there is a vitreous seeding. Recurrence of RB after EBRT continues to be a problem that develops within the first 1-4 years after treatment (Hungerford et al. 1995). Tumour recurrence has been found to be related to the stage of the disease and the tumour size at the time of the treatment. EBRT may induce a second cancer in the field of irradiation. Patients treated with EBRT who are younger than 12 months of age have a greater risk for the second cancers than patients over 12 months of age. It also causes local side effects such as xerophthalmia, cataract, retinopathy and keratopathy (Mohney et al. 1998).

3) **Chemotherapy:** Systemic chemotherapy is the one of the possible treatment modalities, which is free from long-term effects of radiation. A combination of carboplatin, etoposide and vincristine (CEV) is the preferred drug combination for the treatment of RB tumour (**Table 1.2**).

Table 1.2: Chemotherapy vincristine, etoposide, and carboplatin protocol (Bakhshi et al. 2007**)**

A: Drugs
Vincristine 1.5mg/m^2 day1 (0.05mg/kg for children <3 years and max dose 2mg)
Carboplatin 560mg/m^2 day 1 (18.6 mg/kg for children < 3 years)
Etoposide 150mg/m^2 day 1 and 2 (5mg/kg for children < 3 years)
B: Cycles
Every 3-4 weeks
Ensure ANC> 1000 and platelets >100,000/mm^3
C: Number of cycles
2-6 cycles for chemoreduction
6 cycles for chemoprevention
6-12 cycles for systemic disease

It is infused every four weeks, typically for six months. Cyclosporine has also been used in addition to these three anticancer agents by others to avoid multi-drug resistance. However these agents have been associated with adverse effects in some patients including febrile episodes, neutropenia, infections, cytopenia, gastrointestinal distress and vincristine neurotoxicity. Etoposide and carboplatin are also mutagenic. Etoposide therapy is also associated with risk for acute myelocytic leukaemia and secondary leukaemia, hypotension, alopecia, hepatotoxicty and allergic reactions. Carboplatin also act synergistically with etoposide in the induction of secondary leukaemia and also causes neuropathy, nephrotoxicity and hypersensitivity reactions. As these agents are mutagenic, both of these drugs have potential to exacerbate second tumour risk in children with heritable disease.

4) **Intra-arterial chemotherapy**: It is now commonly used to treat RB patients, where the drug adequately reaches the retina via the vascular system to face the intraocular tumour (Shields et al. 2011). However, there are some disadvantages

with this technique which lead to retinal detachment in group ERB patients, where systemic intravenous chemotherapy is preferable (Bakhshi et al. 2007; Shields et al. 2004).

1.2 Chemoprevention of cancer:

Cancer is a growing health problem around the world. The failure of conventional chemotherapy and radiotherapy of human cancers to effect major reductions in the mortality rates for the common epithelial malignancies, such as breast, colon, pancreas, ovary, lung and pharynx, indicate that new approaches to the control of tumour development are critically needed. Unfortunately, most cytotoxic drugs used in cancer therapy also have toxic side effects on a wide spectrum of normal tissues, such as those found in the brain, bone marrow, lung, heart and kidney. Thus, the development and use of new chemopreventive agents with a novel mechanism of action to prevent cancer is most urgent in the field of chemoprevention.

Chemoprevention is defined as using natural or synthetic chemical with the aim of suppressing, interrupting or reversing the carcinogenic processes at early stages (Sporn et al. 2002). Chemopreventive products present low side effects and toxicity, neutralization of carcinogens as well as their effects on cells. Most chemopreventive agents are plant extracts subdivided into two classes:

a) Blocking agent, which inhibit the initiation step by preventing carcinogen activation

b) Suppressing agent, which inhibit malignant cell proliferation during promotion and progression of carcinogenesis (Kelloff et al. 1994) **(Figure 1.6)**.

1.3 Dietary chemopreventive agents:

Many dietary compounds have been identified as potential chemopreventive agents. These include vitamins, minerals, carotenoids and large class of phytochemicals (polyphenols, organosulfur compounds and isothiocynates). Phytochemicals have been used in centuries in the prevention and treatment of various diseases and also to inhibit tumourigenesis. The anti-carcinogenic properties of phytochemicals have been tested *in vivo* using carcinogenic induced and transgenic rodent models. In general, drugs used in chemotherapy are developed by the pharmaceutical companies where they have undergone various

testing not only the efficacy but also the toxicity, mutagenicity and carcinogenicity. In contrast, dietary phytochemicals possessing cancer chemopreventive properties are often assumed to be safe which also bypass some of the detailed toxicological investigations which are required for the chemotherapy drugs. Chemopreventive agents inhibit the development of cancer by altering cellular biology at the molecular level. **Polyphenolic phytochemicals derived from edible plants have been reported to interfere with a specific stage of the carcinogenic process. Many mechanisms have been shown to account for the anti-carcinogenic action of dietary constituents. Chemoprevention by edible phytochemicals is now considered to be inexpensive, readily applicable, acceptable and accessible approach to cancer control and management. Curcumin is one such compound that has been shown to possess such property (Surh et al. 2003).**

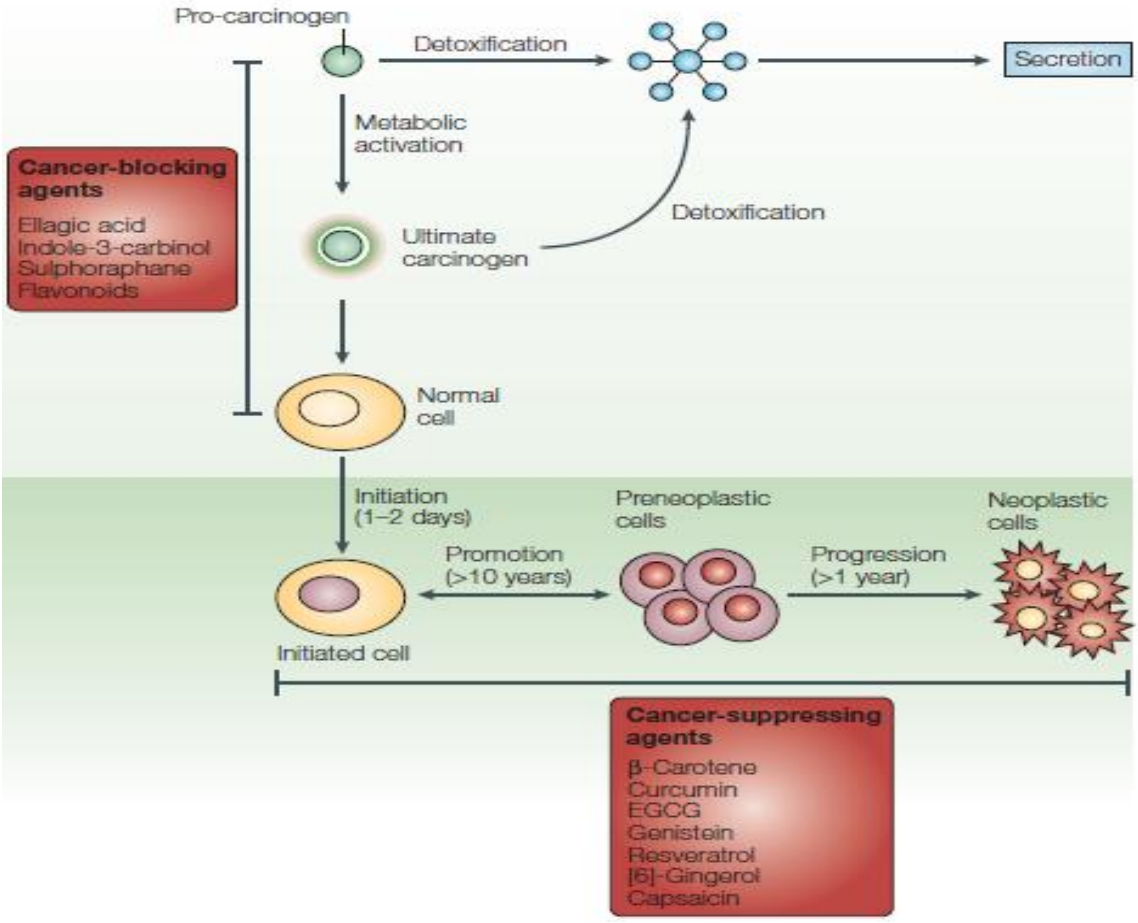

Figure 1.6: Carcinogenesis is initiated with the transformation of the normal cell into a cancer cell. Phytochemicals can interfere with different steps of this process, which can acts as both blocking and suppressing agents (**Surh et al. 1999**).

CHAPTER 2: REVIEW OF LITERATURE

2.1 Curcumin

Curcumin (diferuloylmethane), a major yellow pigment and component of turmeric powder extracted from the rhizomes of the plant, *Curcuma longa* **(Figure 2.1)**. It has a melting point of 183^{o}C, molecular formula of $C_{21}H_{20}O_6$ and molecular weight of 368.37g/mol (Aggarwal et al. 2007). Curcumin has been consumed as spice and a cure for human ailments for thousands of years in Asian countries. The taxonomic position of turmeric (Curcuma longa) is as follows:

Class: Liliopsida
Subclass: Commelinids
Order: Zingiberales
Family: Zingiberaceae
Genus: *Curcuma*
Species: *Curcuma longa*

Figure 2.1: Turmeric plant with Rhizome (Aggarwal et al. 2009)

Extensive research over the past 30 years has indicated the therapeutic potential of curcumin against a wide range of diseases, such as, cancer, lung diseases, cardiovascular, inflammatory, autoimmune and metabolic diseases**.** Curcumin is highly pleiotrophic with anti-inflammatory, hypoglycaemic and antioxidant **(Figure 2.2)**.

Figure 2.2

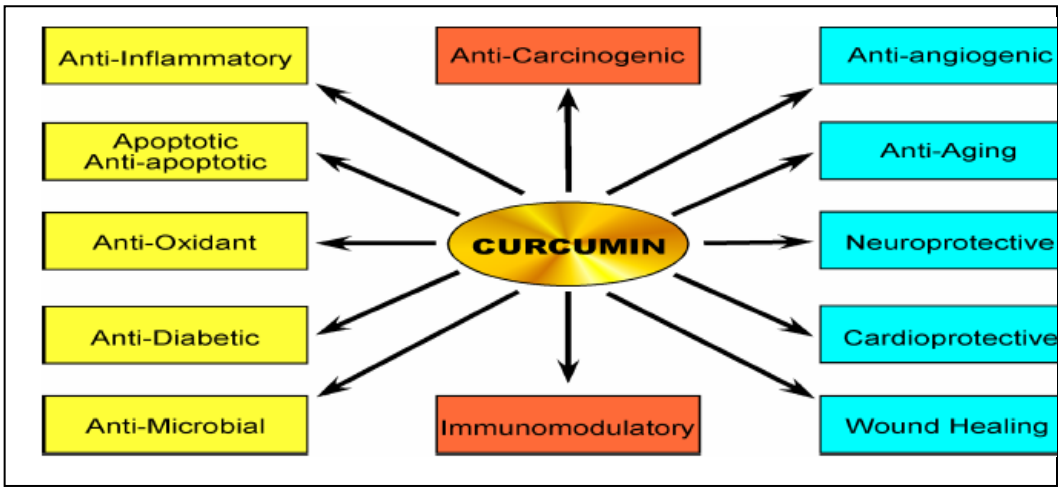

Figure 2.2: Biological activities of curcumin: The biological activities of curcumin in preclinical models and in human studies are shown to illustrate the wide ranging potential of curcumin to treat human diseases (Sa et al. 2010).

It has also been shown to possess chemotherapeutic, chemosensitization and radiosensitization activities as well. Many clinical trials using curcumin as a therapeutic agent are in progress (Aggarwal et al. 2009**)**. The interest in curcumin research has increases markedly over years. More than 4000 articles on curcumin were listed in the National Institute of Health Pubmed data base (http://www.ncbi.nlm.nih.gov/sites/entrez) (**Figure 2.3**).

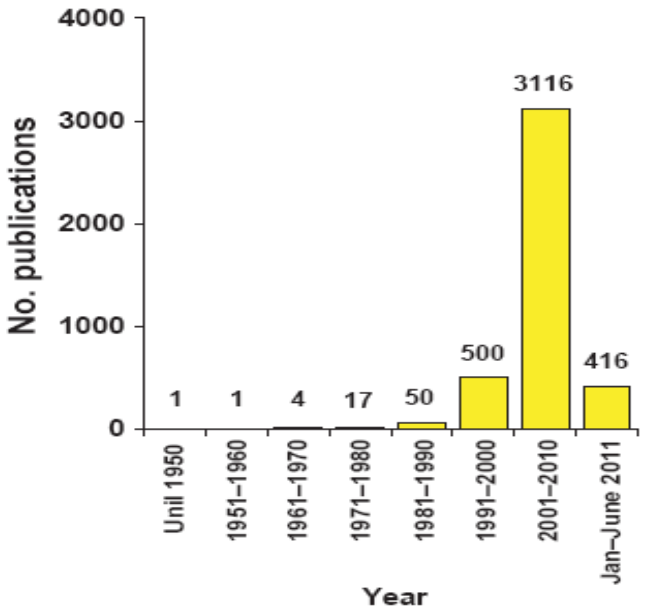

Figure 2.3: Number of publications on curcumin has increased markedly over the years (Gupta et al. 2012).

2.1.1 Structure and chemical properties of curcumin

Curcumin is a bis-α, β-unsaturated β-diketone with a molecular formula of $C_{21}H_{20}O_6$ (M.P.184^oC) and molecular weight is 368.37g/mol. It is insoluble in water but soluble in dichloromethane, chloroform, methanol, ethanol, ethyl acetate, dimethylsulphoxide and acetone. The curcuminoids present along with curcumin are demethoxycurcumin and bisdemethoxycurcumin which exists in two tautomeric structures i.e., keto and enol forms (**Figure 2.4**).

Curcumin shows maximum light absorption at 420nm in UV-Vis spectrophotometer. The presence of hydroxyl groups on phenyl ring is responsible for antioxidant activity of curcumin and the keto groups and double bond is essential for anti-inflammatory, anti-cancer and anti-mutagen activities. Curcumin is stable at acidic pH and degrades within 30 min at basic pH to trans-6-(4-hydroxy-3-methoxyphenyl)-2,4-dioxo-5-hexanal, ferulic acid, vanillin and feruloylmethane (Lin et al. 2000). The presence of foetal bovine serum or addition of antioxidants like ascorbic acid, or glutathione will prevent this degradation in culture media or phosphate buffer at pH 7. In acidic conditions the degradation is slower, with less than 20% of total curcumin decomposed at 1h (Wang et al. 1997).

Figure 2.4

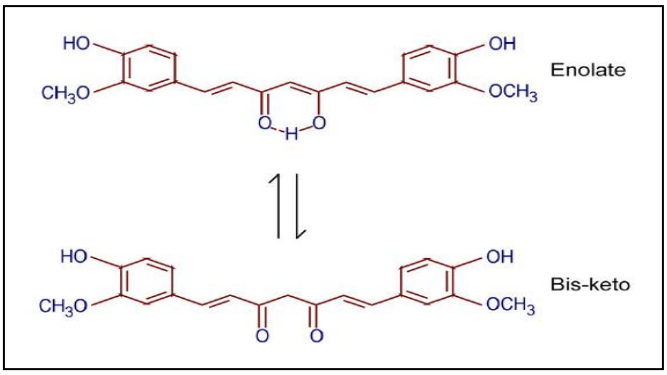

Figure 2.4: Chemical structure of curcumin. The tautomerism of curcumin is demonstrated under different conditions. Under acidic and neutral conditions, the bis-keto form is more predominant than the enolate form (Sa et al. 2010).

2.1.2 Absorption and metabolism of curcumin

Curcumin was first bio-transformed to dihydrocurcumin and tetrahydrocurcumin (THC), and these compounds were further converted to monoglucuronide conjugates. The biotransformation step curcumin→hexahydrocurcumin is rapid,

and the overall rate of curcumin reduction seems slower in human than in rat liver cells. The predominant metabolites of curcumin in rat plasma in vivo are curcumin glucuronide and curcumin sulphate, whereas hexahydrocurcumin and hexahydrocurcuminol as the major metabolites of curcumin in hepatocyte suspensions (Ireson et al. 2001) (**Figure 2.5**). Curcumin when given orally or intraperitoneally to rats is mostly excreted in faeces and only little in the urine (Pan et al. 1999). Only traces of curcumin are found in the liver, heart and kidney (Chattopadhyay et al. 2004).

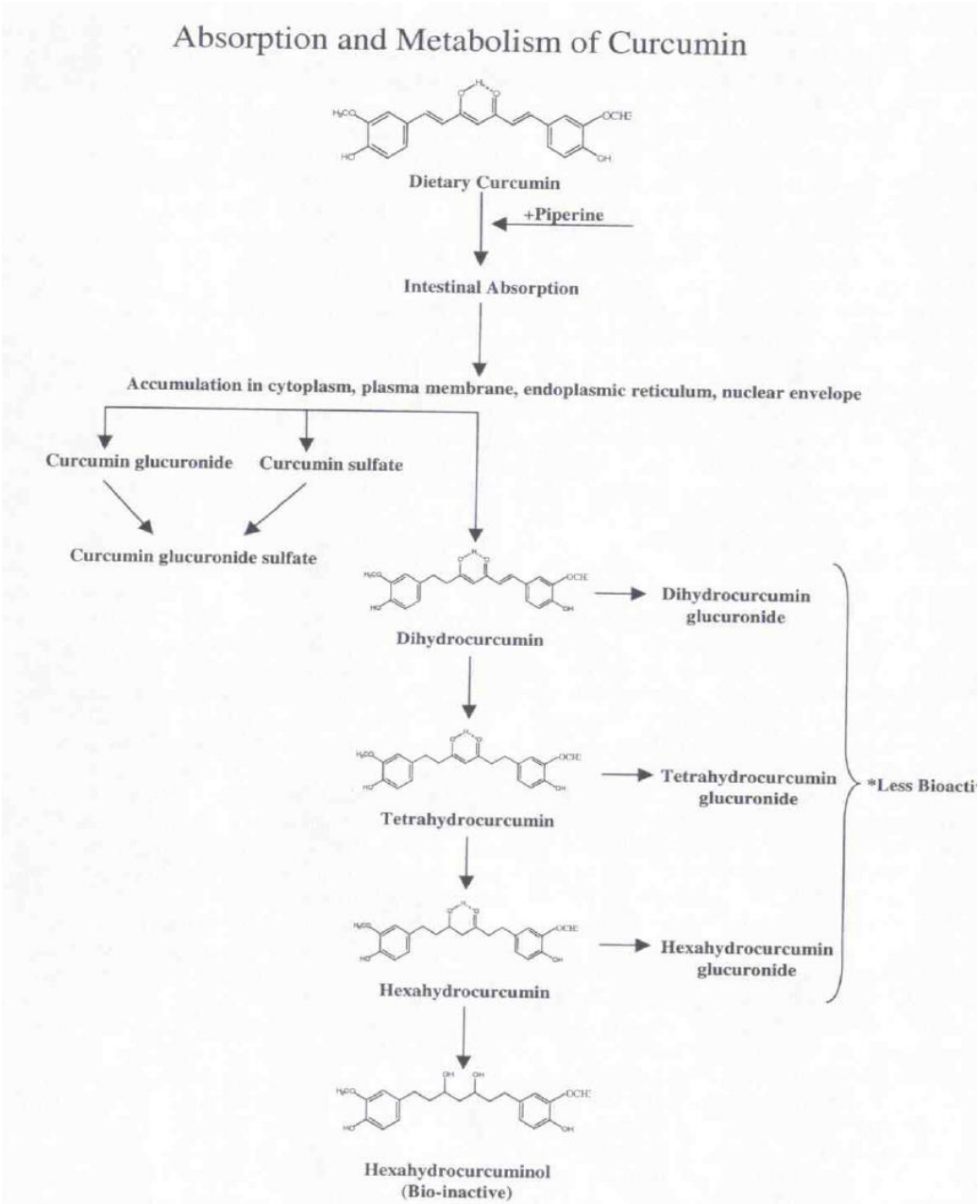

Figure 2.5: Absorption and metabolism of curcumin. The fate of curcumin after oral administration in human and rodents are depicted (Joe et al. 2004).

2.1.3 Biological activities of curcumin

Numerous studies have indicated that curcumin has been shown to possess wide range of pharmacological activities including anti-oxidant, anti-inflammatory, anti-microbial and anti-cancer activities (**Figure 2.6**).

a) Anti-inflammatory activities of curcumin

Extensive research on curcumin has demonstrated that curcumin has been shown to be a useful anti-inflammatory agent. In various animal models, a dose of 100-200mg/kg body weight exhibited good anti-inflammatory activity and seemed to have negligible adverse effects on human systems (Kohli et al. 2005). Curcumin offers anti-inflammatory effect through inhibition of NF-κB activation (Singh et Aggarwal. 1995). The anti-inflammatory role of curcumin is also mediated through down-regulation of cyclo-oxygenase (COX-2) (Goel et al. 2001) and inducible nitric oxide (iNOS) synthase, important enzymes that mediate inflammatory processes, through suppression of NF-κB activation (Surh et al. 1999). It also reduces pro-inflammatory leukotriene synthesis via inhibition of lipooxygenase enzyme (LOX) (Hunag et al. 1991).

Furthermore, the inhibitory action of curcumin on Janus kinase (JAK)-STAT signalling could contribute to its anti-inflammatory activity in the brain and T-lymphocytes (Kim et al. 2003). In summary, the anti-inflammatory activity of curcumin is mainly due to inhibition of arachidonic acid (AA) metabolism, COX, LOX, cytokines and NF-κB.

b) Anti-carcinogenic activity:

Numerous studies have shown that curcumin acts as a potent anti-carcinogenic compound. Among various mechanisms, induction of apoptosis plays an important role in its anti-carcinogenic effect. Curcumin suppresses tumour growth through various pathways. Subtoxic concentrations of curcumin sensitize human renal cancer cells to TRAIL-mediated apoptosis. Nitric oxide and its derivatives play a major role in tumour promotion. Curcumin inhibits iNOS and COX-2 production by suppression of NF-κB activation (Surh et al. 2003). COX-2 has been implicated in the development of many cancers. The tumourigenesis of the skin, mammary gland, oral cavity, fore stomach, intestine, colon and liver have been suppressed by curcumin (Huang et al. 1988; Kuttan et al. 198 7; Chuang et al. 2000). Curcumin induces apoptotic cell death by DNA damage in

human cancer cell lines, TK-10, MCF-2 and UACC-62 by acting as topoisomerase II poison (Martin-Cordero et al. 2003). It also induces apoptosis and inhibits cell-cycle progression, both of which are instrumental in preventing cancerous cell growth in rat aortic smooth muscles (Chen et al. 2000).

Curcumin has been shown to cause apoptosis in mouse neuro2a cells by impairing the ubiquitine-proteosome system through the mitochondrial pathway. It cause rapid decrease in mitochondrial membrane potential and release of cytochrome c to activate caspase 3 and 9 for apoptotic cell death (Jana et al. 2004). On the contrary, it also inhibits programmed cell death in other systems. Curcumin can inhibit apoptosis in T lymphocytes and also in various breast cancer cell lines like MCF-7, MDA-MB 231 and BT-474 cells. In human breast cancer, dietary supplementation with curcumin is found to significantly inhibit cyclophosphamide-tumour regression. These findings show that curcumin can inhibit chemotherapy-induced apoptosis through inhibition of ROS generation and blockade of JNK function (Jones et al. 2000).

c) Anti-oxidant activity:

Curcumin, exhibits strong antioxidant activity, comparable to Vitamin C and E. It is found to be atleast ten times more active as an antioxidant than even Vitamin E (Khopde et al. 1999). The antioxidant mechanism of curcumin is attributed to its unique conjugated structure, which includes two methoxylated phenols and an enol form of b-diketone. The structure shows typical radical trapping ability as a chain breaking antioxidant. It was shown to be capable of scavenging oxygen free radicals such as super anions, hydroxyl radicals, which are the initiators of lipid peroxidation and nitrogen dioxide radicals (Unnikrishnan and Rao et al. 1995).

Curcumin activate expression of several intracellular defense systems *in vitro* and *in vivo*. In vitro, curcumin activates NQO1expression in murine hepatoma cells (Sharma et al. 2005). In human bronchial epithelial cells, it induces the expression of the iron binding protein ferritin and the glutamyl cysteine ligase modulatory (GCLM) and catalytic (GCLC) units, the two sub-units of the rate-limiting enzyme in glutathione biosynthesis. Several cytoprotective genes activated by curcumin, including HO-1, NQO1, ferritin, GCLM are regulated by antioxidant response elements (ARE) (Li et al. 2004).

Figure 2.6

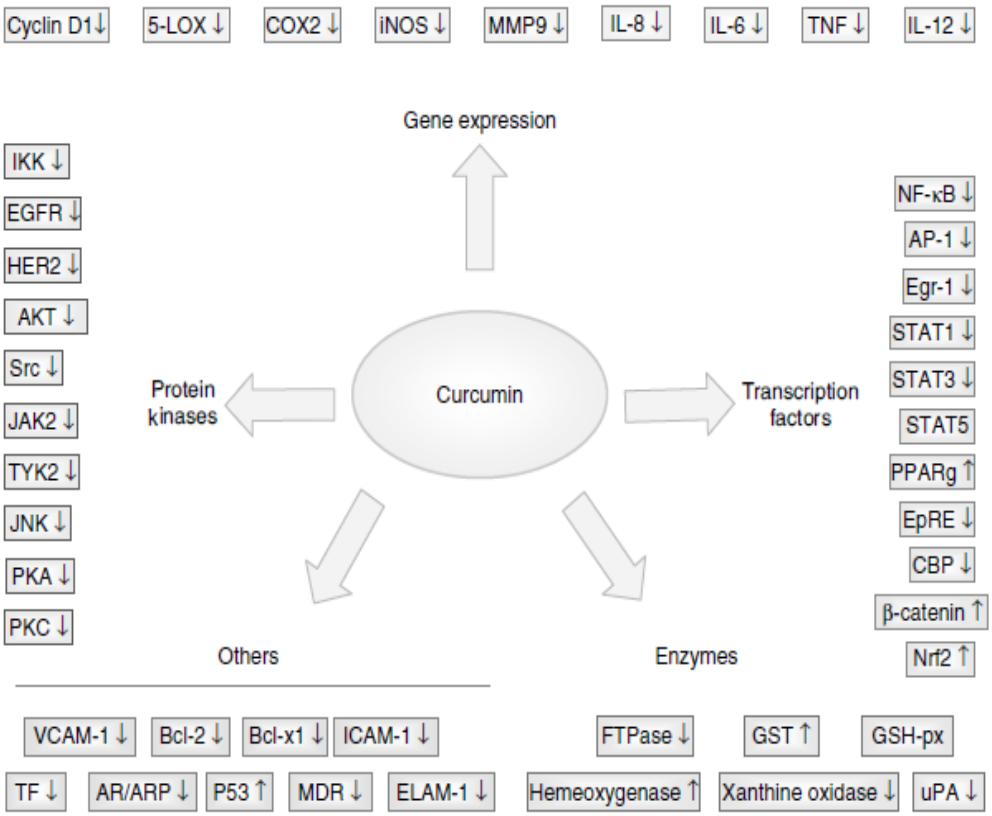

Figure 2.6: Molecular targets shown to be regulated by curcumin (Aggarwal et al. 2005)

2.1.4 Pharmacokinetic studies on curcumin

The pharmacokinetic properties of curcumin have been studied in rodent models. When administered orally, about 75% of the curcumin was excreted in faeces and only about 35% was excreted unchanged, the remaining 65% excreted as metabolites of curcumin. It is biotransformed to dihydrocurcumin and tetrahydrocurcumin and which further get converted to monoglucuronide conjugates and this metabolic reduction occurred very rapidly. In contrast to extensive studies in rodent model, less data is available from human studies. It was found that administration of curcumin to healthy volunteers showed low curcumin concentration in the serum, but when 1% piperine was co-administered, bioavailability of curcumin was increased to 2000% in the serum. It has been found that the presence of curcumin and its metabolites in the urine samples offers a reliable and convenient way of testing the compliance of volunteers consuming curcumin in clinical trials. Since curcumin's poor systemic

bioavailability following oral dosing compromises its potential therapeutic uses, many researchers have focused on ways to improve its bioavailability. Although systemic preclinical pharmacokinetic data are currently lacking, several experimental strategies have been developed to improve the selective and sustained delivery of curcumin into cancer cells. These include use of curcumin phospholipids complexes, inclusion of curcumin in liposomes/lipidic micelles or the curcumin encapsulation in diverse polymeric nanoparticle based formulations with un-conjugated or conjugated ligand or antibody that specifically targets cancer cell receptor or epitopes (Narayanan et al. 2009; Mohanty et al. 2010; Mohanty et al. 2010).

2.1.5 New synthetic analogs of curcumin:

A potential strategy to enhance the anti-carcinogenic efficacy and overcome the high physical and metabolic instability and poor bioavailability of curcumin may be the use of synthetic analogs of this natural dietary compound with improved physiochemical and pharmacological properties. Studies based on the tautomeric forms of curcumin have led to the development of some synthetic analogs endowed with a better chemical stability and showing more potent anti-inflammatory, anti-oxidant, anti-carcinogenic and anti-angiogenic effects on human cancer cell lines than curcumin (**Figure 2.7**). The 4-OH groups of curcumin through methylation yielded a dimethoxycurcumin analog exhibiting an enhanced metabolic activity *in vitro* and *in vivo* as well as anti-proliferative and apoptotic effects on pancreatic and breast cancer cell line compared to curcumin (Tamvakoupoulas et al. 2007; Fuchs et al. 2009).

Few synthetic analog of curcumin which include FLL11, FLL12, FLL32 and GO-Y030, which are more potent than curcumin inhibiting the migration, growth and colony formation in soft agar of colorectal, pancreatic, prostate, breast, melanoma and hepatocellular carcinoma cells. It has been reported that the anti-carcinogenic effects of these structural analogs of curcumin were mediated through down-regulation of erbb2, Akt, STAT-3 phosphorylated forms. A non-toxic fluorinated curcumin analog, namely EF24 have been reported to display improved pharmacokinetic, bioavailability, growth inhibitory and apoptotic effects than those of curcumin on lung, breast and prostate cancer cell lines *in vitro* and animal models *in vivo* (Lin et al. 2010; Shibata et al. 2009).

Various chemical analogs of curcumin, including ASC-J9 and its derivatives, have been shown to inhibit prostate cancer cell proliferation by enhancing AR degradation or by acting as the pure AR antagonist. Few curcumin analogs, which can function as a 17α-substituted dihydrotestosterone (DHT), has indicated that these compounds display potent anti-androgen activities superior to current clinical anti-androgenic activities superior to current clinical anti-androgenic drug, hydroxyflutamide on AI PC3 and DU145 cells transfected with wild-type AR or mutant LNCaP AR and ARA70 co-activator respectively. Chemically stable curcumin have also been shown to be more effective than free curcumin for eradicating chemoresistant cancer cells with the stem cell-like features from diverse cancer cell lines. Difluorinated analog of curcumin 3, 4-difluoro-benzo-curcumin designated as CDF, alone or in combination with 5-fluorouracil and oxaliplatin, was more potent than curcumin at reducing the number of chemoresistant HCT-116 and HT-29 colon cancer cells expressing CD44 and CD166 stem-cell like markers as well as inhibiting the growth and inducing apoptosis and disintegration of colonospheres *in vitro* (Mimeault et al. 2011).

Figure 2.7

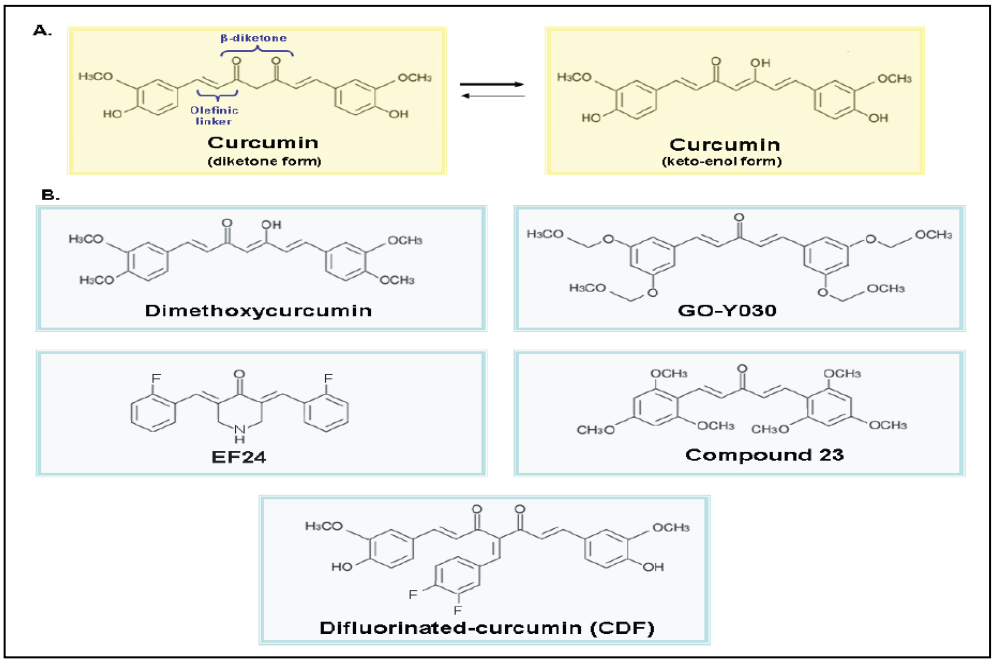

Figure 2.7: Chemical structures of naturally occurring curcumin and its novel synthetic analogs. A) Diketone and keto-enol forms of curcumin. B) Novel synthetic analogs of dietary curcumin showing improved chemical stability and anticarcinogenic properties on different cancer cell lines (Mimeault et al. 2011).

2.1.6 Novel nanotechnologies and delivery system of curcumin:

Apart from the synthetic analogues, several strategies have been evaluated to enhance the bioavailability of curcumin. These include nanoparticles, adjuvant, liposomes, micelles and phospholipids complexes. These various formulations have been discussed below in detail:

1) Adjuvants:

Piperine is known to inhibit hepatic and intestinal glucuronidation. When combined curcumin with piperine, the elimination half-life and clearance of curcumin were significantly decreased, resulting in an increase bioavailability to 154% that of curcumin alone in rats. In contrast, the increase in bioavailability was 2000% in humans, clearly showing the effect of piperine on bioavailability of curcumin, which is greater than in rats. In clinical trial study, human adult male volunteers took 2g of curcumin with and without 5mg piperine in this cross-over design study. One week after drug administration, blood samples were collected from the volunteers the presence of piperine was found to double the absorption of curcumin.

Some other agents that showed a synergistic effect when used in combination with curcumin in various *in vitro* studies look promising for further evaluation. Five patients with familial adenomatous polyposis who has undergone colectomy received 480mg and 20mg quercetin orally 3 times a day. The size of the polyps were assessed baseline and after therapy. There was a decrease in poly number and size, 60.4% and 50.9%, respectively, from baseline after a mean of 6 months of this treatment.

The synergistic inhibitory effect of curcumin and genistein against pesticide-induced growth of estrogen-dependent MCF-7 breast cancer cells shows that, combination of curcumin and gensitein completely inhibited the cell proliferation induced by individual or mixture of pesticides, and the inhibitory effect was superior to the individual effects of either curcumin or genistein.

2) Nanoparticles:

Targeted and triggered drug delivery systems employing nanoparticle technology have emerged as solutions to the problems of enhancing the bioavailability of therapeutic agents and reducing their unwanted side effects. The synthesis, physiochemical characterization and cancer related applications of a polymer

based nanoparticle of curcumin called nanocurcumin were reported. Nanocurcumin was found to have *in vitro* activity similar to that of free curcumin in pancreatic cancer cell lines, inhibiting activation of the transcription factors NF-κB and reducing steady-state levels of pro-inflammatory cytokines such as interleukins and TNF-α. Curcumin loaded solid lipid nanoparticles for topical application were found to be stable for 6 months at room temperature and gave prolonged *in vitro* release of curcumin for up to 12h. An *in vivo* study revealed the improved efficiency of this topical cream containing curcuminoid loaded solid lipid nanoparticle over that containing free curcuminoids. Recently, lipid based nanoparticles provide improved intravenous delivery of curcumin to tissue macrophages. At 6 hr after intravenous injection in rats, curcumin in a nanoparticle delivery system was massively distributed in macrophages of the bone marrow and spleen. Overall, nanoparticle based systems for curcumin delivery, require much progress in this area.

3) Liposomes, micelles and other delivery systems

Liposomes are excellent drug delivery systems since they carry both hydrophobic and hydrophilic molecules. The *in vitro* and *in vivo* antitumor activity of liposomal curcumin showed that curcumin inhibited pancreatic cancer cell growth and also exhibited anti-angiogenic effects.

The preclinical anticancer activity of liposomal curcumin in colorectal cancer was evaluated. This study compared the efficacy of liposomal curcumin with oxaliplatin in colorectal cancer. There was a synergism between liposomal curcumin and oxaliplatin at a ratio of 4:1 in LoVo cells *in vitro*. Significant tumor growth was observed in Colo205 and LoVo xenografts models, and the growth inhibition by liposomal curcumin was greater than that by oxaliplatin in Colo205 cells.

Another study also reported the antitumor and antioxidant activity of neutral unilamellar liposomal curcumin in mice. *In vitro* cellular uptake studies of liposomal and albumin-loaded curcumin showed that liposomal vehicle is capable of loading more curcumin into cells than either human serum albumin or aqueous dimethyl sulfoxide, and lymphoma cells showed a greater uptake of curcumin than lymphocytes. Liposomes were proved to be a more suitable curcumin carrier system since as much as 30% of the photoxic effect caused by curcumin in

cyclodextrin was obtained with about 1/30 of the curcumin concentration in liposomes.

The intestinal absorption and a micellar curcumin formulation with phospholipids and a bile salt were evaluated using an *in vitro* model consisting of everted rat intestinal sacs. This shows that curcumin is biologically transformed during absorption. *In vitro* intestinal absorption of curcumin was found to increase from 47% to 56% when it is prepared in micelles. Pharmacokinetic studies showed that curcumin in polymeric micellar formulation had a 60 fold higher biological half-life in rats than curcumin solubilised in a mixture of polyethylene glycol (PEG) and dextrose.

In another study, the antioxidant effect of liposomal curcumin against copper-induced lipid peroxidation was demonstrated. The feasibility of curcumin microemulsion containing ethyl oleate, lecithin and Tween 80 as an ultrasonic drug delivery carriers was studied. Further more, it was reported that liposomal curcumin formulation had 10 fold higher proliferative activities in human prostate cancer cell line than free curcumin.

4) Phospholipid complexes

In a study, curcumin (100mg/kg) or curcumin-phospholipid complex (100mg/kg curcumin) was administered to rats. The result showed that curcumin-phospholipid complex produced a maximum plasma curcumin level of 600ng/ml 2.33 h after oral administration, while free curcumin yielded a maximum plasma concentration of 267ng/ml 1.62h after oral administration. The curcumin-phospholipid complex yielded a curcumin half-life about 1.5 fold greater than that of free curcumin. These result shows that curcumin-phospholipid complex yielded a 3 fold greater aqueous solubility and a better hepatoprotective effect than free curcumin.

Ina another study, male wistar rats received 340mg/kg of unformulated and formulated curcumin with phosphatidylcholine by oral gavage. Curcumin, the accompanying curcuminoids demethoxycurcumin and bisdemtheoxycurcumin and curcumin sulphate were identified in plasma, intestinal, mucosa and liver of rats. Peak plasma levels of curcumin after administration of Meriva were 5 fold higher than those after administration of unformulated curcumin. Similarly, liver levels of curcumin were higher after administration of Meriva than after administration of unformulated curcumin. Curcumin concentration in the

gastrointestinal mucosa after ingestion of Meriva was somewhat lower than those observed after administration of unformulated curcumin. These results suggest that curcumin formulated with phosphatidylcholine furnishes higher systemic level than the parent curcumin.

5) Curcumin prodrugs:

Two curcumin prodrugs, N-maleoyl-L-valine-curcumin and N-maleoyl-glycine-curcumin, were synthesized and evaluated for the selective inhibition of growth of bladder cancer cell lines. This study showed that activation of curcumin prodrugs via hydrolysis function of cellular esterase could inhibit the growth of tumor cells and reduce the side effects of these drugs on normal diploid cells. DNA-curcumin-tetraglycine was prepared by deoxy-11-mer oligonucleotide, 5'-GTTAGGGTTAG-3', complementary to a repeat sequence of human telomerase RNA template and linked through phosphate and a C-2 linker to a bioactive tetraglycine conjugate of curcumin. This molecule, targeted by antisense mechanism to telomerase, has been found to act as a prodrug affecting cell growth.

6) PEGylation

PEGylation is used mainly to increase the solubility and decrease the degradation of drug molecules. The aqueous solubility of curcumin was increased by formulating it with MePEG-b-PCL. It has been reported that significant increase in solubility of curcumin when conjugated with PEG and cyclodextrin. A bioconjugate with beta-cyclodextrin and PEG was prepared and folic acid was incorporated for targeting purposes. This conjugate, CD-(C6-PEG) 5-FA, formed a complex with curcumin and increased curcumin solubility by about 3200 fold as compared to native beta-cyclodextrins. This conjugation reduced the degradation rates of curcumin at pH 6.5 and 7.2 by 10 and 45 fold, respectively. *In vitro* studies using folic acid receptor over-expressing and non-expressing cells demonstrated that new carrier possesses potential selectivity for the folic acid receptor over-expressing tumor cells. Two conjugates of curcumin with PEG of different molecular weight exhibited greater cytotoxicity than unconjugated curcumin (Anand et al. 2008).

2.1.7 Summary:

The pathology of RB cancer is currently controlled by radiotherapy, surgery and is frequently supported by adjuvant chemotherapy. However, RB cancer is highly resistant to chemotherapy. There is of great interest in developing novel anticancer agents presenting low side-effects, and induce apoptosis or inhibit tumour cell proliferation. Numerous studies over the last few decades have demonstrated that curcumin targets several signalling molecules, thus showing immense challenge for the treatment of cancers. However, till date no study has been reported on RB cancer. Therefore, in this thesis, the role of curcumin (natural polyphenolic compound) in RB cells will be discussed. Hence, we investigated the mechanism by which curcumin exerts its cytotoxic effect on RB cells and non-neoplastic cell lines, with focus on induction of apoptosis, and mechanism of action at a molecular level. Furthermore, whether curcumin reverse drug resistance and sensitize RB cells to chemotherapy drugs has been investigated as well. This study will help to confirm curcumin's potential for chemotherapeutic activity in the treatment of RB cancer. In this thesis, we propose to test the following effects of curcumin:

1. **To study the cytotoxic effect of curcumin on non-neoplastic and RB cell lines.**
2. **To study the effect of curcumin mediated apoptosis in RB cancer cell lines.**
3. **To study the effect of curcumin on the regulation of miRNA and gene expression in RB cancer cell line.**
4. ***In vitro* and *in silico* studies on the effect of curcumin on multi-drug resistance proteins (P-gp, MRP and LRP) in RB cancer cell line.**
5. **To investigate the potential synergistic effects by combination of curcumin with clinically used standard chemotherapeutic drugs.**
6. **To synthesize and study the characterization of curcumin bio-conjugates.**

CHAPTER 3: CYTOTOXICTY AND CELLULAR UPTAKE OF CURCUMIN IN NON-NEOPLASTIC AND RB CELL LINES

3.1 INTRODUCTION

Killing of tumour cells without causing significant toxicity to non-neoplastic cells is one of the most important properties of an anti-cancer agent. Most of the chemotherapeutic agents used in the treatment of cancer not only induce cancer cell apoptosis but also severely damage the normal cells of the host, the effects being particularly severe in case of immune system (Vial et al. 2003). Many naturally occurring plant derived compounds have been reported to be effective in cancer cells without causing damage to normal cells. Curcumin, one of the naturally occurring plant derived compound which is included in our daily food habit and its use in large quantities from ancient times has already proved that it is a safe product. Curcumin preferably induces apoptosis in highly proliferating cells, death is more pronounced in tumour cells than normal cells. Several studies have been conducted to show that curcumin is not toxic to normal cells but has cytotoxic effect in cancer cell lines. It has also been shown that anticancer dose of curcumin arrests non-malignant cells in G0 phase reversibly but does not induces apoptosis in them (Choudhuri et al. 2002). **Thus in the present study, we want to determine the cytotoxic effect of curcumin in non-neoplastic (Muller glial and 3T3 fibroblast) and RB cancer (Y79 and Weri) cell lines by performing absorption and fluorescence spectral studies, cytotoxicity assay, uptake study and DNA fragmentation**.

3.2 Objective

1) To determine the effect of curcumin in non-neoplastic cells (3T3-mouse embryonic fibroblast; MIO-M1-Muller-glial) and human RB cancer (Y79 & Weri) cell line by performing absorption and fluorescence spectral study.
2) To study the cytotoxicity of curcumin in non-neoplastic and RB cell lines by cell viability assay, uptake study and DNA fragmentation.

3.3. Materials and methods:

3.3.1 Chemicals

Curcumin (2mg) was dissolved in 200µl of dimethyl sulphoxide (DMSO) and the stock solution was stored at -20^{0}C. The stock solution was diluted with Rosewell Park Memorial Institute (RPMI-1640 medium) and used for the experiments. Cell culture materials were purchased from Invitrogen (Carlsbad, CA, USA). NIH3T3 cells were obtained from National Centre for Cell Science (NCCS), India. The immortalized MI0-M1 (Muller glial) cell was provided by Prof G.A. Limb, Institute of Ophthalmology, University College, London. Y79 and Weri cells were obtained from Riken Cell Bank (Japan). Absorption spectra were recorded on a DU 800 spectrophotometer (Beckmann) and fluorescence spectra were recorded on a SpectraMax M2 multi-detection microplate reader (Molecular devices, CA, USA).

3.3.2 Cell culture

Y79 and Weri-RB1 cell line in suspension with RPMI-1640 medium and MIO-MI, NIH3T3 cell line as adherent in Dulbeco's Modified Eagle medium (DMEM) were cultured and supplemented with 10% bovine serum albumin, 50ng/mL of streptomycin and 1.25ng/mL of Amphotericin B at 37^{0}C in a humidified atmosphere with 95% O_2 and 5% CO_2. The concentration of DMSO used for the study was within the permissible limits of toxicity (< 1%).

3.3.3 Absorption and fluorescence spectroscopic studies

The non-neoplastic and RB cells (approx 1x10^5 cells/ml) were incubated with curcumin (10µM) for 4h, and the cells were spinned down to 1000 rpm in eppendorf centrifuge for 5 min and washed thrice with ice cold phosphate buffer saline (PBS). The cells were re-suspended into 1 ml of PBS and subjected to absorption and fluorescence spectroscopy studies (Kunwar et al. 2006).

3.3.4 Uptake of curcumin in non-neoplastic and RB cell lines

For the estimation of cellular uptake, RB and non-neoplastic cells were treated with different concentration of curcumin (5-20µM) for 4h. After the incubation period the cells were washed thrice with ice cold PBS. Since curcumin exhibits a green fluorescent signal, the cells were analysed using FACScalibur flow cyotmeter (BD). Fluorescence was detected through a 575nm band filter and quantified using CellQuest Software (Becton Dickinson; Franklin Lakes, NJ). Quantification results are presented as percent increase of mean fluorescence intensity of the curcumin treated samples, compared to untreated cells in triplicate experiments, using gated populations that exclude dead cells and cellular debris (Kunwar et al. 2006)

3.3.5 Sub-cellular fractionation

The RB and non-neoplastic cells (approx $1x10^5$cells/ml) were incubated with curcumin at 20µM concentration for 4h. Following treatment, the fractionation was performed using differential centrifugation. In brief, cells were treated with 0.5ml of hypotonic buffer, allowed to swell on ice for 15min, and then NP-40 (0.6%) was added. The sample was homogenised and subjected to various centrifugal speed of 2000xg for 10 min, 10,000xg for 15 min and 100,000xg for 45 min respectively to collect the nuclear, mitochondrial and membrane fraction in the pellet and cytosolic fraction as supernatant. All fractions were washed thrice with ice cold PBS, air dried and suspended in 0.5ml of methanol. Absorption spectra of curcumin from all the fractions were recorded (Kunwar et al. 2006).

3.3.6 Cell survival and therapeutic index:

Non-neoplastic and RB cells were seeded into 96-well plate at density of $5x10^3$cells/well and incubated overnight. Next day medium containing varying concentration of curcumin (vehicle control 0.5% DMSO) was added and cells were incubated for 48h, after which the cell viability was measured using MTT. Thereafter, 10µl MTT (5mg/ml in PBS) was added and incubated for 4h. Cells that are viable form formazan crystals by active mitochondria respiration. Crystals were dissolved with 100µl DMSO, after which the reading was taken spectrophotometrically at 570nm using an ELISA reader (Mosmann et al. 1983).

Percentage cell viability was calculated as:

Test absorbance/ Control absorbance x 100.

For therapeutic index (Cha et al. 2005)**, the formula used for calculation was**

Therapeutic index = Normal cell IC_{50} / Tumour cell IC_{50}

3.3.7 Cell morphology study:

Non-neoplastic and RB cells were seeded into 12-well plate at a density of $5x10^4$ cells/well and treated with different concentration of curcumin (20 and 30µM) for 48h and the morphology was examined under phase contrast microscope after the incubation period (Shi et al. 2006).

3.3.8 DNA fragmentation

5×10^4 cells/well were seeded in 24-well plates with 500 µl of culture media and incubated at 37^0C for 48h. The cells were then exposed to different concentration of curcumin (20 and 30µM) and incubated for 48h. DNA was extracted from the cell pellet using DNA isolation kit (Qiagen, USA) as per the manufacturer's instructions. The isolated DNA was then electrophoresed at 100V in a 2% agarose gel with 0.5 % ethidium bromide. The bands were visualized under UV light with a gel documentation system (BioDoc-It Imaging system, UVP, USA).

3.3.9 Statistical analysis

In all the experiments, the untreated cells with only the culture medium served as control. The statistical analysis between different groups for significance was done using Student's t-test. A value of $p<0.05$ was considered as statistically significant.

3.4 Results

3.4.1 Uptake of curcumin in non-neoplastic and RB cell lines

The cellular uptake of curcumin in non-neoplastic and RB cell lines was calculated at different concentrations. The result indicated that the uptake increased with increase concentration of curcumin in all different cell lines. It was observed that the RB cells (Y79 and Weri) show significantly higher uptake of curcumin (2-3 folds) when compared with the non-neoplastic cells (MIO-M1), indicating curcumin absorption for its increased anti-proliferative effect only in the RB cells and not on the no-neoplastic cells (**Figure 3.1**)

Figure 3.1

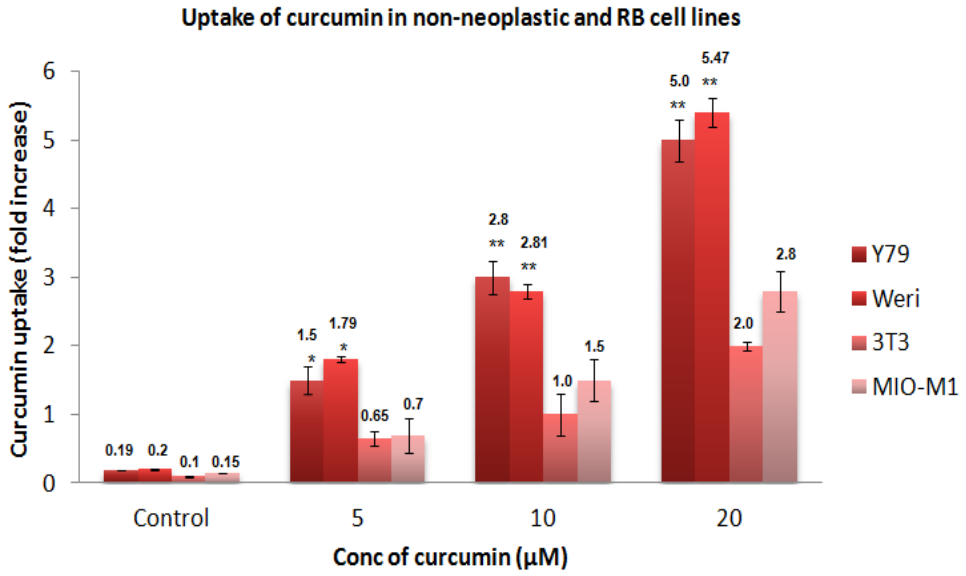

Figure 3.1: Cellular uptake of curcumin in non-neoplastic and RB cell lines: RB and non-neoplastic cells were treated with different concentration of (5-20 µM) curcumin for 4h. Curcumin uptake was measured by flow cytometry. Results presented as mean ± S.D, n=3. * p <0.05, ** p< 0.01; indicates significant difference beween the non-neoplastic and RB cell lines.

3.4.2 Spectroscopic studies of intracellular curcumin

Figure 3.2a&b shows the absorption and fluorescence spectra of curcumin. The absorption spectra from the methanolic extract of curcumin showed a maximum absorption at 420 nm in both the non-neoplastic and RB cell lines. The fluorescence spectra of curcumin in non-neoplastic cell line (MIO-M1 and 3T3) showed absorption maximum at 510nm and 530nm, respectively. In RB cell lines (Y79 and Weri) it showed a fluorescence spectrum with an absorption maximum of 520 and 515nm, respectively. The fluorescence intensity was found to be higher in the RB tumour cell lines (Y79 & Weri) when compared with the non-neoplastic cell (3T3 & MIO-M1) lin

Figure 3.2a&b

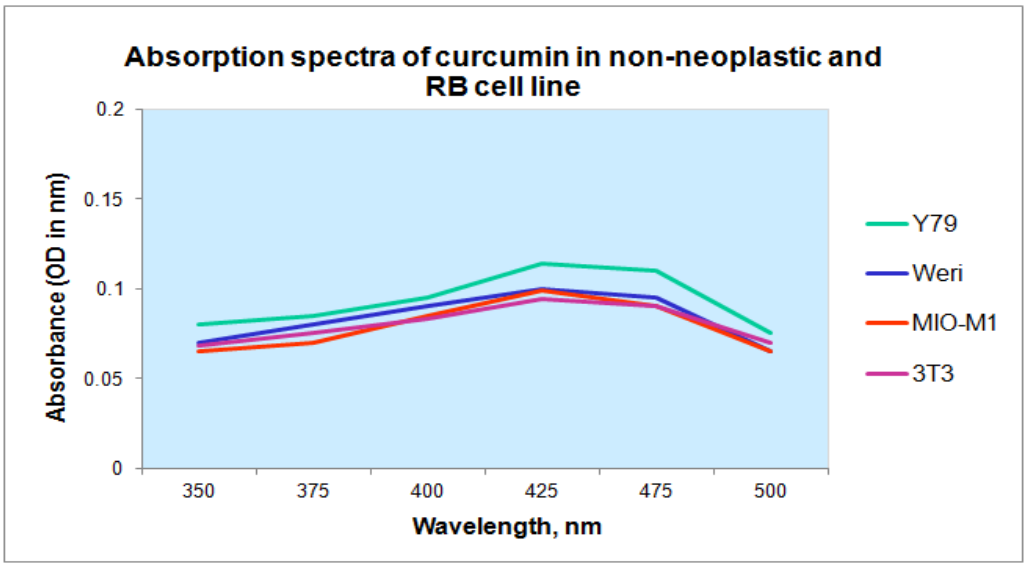

Figure 3.2a: Absorption spectra of curcumin extracted into 1of methanol from RB and non-neoplastic cell lines ($1x10^5$cells/ml) after treatment with 10µM concentration of curcumin for 4h. Results are presented as mean ±SD, n=3.

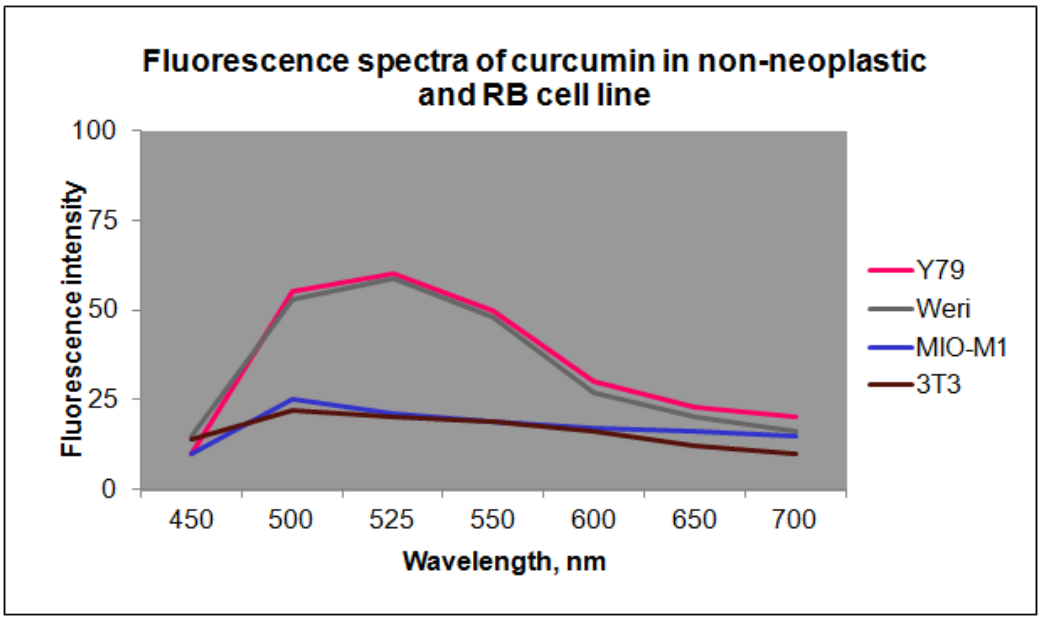

Figure 3.2b: The cells for recording fluorescence spectra were treated with 10µM concentration of curcumin for 4h and the fluorescence spectra of curcumin after excitation at 420nm were noted. Results are presented as mean ±SD, n=3.

3.4.3 Sub-cellular distribution of curcumin in non-neoplastic and RB cell lines

The sub-cellular distribution of curcumin showed maximum absorption of curcumin in RB cell lines when compared with the non-neoplastic cell lines. The absorption spectra of curcumin from different sub-cellular fractions have been

calculated by comparing the absorbance at 428nm with the percentage of curcumin accumulated in different cellular compartments. The accumulation of curcumin was more in the membrane followed by its distribution in cytoplasm, nucleus and mitochondria (**Figure 3.3**).

Figure 3.3

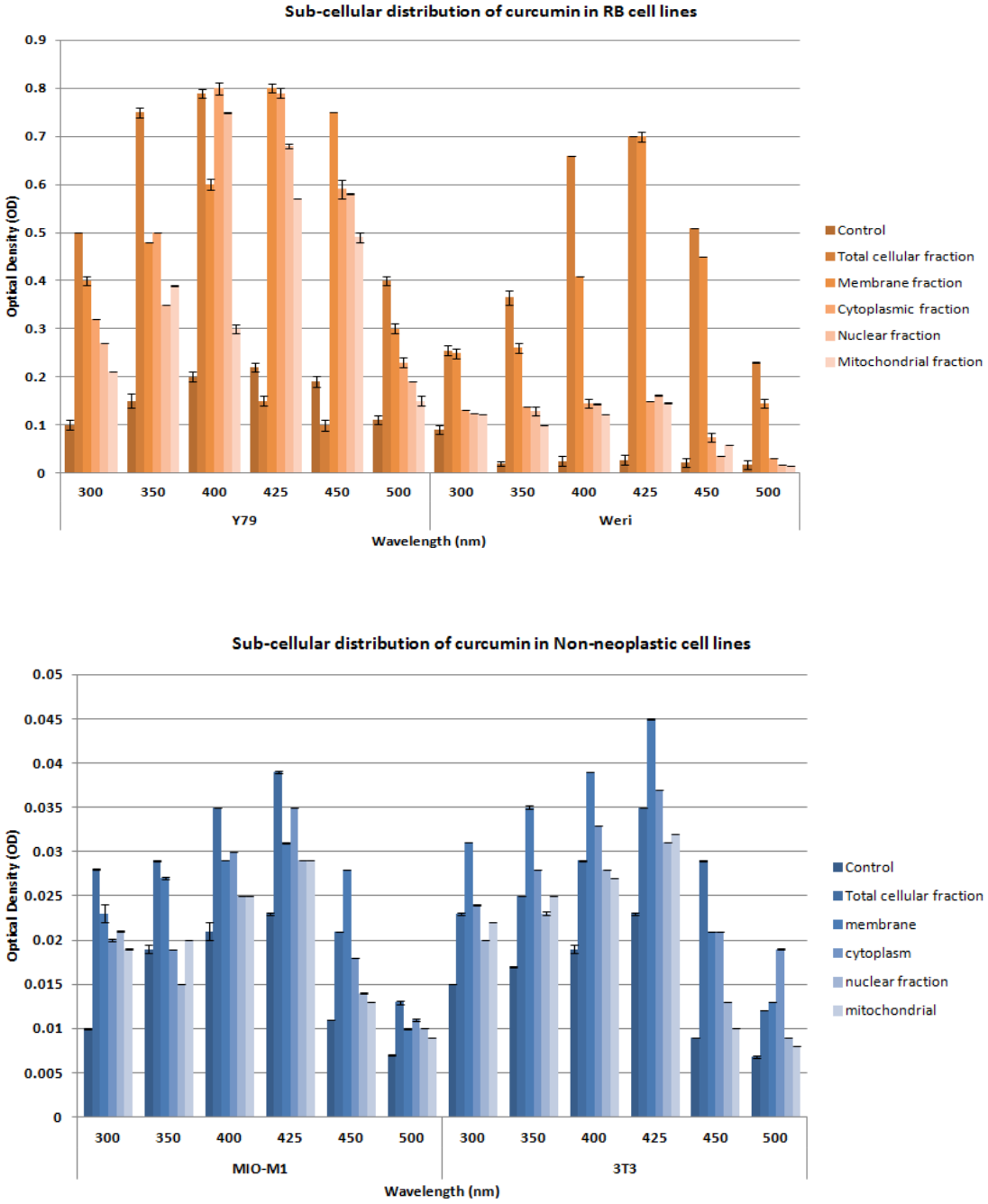

Figure 3.3: Absorption spectra of curcumin extracted into 0.5ml of methanol solution from different sub-cellular fraction of non-neoplastic and RB cancer cell lines after treatment with 20µM curcumin. Results presented as mean ± S.D, n=3.

3.4.4 Cytotoxicity measurements

Figure 3.4 shows the cell survival and therapeutic index of curcumin at different concentrations in RB and non-neoplastic cell lines. The results indicate that there is an increase in the cytotoxicty of curcumin with increase concentration in different cell lines. RB cell lines (Y79 and Weri) showed higher sensitivity towards the cytotoxic effect of curcumin when compared with the non-neoplastic cell line (NIH-3T3 and MIO-M1). The therapeutic index data also showed that curcumin have greater toxicity in RB cells than the non-neoplastic cells, since the therapeutic value was found to be greater than 1 in both the RB cell lines.

Figure 3.4: Cytotoxicity assay of curcumin in RB and non-neoplastic cell lines

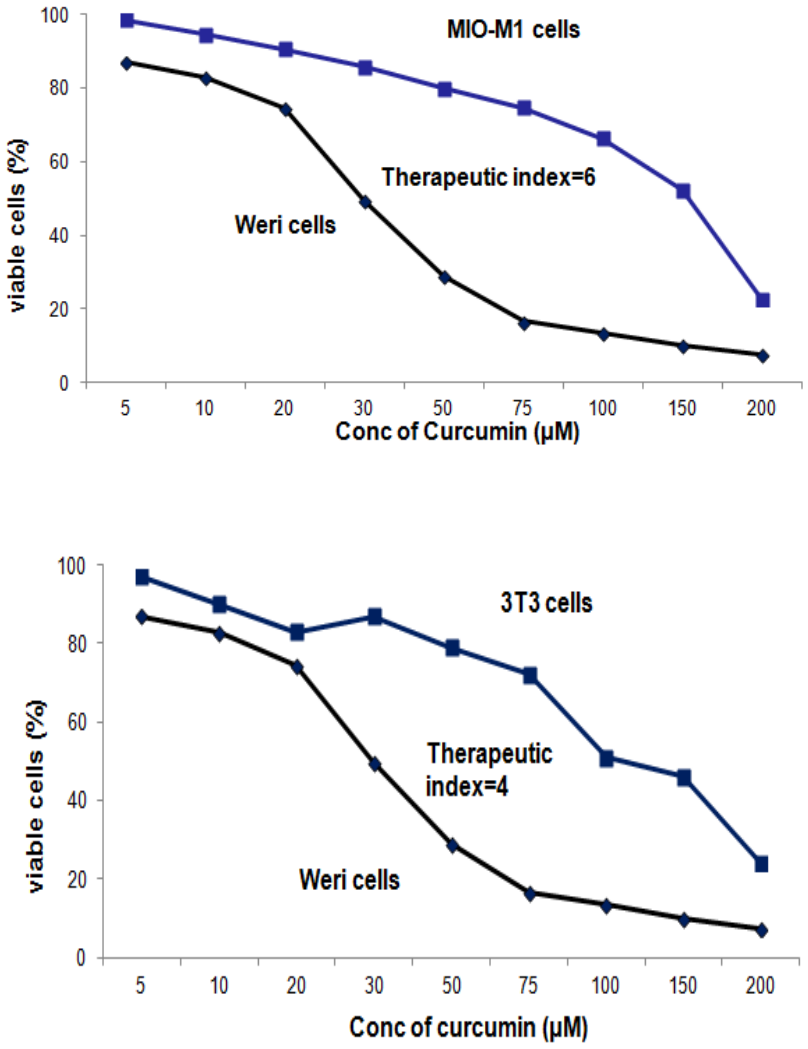

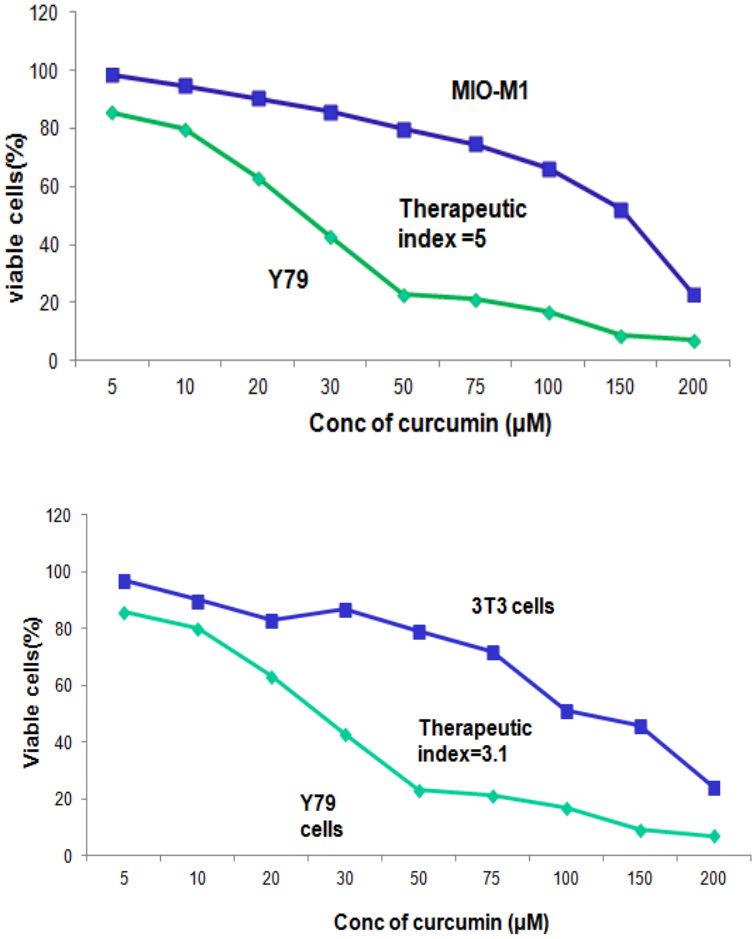

Figure 3.4: Effect of curcumin on cell survival and therapeutic index. Cells were treated with different concentration of curcumin (5-200 µM) and incubated for 48h and the cell viability was measured using MTT assay. Therapeutic index for curcumin between non-neoplastic and RB cell lines was calculated at the IC_{50} concentration. Results presented as mean ± S.D, n=3.

3.4.5 Effect of curcumin on cell morphology in non-neoplastic and RB cell lines

To determine curcumin induced apoptosis of RB cells, we first examined the changes in cell morphology after exposure to curcumin in both RB and non-neoplastic cell lines. The cells were observed under phase contrast microscope after curcumin treatment, which showed obvious change in the morphology in RB cancer cell lines. The RB cells showed shrinking in cell size, chromatin condensation and less number of cluster formation. In contrast, no morphological changes of non-neoplastic cells treated with curcumin were observed, suggesting non-toxic effects of these compounds to non-neoplastic cells (**Figure 3.5**).

Figure 3.5: Effect of curcumin on cell morphology in RB and non-neoplastic cell lines

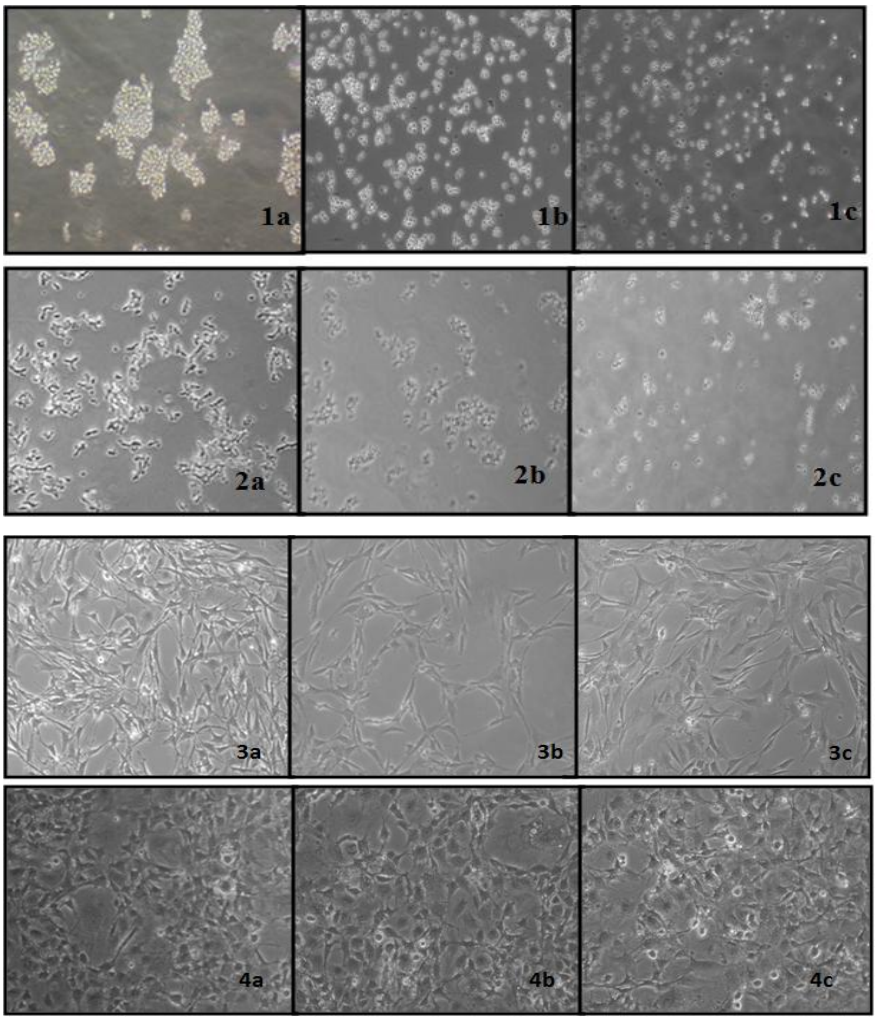

Figure 3.5: Morphological changes of non-neoplastic and RB cells after 48h of treatment with curcumin observed under phase-contrast microscope. Figure 1 & 2 - Y79 and Weri cells and Figure 3 & 4 - MIO-M1 and 3T3 cells. 1a, 2a, 3a= Respective control cells, 1b, 2b, 3b= 20µM curcumin and 1c, 2c, 3c= 30µM curcumin. Cells were photographed with a Leica DM IL inverted phase contrast microscope.

3.4.6 Effect of curcumin on DNA fragmentation in non-neoplastic and RB cell lines

We next examined the DNA pattern in curcumin treated non-neoplastic and RB cells by performing gel electrophoresis. RB cells showed typical ladder pattern of internucleosomal fragmentation in curcumin treated cells when compared with the control cells. In curcumin treated non-neoplastic cells, the DNA was found to be intact, which shows that curcumin did not have any effect on non-neoplastic cell lines (**Figure 3.6**).

Figure 3.6: Effect of curcumin DNA fragmentation in non-neoplastic and RB cancer cell lines

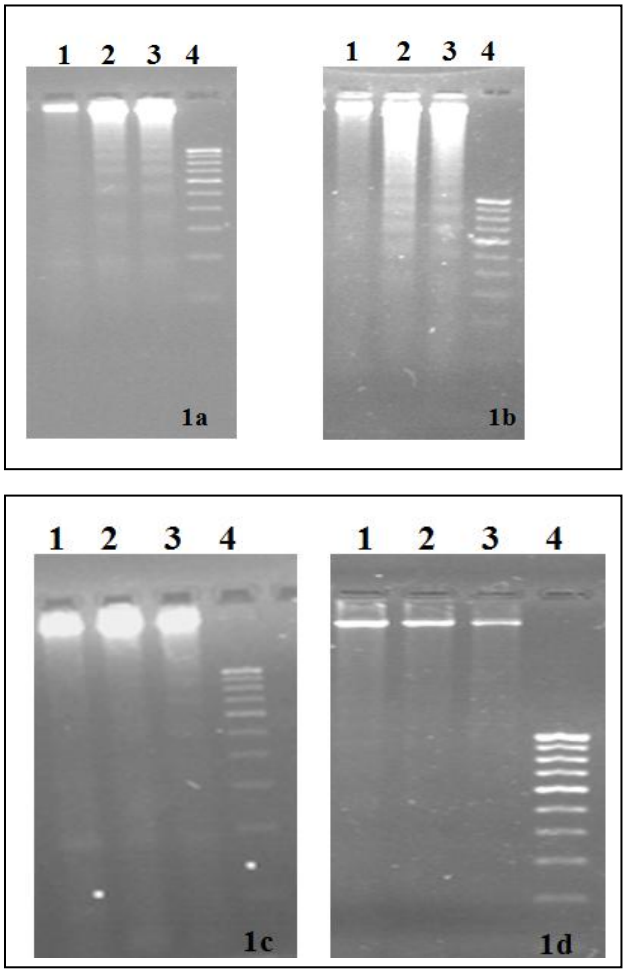

Figure 3.6: Detection of DNA fragmentation by agarose gel electrophoresis in non-neoplastic and RB cells. Both the cells were treated with curcumin (20 and 30 µM) and the control was treated with medium containing DMSO only. After the incubation period, the cells were harvested and lysed. DNA fragmentation was examined by agarose gel electrophoresis. Figure 1a-Y79 cells, 1b-Weri cells, 1c-MIO-M1 cells and 1d -3T3 cells. Lane 1- Respective control cells, Lane 2-20µM curcumin, Lane 3-30µM curcumin, Lane 4- 100 Basepair ladder (Bangalore genei).

3.5. Discussion:

Curcumin is the major ingredient of turmeric and has been used as an herbal medicine for years in the Southeast Asia. Recent studies shows that curcumin possess various biological properties in a variety of tumour cells. However, only few studies have been reported on the uptake and localization of curcumin in certain cell lines. In the present study, we have investigated the cytotoxic and cellular uptake of curcumin on the non-neoplastic (3T3, MIO-M1) and RB (Y79, Weri) cell lines. Our results showed that **curcumin inhibited** the **cell proliferation in all these cell lines in a dose and time-dependent manner**,

which showed **more toxicity in RB cancer cell lines when compared with the non-neoplastic cells**. Kunwar et al. also found that addition of curcumin showed higher sensitivity in tumour cells when compared to the non-neoplastic cell lines (Kunwar et al. 2008). Curcumin, being a lipophilic compound, easily interacts with the cellular components like the cell membrane and easily gets transported inside the cell (Kunwar et al. 2006). Our study also showed that the sub-cellular fraction of all the cell lines showed **more accumulation of curcumin in the membrane of RB cells followed by its presence in the cytoplasm and nucleus**. The cellular uptake and the fluorescence spectrum study also showed that the uptake **of curcumin is more in the RB cells compared with the non-neoplastic cell lines**. The higher uptake of curcumin seen more in tumour cells than the non-neoplastic cell may be due to factors like difference in cell size, its structure and protein composition. Kunwar et al. also reported accumulation of curcumin is seen more in the MCF-7 breast cancer cell line than the NIH3T3 fibroblast cells (Kunwar et al. 2008).

In this study, we also observed significant morphological changes and **intranucleosomal fragmentation of DNA in RB cancer cells** treated with curcumin and no change in the non-neoplastic cell lines. Syng-ai et al. also showed DNA fragmentation in MCF-7 and MDA-MB treated cells and not in normal rat hepatocytes (Syng-ai et al. 2004). Hence, our findings showed that **curcumin possesses an anti-cancer property only in RB cancer cells, without causing damage to the non-neoplastic cell lines**.

3.6 Chapter summary

- RB tumour cells show preferentially more uptake of curcumin compared to the non-neoplastic cell lines.
- Fluorescence spectra of cellular curcumin showed higher fluorescence intensity in RB cell lines compared to the non-neoplastic cells.
- Cellular fractionation studied showed localization of curcumin in different compartments of the cells (nucleus, cytoplasm, membrane, mitochondrial) with maximum in the membrane of all the cell lines.
- Cytotoxicity studied showed inhibition in the cell proliferation in the RB cells when compared with the non-neoplastic cells with a therapeutic index value of greater than 1 in both the RB cell lines.

- Cell morphology and DNA fragmentation study showed change in cell size and shape with internucleosmal DNA fragmentation in the RB cell lines and no change was observed in the non-neoplastic cell lines.

CHAPTER 4: INDUCTION OF APOPTOSIS BY CURCUMIN IN HUMAN RB CELLS THROUGH MITOCHONDRIAL MEDIATED PATHWAY

4.1 Introduction

Retinoblastoma (RB) is the most common primary intraocular tumour of childhood (Vogel et al. 1979). Surgery, chemotherapy and radiation have been used for the treatment of RB. Chemotherapy is the treatment of choice following enucleation in patients with optic nerve and choroid invasion and orbital extension (Krishnakumar et al. 2004). Although chemotherapy is a common therapeutic strategy, its use has been toxic to normal tissues and limits their use (Walker et al. 1986). Recent studies show that many naturally occurring plant-derived compounds have been identified that can inhibit, retard, or reverse the process of multistage carcinogenesis in various cancers (Newman et al. 2003).

Curcumin (1,7-bis (4-hydroxy-3-methoxyphenyl)-1,6-heptadiene-3,5-dione]), is a naturally occurring phenolic compound extracted from the rhizomes of the plant C*urcuma longa* (Campbell et al. 2005). It has been used as an herbal medicine on the skin for wounds, blistering diseases, parasitic infection, acne and several other conditions (Chainani-Wu et al. 2003). Several studies have shown that curcumin possesses various properties like antibacterial, antitumor, anti-cancer and antioxidant activity (Chattopadhyay et al. 2004). It inhibits proliferation and induces apoptosis in cancer cells of breast, lung, pancreas, bladder, cervix, head and neck, bone marrow, brain, kidney, prostate, ovary and skin (Aggarwal et al. 2006; Dorai et al. 2001; Moragado et al. 2001; Anto et al. 2002; Chakraborty et al. 2006; Chen et al. 2006; Dorai et al. 200).

Apoptosis is a tightly regulated mechanism by which cells undergo programmed cell death in various physiological and pathological situations (Reuter et al. 2008; Fulda et al. 2004). Killing of tumour cells using anticancer drugs, γ-irradiation or immunotherapy has been shown to mediate apoptosis in target cells (Debatin et al. 2004). Mostly cancer cells become resistant to apoptosis, with the loss of pro-apoptotic signals and gain of anti-apoptotic protein thereby leading to tumourigenesis (Kabore et al. 2004). Curcumin being a hydrophobic molecule can enter the lipid bilayer and induce structural and functional changes of the cellular membrane, such as membrane blebbing and phosphotidylserine exposure (Jaruga et al. 1998). Induction of apoptosis by curcumin involves various

mechanisms which include up-regulation of Bax (Pal et al. 2001), activation of caspases (Bush et al. 2001)' generation of free radicals (Khar et al. 1999) and impairment of the ubiquitin proteasome pathway (Jana et al. 2004). Curcumin also suppresses the activation of nuclear factor kappa B (NF-kB), signal transducer and activator of transcription 3 (STAT3) and the AKT pathway. It has been also shown to down-regulate the expression of various regulated genes of NF-kB, including B-cell lymphoma 2 (Bcl2), cyclooxygenase (COX2), matrix metallopeptidase (MMP-9), tumor necrosis factor (TNF), cyclinD1, and adhesion molecules (Aggarwal et al. 2006).

Based on the previous reports, it was suggested that curcumin could inhibit cell proliferation and induces apoptosis. The facts that no apoptosis studies of RB cell line is performed, to our knowledge, to this date. Thus in the present study we demonstrate the effect of curcumin on RB cells *in vitro*, and investigated the possible underlying molecular mechanisms.

4.2 Objectives:

- To determine the effect of curcumin on the viability of two human RB cell lines (Y79 and Weri) in a dose and time dependent manner.
- To study the effect of curcumin on the mitochondrial membrane potential (MMP) in RB cell lines
- To study the effect of curcumin on the apoptosis related proteins (Bax, Bak, Bcl-2, cytochrome c) in RB cell lines
- To study the effect of curcumin on the activity of caspase 3 and 9 in RB cell lines.

4.3. Methods

4.3.1 Cytotoxicity assay by MTT

RB cells (Y79 and Weri) were seeded into 96-well plate at density of $5x10^3$cells/well and incubated overnight. Next day, medium containing varying concentrations of curcumin from 5-100µM (vehicle control 0.5% DMSO) was added and cells were incubated for 24-96h, after which the cell viability was measured using MTT. Thereafter, 10µl MTT (5mg/ml in PBS) was added and incubated for 4h. Cells that are viable form formazan crystals by active

mitochondria respiration. Crystals were dissolved with 100µl DMSO, after which the reading was taken spectrophotometrically at 570nm using an ELISA reader. Percentage cell viability was calculated as test absorbance/ control absorbance x 100.

4.3.2 Examination of apoptosis by 4,6-diamidino-2-phenylindole dihydrochloride (DAPI) staining

RB cells were plated in a 12-well plate at a density of 1x 10^4cells/well. After 24h, cells were treated with or without various concentration of curcumin (0, 10, 30 and 50 µM) for 48h. The cells were collected, washed with ice-cold phosphate buffer saline (PBS) and fixed with methanol: acetic acid (3:1) for 30 min at RT. Cells were stained with DAPI (1µg/ml) for 20 minutes at RT and observed under Nikon TS100 phase-contrast fluorescent microscope mounted with Retiga Exi monochrome cooled CCD camera (Mosmann et al. 1983).

4.3.3 Annexin V fluos staining by flow cytometry

RB cells (1x10^5cells/cm^2) were plated in 12-well plate for overnight at 37^0C. After overnight incubation, the cells were treated with different concentrations of curcumin (10, 30 and 50µM) and incubated for 48h. AnnexinV-fluos staining was performed using an AnnexinV-fluos apoptosis detection kit (Roche, Indianapolis) in accordance with the manufacturer's instructions. In brief, treated cells were centrifuged, re-suspended in 100µl of Annexin-V-Fluos reagent and incubated for 10-15min at RT in the dark. After incubation period, flow cytometry analysis was immediately performed. Data acquisition and analysis were performed by a FACScalibur flow cytometer using Cell Quest software. Cells that were Annexin V (-) and PI (-) were considered viable cells whereas cells that were Annexin V (+) and PI (-) or Annexin V (+) and PI (+) were considered early stage or late-stage apoptotic cells, respectively.

4.3.4 Mitochondria membrane potential assay

RB (1x10^5) cells were incubated with 2µM rhodamine 123 for 10 minutes at 37^0C. After 2h, the cells were incubated with 50µM curcumin for different time intervals (30min, 60min, 2h and 4h). After incubation period, the cells were washed twice with PBS and finally re-suspended in 1ml PBS. The fluorescence

intensity of the control and curcumin treated RB cells were measured at an excitation wavelength 480nm and an emission wavelength 530nm in a fluorescence spectrophotometer. The fluorescence intensity was used as an arbitrary unit representing the mitochondria transmembrane potential (Lin et al. 2005).

4.3.5 Effect of curcumin on apoptosis related proteins by semi-quantitative RT-PCR

RB cells ($1x10^5$cells/cm^2) were plated in 12-well plate and after overnight incubation at 37^0C the cells were treated with 0, 10, 30 and 50µM curcumin for 48h. Total RNA from each sample was extracted using Trizol reagent (Invitrogen, USA), following the manufacturer's instructions. Turbo DNase treatment was done to remove endogenous DNA contamination. For single-strand cDNA synthesis, 2µg of total RNA from each sample was reverse transcribed (sensiscript, Qiagen) at 37^oC for 1h using sensiscript reverse transcriptase. PCR amplification was carried out in an Eppendorf PCR system using the gene specific primers (**Table 4.1**), **Bax, Bak and Bcl-2:** 95^oC for 45sec, 69^oC for 1min and 72^oC for 1 min and **GAPDH:** 94^0C-5 min, 94^0C-45sec, 63^0C-45sec, 72^0C-45sec and final elongation 72^0C-2min. Numbers of cycles were 35 for all the reaction and glyceraldehydes-3-phosphate dehydrogenase (GAPDH) gene was used for normalization of the results. PCR products were fractionated by electrophoresis using 2% agarose gel containing 0.5% Ethidium bromide.

4.1 Primers used for quantitative reverse transcriptase polymerase chain reaction (qRT-PCR)

Gene	Primer sequence	PCR Product size
Bcl-2	**FP** 5'-AGATGTCCAGCCAGCTGCACCTGAC-3'	366bp
	RP 5'-AGATAGGCACCCAGGGTGATGCAAGCT-3'	
Bax	**FP** 5'-AAGCTGAGCGAGTGTCTCAAGCGC-3'	365bp
	RP 5'-TCCCGCCACAAAGATGGTCACG-3'	
Bak	**FP** 5'-TCCAGATGCCGGGAATGCACTGACG-3'	1191bp
	RP 5'- TGGTGGGAATGGGCTCTCACAAGG-3'	
GAPDH	**FP** 5'-GCCAAGGTCATCCATGACAAC-3'	498bp
	RP 5'-GTCCACCACCCTGTTGCTGTA-3'	

4.3.6 Effect of curcumin on apoptosis related proteins by western blot

RB cells ($1x10^5$cells/cm^2) were plated in 12-well plate and after overnight incubation at 37^0C the cells were treated with 0, 10, 30 and 50µM curcumin for 48h. The cells were collected and lysated with 100µl RIPA buffer and sonicated at 50-60 cycles/30sec. After sonication, the protein concentration in the lysate was measured by the Lowry method **(**Lowry et al. 1951**).** The lysates (50µg) were run on 10% sodium dodecyl sulphate-polyacrylamide gel electrophoresis (SDS-PAGE) (BioRad, Hercules, CA) and then electrophoretically transferred onto the nitrocellulose membranes (Amersham) at 100V for 1h at 4^0C. Transfer of proteins was checked by staining the membrane with 0.1% Ponceau stain (Sigma) and non-specific sites were blocked with 5% non-fat dry milk for 1h. The blots were incubated with primary antibody solution (Bak, Bcl-2 and Bax procured from Santa Cruz Biotechnology, Inc. (CA, USA) was diluted at 1:1000 for overnight. After washing with TTBS the blots were incubated with the respective HRP-conjugated secondary antibody (Pierce, Italy) diluted 1:2000 for 2h at RT. After further washing with TTBS, the immunoreactive bands were visualized using an enhanced chemiluminescence (ECL) kit (Amersham Life Sciences). To normalize band intensity, the membranes were probed with β-actin antibodies (Sigma Aldrich, USA).

4.3.7 Measurement of cytochrome c release

Cytosolic extracts of the cells were prepared as described (Diaz et al. 2003). RB cells were collected after treatment with curcumin (0, 10, 30 and 50µM) for 48h and mixed with 100µl of lysis buffer, followed by centrifugation at 12,000rpm for 30 min at 4^0C. 100µg of protein was electrophoresed on a 12% SDS-PAGE and transferred onto nitrocellulose membrane. Cytochrome c was detected using polyclonal anti-cytochrome c antibody (1:300 dilutions for overnight). After washing, anti-rabbit horse radish peroxidase (HRP) conjugate antibody was added and incubated for 2h. Protein bands were visualized using an ECL kit.

4.3.8 Measurement of caspase 3 and 9 activity

RB cells ($1x10^6$ cells/cm^2) were plated in 12 well plates and treated with different concentrations of curcumin for 48h. Cells were washed with ice-cold PBS and resuspended in a buffer containing 5mmol/L Tris (pH 8), 20mmol/L

ethylenediamine tetraacetate (EDTA) and 0.5% Triton-X 100 on ice for 30 min. After incubation, lysates were centrifuged for 5 min at 13,000rpm and the clear supernatant was taken for caspase activity. Reactions were carried out with 50µg of protein, 20mmol/L4-(2-hydroxyethyl)-1-piperazineethanesulfonic acid (HEPES) (pH 7), 10% glycerol, 2mmol/L dithiothreitol and 200 µmol/L *N*-acetyl-Asp-Glu-Val-Asp (DEVD)-*p*NA substrate (caspase 3) and Leu-Glu-His-Asp (LEHD)-pNA substrate (caspase 9), in the presence and absence of caspase 3(Ac-DEVD-CHO) and 9(Ac-LEHD-CHO) inhibitor, respectively. Reaction mixtures were placed into a flat-bottomed microtiter plate and read with a 405 nm filter using a microtiter plate reader. Caspase activities were detected by measuring the proteolytic cleavage of the coloured substrates.

4.3.9 Statistics

Results are expressed as mean ± standard deviation. Data were analyzed by a one-way ANOVA (SPSS 11.0) and $p<0.05$ were considered to be statistically significant.

4.4. Results

4.4.1 Cytotoxic effect of curcumin on RB cells

The toxic effect of curcumin on RB cells after 24-96h treatment was assessed by MTT assay. The IC_{50} of curcumin was 30, 25 and 20µM at 48, 72 and 96h, respectively which cause 50%, cell death in Y79 cells. Similarly in Weri cells the IC_{50} was found to be 25, 17.5 and 15, respectively at 48, 72 and 96h respectively (**Figure 4.1a & b)**.

Figure 4.1a: MTT assay for curcumin in Y79 cell line

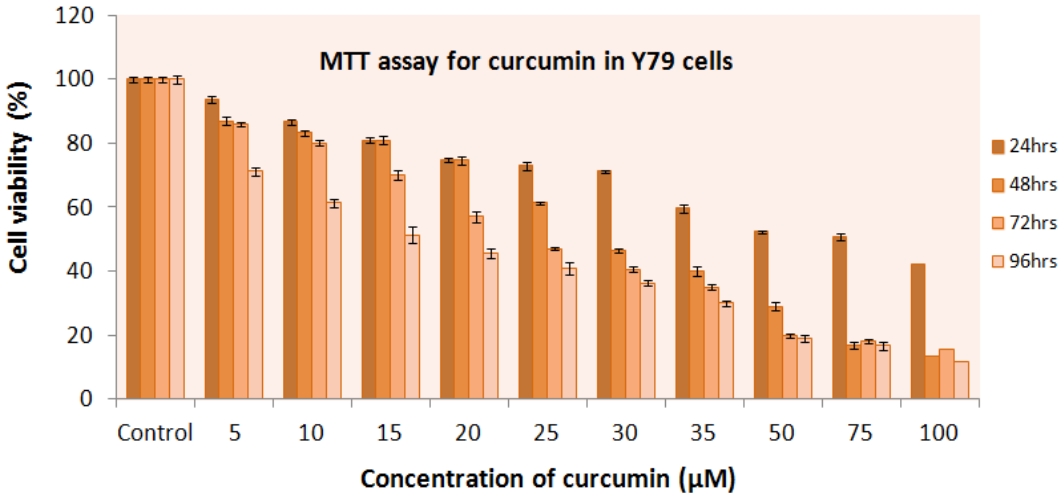

Figure 4.1b: MTT assay for curcumin in Weri cells

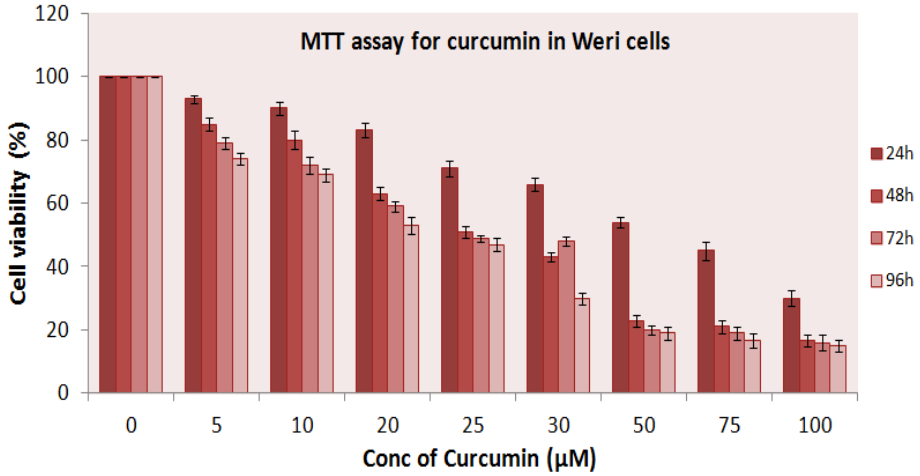

Fig 4.1a&b. Effect of curcumin on cell viability of human RB cell lines: RB cells (Weri and Y79) were plated on 96 well plates; cells were treated with different concentrations of curcumin for 24, 48, 72 and 96h. The cell viability was then determined by MTT assay. Experiments were done in triplicates. Values represent mean (± SD) cell viability as a percentage of untreated control samples.

4.4.2 Curcumin-induced apoptosis examined by DAPI staining

Apoptosis was detected by the DAPI staining method after 48h of exposure to curcumin followed by fluorescence microscopy. As shown in (**Figs. 4.2a and b,** curcumin induced apoptosis in RB cells compared with control cells and this

effect was in a dose-dependent manner. Percentage increase in apoptotic cells is represented as bar diagram in both the cell lines (**Figure 4.2c**)

Figure 4.2a: DAPI stain in Y79 cells

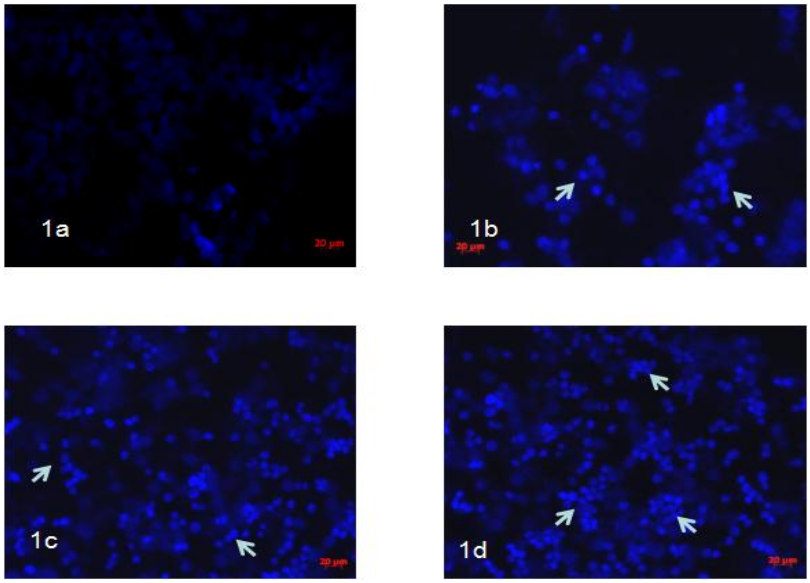

Figure 4.2b: DAPI stain in Weri cells

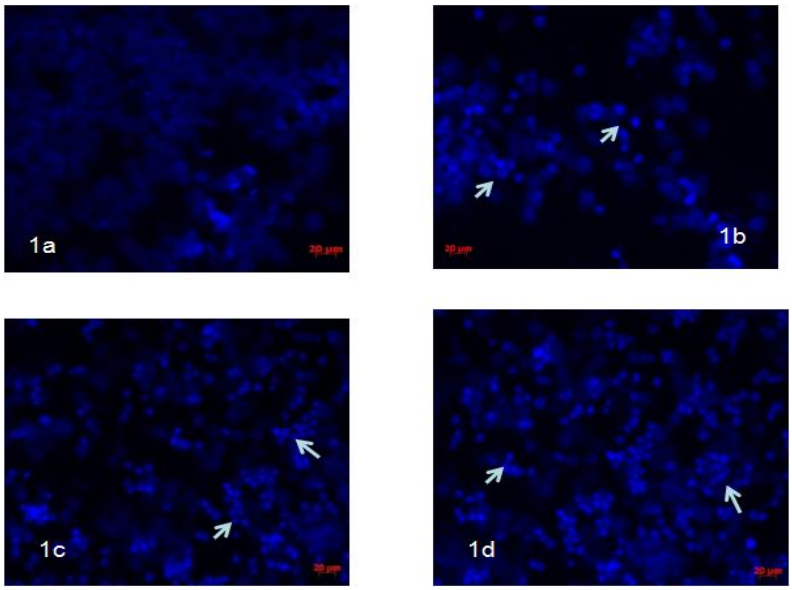

Figure 4.2c: Percentage increase in apoptotic cells in both Weri & Y79 cells

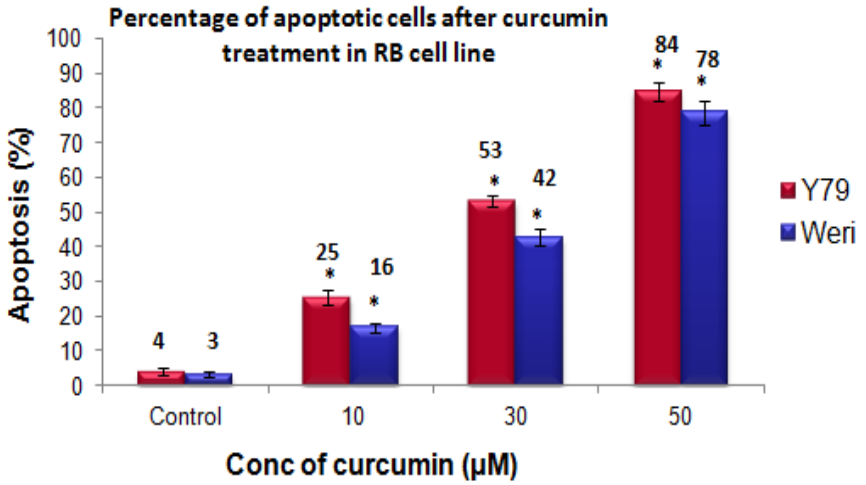

Fig.4.2. Effect of curcumin on cell nuclear morphology: **a**) Y79 **b)** Weri cells were treated with different concentration of curcumin for 48h and untreated cells served as control (1a-control, 1b-10µM curcumin, 1c-30µM curcumin and 1d-50µM curcumin). Arrows indicate the apoptotic cells with condensed and fragmented nuclei. Nuclear staining was examined under a fluorescence microscopy. **c)** Cells were counted in 5 different fields and the mean values of triplicate samples expressed in percentage are shown.

4.4.3 Effect of curcumin treatment on RB cells apoptosis

The effect of a 48h curcumin treatment on RB cells apoptosis was obtained by Annexin V-fluos/PI staining using flow cytometry analysis (**Fig. 4.3A&B)**. The number of cells corresponding to the early or late apoptosis was increased at 30 and 50µM concentration of curcumin but was not observed at 10µM concentration. Further, quantitation of apoptotic cells further demonstrated that 30 and 50µM curcumin resulted in significantly increased number of apoptotic cells **(Table 4.2**).

Figure 4.3a: Annexin stain in Y79 cells

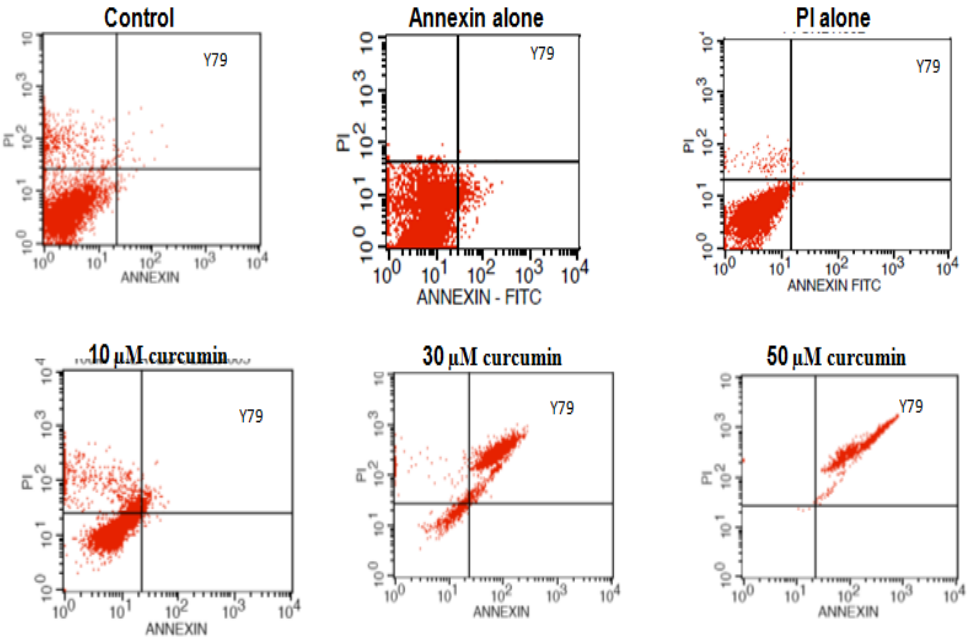

Figure 4.3b: Annexin stain in Weri cells

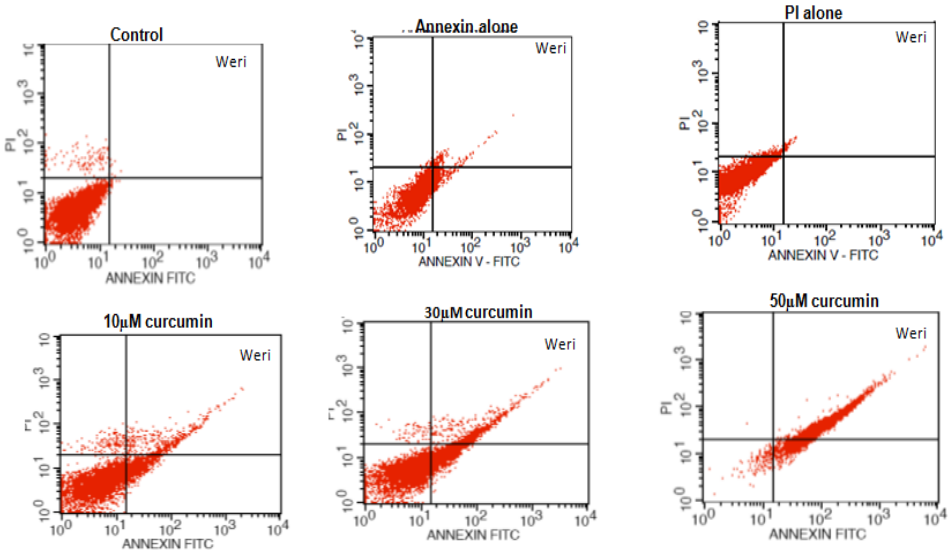

Fig.4.3. Annexin-V-fluos staining in RB cells: a&b) RB cells were treated with different concentration of curcumin (10,30 and 50 µM) for 48h, and subsequently stained with fluorescein-conjugated Annexin V and propidium iodide and analyzed by flow cytometry. Atleast 10,000 cells were analyzed per sample, and quadrant analysis was performed. The cells falling in the right upper square in each scatter diagram are considered as the apoptotic cells.

Table 4.2

Effect of curcumin in inducing apoptosis of Y79 RB cells by flow cytometry

Quadrant (%Total)	Control	10µM	30µM	50µM
UL (Necrotic)	15.45	17.54	3.04	0.20
UR (Late apoptotic)	0.31	2.83	88.64	99.7
LL (Live cells)	83.98	79.24	8.26	0.1
LR (Early apoptotic)	0.26	0.39	0.07	0.0

Effect of curcumin in inducing apoptosis of Weri RB cells by flow cytometry

Quadrant (%Total)	Control	10µM	30µM	50µM
UL (Necrotic)	1.86	0.02	1.11	2.47
UR (Late apoptotic)	0.15	82.0	12.95	8.35
LL (Live cells)	97.59	2.64	58.51	72.33
LR (Early apoptotic)	0.39	15.25	27.44	16.84

4.4.4 Effect of curcumin on loss of mitochondrial membrane potential ($\Delta\Psi_m$) of RB cells

In order to understand the mechanism of curcumin-induced apoptosis in RB cells, we used Rhodamine 123 to acquire the $\Delta\Psi_m$ by examining its fluorescent intensity. As shown in **Figure 4.4** there was a time dependent decrease of Rhodamine 123 fluorescence after treated with curcumin, compared with the control group. This indicates that curcumin was able to induce $\Delta\Psi_m$ disruption in RB cells **Figure 4.4**

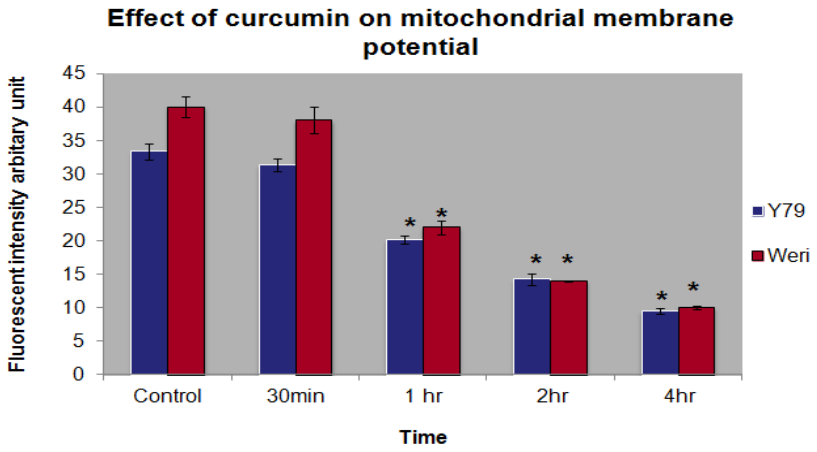

Figure 4.4: Effect of curcumin on the mitochondrial membrane potential of RB cell line. RB cells were treated with and without curcumin at different time intervals, and then incubated with 2µM Rhodamine 123. Experiments were done in triplicates. *p<0.05 was considered as statistically significant.

4.4.5 Effect of curcumin treatment on RB cells Bax, Bak and Bcl-2 mRNA and protein expressions

To investigate the cellular mechanism underlying curcumin-induced apoptosis in RB cells, we analyzed the expression of Bcl-2, Bax and Bak mRNA expression following 48h exposure to various concentration of curcumin by qRT-PCR. Pro-apoptotic gene Bax and Bak mRNA expression significantly increased whereas Bcl-2 mRNA expression significantly decreased after curcumin exposure (**Figure 4.5A**). The result of western blotting also showed similar results where Bax and Bak protein expression was increased and Bcl-2 level was decreased in response to curcumin treatment (**Figure 4.5B**). The Bax/Bcl-2 and Bak/Bcl-2 ratio was significantly increased in cells exposed to 10, 30 and 50µM curcumin ($p<0.05$).

4.5A) mRNA expression of apoptosis related protein in RB cell line

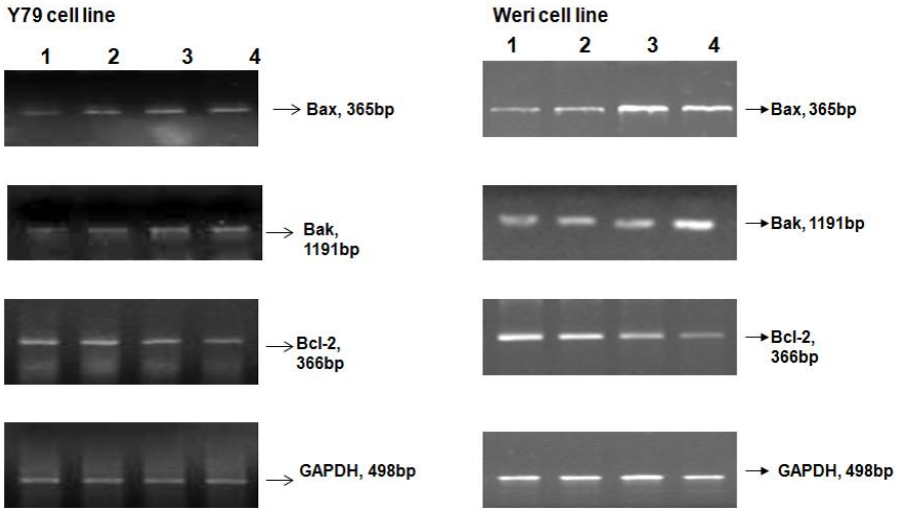

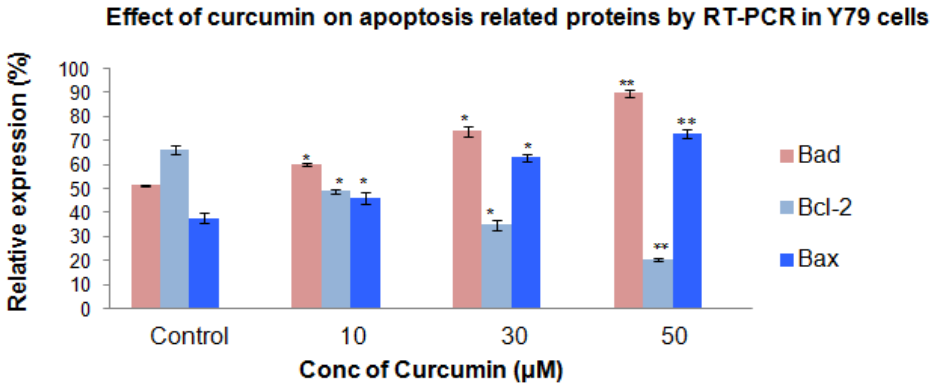

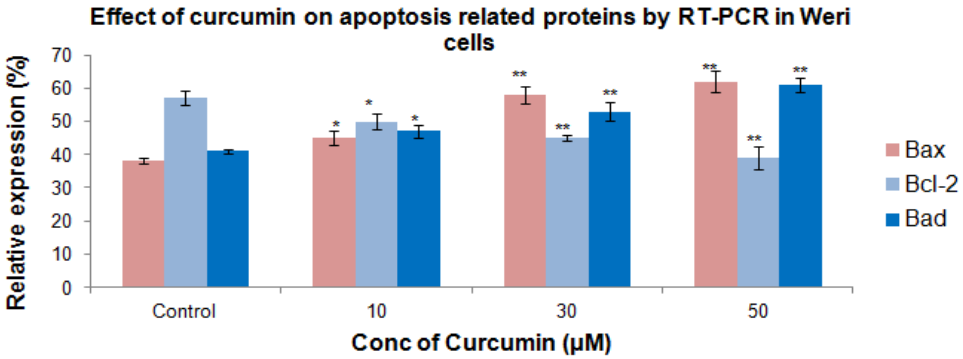

Figure 4.5A: Effect of curcumin treatment on mRNA expression of Bax, Bak and Bcl-2 in Weri and Y79 cells: RB cells were treated with different concentration of curcumin for 48h. After curcumin treatment cells were harvested for RNA isolation. RT-PCR was performed as described in methods. PCR products were resolved on a 2% agarose gel and visualized using ethidium bromide. GAPDH served as an internal control. The mRNA levels of Bax, Bcl-2 and Bak quantified by densitometric analysis of the three autoradiographs. *p<0.05 and **p<0.01 vs control.

4.5B) Protein expression of apoptosis related protein in RB cell line

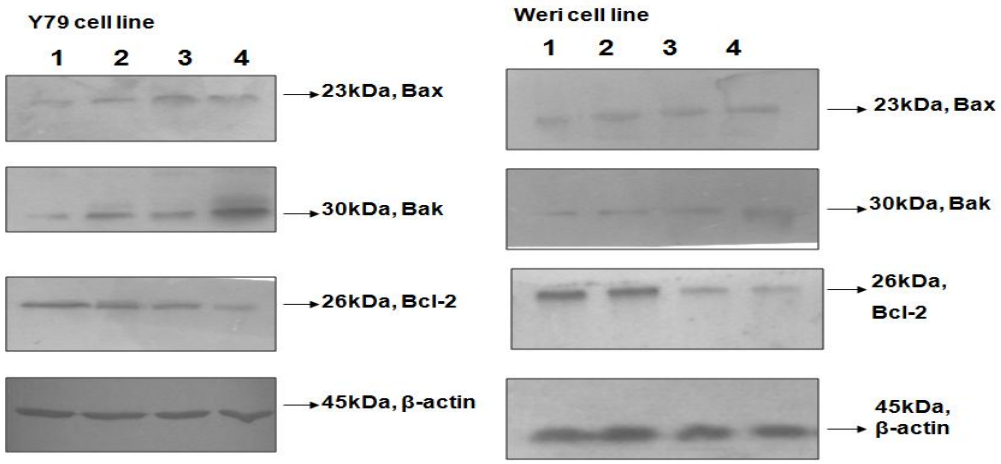

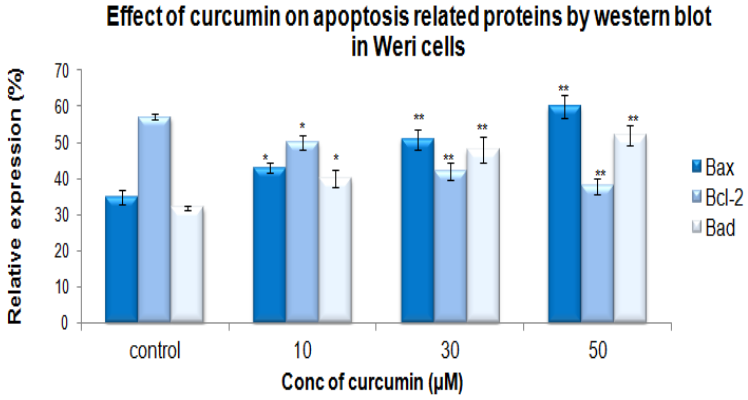

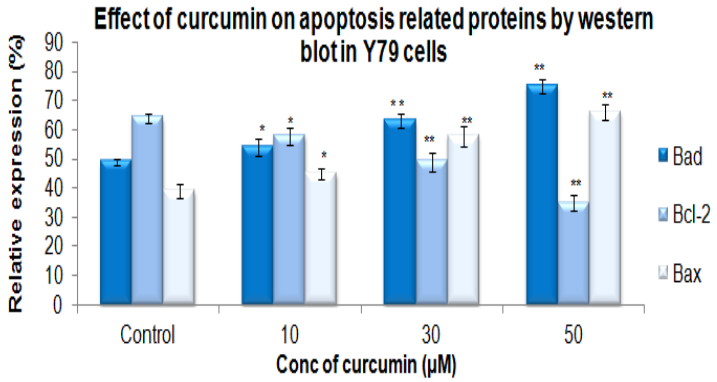

Figure 4.5B: Effect of curcumin treatment on protein expression of Bax, Bak and Bcl-2 in Y79 & Weri cells: RB cells were treated with different concentration of curcumin for 48h. After curcumin treatment cells were harvested for protein extraction. Cell lysates were subjected to immunoblot analysis. Equal amounts of total protein (100µg) were resolved on 12% SDS-PAGE and β-actin was used as an internal control. The protein levels of Bax, Bcl-2 and Bak quantified by densitometric analysis of the three autoradiographs. *$p<0.05$ and **$p<0.01$ vs control.

4.4.6 Effect of curcumin on cytochrome c release

The release of cytochrome c from mitochondria is the key event in apoptosis induced by various stimuli. In order to analyze the involvement of mitochondria in the apoptosis induced by curcumin, the cytosolic level of cytochrome c was studied. The release of cytochrome c was significantly increased in RB cells incubated with 10-50µM concentration of curcumin (**Fig. 4.6**).

Figure 4.6: A) Y79 and B) Weri cells

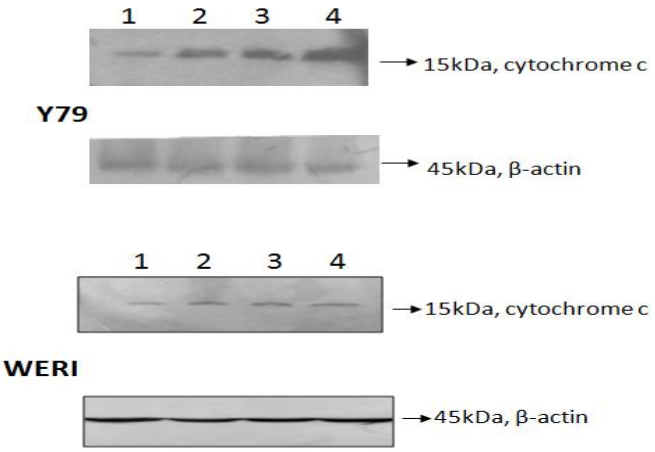

Figure 4.6: Effect of curcumin on release of cytochrome c: **A)** Y79 **B)** Weri cells were treated with indicated concentration of curcumin for 48h. The cytochrome c in cytosolic fraction was assayed by western blot. Lane 1: Control, Lane 2: 10µM curcumin, Lane 3: 30µM curcumin and Lane 4: 50µM curcumin. Data are presented as the means of triplicate experiments.

4.4.7 Effect of curcumin on caspase 3 and 9 activities in RB cells

To examine whether caspase 3 and 9 activity is involved in curcumin induced apoptosis in RB cells. In cells treated with different concentration of curcumin (10, 30, 50 µM) for 48h, the activity of caspase 3 and 9 was significantly increased, moreover the activity was decreased in the presence of caspase-3 (Ac-DEVD-CHO) and caspase 9 (Ac-LEHD-CHO) inhibitor in RB cells. These results suggest that caspase-3 and 9 is involved in curcumin-induced apoptosis in both the RB cells (**Figure 4.7a,b,c,d**).

Figure 4.7a

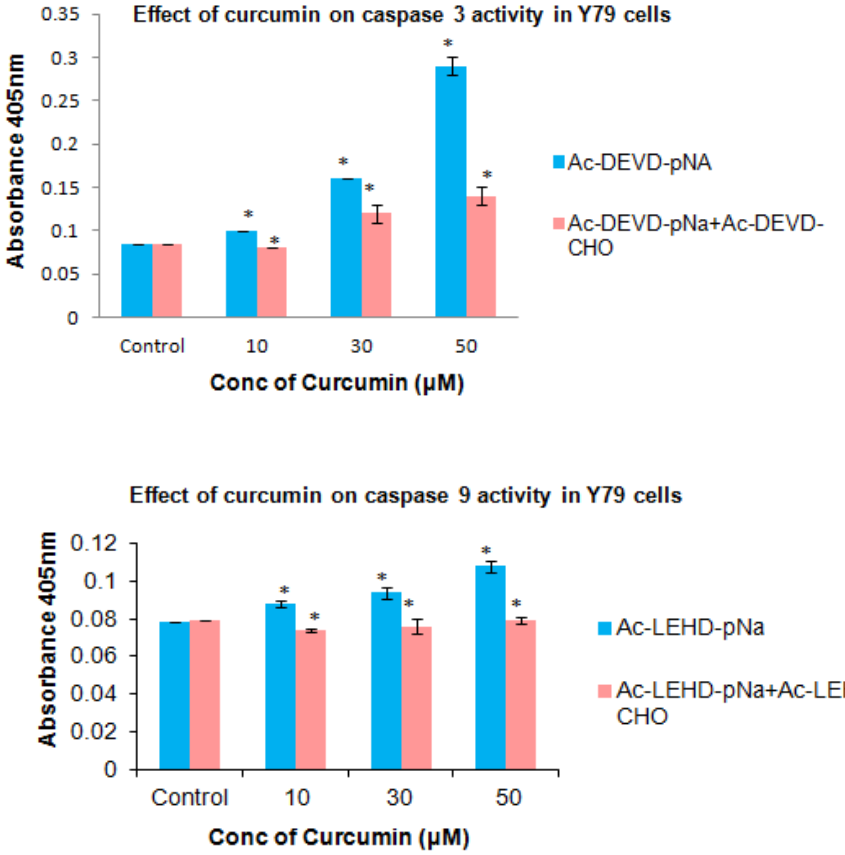
Effect of curcumin on caspase 3 activity in Y79 cells
Absorbance 405nm
0.35
0.3
0.25
0.2
0.15
0.1
0.05
0
Control
10
30
50
Conc of Curcumin (µM)
Ac-DEVD-pNA
Ac-DEVD-pNa+Ac-DEVD-CHO
Effect of curcumin on caspase 9 activity in Y79 cells
Absorbance 405nm
0.12
0.1
0.08
0.06
0.04
0.02
0
Control
10
30
50
Conc of Curcumin (µM)
Ac-LEHD-pNa
Ac-LEHD-pNa+Ac-LEHD-CHO

Figure 4.7b

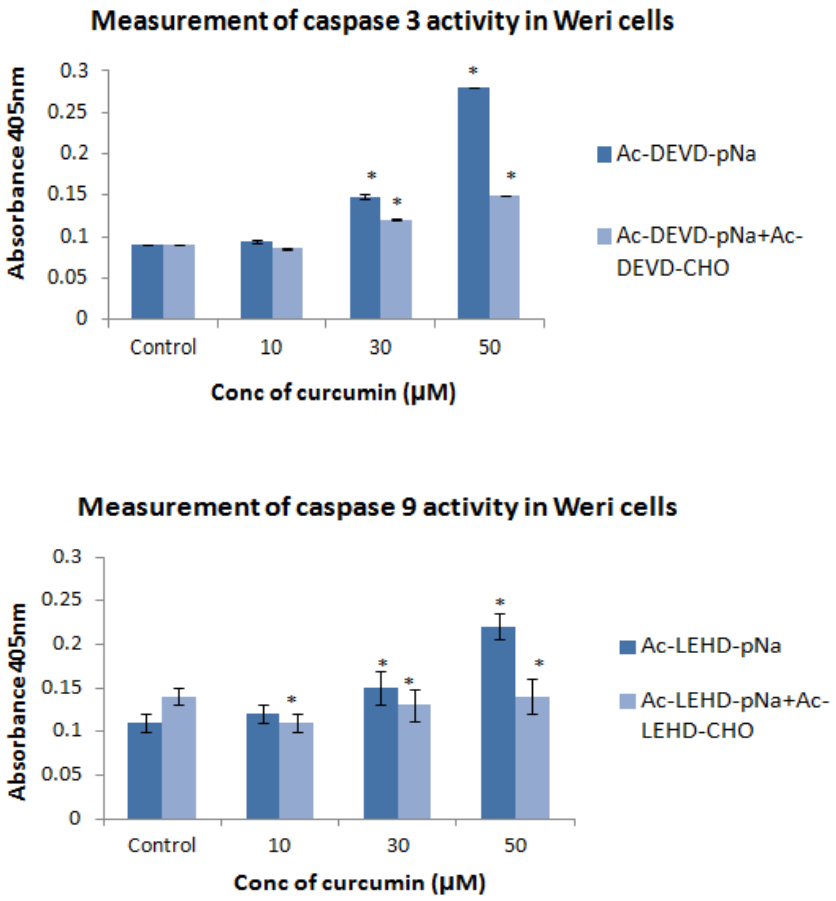

Figure 4.7: Effect of curcumin on caspase 3 and 9 activity in RB cells: **a)** Y79 and **b)** Weri cells were treated with different concentration of curcumin (10, 30 and 50µM) and caspase activity was determined by incubation of 50µg protein with DEVD-pNA substrate (caspase3) and LEHD-pNa substrate (caspase9) and with its respective inhibitor. Data are mean ±SD from three separate experiments. *p<0.05 was considered as statistically significant.

4.5 Discussion

One of the major modes of curcumin anti-cancer effects may be through activation of apoptosis. Many studies have demonstrated that curcumin; a well-studied cytotoxic compound induces apoptosis in various human cancer cells (Kuo et al. 1996; Shi et al. 2006; Lu et al. 2010**)**. However, there is no information available on the influence of curcumin on RB and especially on apoptosis.

Curcumin-induced apoptosis was observed by the changes in nuclear morphology by DAPI staining in RB cells. The two major signalling pathways involved in apoptosis are the mitochondria and death receptor pathways (Lu et al. 2009).

Many studies have shown that the loss of mitochondrial membrane potential ($\Delta\Psi_m$) is a hallmark for apoptosis (Mantymaa et al. 2000**)**. Depolarization of the $\Delta\Psi_m$ is observed in some anticancer compounds thereby inducing apoptosis in cancer cell lines (Kim et al. 2006). Our data demonstrated **reduced $\Delta\Psi_m$ as indicated by Rhodamine 123 (fluorescent dye) following treatment with curcumin at different concentrations**. This indicates that curcumin-induced apoptosis in RB cells is related to the collapse of the $\Delta\Psi_m$. The mitochondrial release of cytochrome c plays an important role in the induction of apoptosis. It is located in the space between the inner and outer mitochondrial membranes. During apoptosis, cytochrome c is released from the mitochondria into cytosol where it binds with apoptotic protease activating factor -1(Apaf-1). The cytochrome c/Apaf-1 complex activates caspase-9 which in turn activates caspase-3 thereby leading to cell death. Curcumin induced cytochrome c release has been observed in various cancer cell lines (Rashmi et al. 2003; Cao et al. 2007; Sen et al. 2005). In this study, we also observed that **curcumin markedly increased the release of cytochrome c from the mitochondria to cytosol in human RB cells**.

The Bcl-2 family is composed of anti-apoptotic (Bcl-2 and Bcl-x_L) and pro-apoptotic (Bax and Bad) proteins, which plays an important role in the control of mitochondrial mediated pathway. Over-expression of Bax promotes cell death and Bcl-2 represses the function of Bax thereby leading to cell survival (Miyashita et al. 1994). We assessed the effects of curcumin on Bcl-2 family proteins, and our data showed that curcumin resulted in a significant increase in the Bax/Bcl-2 ratio that is regarded as a driving force for apoptosis in RB cells. Thus, activation of mitochondrial pathway by curcumin may be through modulation of Bax and Bcl-2 expression, leading to RB cell death. Many anti-cancer agents have been shown to cause apoptotic cell death through activation of caspase. Caspases are a family of cysteine proteases that have been shown to be activated during apoptosis in many cell systems. They play critical roles in both the initiation and the execution of apoptosis (Cohen et al. 1997). Caspase can be activated by different stimuli such as mitochondrial and receptor pathway involving caspase 9 (Park et al. 2007). In our study we also found **increase in the activity of caspase 3 and 9 after curcumin treatment in RB cells**.

In summary, apoptosis induced by curcumin was associated with the release of cytochrome c, caspase activation, up-regulation of Bax, Bad and down-regulation

of Bcl-2 levels, in human RB cells. Thus, curcumin-induced cell death involves the mitochondrial pathway, which then stimulated the molecular cascade of apoptosis.

4.6 Chapter summary

- Curcumin inhibited cell proliferation in a dose and time-dependent manner in both the RB cancer cell lines
- Annexin V fluos staining showed increased in the percentage of apoptotic cells with increase concentration of curcumin treatment.
- An increase in the expression of pro-apoptotic factor Bax, Bak, cytochrome c and a decrease in the expression of anti-apoptotic protein Bcl-2 were observed after curcumin treatment.
- Curcumin treated RB cells showed decrease in the membrane mitochondrial potential in RB cell lines.
- Curcumin also decreased the activity of caspase 3 and 9 in a dose-dependent manner.
- These data suggest that curcumin induce apoptosis signalling in human RB cells by mitochondrial and through regulation of apoptosis-related proteins (**Figure 4.8**).

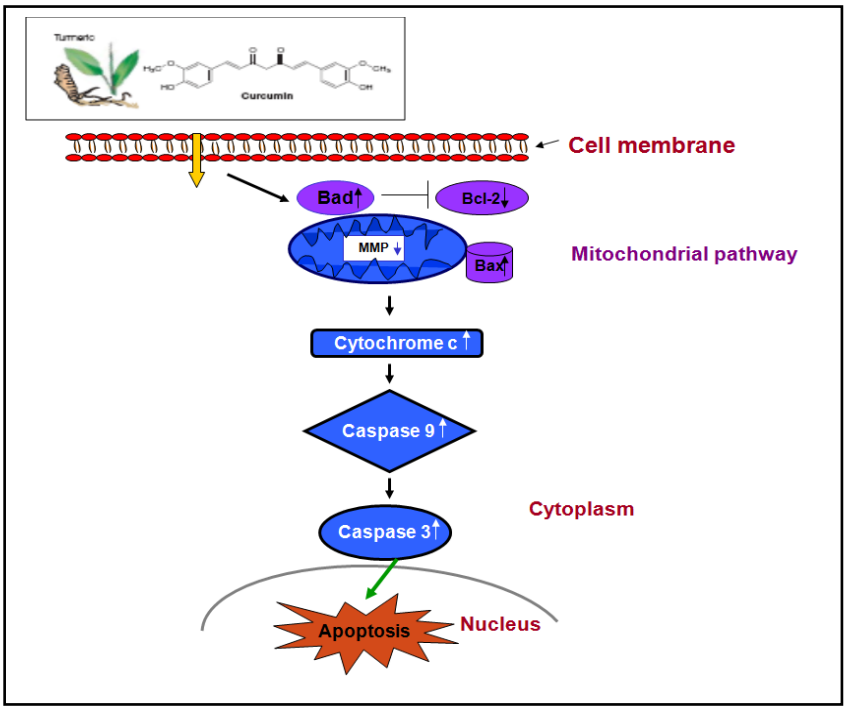

Figure 4.8: Schematic representation of curcumin inducing apoptosis through mitochondrial mediated pathway in RB cell lines

CHAPTER 5: EXPRESSION PROFILE OF GENES REGULATED BY CURCUMIN IN RB CELL LINE

5.1 INTRODUCTION

Retinoblastoma (RB) is the most common intraocular tumor of childhood. It is caused by mutations in the RB gene, which functions as a tumor suppressor (Dunn et al. 1988). RB patients who present with optic nerve and choroid invasion and orbital extension are treated by enucleation followed by chemotherapy (Krishnakumar et al. 2004)**.** Current anticancer therapies, however, are based on modulation of single target which is highly toxic and expensive. Therefore, the current paradigm for cancer treatment is to design drugs that modulate multiple targets (Gupta et al. 2011). The recent recognition of several natural dietary compounds having anti-carcinogenic properties has expanded our pool of potential chemopreventive agents (Sarkar et al. 2006). For example, phytochemical dietary compounds have been evidenced to suppress mammalian inflammatory processes that may otherwise lead to cellular transformation, hyperproliferation and initiation of carcinogenesis (Aggarwal et al. 2006). Curcumin (diferuloylmethane), a naturally occurring polyphenolic compound present in turmeric (*Curcuma longa*), is a potent inducer of apoptosis in various cancer cells **(**Gupta et al. 2011; Singh et al. 1995; Chainani-Wu et al. 2003**)**. Our earlier results have shown that curcumin had an anti-proliferative effect and modulated the expression of a drug resistance protein (lung resistance related protein, LRP) in Y79 RB cells **(**Thiyagarajan et al. 2009).

Recent studies have shown that curcumin has chemo-preventive properties, which are mainly due to its ability to arrest the cell cycle and to induce apoptosis by several pathways **(**Reuter et al. 2008**)**. The anticancer mechanism of curcumin is diverse **(**Chen et al. 2004). Curcumin has been shown to bind directly to numerous signalling molecules, such as transcription factors like activator protein 1(AP-1), NF-κB, SP-1 transcription factor, signal transducer and activator of transcription 3 (STAT3), inflammatory molecules like (tumour necrosis factor –α, cyclooxygenase, myeloid differentiation protein 2), protein kinases (protein kinase C, ErbB2, phosphorylase kinase), carrier protein like (casein, albumin and

fibrinogen) etc, and variation in the gene expression profile can be expected (Gupta et al. 2011; Ramachandran et al. 2005; Jana et al. 2004).

The microarray is a powerful technique for simultaneously monitoring the relative expression of thousands of genes in a single experiment (Xiang et al. 2000). Thus in the present study, we understand the molecular mechanism by which curcumin exerts its effect on RB cells, by determining the deregulated genes in curcumin treated RB cells.

5.2. Objectives:

- To study the expression profiles of genes regulated by curcumin in RB cell lines by microarray
- To validate selected genes from microarray data by real-time quantitative polymerase chain reaction (qRT-PCR)
- To study the effect of curcumin on cell cycle changes in human RB cells
- To study the effect of curcumin on DNA laddering pattern in curcumin treated RB cell lines

5.3. Methods:

5.3.1 Cell cycle analysis

Y79 RB cells were treated with curcumin (5-20µM) for 48h, then harvested by centrifugation, washed twice with ice-cold PBS, and fixed by 70% ethanol at -20^{o}C overnight. The fixed cells were then washed twice with ice-cold PBS and treated with 10 mg/ml RNAse for 30 min at 37^{o}C. Cells were stained with propidium iodide buffer (0.1 mM EDTA, 0.1% Triton X‑100, 50 mg/ml propidium iodide, PBS pH 7.4) for 15 min in the dark at room temperature. Cell cycle distribution was analyzed on a FACS Calibur flow cytometer. Data for 10,000 cells per sample were collected and analyzed using CellQuest software program (BD Biosciences, San Jose, CA).

5.3.2 DNA fragmentation

5×10^4 cells/well were seeded in 24-well plates with 500 µl of culture media and incubated at 37^{0}C for 48 h. The cells were then exposed to different concentration

of curcumin (20 and 30µM) and incubated for 48h. DNA was extracted from the cell pellet using DNA isolation kit (Qiagen, USA) as per the manufacturer's instructions. The isolated DNA was then electrophoresed at 100V in a 2% agarose gel with 0.5 % ethidium bromide. The bands were visualized under UV light with a gel documentation system (BioDoc-It Imaging system, UVP, USA).

5.3.3 cDNA microarray analysis

Y79 RB cells were treated with 20µM curcumin for 48h and untreated cells were considered as control (**Sample treatment at sankara nethralaya**).

After the incubation period, the cells were collected in RNA later solution and sent to Genotypic for RNA extraction and further proceeding with microarray. Total RNA was isolated from control and curcumin treated Y79 RB cells using TRIZOL reagent (Invitrogen) and purified using an RNeasy Mini Kit (Qiagen), combined with DNase treatment following the manufacturer's instructions. The samples for gene expression were labelled using Agilent Quick Amp Kit PLUS.

0.5µg of sample was incubated with reverse transcription mix at 42^{o}C and converted to double stranded cDNA primed by oligodT with a T7 polymerase promoter. The cleaned up double stranded cDNA were used as template for RNA generation. RNA was generated by in vitro transcription and the dye Cy3 CTP (Agilent) was incorporated during this step. The cDNA synthesis and in vitro transcription steps were carried out at 40°C. Labelled cDNA was cleaned up and quality assessed for yield and specific activity.

5.3.4 Hybridization and scanning

The labelled cDNA samples were hybridized onto a Whole Genome Human Array 4x44k. About 1650ng of cy3 labelled samples were fragmented and hybridized. Fragmentation of labelled cDNA and hybridization were done using the Gene Expression Hybridization kit of Agilent. Hybridization was carried out in Agilent's Surehyb Chambers at 65º C for 16 h. The hybridized slides were washed using Agilent Gene Expression wash buffers and scanned using the Agilent Microarray Scanner G Model G2565BA at 5 micron resolution.

5.3.5 Feature extraction

Normalization of the data was done in Gene Spring GX using the recommended one colour Per Chip and Per Gene Data Transformation. One folds and above differentially regulated genes was filtered from the data. Ontology based biological analysis was done using Gene Ontology browser in Gene Spring GX.

Further, biological analysis was performed using Genotype's Biointerpreter web-based biological interpretation tool which was provided by Genotypic technology to us at sankara nethralaya. For microarray analysis, the genes were considered for expression analysis when they satisfied the following two criteria: p≤0.05 and log ratio of atleast 2.0 for up-regulation, and log ratio of 0.5 for down-regulation (keeping a median log ratio of 1 in both biological replicates. Values are expressed as mean ±S.D. of duplicate values.

5.3.6 Quantitative real time polymerase chain reaction (qRT-PCR)

We performed qRT-PCR to validate microarray data. Control and 20µM curcumin treated Y79 cells were investigated by real-time PCR. Total RNA was isolated from the samples and the concentration was checked by Nano-drop method. 0.5µg of total RNA from each sample was reverse transcribed using sensiscript reverse transcriptase (Qiagen, Germany).

Quantification of specific gene expression was performed in triplicate in a 20µl volume reaction mixture (0.5µg of cDNA, specific primer and SYBR green reagent; Invitrogen (Carlsbad, CA, USA) in 96-well plates on a real-time PCR system (Prism 7300; ABI Lab India Instruments, Gurgaon, India). GAPDH was used as an internal control and the detection was carried out by measuring the binding of fluorescence dye SYBR green to double stranded DNA. After cycling, relative quantitation of tested gene cDNA against the internal control was calculated using a ΔC_T method. The difference (ΔC_T) between the mean values in triplicate samples of tested gene cDNA and those of the internal control were calculated by Microsoft excel and the relative quantitation value was defined as $2^{-\Delta C_T} \times K$, where K is a constant).

Table 5.1: mRNA primers used for RT-PCR

Gene	Primer sequence	PCR product

		size
CDKN1A	FP 5′-ATGTCAGAACCGGCTGGGGAT-3′ RP 5′-TAGGGCTTCCTCTTGGAGAAG-3′	230 bp
CCNL2	FP 5’-CGGAATTCGCCACCATGGCGGCGGCGGCG-3’ RP 5’-GCTCTAGACTCCTCCGATGCCTGCTGTGT-3’	310 bp
CCNH	FP 5’-TTCTTCCGAATGATCCAGTCTTTC-3’ RP 5’-TGGCTTAAACACCGAACAGAATT-3’	210bp
LATS1	FP 5'-ACCGCTTCAAATGTGACTGTGATGCCACCT-3' RP 5'-CTTCCTTGGGCAAGCTTGGCTGATCCTCT-3'	280 bp
PAK6	FP5’-CCACAGAACTTCCAGCTCCGTCTCCTCACCTCCTTC-3’ RP 5’- GAAGGAGGTGAGAGGAGACGGACGGAAGTTCTGTGG-3’	325bp
SKP2	FP 5’-CGTGTACAGCACATGGACCT-3’ RP 5’-GGGCAAATTCAGAGAATCCA-3’	199bp
BFAR	FP 5’- GGAGGACATCGTCACCAAGC RP 5’- AGTATTTGACCAGGAACTCTCTCCA	350bp
BAG4	FP 5’- CGGGGTACCC-3’ RP 5’- AAGAATGCGGCCGCTA-3’	210 bp
TP53I3	FP 5’-TCTCTATGGTCTGATGGG-3’ RP 5’- TTGCCTATGTTCTTGTTG-3’	195 bp

5.4 Results

5.4.1 Whole genome microarray analysis of Y79 RB cells after curcumin treatment

The microarray of curcumin treated retinoblastoma cells has revealed differential expression of several categories of genes involved in various cellular processes **(Figure 5.1).** The comphrehensive list of genes differentially regulated on curcumin treatment in retinoblastoma cells is presented in **Appendix III** (**Table 1a and b)**, that play an important role in various biological function. The present oligonucleotide microarray data were submitted to NCBI’S Gene Expression Omnibus and is accessible through GEO series accession number **GSE 17034**.

Figure 5.1

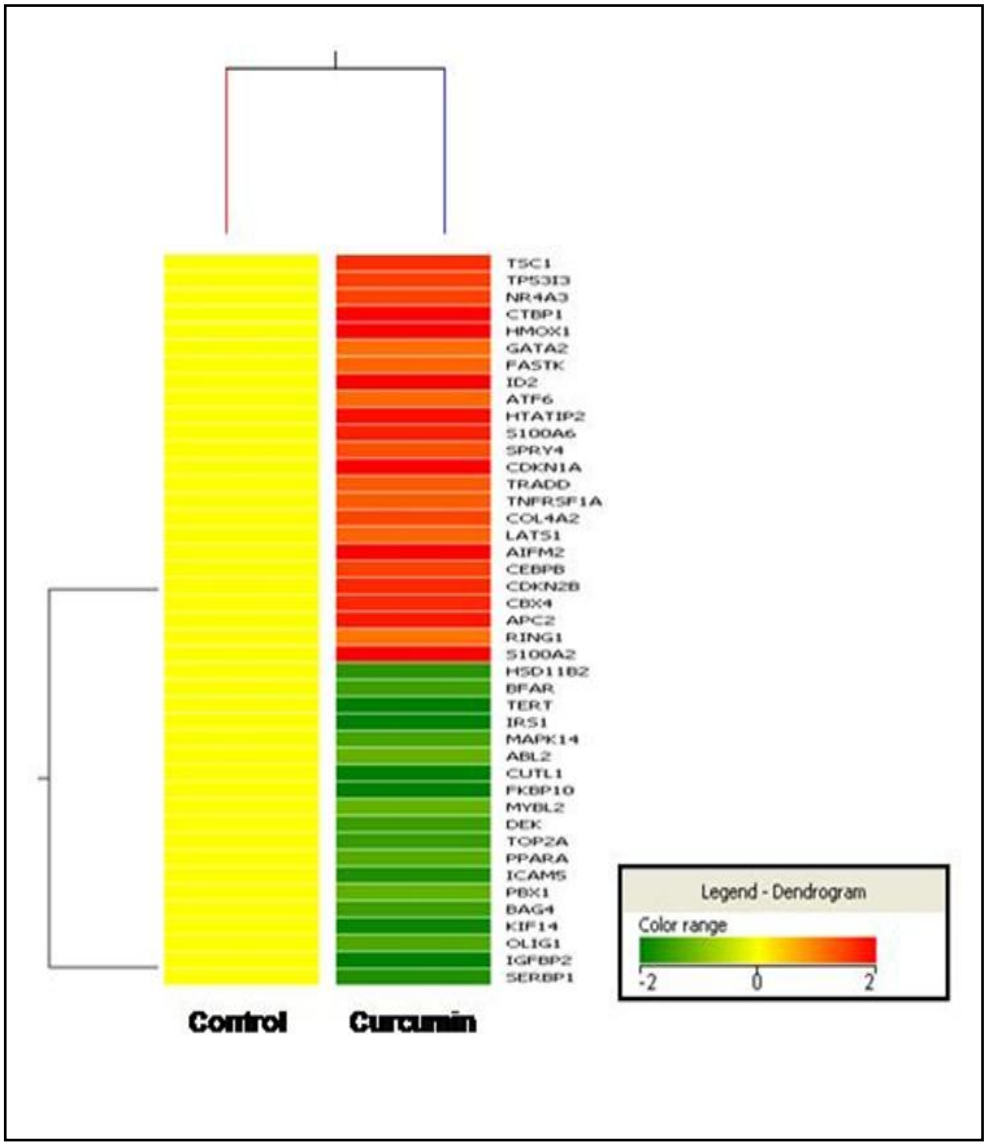

Figure 5.1: Change in gene expression profiling of Y79 RB cells determined by microarray. Heat map represents the overall differential expression of genes in Y79 retinoblastoma cells when subjected to 20µM concentration of curcumin treatment for 72h. Red and green colours represent the up-regulation and down-regulation of genes respectively relative to untreated control Y79 RB cells.

5.4.2 Up-regulated genes in curcumin treated Y79 RB cells

Curcumin treated Y79 RB cells, revealed up-regulated genes involved in various functions:

Apoptosis (22%): TNFRSF1A-associated via death domain (TRADD), Fas-activated serine/threonine kinase (FASTK), Apoptosis-inducing factor, mitochondrion-associated, 2 (AIFM2), insulin-like growth factor binding protein 6 (IGFBP6), interferon regulatory factor 1 (IRF1), Tumor protein p53 inducible protein 3 (TP53I3), serine/threonine kinase 17a (STK17A), tumour necrosis factor (ligand) superfamily (TNFSF13B).

Tumour suppressor genes (22%): Large tumor suppressor, homolog 1 (LATS1), sprouty homolog 4 (SPRY4), arginine-rich, mutated in early stage tumours-like 1 (ARMETL1), Exostosin 1 (EXT1), sema domain, immunoglobulin domain (Ig), short basic domain, secreted, (semaphorin) 3B (SEMA3B), TSPY-like 2 (TSPYL2), Pleckstrin homology-like domain, family A, member 2 (PHLDA2), cytoplasmic FMR1 interacting protein 1 (CYFIP1), slit homolog 2 (SLIT2).

Cell cycle genes (20%): Never in mitosis gene a-related kinase 11 (NEK11), CDKN1A interacting zinc finger protein 1 (CIZ1), ras homolog gene family, member B (RHOB), oxidative stress induced growth inhibitor 1 (OSGIN1), cyclin-dependent kinase inhibitor 1A (CDKN1A), cyclin-dependent kinase inhibitor 2B (CDKN2B), p21 (CDKN1A)-activated kinase 6 (PAK6), cyclin L2 (CCNL2), early growth response 1 (EGR1).

Heat shock proteins (15%): suppressor of hairy wing homolog 1 (SUHW1), heat shock 22kDa protein 8 (HSPB8), heat shock 70kDa protein 1-like (HSPA1L), heat shock 70kDa protein 5 (HSPA5), heat shock 70kDa protein 1A (HSPA1A), heat shock 70kDa protein 6 (HSPA6).

phosphatase activity (13%): protein phosphatase 1, regulatory (inhibitor) subunit 3C (PPP1R3C), protein phosphatase 1, regulatory (inhibitor) subunit 15A (PPP1R15A), protein phosphatase 1, regulatory (inhibitor) subunit 10 (PPPIR10).

Inactivation of MAPK family kinases (8%): dual specificity phosphatase (DUSP10, DUSP18, DUSP13, DUSP23 and DUSP2).

5.4.3 Down-regulated genes in curcumin treated Y79 RB cells:

Curcumin treated Y79 RB cells, revealed down-regulated genes involved in:

Transcription factor (25%): sterol regulatory element binding transcription factor 2 (SREBF2), POU class 4 homeobox 2 (POU4F2), member RAS oncogene family (RAB26), transcription factor A, mitochondrial (TFAM), proliferation-associated 2G4 (PA2G4), V-myb myeloblastosis viral oncogene homolog (avian)-like 2 (MYBL2), DEK oncogene, DNA binding (DEK), ***Insulin receptor substrate 1 (***IRS1), V-abl Abelson murine leukemia viral oncogene homolog 2 (ABL2), SERPINE1 mRNA binding protein 1 (SERBP1)

Angiogenesis genes (14%): Transforming growth factor, beta 2 (TGFB2), EGF-like-domain, multiple 7 (EGFL7), phosphoglycerate kinase 1 (PGK1), insulin-like growth factor binding protein 2 (IGFBP2), neurotrophic tyrosine kinase, receptor, type 1 (NTRK1).

Cell cycle genes (38%): anaphase promoting complex subunit 7 (ANAPC7), Cyclin division cycle 2 (CDC2), S-phase kinase-associated protein 2 (SKP2), cyclin E2 (CCNE2), cyclin H (CCNH), v-myb myeloblastosis viral oncogene homolog (MYB), MAD2 mitotic arrest deficient-like 1 (MAD2L1), minichromosome maintenance complex component 7 (MCM7), cyclin F (CCNF), NIMA (never in mitosis gene a)-related kinase 2 (NEK2), NSL1, MIND kinetochore complex component, homolog (NSL1), kinesin family member 14 (KIF14), kinesin family member 20A (KIF20A); cell adhesion: Intercellular adhesion molecule 5 (ICAM5), Cbp/p300-interacting transactivator, with Glu/Asp-rich carboxy-terminal domain, 1 (CITED1), v-crk sarcoma virus CT10 oncogene homolog (avian)-like (CRKL), peroxisome proliferator activated receptor (PPARA).

Cell migration (11%): laminin, alpha 1 (LAMA1), peptidylprolyl isomerase A (PPIA), Y box binding protein 1 (YBX1).

Anti-apoptosis (6%): Bifunctional apoptosis regulator (BFAR), BCL2-associated athanogene 4 (BAG4).

Functional grouping of the deregulated genes were examined for their known biological function according to the gene ontology convention and grouped in the respective functional category. The proportion of each functional category from the total number of selected genes was taken as 100%. Among the de-regulated genes, 36% of down-regulated genes belong to cell cycle and differentiation and 22% up-regulated genes belong to cell cycle arrest. Hence the

antiproliferative effect of curcumin may be due to disruption of genes involved in cell cycle pathway. Other genes belong to angiogenesis, cell migration, cell adhesion, tumour suppressor, heat shock proteins, transcription factors and inactivation of MAPK family (**Figure 5.2**). **Figure 5.3** shows schematic representation of various pathway's gene list differentially regulated on curcumin treatment in Y79 RB cells.

Figure 5.2

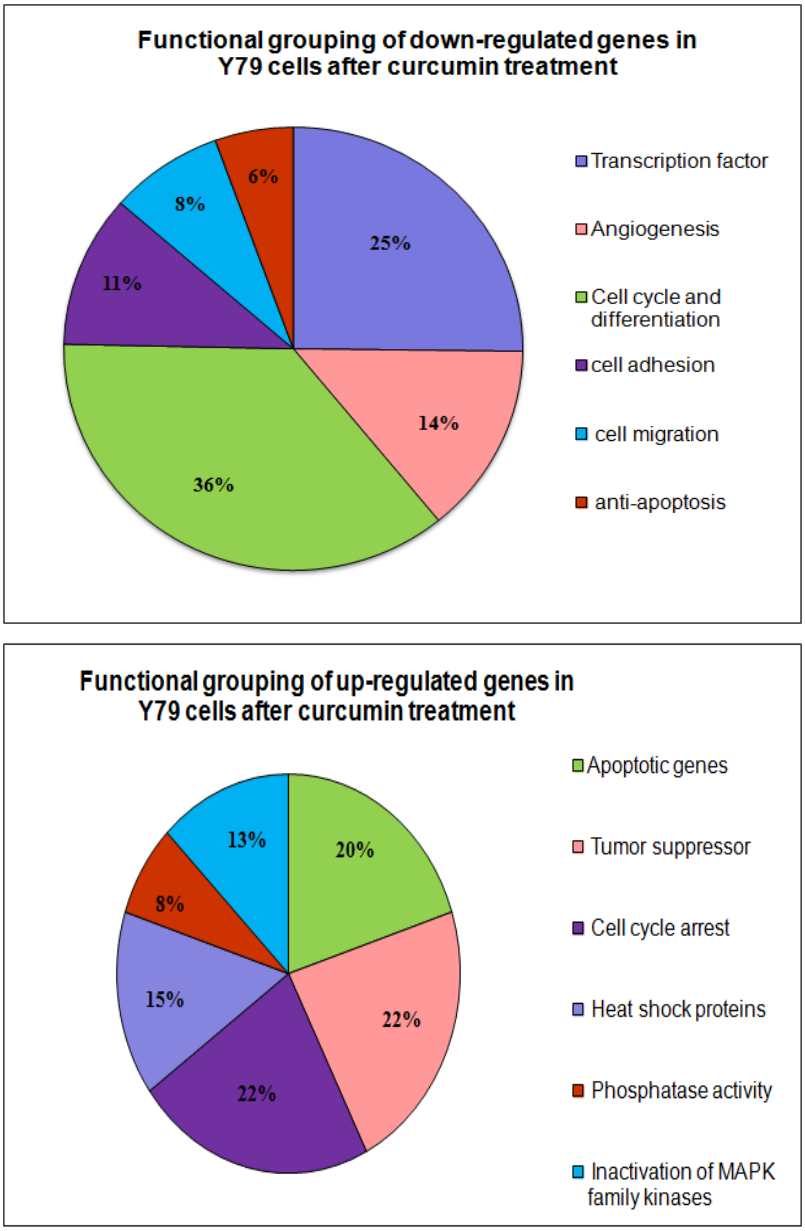

Figure 5.2: Functional grouping of up and down-regulated genes in Y79 cells treated with 20µM curcumin after 72 h. All the gene identifications were examined for their known biologic function according to gene ontology convention and grouped in the respective functional category. The proportion of each functional category in the total number of selected identified genes (taken as 100%) is shown.

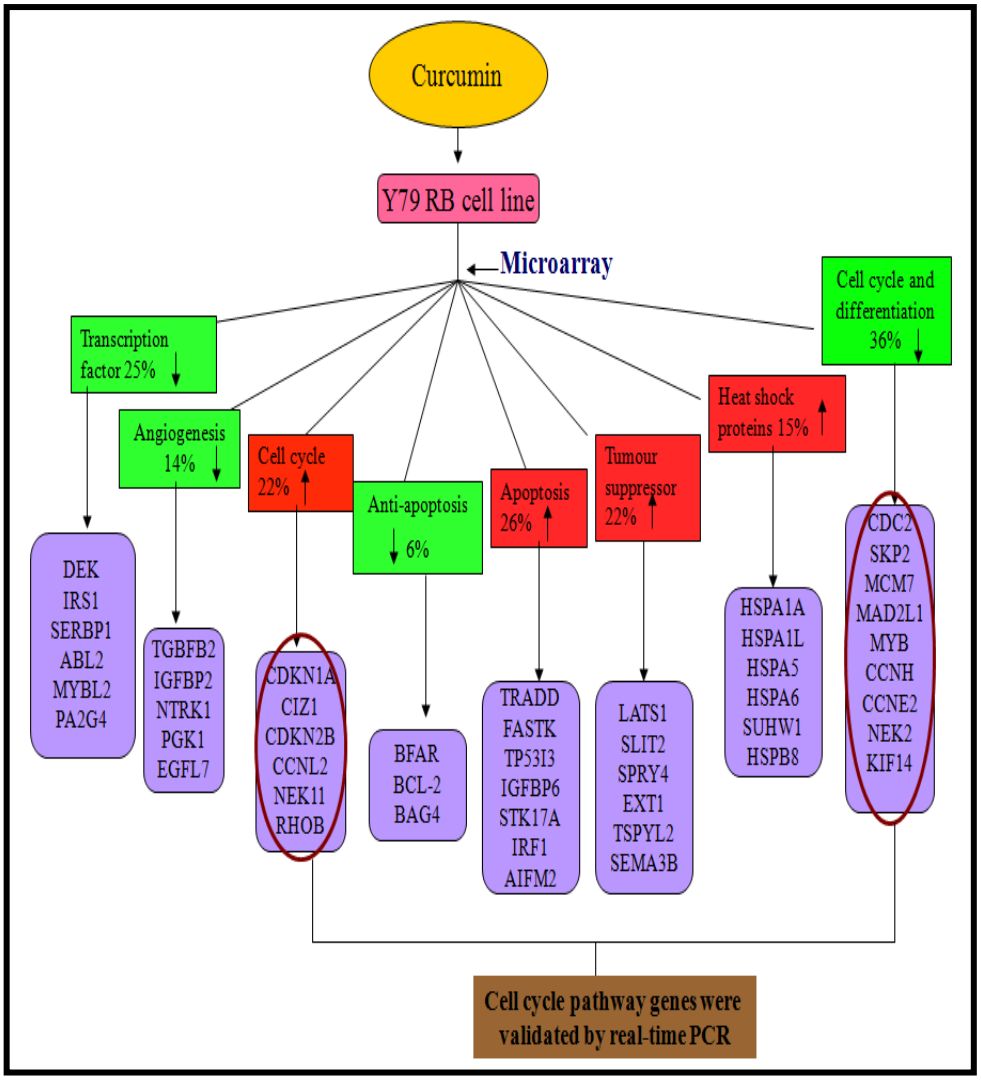

Figure 5.3: Schematic representation of differentially regulated genes regulated on curcumin treatment in Y79 RB cells. The genes that are up or down-regulated in each pathway are shown.

5.4.4 Validation of curcumin regulated genes identified by cDNA microarray by qRT-PCR

To substantiate the results of the microarray studies, RTQ-RT-PCR was performed to assess the mRNA expression of 9 of the curcumin regulated genes (6 for up-regulation and 7 for down-regulation). The mRNA levels of 13 different genes (CDKN1A, CDKN2B, CDC2, MCM7, MAD2L1, CCNL2, CCNH, LATS1, SKP2, PAK6, BFAR, BAG4, and TP53I3) were confirmed to be regulated at 72h of curcumin treatment (20µM) by qRT-PCR in Y79 RB cells, which were consistent with our microarray data (**Figure 5.4)**.

Figure 5.4

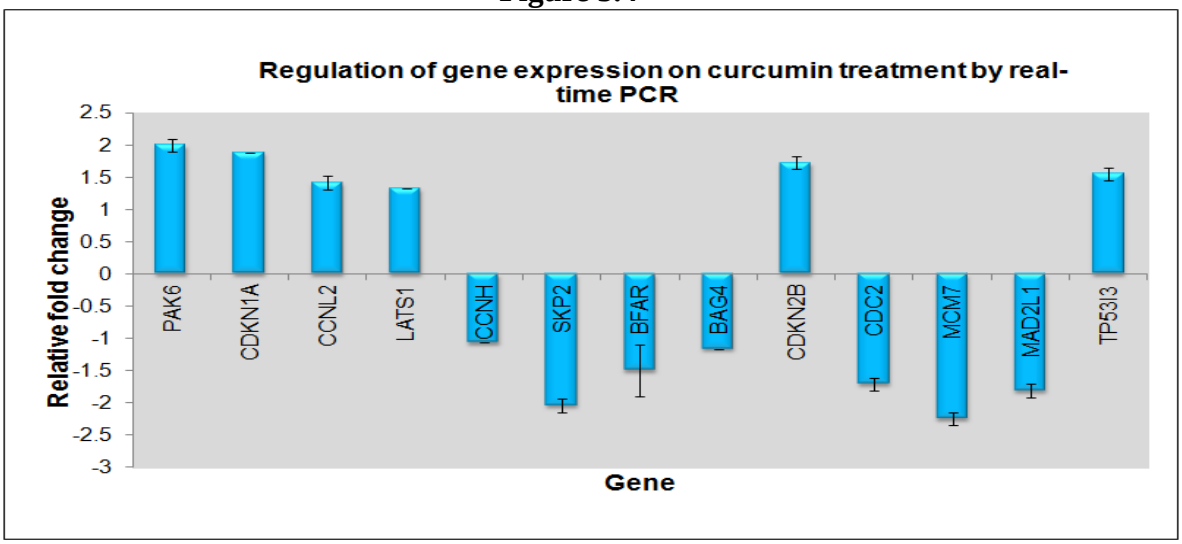

Cell cycle genes:

PAK6- p21 (CDKN1A)- activated kinase 6
CDKN1A-cyclin dependent kinase inhibitor 1A
CCNL2-cyclin L2
LATS1-large tumour suppressor
CDKN2B-cyclin dependent kinase inhibitor 2
TP53I3-Tumor protein p53inducible protein 3

SKP2-S-phase kinase-associated protein 2
BFAR-Bifunctional apoptosis regulator
BAG4-BCL-2 asociated athanogene 4
CDC2-cyclin division cycle 2
MCM7-minichromosome maintenance complex component 7
CCNH-cyclin H
MAD2L1-MAD2 mitotic arrest deficient like 1

Figure 5.4: Validation of microarray data with Real-time quantitative reverse transcriptase PCR (Q-RT-PCR) in Y79 cells: cDNA from curcumin treated and untreated Y79 cells from three different independent experiments were used for validation of the gene expression obtained from microarray analysis. The Q-RT-PCR results are consistent with microarray results. The results are represented as fold change relative to un-induced Y79 cells (control). Values are expressed as mean • ±S.D. of triplicate values.

5.4.5 Curcumin induced cell cycle arrest of Y79 RB cells

To investigate the effect of curcumin on cell-cycle status, Y79 RB cells were treated with different concentration of curcumin for 48h and then analyzed for cell- cycle alteration by flow cytometry. We observed that curcumin caused a dose-dependent decrease in the percentage of G_0/G1 phase cells and increase in the percentage of cells in the G_2/M phase **(Table 5.2 and Figure 5.5)**.

Figure 5.5

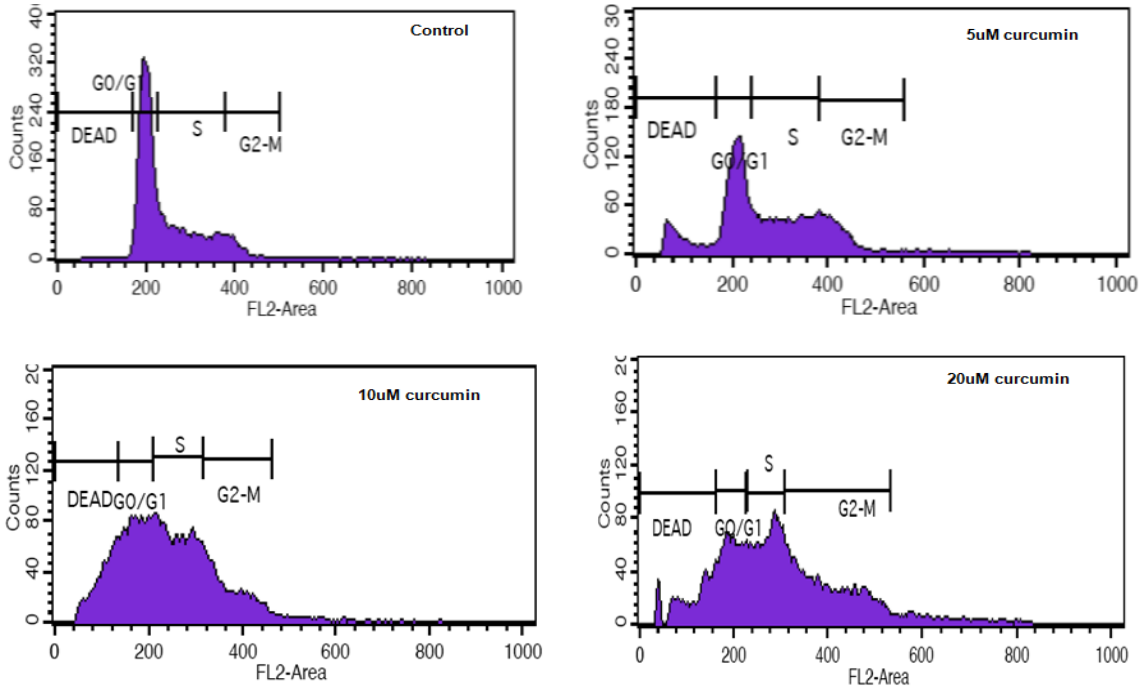

Figure 5.5: Cell cycle distribution in Y79 RB cells was assessed by flow cytometry. Y79 cells were exposed to various concentrations of curcumin (control, 5µM, 10µM and 20µM) for 48h. Percent cell cycle was evaluated after propidium iodide staining and flow cytometry of 10,000 acquired events. The flow cytometry analysis revealed that curcumin decreased the percentage of cell cycle at G_0/G1 and increased at G2/M phase. Data represent means ± SE of three independent experiments. ($p<0.05$ was considered as significant).

Table 5.2: Cell cycle phase distribution of Y79 RB cells after exposure to curcumin

	Distribution (%cells)			
Group	**G0/G1**	**S**	**G2/M**	**Dead**
Control	56.55±2.1	34.03±1.28	7.47±2.3	1.22±0.50
5µM curcumin	35.73±1.54*	35.18±1.75	16.23±2.1*	10.81±0.25*
10 µM curcumin	27.73±2.5*	36.78±2.1	19.07±1.35*	15.22±0.32*
20 µM curcumin	20.72±1.75*	29.46±1.95	33.73±2.10*	12.50±2.2*

***p<0.05= was considered as significant**

5.4.6 Analysis of curcumin induced DNA fragmentation in RB cell line:

The fragments of DNA were checked by agarose gel electrophoresis. With increase in concentration of curcumin, an intense pattern of DNA fragments were

detected. No fragment was observed with DNA extracted from control cells (**Figure 5.6**).

Figure 5.6

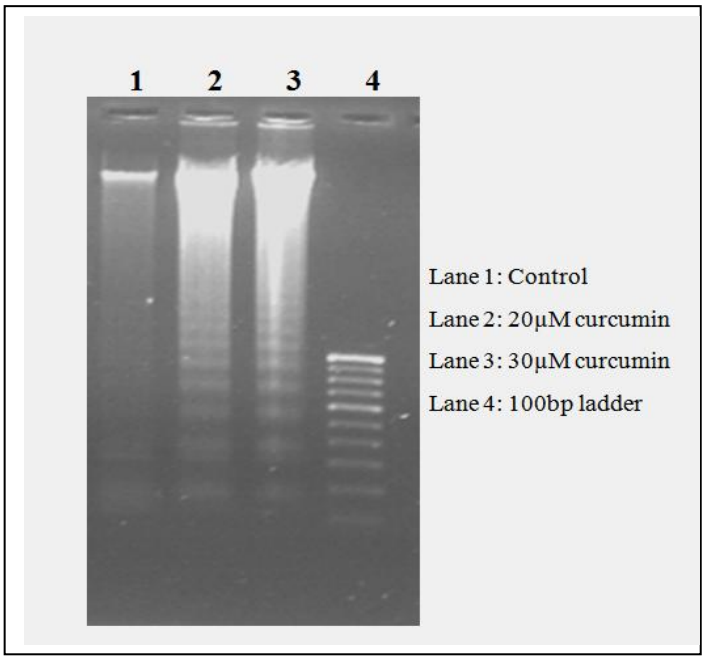

Figure 5.6: Detection of DNA fragmentation by agarose gel electrophoresis. RB cells were treated with different concentration of curcumin (20 &30 µM) and the cells were collected for DNA extraction. Lane 1: Control cells, Lane 2: 20µM curcumin, Lane 3: 30µM curcumin, Lane 4: Base pair marker.

5.5 Discussion:

Normal cell development relies on the regulation of gene expression, but in diseases like cancer, loss of this regulation induces differential gene expression and contributes to the malignant state. Curcumin, a natural polyphenolic compound, appears to exert multiple inhibitory effects on cancer cells through regulation of several signal transduction pathways (Singh et al. 1995). Although, the anti-tumour effects of curcumin have been investigated extensively in various cancers, its gene regulatory effects have not been studied in RB cancer. The aim of this study was to investigate the effect of curcumin on Y79 RB cells by performing a gene expression microarray profiling at 20µM concentration of curcumin for 48h and compared with vehicle-treated RB cells. We observed that curcumin reduced the cell viability and altered the cell cycle of Y79 RB cells. In addition, cDNA microarray analysis identified **1319 genes were up-regulated and 903 genes were down-regulated** in response to curcumin treatment, in

comparison to control Y79 cells. These results demonstrated that curcumin **regulated important genes that belong to cell cycle and differentiation**.

The **cell cycle regulatory genes like EGR1, CDKN1A, CCNL2 and CDKN2B are up-regulated on curcumin treatment**. It is likely that the up-regulation of these genes is one of the causes for the inhibition of cell cycle progression in RB cells.

CDKN1A belongs to cyclin dependent kinase inhibitor (CDKI) family and inhibits cell cycle progression by inhibiting CDK2 and CDK4 and causes arrest at G1, S and G2 phases. CDKN2B also belongs to the CDKI family and binds to CDK4 and CDK6 to prevent their association with cyclin D, thereby blocking the cell cycle at G1 phase (Padua et al. 2009). CCNL2, a novel member of cyclin gene family up-regulated in RB cells, has been observed to promote apoptosis in *in vitro* studies with human cancer cell lines. Over-expression of cyclin L2 have direct anti-proliferative effect on A549 cells, and also able to induce apoptosis *in vitro* (Li et al. 2007). We found increase in the expression of early growth response-1 (EGR1), which regulates expression of genes involved in the control of growth and apoptosis by transactivating p21. A similar result was reported by Calogero et al, indicating the increased in the expression of EGR1 induced by curcumin, thereby activating the expression of p21 protein (Calogero et al. 2004).

The **cell cycle CDC2, MCM7, SKP2, CCNE2 and differentiation genes CCNH are down-regulated in the curcumin treated Y79 RB cells**.

CCNH is the regulatory subunit of the cdk-activating kinase and is distinct from mitotic cyclins because it is expressed constantly throughout the cell cycle. It is identified as a biomarker for determining proliferative activity in endometrial hyperplasia and adenocarcinoma (Kayaselcuk et al. 2006). MCM7, one of the down-regulated genes, a critical component of the DNA replication licensing complex and over-expression of this gene was found to increase cancer progression and invasion in prostate cancer (Ren et al. 2006). SKP2 is the positive regulator of G1-S transition and over-expression of this gene is implicated in cell transformation and oncogenesis in both *in vitro* and *in vivo* models (Yang et al. 2002). CCNE2 functions as a regulator of CDK, which play a role in the cell cycle G1/S transition. Increased expression of CCNE2 is observed in various malignancies such as lung, ovarian, colorectal and non-small cell lung cancer (Caldon et al. 2010).

Curcumin also **deregulated** the expression of many other **genes involved in various cellular functions that play an important role in apoptosis, tumor suppressor, cell adhesion, angiogenesis and transcription factors**. **In summary, this is the first report which shows that curcumin exerts its anti-proliferative effect in RB cells by regulating various genes involved in cell cycle signalling pathway**. Disruption involves increased expression of p21, p15 and down-regulation of few genes involved in cell cycle progression.

5.6: Chapter Summary

- Curcumin decreased cell viability and altered cell cycle of Y79 RB cells.
- Microarray analysis showed around 903 down-regulated genes and 1319 up-regulated genes were regulated upon curcumin treatment.
- Curcumin regulated the expression of many genes that are involved in the regulation of apoptosis, tumour suppressor, cell, adhesion, angiogenesis, transcription factor, cell cycle and differentiation.
- Thus treatment of curcumin affects the expression of genes that are involved in various cellular functions that play an important role in tumour metastasis and apoptosis.

CHAPTER 6: EFFECT OF CURCUMIN ON MICRORNA EXPRESSION PROFILE IN HUMAN RB CELL LINE

6.1 INTRODUCTION:

MicroRNAs are small non-coding, single-stranded RNAs of 18-25 nucleotides long that negatively regulate gene expression at a post-transcriptional level (Bagnyukova et al. 2006). These miRNAs interact with the 3'-untranslated region (UTR) of the target mRNA, induce its degradation and repress the target protein activity (Doe et al. 2008). Various studies have shown that miRNA regulates many biological processes, such as differentiation, proliferation, and apoptosis in cancer (Bagnyukova et al. 2006). Although the biological functions of miRNAs are not completely understood, regulation of gene expression by miRNAs provides a new tool for gene functional study and drug development (Liu et al. 2008). MiRNA deregulation is seen in various cancers like breast (Iorio et al. 2005), glioblastoma (Lu et al. 2005), lung (Takamizawa et al. 2004), colon (Volinia et al. 2006), pancreatic tumours (Lee et al. 2007), and thyroid (He et al. 2005).

6.1.2 miRNA in RB

RB is the most common form of ocular cancer in children. Alterations or loss of the RB1 gene is a defining molecular characteristic of this cancer and is thought to be the tumour-initiating event. Other genomic alterations in oncogenes and tumour suppressor genes have been identified in RB and these changes may be important in RB tumour progression. MiR-17~92 clusters are potent microRNA-encoding oncogenes. High expression of miR-17~92 and miR-106b-25 has been observed in primary human retinoblastoma and over-expression of miR-17~92 accelerates retinoblastoma development in mice by promoting proliferation, in part by reducing expression of the cell cycle inhibitors (Conkrite et al., 2011).

Similarly, a cluster of miRNA was identified as highly expressed in RB tumours, including hsa-miR-494, hsa-let- 7e, hsa-miR-513–1, hsa-miR-513–2, hsa-miR-518c*, hsa-miR- 129–1, hsa-miR-129–2, hsa-miR-198, hsa-miR-492, hsa-miR-498, hsa-miR-320, hsa-miR-503, and hsa-miR-373*. These miRNA are reported in RB tumours which may play important roles in regulating tumorigenesis (Zhao JJ et al., 2009). The tumor specific patterns of miRNA expression give very

useful diagnostic information in determining how various anticancer agents are effective in the treatment or prevention of cancer.

Recent studies have shown that natural agents like indole-3-carbionol (I3C) (Li et al. 2009), isoflavone, diindolylmethane (DIM) (Melkamu et al. 2010), curcumin (Sun et al. 2008) and epigallocatechin gallate (EGCG) (Tsang et al. 2010) alter the expression of specific miRNAs, thereby leading to increased sensitivity of cancer cells to the anti-cancer agents (Tsang et al. 2010). Curcumin is considered one of the most powerful chemopreventive and anti-cancer agents. Extensive studies have shown that most biological effects of curcumin are through regulation of cellular signalling pathways, including NF-κB, protein kinase B (PKB/Akt), mitogen-activated protein kinase (MAPK) and other pathways (Sarkar et al. 2004; Mukhopadhyay et al. 2001). However, there is no report on the effect of curcumin on miRNA regulation in RB cells. In this study, we have used microarray technology to investigate the effect of curcumin on the expression profile of miRNAs in Y79 RB cells.

6.2 Objective

- To study the expression profiles of miRNA regulated by curcumin in RB cell lines by microarray analysis
- To validate selected miRNA from microarray data by real-time quantitative polymerase chain reaction (qRT-PCR)
- To transfect significantly altered miRNA and study the biological function of its known targets in RB cell lines.

6.3 Materials and Methods:

6.3.1 Cell treatment

Cells were plated in 12-well plates at a seeding density of 50,000 cells/cm^2 to a volume of 1 ml per well. Treatments were made from dilutions of a stock made from fresh prior to each treatment. The stock solution was filtered through a 0.22 µm polyethersulfone filter prior to additional dilution. After seeding for 24h, cells were drained of media and treated with 1ml of RPMI 1640 media with 20µM

concentration of curcumin. After 48h of incubation, the cells were taken for RNA isolation.

6.3.2 Total RNA isolation

After the RB cells were treated with 20 µM curcumin (done at Sankara Nethralaya), cells were collected and placed in RNA later solution and sent for miRNA microarray (Genotypic technology, Bangalore).

Total RNA was extracted from Y79 RB cells with control and 20µM of curcumin using the mirVana^{TM} miRNA Isolation kit (Ambion) according to the manufacturer's instructions. The treatment of 20µM was chosen because 80% of the cells were viable by MTT assay. Briefly, about 10^6 cells were collected from each of 2 biological replicate treatments and pelleted by centrifuging at 1000 rpm. The pellet was resuspended in 1ml of phosphate buffered saline (PBS) and repelleted at 1000 rpm. The cells were then placed on ice. The excess PBS was then drained and 500µl of Lysis/Binding Solution was added and vortexed with the cells at 1000 rpm. 50µl of miRNA Homogenate Additive was added to the cells and mixed by vortexing. The mixture was then placed on ice for 10min, 500µl of Acid-Phenol:Chloroform was added and the cells were vortexed for 60 sec. The cells were centrifuged for 5 min at maximum speed. The aqueous phase was removed and transferred to a new tube and its volume was recorded. 1.25 times the aqueous phase volume of room temperature 100% ethanol was added to the aqueous phase and mixed. Each sample was transferred to its own filter cartridge collection tube and centrifuged for 15 seconds at 10,000 rpm. The flow-through was discarded and the sample was centrifuged until all of the lysate/ethanol mixture had passed through the filter. miRNA Wash Solution 1 (700µl) was then added to the filter cartridge and centrifuged for 10 sec and the flow-through was discarded. Wash Solution 2/3 (500µl) was then added and centrifuged through the filter as previously performed. This was completed twice, with each flow-through discarded. The cartridge filter was centrifuged a final time for 1 minute at 10,000 rpm. RNA concentration and purity was quantified using Nanodrop (Nanodrop Santa Clara, CA) spectrophotometer by nanodrop ribogreen assay and quality of total RNA was determined on an Agilent (Agilent, Santa Clara, CA) bioanalyzer.

6.3.3 miRNA microarray and data analysis

Hybridization and detection

MiRNA expression profiling was performed as recommended by the manufacturer's instructions (Agilent Technologies Genotypic, Bangalore, India). Human miRNA V2 8x15k Agilent arrays, which represent 723 human and 76 human viral miRNAs, were used for miRNA analysis. Total RNA underwent phosphatase treatment. The 3'end of dephosphorylated RNA was ligated with one molecule of (3- pCp), cyanine 3-cytidine bisphosphate (pCp) as this reagent selectively labels and hybridizes mature miRNAs, with more than 90% efficiency. Hybridization cocktail was added to the arrays and hybridization was performed in the hybridization oven set at 55ºC for 20h. The microarray was washed using Agilent wash buffer. Scanning and extraction were performed using the Agilent feature extraction software. The intensity and background subtracted were taken from the Raw Data file generated from the Agilent Feature Extraction software (Agilent). The normalization was done using GeneSpring GX 11 Software. The study was done in biological duplicates and the mean value was obtained from the duplicate samples.

Once the result of miRNA microarray was generated, the data of the miRNA microarray was analyzed at Sankara nethralaya using miRBase data software and preceded with further experiments.

6.3.4 Quantitative real time PCR (qRT-PCR) of miRNA expression

Quantitative real-time polymerase chain reaction (qRT-PCR) was used to confirm results. Cells were treated with 20µM curcumin for 48h and the total RNA was isolated from the cells as mentioned above. Purity and concentration of samples were assessed with a Nanodrop ND-1000 spectrophotometer. MicroRNA reverse transcription was performed with specific primers let-7g*, hsa-miR-22, 503, 200c, 135b, 210, 25*, 95, 514, 106b*, 92a-1*, 34c-3p, and U6 was taken as an internal control (**Table 6.1**). Quantification of miRNA expression was performed in triplicate in a 96-well plate on a real-time PCR system (Prism 7500; ABI, Lab India Instruments, Gurgaon, India). The PCR reaction volume of 20µl contained 0.5µg of cDNA, specific primer and SYBR green reagent. The relative amount of each miRNA to U6RNA was calculated using $2^{-\Delta\Delta Ct}$, where C_t is the number of cycles at which amplification reaches a threshold, determined by using commercial software (SDS software v 1.3; ABI) **(**Livak et al., 2000**)**.

Table 6.1: miRNA primers used for real-time PCR:

Gene	Sequence of PCR Primers (5'-3')
let-7g*	F: CTGTACAGGCCACTGCCTTGC
miR-22	F: AAGCTGCCAGTTGAAGAACTGT
miR-503	F: TAGCAGCGGGAACAGTTCTGCAG
miR-200c	F: TAATACTGCCGGGTAATGATGGA
miR-210	F: CTGTGCGTGTGACAGCGGCTGA
miR-135b	F: TATGGCTTTTCATTCCTATGTGA
miR-514	F: ATTGACACTTCTGTGAGTAGA
miR-106b	F:TAAAGTGCTGACAGTGCAGAT
miR-34c-3p	F: AATCACTAACCACACGGCCAGG
miR-92a-1	F: TATTGCACTTGTCCCGGCCTGT
miR-25	F: CATTGCACTTGTCTCGGTCTGA
miR-95	F: TTCAACGGGTATTTATTGAGCA
U6	F: GCTTCGGCAGCACATATACTAAAAT

6.3.5 miRNA transfection

The miR-22 mimics and inhibitors were chemically synthesized by Sigma-Aldrich (USA). Y79 RB cells were plated in 12-well plates at 2 x 10^5 cells/well and incubated for 24h and then transfected with 30nM of the respective mimics or inhibitor of miR-22 or negative control RNA as control using Lipofectamine 2000 and OPTI-MEM I reduced serum medium (Invitrogen, CA, USA) for 48h. Efficiency of over-expression or suppression of miR-22 was measured by Real-time RT-PCR as mentioned above.

6.3.6 MTT assay

Cell viability was assessed calorimetrically using MTT assay. Briefly, cells were seeded at a density of 5 x10^3 cells per well in 96-well plates after 48h of miR-22 transfection. 10µl of MTT solution was added into each well, and the cells were incubated for an additional 4h. The absorption value at 570nm was read using a microplate reader (Bio-Rad, CA, USA) with a reference wavelength of 630nm. Experiments were done in triplicates, and the data were expressed as mean ±SD.

6.3.7 In-vitro scratch migration assay

Y79 RB cells after miR-22 transfection were seeded on 12 well plates and grown to confluent. A scratch was performed using 200µl pipette tip and the cells were incubated for 24h. The images were captured and the distance between the cells was measured. Relative cell migration (%)= No. of treated cells migrated into wounds/No. of control-miRNA treated cells that migrated into wounds x 100.

6.3.8 Western blotting

Y79 miR-22 transfected cells were lysed in 0.5ml of radioimmunoprecipitation (RIPA) buffer. Lysates were separated by electrophoresis, blotted onto nitrocellulose membrane and treated with primary antibody Erbb3 (Santa Cruz Technology, USA). After incubation with a primary antibody, the blots were incubated with a HRP-conjugated secondary antibody (Pierce, Italy). The immunoreactive bands were visualized using an enhanced chemiluminescence (ECL) kit (Amersham Life Sciences). To normalize band intensity, the membranes were probed with β-actin antibodies (Sigma Aldrich, USA).

6.3.9 Identification of predicted target genes

The miRNAs which showed regulation after curcumin treatment were selected for target prediction. Putative target genes were identified using miRBase (http://microrna.sanger.ac.uk), TargetScan (http://genes.mit.edu/targetscan) and PicTar (http://pictar.bio.nyu.edu) database algorithm (Cho et al., 2007).

6.3.10 Statistical analysis

Data were expressed in terms of means ± SD, and analyzed statistically by Student's t-test. Analyses were performed using SPSS 12.0 statistical software. P-value less than 0.05 were considered significant.

6.4 Results

6.4.1 MiRNA microarray analysis of gene expression of Y79 RB cells after curcumin treatment

We used the human miRNA V28x15k array to identify the differential miRNA expression pattern of Y79 cells treated with curcumin for 48h. MiRNA expression was changed by the drug treatment. The data discussed in this

publication have been deposited in NCBI's Gene Expression and are accessible through GEO Series accession number GSE21126. As shown in **Figure 6.1**, the array results of miRNA gene expression showed the number of genes regulated on curcumin treatment. Five miRNAs (miR- 200c, 503, let-7g*, 923, 22) were significantly up-regulated and sixteen miRNAs were significantly down-regulated (miR-210, 598, 181a*, 181a, 34b*, 34c-5p, 216a, 216b, 106b*, 95, 124*, 217, 25*, 135b, 92a-1*, 514) on curcumin treatment when compared with the control Y79 RB cells **(Table 6.2)**.

Figure 6.1

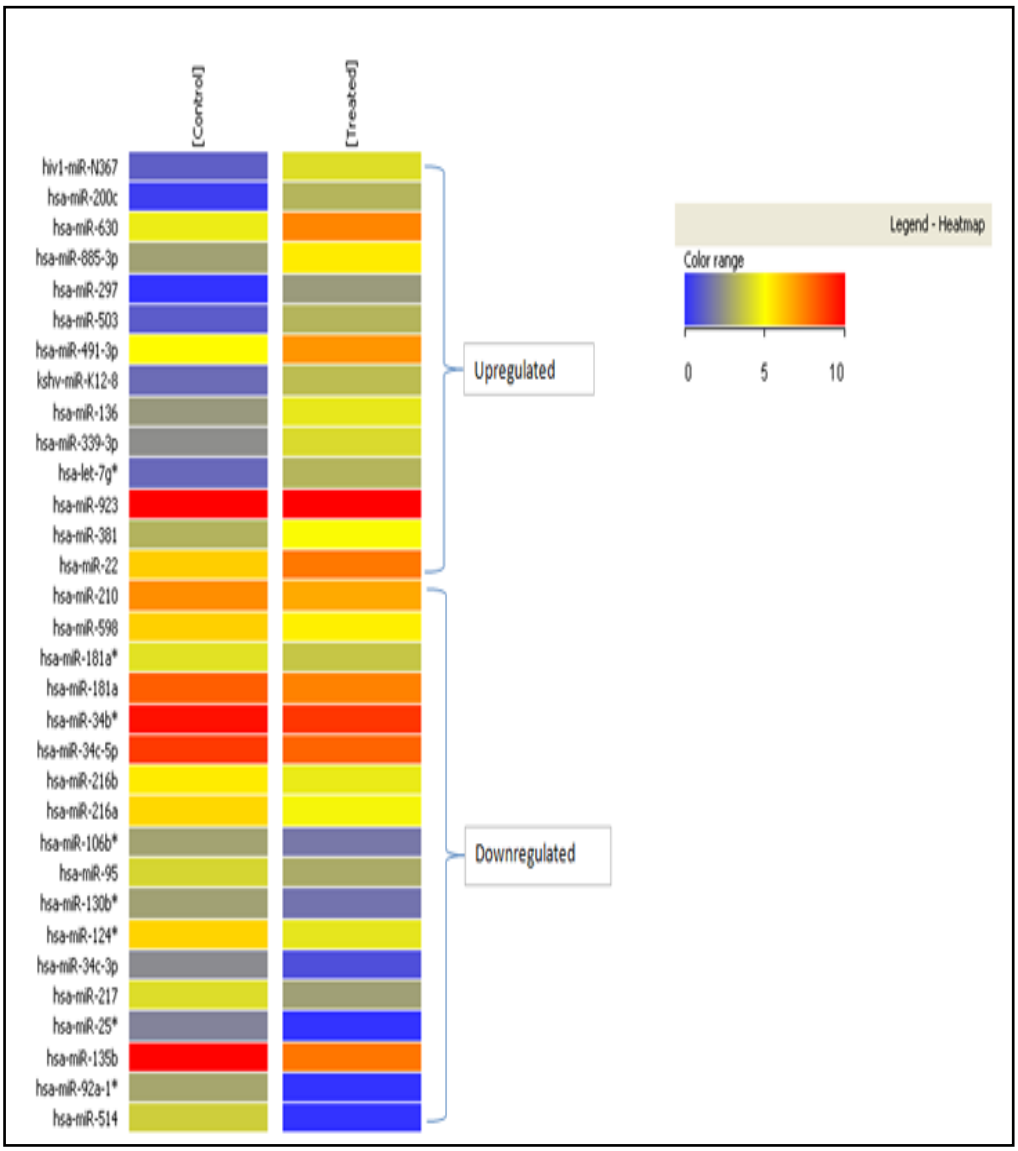

Figure 6.1: Changes in the miRNA expression profiling on curcumin treated Y79 retinoblastoma cells determined by microarray. Y79 cells were treated with 20µM curcumin for 48h and untreated cells were considered as control. The heat map represents the expression profile of differentially regulated miRNA in response to curcumin in Y79 RB cells compared to untreated cells. Red and green indicate increased and decreased expression, respectively, relative to control RB cells

Figure 6.2:

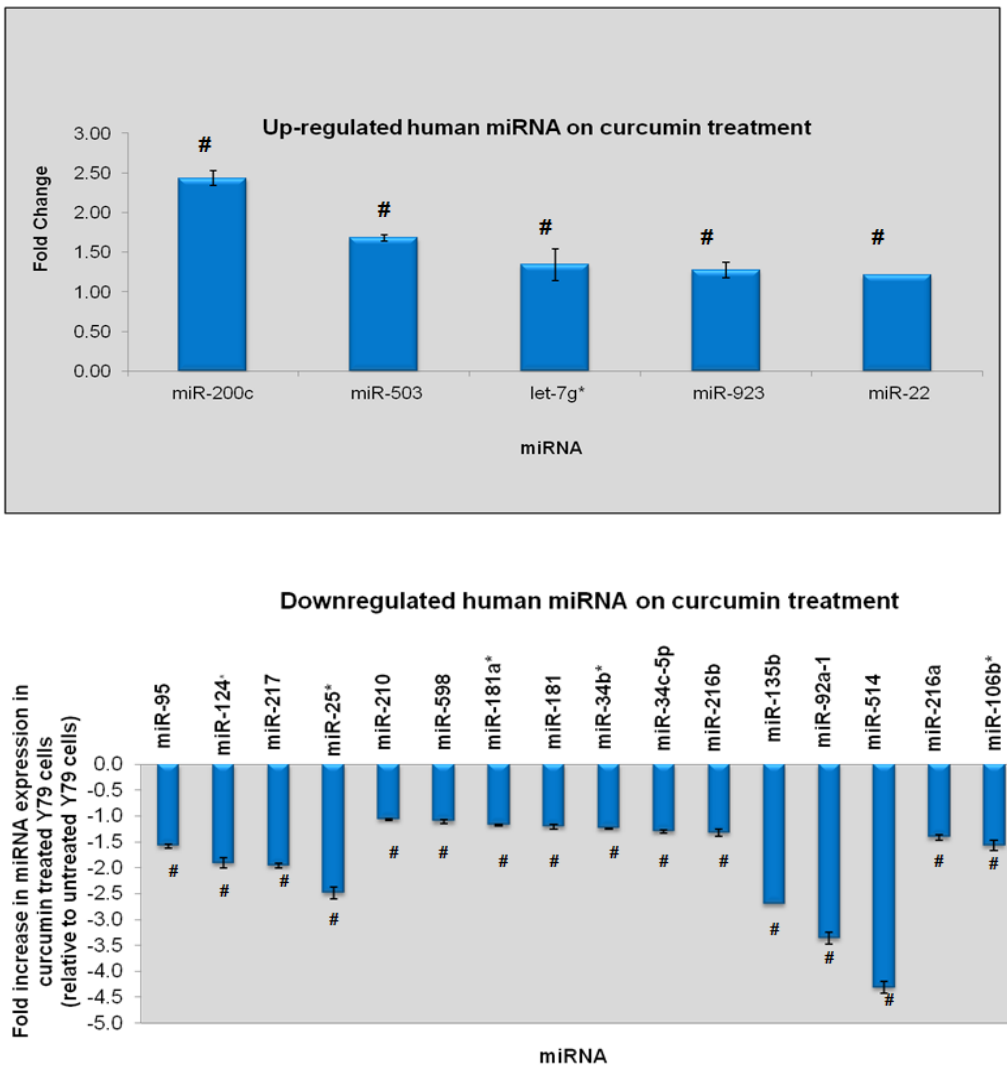

Figure 6.2: Fold change in the **e**xpression of altered miRNA after curcumin treatment. 32 miRNA were found to be regulated between curcumin treated and untreated Y79 RB cells. Of these 5 were significantly up-regulated and 16 were significantly down-regulated. Data are expressed in terms of means ±S.E.M for the fold change in miRNA expression in log2 scale between control Y79 cells with respect to curcumin treated cells. (# $p<0.05$) is considered as significant when compared with the control Y79 cells as calculated by students t-test.

Table 6.2: Expression profiling of miRNA genes in curcumin treated Y79 cells.

miRNA	Chromo -some location	Up/down-regulation	Putative targets	Fold changes	p-val ue
hsa- let-7g*	3p21.1	Up	NRAS, HMGA2, TGFBR1 IGF1R, MYCN, MAPK6, TP53	1.34	0.012
hsa-miR-22	17p13.3	Up	ESR1, BCL9L, ERBB3, SP1, SATB2, RAB5B, CAV3	1.21	0.00
hsa- miR-503	Xq26.3	Up	CBX4, IGF1,M CPEB2, PIK3R1	1.6	0.014
hsa-miR-923	17	Up	No previously reported targets	1.2	0.042
hsa-miR-200c	12p13.31	Up	ZEB1, TIMP2, MYB, BCL2	2.44	0.024
hsa- miR-135b	1q32.1	Down	STAT6, TET3, MRAS, MMP11	-2.77	0.003
hsa- miR-181a	1q31.3	Down	TRIM2, E2F1, RET, SP8	-1.2	0.025
hsa-miR-181a*	1q31.3	Down	No previously reported targets	-1.1	0.010
hsa- miR-210	11p15.5	Down	EFNA3,BDNF, PCDH17	-1.0	0.006
hsa- miR-216a	2	Down	SP1, CDC23	-1.41	0.024
hsa- miR-216b	2	Down	BCL2L11, SERBP1, TCF4	-1.3	0.031
hsa- miR-217	2p16.1	Down	RICTOR, FAM60A	-1.98	0.021
hsa- miR-514	X	Down	SERBP1, PTEN, TIAM1, FOXO4	-4.31	0.017
hsa- miR-598	8p23.1	Down	ZEB2, HOXOA3	-1.1	0.022
hsa-miR-25*	7q22.1	Down	MAP2K4, RAB23, MALAT1	-2.49	0.030
hsa-miR-95	10p13	Down	NR4A2, SELS, GNAI2, OAZ2	-1.5	0.017
hsa-miR-34b*	11q23.1	Down	ASB1, SGPP1	-1.2	0.003
hsa-miR-34c-5p	11q23.1	Down	DLL1, FLOT2, NAV1	-1.3	0.014
hsa-miR-106b*	7q22.1	Down	ZBTB7, ITGB8	-1.5	0.040
hsa-miR-92a-1*	13q31.3	Down	CPEB3, NFYC, HIPK3	-3.3	0.022
hsa-miR-124*	8p23.1	Down	OSR1, CDH11, PTPN12	-1.9	0.032

1. The data presented fold change of curcumin treated cells with the control Y79 cells.
2. Putative targets are targets identified from the miRBase, pictar and target scan computational algorithm.
3. $p<0.05$ was considered as significant when compared with the control Y79 retinoblastoma cells.

6.4.2 Confirmation of microarray results by quantitative real time polymerase chain reaction

To confirm the miRNA microarray data, qRT-PCR was performed to further determine the expression of 12 selected miRNAs of Y79 RB cells induced by curcumin. The selected miRNAs included eight down-regulated oncomirs (miR-135b, 210, 25*, 95, 514, 106b*, 34c-3p, and 92a-1*) and four up-regulated tumor suppressors (let-7g*, miR-22, 503 and 200c). MiRNA which was used for the microarray analysis was reverse transcribed and amplified in the ABI 7500 sequence detection system. From the real time PCR results it was found that all selected miRNAs mentioned above were regulated and the results were consistent with the microarray data (**Figure 6.3**). (# $p<0.05$ was considered as significant when compared with the normal control values in the absence of curcumin).

Figure: 6.3

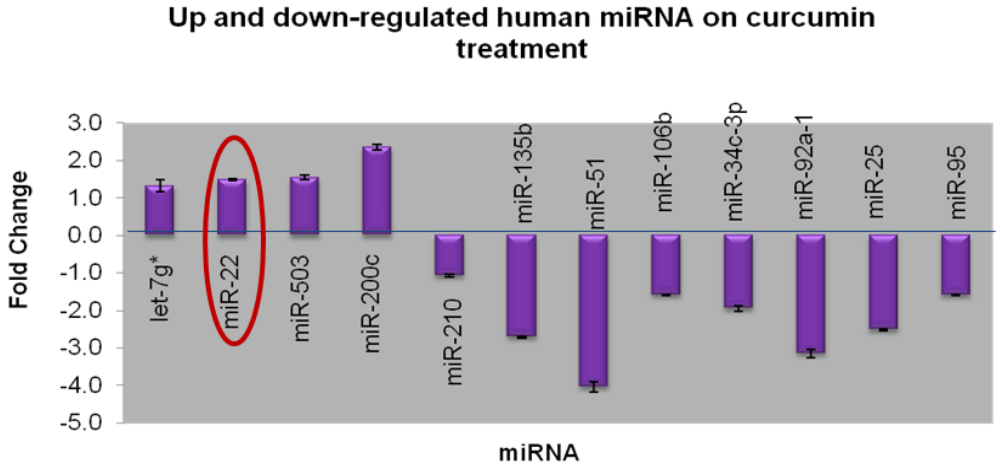

Figure 6.3: Validation of microRNA microarray data of selected miRNA by real-time PCR. QRT-PCR was performed on twelve differentially expressed miRNAs (eight down-regulated**:** miR-135b, 210, 25*, 95, 514, 106b*, 34c-3p, and 92a-1*; and four up-regulated: let-7g*, miR-22, 503 and 200c) to confirm the microRNA microarray data. The expression changes observed from three independent experiments, ± SD (n=3) by qRT-PCR were comparable with the microarray data.

Among the differentially expressed miRNA in RB cells after curcumin treatment, we have selected miR-22 (tumour suppressor gene) for further studies which have been found to have complex role in regulating cell proliferation and invasion in various cancers. However the role of miR-22 has not been studied in RB cancers, thus in the present study, we studied the effect of miR-22 over-expression on RB cell line.

6.4.3 miR-22 over-expression by transfection leads to decreased cell proliferation and invasion in Y79 RB cells

The altered expression of miR-22 after transfection was confirmed by real-time PCR. TaqMan real-time PCR revealed significantly increased levels of miR-22 (10-fold), when compared with those transfected with control oligonucleotide after 48h **(Figure 6.4).**

Figure 6.4

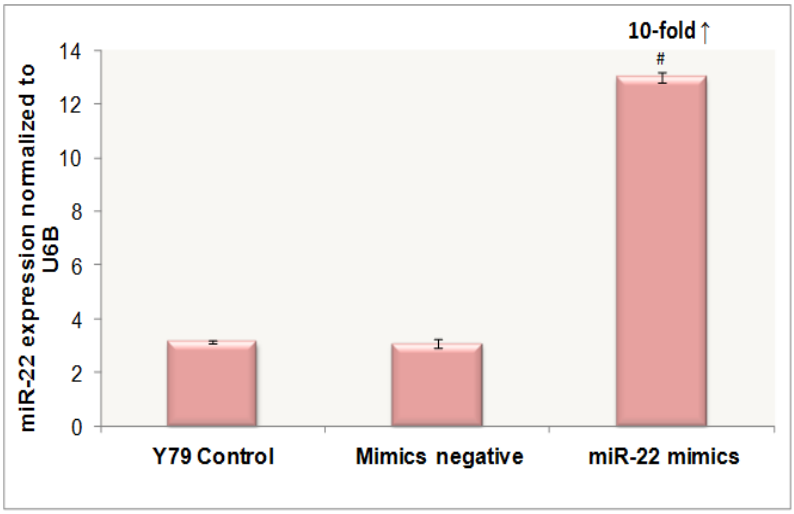

Figure 6.4: Over-expression of miR-22 in Y79 RB cells by transient transfection **a**) Y79 cells were treated with miR-22 mimics and control oligonucleotide containing Opti-MEM and Lipofectamine reagent for transfection for 48h. Cellular total RNA was isolated after transfection with miR-22 mimics and mimics negative control and the miR-22 expression was analyzed by TaqMan quantitative real-time PCR in Y79 RB cells. The results are normalized to U6 expression and are presented as the relative miR-22 expression.

6.4.4 Cell viability assay

To assess the role of cell proliferation on miR-22 transfected cells, MTT assay was performed. **Figure 6.5** demonstrates that the miR-22 transfected cells showed a significant reduction in cell proliferation when compared with control oligonucleotide transfected cells.

Figure: 6.5

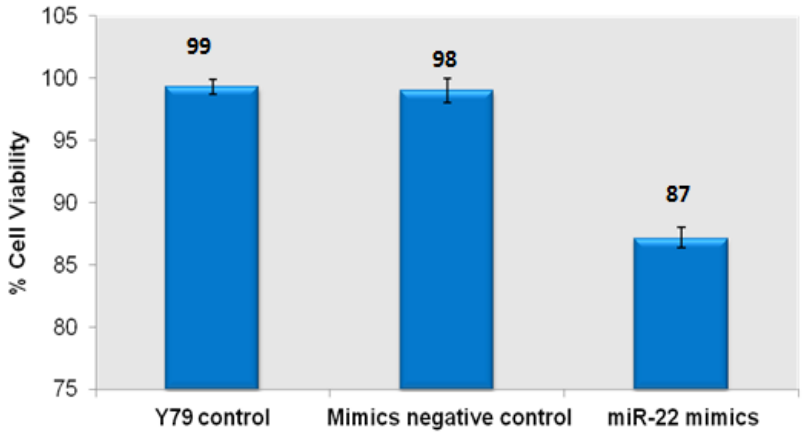

Figure 6.5: Over-expression of miR-22 in Y79 RB cells and its effect on Y79 cell proliferation: Cell proliferation was analyzed by a MTT assay after transfection with miR-22 mimics and mimics negative control in Y79 RB cells. The data are represented against control Y79 cells, mimics negative control and are presented as relative cell proliferation.

6.4.5 Effect of miR-22 on cell migration

In our results transfection with miR-22 mimics reduced the number of Y79 cells that migrated over wounds compared with the control oligonucleotide transfection **(Figure 6.6)**.

Figure: 6.6

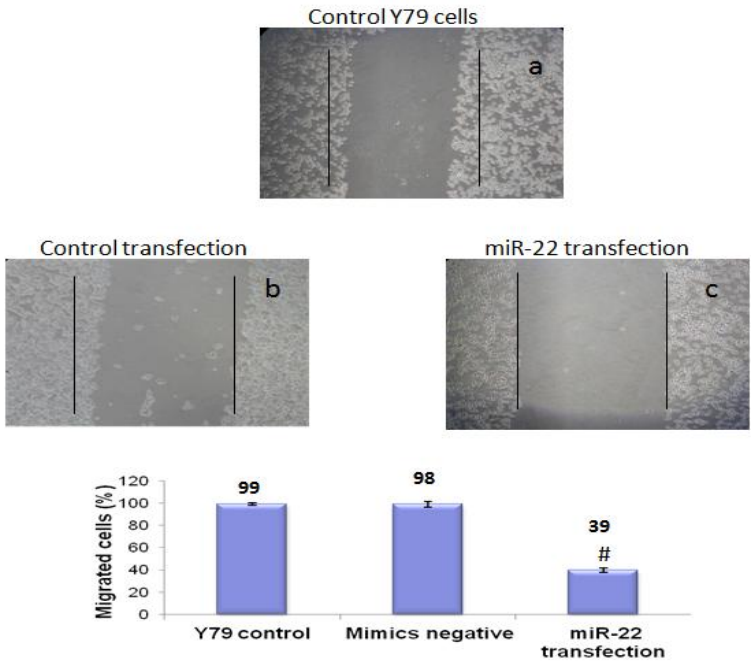

Figure 6.6: Cell invasion was evaluated in Y79 RB cells after transfection by *in vitro* scratch migration assay (a- Normal Y79 cells, b-Control transfetcion, c- miR-22 transfection). The data are presented as relative cell invasion and are representative of three independent experiments (n=3, *$p<0.05$).

6.4.6 MiR-22 controls Erbb3 expression in Y79 RB cells

To investigate the role of miR-22 in Erbb3 expression, we transfected Y79 RB cells with miR-22 mimics and mimics negative control or control Y79 cells, and then measured Erbb3 protein expression by western blot. Western blotting revealed a significant inhibition of Erbb3 protein expression in miR-22 transfected Y79 cells **(Figure 6.7)**. Our data indicate that Erbb3 is a potential target for miR-22 and over-expression of miR-22 inhibited cell proliferation and invasion may be through down-regulation of Erbb3.

Figure: 6.7

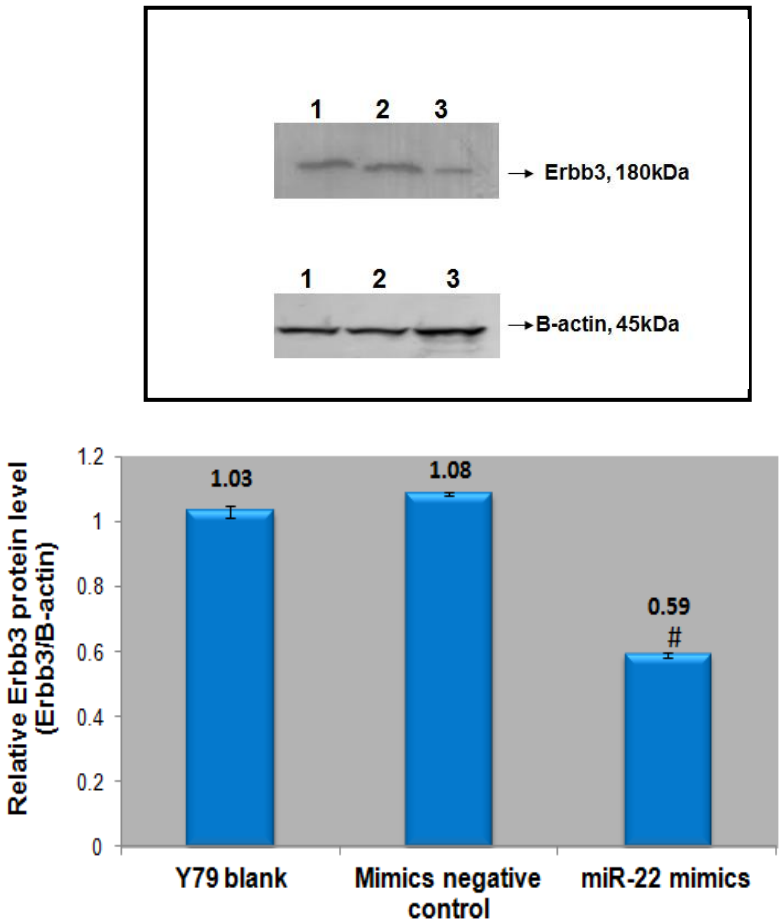

Figure 6.7: Effect of miR-22 on Erbb3 protein expression. Western blot analysis for Erbb3 and β-actin in transfected Y79 cells. Y79 cells were transfected with miR-22 mimics and mimics negative control and then incubated for 48h. Cell lysates were immunoblotted for Erbb3 (Lane 1: Normal Y79 cells, Lane 2: Control transfection, Lane 3: miR-22 transfection). Quantification was done by densitometry for Erbb3 in Y79 transfected cells.

6.5. Discussion:

Several studies have been reported that natural dietary compounds induce differential expression of miRNAs in variety of cancer cell lines (Saini et al. 2010). Certain miRNAs are up-regulated or down-regulated in human cancer,

with some overlapping miRNA profiles on tissue origin. However, no study has been reported on the effect of natural products on miRNA expression in any organism *in vivo* or *in vitro*. In this study, we report of the first time the effect on the miRNA expression profile after 48h of treatment with 20µM curcumin concentration.

The present study demonstrated that curcumin, a natural polyphenolic compound from ***Curcuma longa,*** **altered miRNA expression in human RB cells**, including **5 up-regulated and 16 down-regulated miRNA**s. We found that certain miRNAs up-regulated by curcumin are tumour suppressors. These include miR-22, miR-200c, let-7g* and miR-923, and these findings were consistent with our qRT-PCR. Among the four tumour suppressor miRNA, miR-22 was selected for further study whose down-regulation has been reported in various human cancers (Xiong et al. 2010; Pandey et al. 2009; Zhang et al. 2008)**.** In our study, **miR-22 was over-expressed to study its functional changes in RB cells**. miR-22 showed an inhibition in the growth of Y79 cells after transfection, and the cells transfected with miR-22 showed a decrease in the cell migration compared with the control oligonucleotide transfected cells.

It has been studied earlier that miR-22 acts as a tumor suppressor in certain cancers through various signalling pathways (Li et al. 2010). miR-22 is a well-studied regulator of oncogenic activity, and has been demonstrated to down-regulate endogenous estrogen receptor alpha protein levels that inhibit the proliferation of MCF-7 cells (Pandey et al. 2009). Moreover, up-regulation of miR-22 by curcumin or by transfection was shown to suppress the expression of SP1 transcription factor and estrogen receptor 1 (ESR1) in a human pancreatic cancer cell line (Sun et al. 2008). miR-22 targets multiple proteins such as estrogen receptor alpha, c-myc binding protein (MYCBP), Myc associated factor X (Max) and PTEN suggesting that miR-22 may be implicated in tumorigenesis (Chang et al. 2008). In our study, we used miRBase computational algorithm (Lewis et al. 2003) to predict the target genes of miR-22, and selected Erbb3 for further study. It has been reported earlier, that the expression of Erbb3 has been over-expressed in several cancers including RB tumor which play an important role in cancer development and progression (Chakraborty et al. 2007). Patel et al showed that over-expression of miR-22 reduced the levels of Erbb3 in breast cancer cells confirming that Erbb3 is one of the targets of miR-22 (Patel et al.

2011). Our western blot results showed that the **over-expression of miR-22 inhibited the expression of Erbb3 in Y79 RB cells**. Yan et al. reported that in MDA-1986 squamous carcinoma cell line the expression of Erbb3 was down-regulated upon curcumin treatment (Yan et al. 2005)**.**

In our study, the miRNAs regulated on curcumin treatment were well characterized and had been previously implicated in various cancers. Curcumin treatment could induce the differential expression of a set of miRNAs, which could potentially regulate the expression of oncomirs and tumor suppressor genes. MicroRNA-based gene therapy makes miRNA research applicable to a wide variety of medical fields, not limited to cancer research. Specific miRNA alterations using microRNA mimics or antagomirs or siRNA can alter their expression in tumor cells, thus down-regulating the expression of oncomirs and thereby helping in the prevention of RB cancer initiation and metastasis (Huang et al. 2007).

These novel findings suggest that the use of **natural agents could open new avenues for the successful treatment of cancers, especially by combining conventional therapeutics with natural chemopreventive agents** that are known to be non-toxic to humans (Li et al. 2010).

6.6: Chapter summary

- Curcumin altered miRNA expression profile in human Y79 RB cells, of which 5 were up-regulated and 16 were down-regulated.
- Curcumin up-regulated some of the tumour suppressor miRNAs and down-regulated oncomeric miRNAs.
- miR-22, one of the tumour suppressor miRNA was up-regulated on curcumin treatment. Transfection of miR-22 in Y79 cells inhibited cell proliferation and migration and suppressed one of its target oncogene Erbb3.
- These suggest that curcumin modulate miRNA expression profile, thereby exerting its anti-cancer effect on RB cells (**Figure 6.8**).

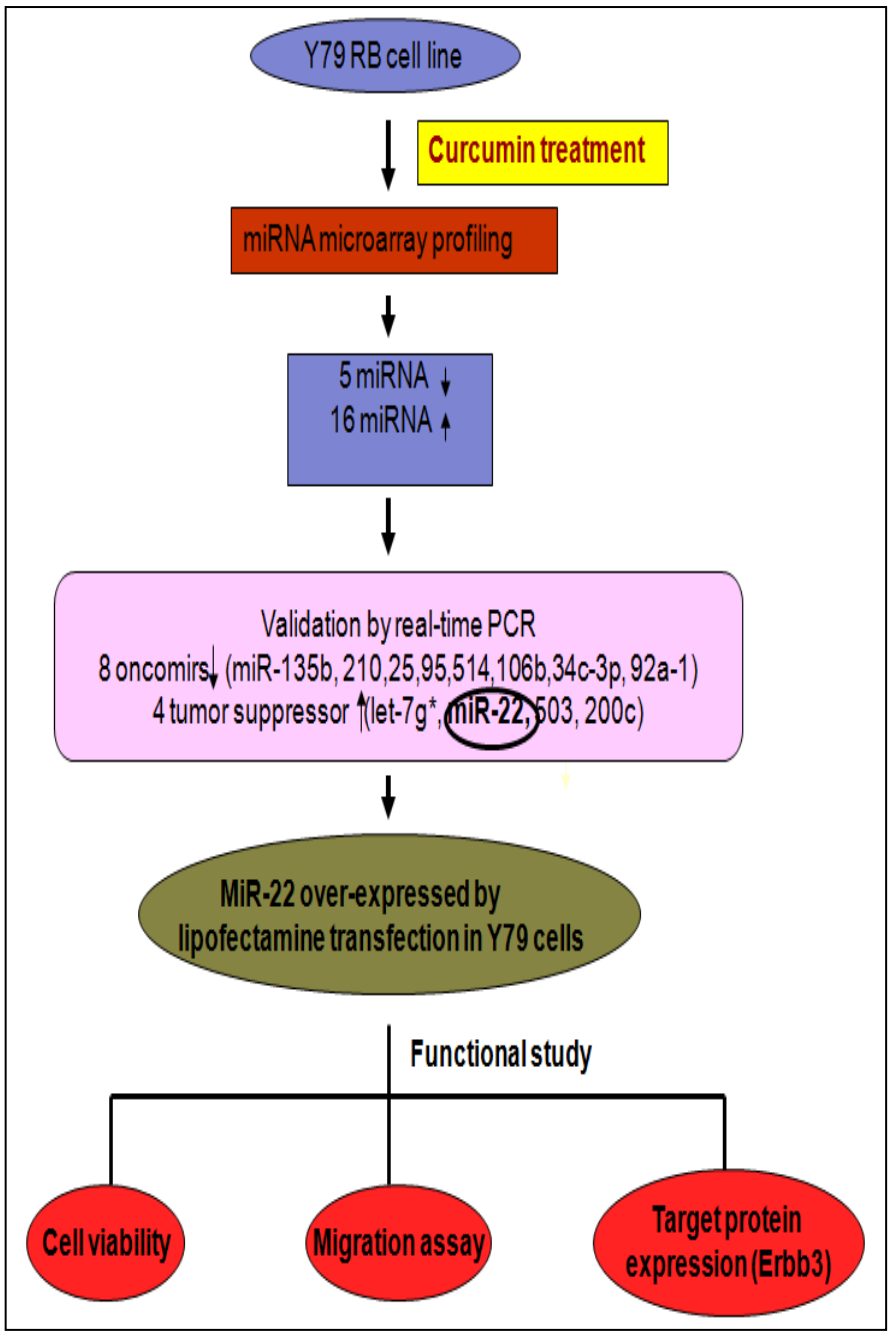

Figure 6.8: Effect of curcumin on miRNA expression in human Y79 RB cells. This work has been published in **Current Eye Research 37(5), 421-28, 2012**

CHAPTER 7: *IN VITRO* AND *IN SILICO* STUDIES ON INHIBITORY EFFECTS OF CURCUMIN ON MULTI DRUG RESISTANCE PROTEINS IN RB CELLS

7.1 Multi-drug resistance in RB cancer

RB cancer is currently treated by surgery and radiotherapy, and frequently involves the incorporation of chemotherapy drugs. Chemotherapy plays an important role in the treatment of RB cancer. The triple drug therapy treatment (carboplatin, vincristine and etoposide) are well established the most active agents for RB cancer.

Although chemotherapy forms part of sucessful treatment in many cases, drug resistance is a major problem in the management of RB cancer (Gallie et al. 1996). The mechansim of drug resistance involves altered expession/activity of drug efflux pumps, nuclear DNA-binding enzymes, mismatch repair deficiency and metabolozing and conjugating enzymes.

a) Multi-drug resistance 1(MDR1), Multidrug resistance associated protein (MRP1) and Lung resistance related protein (LRP) contribute to drug resistance:

A number of mechanisms of MDR have been identifie by usina in vitro cell culture models. Among these mechansim, several of the transmembrane drug efflux pumps belong to ATP-binding casette (ABC) transmembrane protein superfamily that utilises énergy frome ATP hydrolysis to translocate substrates across cell membranes (Lee et al. 2004).

It is known that MDR1 gene is normally overexpressed in the adrenal glands, colon, liver and kidney. In addition, the MDR1 gene is shown to be regulated in response to cellular stress triggered by anti-cancer drugs, heavy metals, heat shock, ultra-violet, serum starvation and phorbol esters in some cultured human cancer cells. **Expression of P-gp is more frequently observed in well-differentiated RB tumours, especially those treated by chemotherapy before enucleation** (Filho et al. 2005).

Another protein MRP1 tends to increase with disease stage and invasiveness in prostate cancer. In prostate cancer cell line, over-expression of MRP1 confers chemoresistance to doxorubicin treatment. Similarly another *in vitro* studied showed that over-expressing MRP1 cells tend to expel anti-androgen compounds,

thereby leading to failure of anti-androgen therapy (Munoz M et al. 2007). A report of increased expression of MRP1 is observed in other cancers like neuroblastoma and breast cancer. **Failure of chemotherapy due to over-expression of MRP1 is one of the major causes in RB tumour** (Chan et al. 1997).

Another drug resistance protein which does not belong to the ABC transporter family, named lung resistance related protein (LRP) is found to be highly expressed in some tumours and drug resistant cell lines (Suprenant et al. 2002). The LRP was first identified as the major vault protein (MVP), the main component of vaults (Scheffer et al. 1995). In 1993, Scheper et al identified LRP to be highly expressed in non-Pgp MDR cell lines (Scheper et al. 1993). It has been demonstrated that LRP is involved in the efflux of anthracyclines in resistant cells and over-expression of this protein in colon carcinoma cells lead to lowered sensitivity to vincristine, etoposide and paclitaxel. **In our study also, we found that LRP was expressed intrinsically in RB tumour that play a role in drug resistance** (Krishnakumar et al. 2004). Other cancers where LRP is highly expressed include neuroblastoma, melanoma and osteosarcoma (Ramani et al. 1995).

b) Defect of apoptosis contributes to drug resistance:

Apoptosis in tumour cells play a critical role in chemotherapy induced cell death. Many antitumor agents have been reported to exhibit apoptosis in tumour cells. Altered expression of proteins involved in apoptosis/ cell cycle regulation has been proposed to explain drug resistance in different cell lines. Drug resistance has been made to understand the biochemical alterations of apoptotic pathways in cancer, thus it is highly possible that the inability to activate apoptotic responses represents a mechanism of drug resistance (Toomey& Simoni et al. 2002).

7.1.2 Role of natural compounds in overcoming multi-drug resistance

Natural compounds like fruits and vegetables contain various phytochemicals that provide various health benefits. These phytochemicals present in the plant possess various biological activity and some of the important ones are curcumin, capsaicin and epigallocatechin gallate with chemopreventive properties. These natural compounds have been found to reverse multi-drug resistance by the inhibition of the drug efflux transporter like P-gp, MRP etc (Conseil et al. 1998).

Curcumin is one of the most extensively studied modulator of multi-drug resistance proteins in various cancer cell lines. It has been reported that curcumin increased the accumulation of daunorubicin in KB-C2 cells (Kitagawa et al. 2004). Similarly the cellular accumulation of rhodamine 123 was increased in the presence of curcumin, indicating the inhibition of efflux transporter P-gp by curcumin (Nabekura et al. 2005). Another study also showed that curcumin inhibited the function of MRP1 in HEK-293 cells (Chearwae et al. 2006). These findings suggest that curcumin has the inhibitory effect on P-gp and MRP expression, which may be due to its chemosensitizing property. **Thus in the present study we want to determine the modulatory effect of curcumin on MDR expression and function (P-gp, MRP and LRP) in RB cell lines.**

7.2 Objective

- To study the expression of MDR proteins (P-gp, MRP1 and LRP) in Y79 RB cell lines.
- To study the effect of curcumin on the expression and function of MDR proteins by western blot, RT-PCR and functional assay in RB cells.
- To perform *in silico* docking study to understand the molecular interactions conferred by curcumin on MDR proteins.

7.3 Materials and Methods

7.3.1 Expression of MDR mRNA (P-gp, MRP and LRP) by RT-PCR in RB cell lines:

Cells were collected and the total RNA was extracted by the Trizol method. The harvested cells were collected and centrifuged at 10,000 rpm for 5-10 min and the supernatant is discarded using a pipette. To the pellet added 1ml Trizol reagent and vortexed nicely. Added 500µl of $CHCl_3$ and shaked well for 15sec. Cells were centrifuged at 12,000 rpm for 15 min. Aqueous layer that has RNA was collected and transferred to new vial and added 500µl isopropanol and incubated at RT for 10 min. Cells were centrifuged at 12,000 rpm for 10 min and supernatant was discarded and to the pellet added 75% alcohol and mixed well. Cells were centrifuged at 12,000rpm for 5 min and the supernatant was discarded. The pellet was air dried at RT for 2 min and added 25µl DEPC treated water. 5µl of the total RNA extracted was run in 2% agarose gel to see the quality of RNA

extracted and the rest was stored at -80^{0}C before use. CDNA was performed using sensiscript reverse transcriptase and the RT-PCR was performed using specific primers (**Table 7.1**). PCR products were fractionated by electrophoresis using 2% agarose gel containing 0.5% Ethidium bromide with molecular marker *Hinf I* Φ *X* digest to confirm the size of the resultant product.

Table 7.1: Primers used for semiquantitative RT-PCR

Gene	Primer sequence	PCR Product size
P-gp	**FP** GGAAGCCAATGCCTATGACTTTA **RP** GAACCACTGCTTCGCTTTCTG	193bp
MRP1	**FP** CGTCTACTCCAACGCTGAC **RP** CTGGACCGCTGACGCCCGTGAC	325bp
LRP	**FP** TGGCTTTGAGACCTCGGAAG **RP** TCCAGTCTCTGAGCCTCATGC	235bp

7.3.2 Expression of MDR proteins (P-gp, MRP and LRP) by western blot in RB cell lines:

Cells were collected and centrifuged at 10,000rpm for 5-10 min. The obtained cell pellet is washed thrice with phosphate buffered saline at 12,000rpm for 5min. The cell pellet is re-suspended in 200µl-300µl of the RIPA buffer and kept at 4^{0}C and sonicated at 50-60 pixels for1min (thrice). After sonication the protein concentration in the lysate was measured by the Lowry method and the concentration was noted. SDS-PAGE was performed with the prepared lysate depending on the percentage of proteins. The electrophoresed gel was transferred with nitrocellulose membrane and the membrane was blocked with skimmed milk for an hour. The membrane was treated with different primary antibody for the detection of the drug resistance proteins. Detection was done using ECL method.

The expression of drug resistance proteins was detected in RB cell line and further we studied the modulating effect of curcumin on the expression of these drug resistance proteins.

7.3.3 P-glycoprotein

7.3.3.1 Transient transfection with pMDR1-EGFP in RB cell line

Transient transfection were performed by using Lipofectamine 2000 and OPTI-MEM I reduced serum medium (Invitrogen, Carlsbad, CA), following the manufacturer's protocol. Y79 RB cells were plated in 12-well plates at 2 x 10^5 cells/well and incubated for 24h and then transfected with pMDR1-EGFP (a kind gift by S.Simon, The Rockefeller University, New York, (**Figure 7.1**) for 48h. After transfection, the efficiency of over-expression of P-gp was measured by western blot.

Figure 7.1

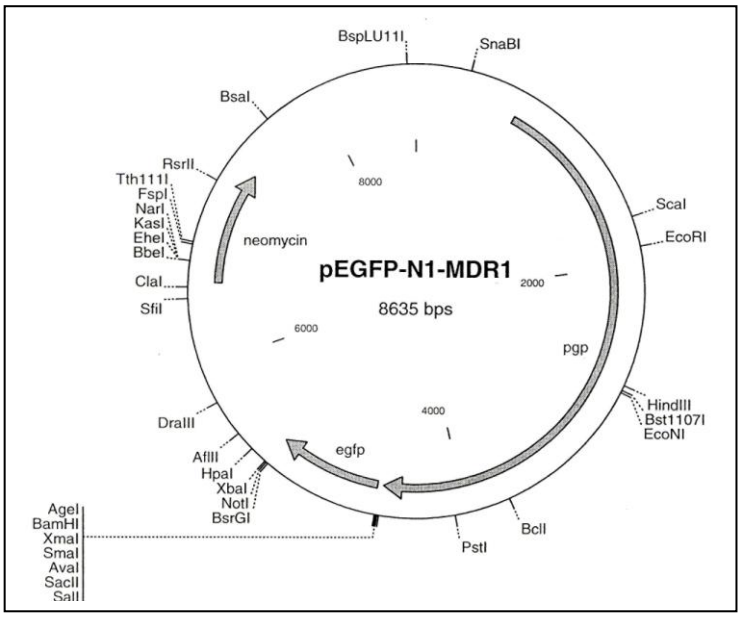

Figure 7.1: pMDR1-EGFP map

7.3.3.2 Effects of curcumin on MDR1 mRNA and protein expression in RB cell line:

RT-PCR was performed for MDR1 mRNA and proteins on curcumin treated (2-10µM) & untreated Y79 RB cells. RNA was extracted and 2µg of it was taken and converted to cDNA. cDNA were amplified for 35 cycles using specific primers and the amplification product was fractionated by electrophoresis using 2% agarose gel containing 0.5% Ethidium bromide. Further, for studying the protein expression, curcumin treated and untreated cell lysates (50µg) were loaded onto 8% polyacrylamide gels and the western blot for P-gp (1:4000) and β-actin (1:4000) was performed. Protein bands were visualized using a chemiluminescence kit. The relative amount of P-gp mRNA and protein

expression was determined by densitometer.

7.3.3.3 Effect of curcumin on accumulation and efflux of Rhodamine 123 by flow cytometry (P-gp)

Y79-MDR1 cells ($3x10^5$/well) were incubated with 1µg/ml of Rh123 in the presence of curcumin in the dark at 37^0C in 5% CO2 for 3hrs. After incubation cells were washed twice with ice-cold HBSS with 10%FBS, and were analyzed using FACScan flow cytometer (Becton-Dickinson) equipped with 488nm argon laser. The green fluorescence of Rh123 was measured at 530nm. A minimum of 10,000 events was collected for each sample. For determination of Rh123 efflux, cells were treated with Rh123 for 60 min in the absence of curcumin, and then the medium was replaced with drug free medium containing curcumin. After the incubation, the cells were washed twice with ice-cold HBSS and analyzed under flow cytometry.

7.3.3.4 ATPase activity of P-gp

Y79-MDR1 cells expressing P-gp were incubated at 37^0C for 30 min with varying concentration of curcumin in the presence and absence of sodium orthovanadate (Vi, 0.3mM) in ATPase assay buffer to measure the amount of inorganic phosphate that is being released. Membrane extracts were incubated with increasing concentration of curcumin in the presence and absence of verapamil. The reaction was initiated by the addition of 5mM ATP and incubated for 20 min at 37^0C. SDS (0.1ml of 5% SDS) solution was added to terminate the reaction, and the amount of inorganic phosphate released was quantified with a colorimetric reaction.

7.3.3.5 Photo-cross-linking of P-gp with 8-azido-ATP-bitoin

Crude membrane of P-gp expressing in transfected Y79-MDR1 cells (100µg protein) were incubated with 5mM $Mgcl_2$ and 100µM 8-azido-ATP-biotin in the dark on ice for 5 min in the presence and absence of 10µM curcumin. The mixture was photolinked using UV light for 10 min. Blotting was performed on the photolinked sample using P-gp monoclonal antibody. The protein band was visualized with streptavidin horseradish peroxidase.

7.3.3.6 *In silico* Analysis

Three dimensional structure of P-gp is yet to be elucidated. Hence, homology search was performed for P-gp (Accession ID: **P08183**) using BLASTp against PDB with optimal parameters to identify suitable templates for homology modelling. BLASTp results revealed that Multi-drug resistance protein 1a (PDBID: **3G5U**) of Mus musculus as an optimal template as it shared a sequence identity and similarity of 88% and 94%, respectively. Further, homology based structure prediction was attempted to determine the plausible 3D structure of P-gp using MODELLER 9V7 software (Dawson et al. 2006). Among the 100 models generated for P-gp, the one with significant Probability Density Function (PDF) and Discrete Optimized Potential Energy (DOPE) as calculated by the MODELLER 9V7 was chosen as the best model and was subjected to further refinement and analysis.

Further, the refined structure was geometry optimized using GROMACS 4.3.1, a molecular dynamics package (Eswar et al. 2008; Van Der Spoel et al. 2005)**.** The stereo chemical aspects of the refined model was inspected by checking the Phi-Psi angles through visualizing Ramachandran plot generated by Procheck (Summa et al. 2007). The structure was also validated using ProSA II server (Laskowski et al. 1993). The structural quality of the protein was further assessed by comparing the topology of the protein through the more sensitive TM-score calculation implemented through TM align (Wiederstein et al. 2007). The possible ligand binding cavities within the generated model was predicted using DEPTH (Xu et al. 2010). The structural coordinates of curcumin (ACD0022) was retrieved from Indian Plant Anticancer Compound Database (Tan et al. 2011) and was geometry optimized using PRODRG2 sever (Vetrivel et al. 2009) with the full charges and optimal chirality.

Molecular Docking study was carried out using AutoDock 4.2. Initially, the energy optimized macromolecules and the ligands were prepared by adding polar hydrogen's. Further, the receptor and ligand were optimized by adding Kollman united atom charges and Gasteiger charges, respectively. Flexibility of the ligand was assigned based on its torsional degrees of freedom through Autotors, with the protein fixed to rigid throughout the process of docking simulation **(**Schüttelkopf et al. 2004; Goodshell et al. 1996).

Grid box covering the entire surface of P-gp (126×126×126; 0.825Å) was constructed and used for all docking process. Further, Grid maps were generated for each atom within the ligand of P-gp using Autogrid. Docking calculation was performed using Lamarckian genetic algorithm (LGA) with default parameters, except for the number of GA runs which was set to 100. Further, cluster analysis was performed to find the optimal binding orientation of the ligand.

Potential binding pose of curcumin with P-gp was predicted based on the binding energy and inhibitory constant. Moreover, polar and non polar interactions were also analyzed and visualized using PyMOL (www.pymol.org) and Ligplot (Corbeil et al. 2007). All the molecular modelling and simulation studies were carried out on Open Discovery Linux platform (Vetrivel et al. 2008).

7.3.4 Multi-drug resistance protein (MRP1)

7.3.4.1 Effects of curcumin on MRP1 expression in RB cell line:

RT-PCR study for MRP1 on curcumin treated (2-10µM) & untreated Y79 RB cells were performed with 2µg of total RNA from each sample. The cDNA products were amplified for 35 cycles using specific primers and the amplification product was fractionated by electrophoresis. Further, for protein expression studies, the curcumin treated and untreated cell lysates (50µg) were loaded onto 8% polyacrylamide gels and the western blot for MRP1 (1:2000) and β-actin (1:4000) was performed. Protein bands were visualized using a chemiluminescence kit. The relative amount of MRP1 mRNA and protein expression was determined by densitometer.

7.3.4.2 MRP1 functional study using calcein-AM by flow cytometry:

The accumulation of calcein-AM, which is a fluorescent substrate for MRP1, was used for the functional study. $5x10^4$ Y79 cells were collected and 0.5µM of calcein-AM was added in the presence and absence of 10µM curcumin and incubated at 37^0c in the dark for 30 min. Similarly, the inhibitors of MRP1 (1mM probenecid and 100µM indomethacin) was added and the accumulation of calcein was measured. After the incubation period, the cells were pelleted by centrifugation at 5000rpm for five min. To the pellet, 500µl of PBS containing 0.1% BSA was added and analysed immediately by flow cytometry.

7.3.4.3 *in silico* Analysis: (MRP1)

The sequence information's of MRP1 (UniProt ID: **P33527**) were retrieved from Uniprot (http://www.uniprot.org/). Three dimensional structures for the entire MRP1 have not been elucidated. Hence, BLASTp analysis has been performed against Protein Data Bank (PDB) to identify the suitable templates for MRP1. Sequence analysis of MRP1 revealed that homodimeric multidrug exporter Sav1866 (PDB ID: **2HYD**) of *Staphylococcus aureus* (Dawson et al. 2006) shared an overall sequence identity of 28% and similarity of 49% with MRP1.

For generating the homology based models of MRP1, sequence alignments were produced using ClustalW2 with default parameters. With specific to these alignments, three dimensional structures of MRP1 were generated using Modeller9v8 (Eswar et al 2008). Among the 100 models generated for MRP1, the one with significant molecular PDF and discrete optimized potential energy (DOPE) (Shen et al. 2006) was subjected to refinement.

Further, the modelled structures were energy optimized through GROMACS 4.3.1; molecular dynamics package (Vander Spoel et al. 2005). The optimized models were evaluated for the stereo chemical aspects using PROCHECK (Laskowski et al. 1993) and for the energy profile using ProSA II server (Wiederstein et al. 2007). The structural quality of the protein was further evaluated by comparing the topology of the protein through structural superposition. The more sensitive TM-score was generated using TM align to check the probability of proteins sharing the same fold at the structural level. TM-Score > 0.17 is suggestive of a model and template sharing the similar topology (Xu et al. 2010).

The possible ligand binding cavities within the generated model was predicted using castP (Liang et al. 1998). The structural co-ordinates of curcumin (ACD0022) was retrieved from Indian Plant Anticancer Compound Database (Vetrivel et al. 2009) and geometry optimized using PRODRG2 sever (Schüttelkopf et al. 2004).

Molecular Docking studies were carried out using AutoDock 4.2. Initially, the energy optimized macromolecules and the ligands were prepared by adding polar hydrogen. Further, the receptor and ligand were optimized by adding Kollman united atom charges and Gasteiger charges, respectively. Flexibility of the ligand

was assigned based on its torsional degrees of freedom through Autotors, with the protein fixed to rigid throughout the process of docking simulation (Goodshell et al. 1996**; http://www.pymol.org/).** Grid box covering the complete binding cavity as predicted using CASTp for MRP1 (104×104×104; 0.667Å) was built and used for docking process. Further, Grid maps were generated for each atom within the ligand of MRP1 using Autogrid. Docking calculation was performed using Lamarckian genetic algorithm with default parameters, except for the number of GA runs which was set to 100. Further, cluster analysis was performed with a threshold RMSD set to 2.0Å to find the optimal binding orientation of the ligands. Potential binding pose of curcumin with MRP1 was predicted based on the binding energy and inhibitory constant. Finally, bonded and non-bonded interactions were also analyzed and visualized using PyMOL (http://www.pymol.org/). All the major structural bioinformatics tools used in this study were run on Open Discovery Linux platform installed in Dell Precision Multicore workstation (Corbeil et al. 2007).

7.3.5 Lung resistance protein (LRP)

7.3.5.1 Effect of curcumin on LRP mRNA and protein expression in RB cell line

Total RNA from RB cells was extracted according to the manufacturer's recommended protocol. For single-strand cDNA synthesis, 2µg of total RNA from each sample was reverse transcribed using sensiscript reverse transcriptase PCR amplification was carried out in an Eppendorf PCR system for 35cycles. PCR product of 230bp encoding LRP and 498bp encoding GAPDH was fractionated by electrophoresis using 2% agarose gel containing 0.5% Ethidium bromide with molecular marker *HinfI* ϕ□digest to confirm the size of the resultant product.

Similarly for the LRP protein expression studies, following curcumin treatment, lysates of untreated and curcumin treated cells (100µg) were loaded onto 10% polyacrylamide gels and the western blot for LRP was performed, as described above. The relative amount of LRP mRNA and protein expression was determined by densitometry.

7.3.5.2 *In silico* analysis (LRP):

The sequence information's of LRP (Accession ID: **Q14764**) were retrieved from Swissprot database (http://expasy.org/sprot/). In LRP (PDBID: **1Y7X**) (Kozlov et al. 2006), the functional domain mediating drug interaction has been experimentally determined, so these structures were utilized for further studies.

7.3.5.3 Model Refinement and validation

WHATIF package was utilized to remove the steric clashes (bumps) (http://swift.cmbi.ru.nl/servers/html/index.html) in the generated model. Further, the structures were optimized using OPLS force field with 1000 runs of energy minimization using steepest descent through GROMACS 4.3.1, a molecular dynamics package (Vanderspoel et al. 2005; Laskowski et al. 1993).

The stereo chemical aspects of the refined models were inspected by checking the Phi- Psi angles through visualizing Ramachandran plot. The quality of the model was assessed through Goodness factor (G-Factor) as predicted using Procheck (Laskowski et al 1993). G-factor describing the Dihedral angles and Main-chain covalent forces were evaluated to assess the optimality of the generated model. Moreover, Planarity of the sidechains was also checked. Final optimized three dimensional structures were validated based on energy criteria by comparing with the potential of mean force derived from the known protein structures using ProSA II server (Wiederstein et al. 2007). The structural quality of the protein was further assessed by comparing the topology of the protein. The more sensitive TM-score was generated using TM align to check the probability of proteins sharing the same fold at the structural level. TM-Score > 0.17 is suggestive of a model/ template sharing the similar topology (Xu et al. 2010).

7.3.5.4 Ligand Optimization

The structural co-ordinates of curcumin (**IUPAC Name:** (1E, 6E)-1, 7-bis (4-hydroxy-3-methoxyphenyl) hepta-1, 6-diene-3, 5-Dione) (**CID 969516**) and Adenosine Triphosphate (ATP) (**CID 5957**) were retrieved from NCBI-Pubchem database (E.http://www.acscomp.org/Publications/ARCC/volume4/chapter12.htmlBolton, Y**)**. The structures were geometry optimized through energy minimization using PRODRG2 sever (Schuttelkopf et al. 2004) with the full charges and optimal

chirality.

7.3.5.5 Molecular Docking Simulation

Molecular Docking of Curcumin with MDR proteins was carried out using AutoDock 4.2 in combination with Lamarckian genetic algorithm (LGA) to find the global optimised conformation of the ligand. Initially, the energy optimized macromolecules and the ligands were prepared by adding polar hydrogens. Further, the receptor and ligand were optimized by adding Kollman united atom charges and Gasteiger charges, respectively. Atomic solvation parameters were assigned using the ADDSOL utility of Auto Dock 4.2. Flexibility of the ligand was assigned based on its torsional degrees of freedom through Autotors, with the protein fixed to rigid throughout the process of docking simulation (Goodshell et al. 1993; Corbeil et al. 2007).

Grid box covering the entire surface of LRP (92×92×126; 0.403Å) was constructed and used for all docking process. Further, Grid maps were generated for each atom within the ligand of LRP respectively Autogrid. Docking calculation was performed using LGA with default parameters, except for the number of GA runs which was set to 100. Further, cluster analysis was performed to find the optimal binding orientation of the ligand.

Potential binding pose of curcumin with LRP were predicted based on the binding energy and inhibitory constant. Moreover, polar and non polar interactions were also analyzed and visualized using Ligplot**.** These studies were carried out in Open Discovery- Linux Platform through Dell Precision workstation with 8 core processors (Vetrivel et al. 2008).

7.4 Results:

7.4.1 Expression of drug resistance (P-gp, MRP1 and LRP) proteins by RT-PCR and western blot in RB cell lines:

a) LRP: LRP mRNA and protein expression was determined using a RT-PCR and western blot method. In the Y79 cells, a 230bp band corresponding to LRP mRNA was observed. A similar band was observed in the LRP over expression HCT-15 cells. In the Y79 cells, a band at 110kDa corresponding to LRP protein

was observed. A similar band was detected in the immunoblots of the LRP over expression HCT-15 cells (**Figure 7.2a,b)**

Figure 7.2a: Expression of LRP by western blot

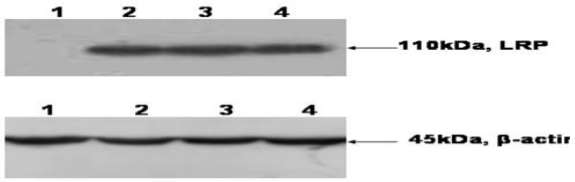

Figure 7.2b: Expression of LRP by RT-PCR

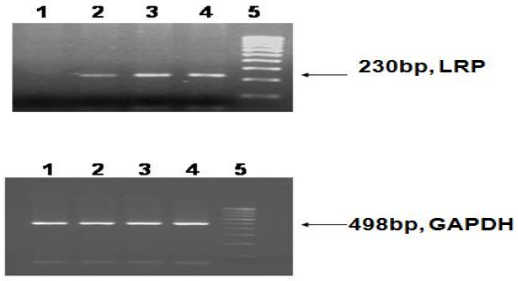

Figure 7.2: LRP mRNA and protein expression in RB cell line. **a)** Western blot for the LRP protein expression was performed with LRP56, a specific anti-LRP antibody. 50µg of protein were loaded on SDS-PAGE. Lane 1: Negative control, lane 2: Retina, lane 3: Y79 cells, Lane 4: HCT-15 cells (LRP positive control). **b)** 2µg of total RNA was subjected to RT-PCR for LRP gene expression and the PCR products were separated on a 2% agarose gel. Lane 1: Negative control (SiHa cells), lane 2: Retina, lane 3: Y79 cells, lane 4: HCT-15 cells (LRP positive cells), lane 5: *HinfI* φX digest.

b) MRP1: Similarly MRP1 mRNA and protein was detected both by RT-PCR and western blot. MRP1 was positive in both A549 and Y79 cell line. A 325bp corresponding to MRP1 mRNA and 170-190kDa protein was observed (**Figure 7.3a, b)**.

Figure 7.3a: MRP1 protein expression by western blot

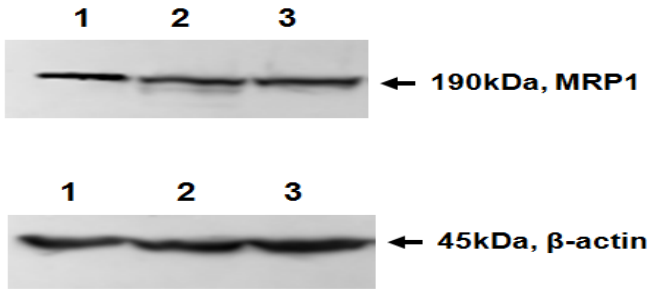

Figure 7.3b: MRP1 mRNA expression by RT-PCR

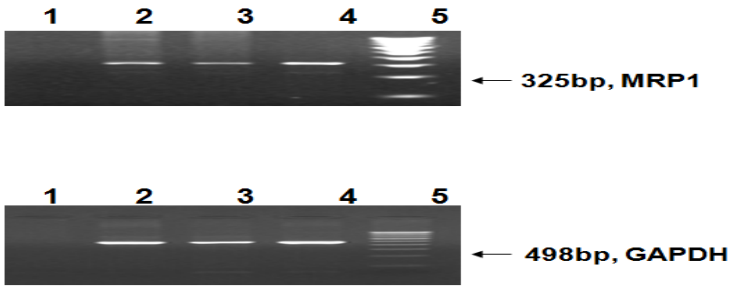

Figure 7.3: a) MRP1 mRNA and protein expression in Y79 RB cell line. Western blot for the MRP1 protein expression was performed with MRP1 antibody (clone QCRL-1), a specific anti-MRP1 antibody. 50µg of protein were loaded on SDS-PAGE. Lane 1: retina, lane 2: Y79 cells and lane 3: A549 (MRP1 positive control). **b)** 2µg of total RNA was subjected to RT-PCR for MRP1 gene expression and the PCR products were separated on a 2% agarose gel. Lane 1: Negative control, lane 2: Y79 cells, lane 3: retina, lane 4: A549 cells (positive control) cells, lane 5: Base pair ladder.

c) P-gp: P-gp protein was not detected in RB cell line, whereas the mRNA expression of P-gp was detected by RT-PCR. HCT-15 showed both the mRNA (193bp) and protein expression of P-gp (150-170kDa), which served as a positive control (**Figure 7.4**).

Figure 7.4

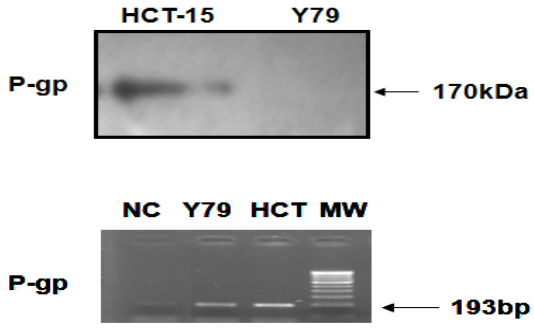

Figure 7.4: P-gp expression by western blot and RT-PCR: P-gp was negative in RB cell line, whereas HCT-15 (positive control) showed expression for P-gp. Similarly RT-PCR study showed the expression of P-gp in both Y79 and HCT-15 cell line.

7.4.2 Expression of P-gp in transfected RB cells

The expression of P-gp protein was observed in RB cells transfected with pMDR1-EGFP and no band were observed in untransfected RB cells by western blot (**Figure 7.5a**).

Figure 7.5a: Expression of P-gp by western blot

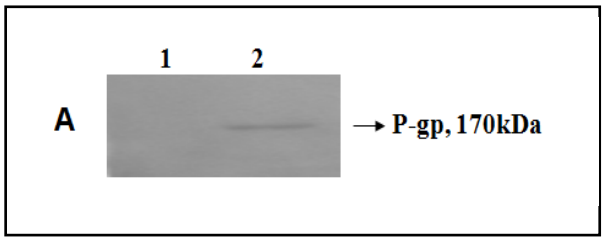

Figure 7.5a: Expression of P-gp in transfected RB cells: Lane 1: No P-gp band seen in untransfected RB cell line. Lane 2: Transfected cells show P-gp positive in RB cell line.

7.4.2.1 Effect of curcumin treatment on P-gp (MDR1) expression by RT-PCR and western blot analysis in RB cells

To verify if curcumin could modulate the P-gp expression, 2-10µM curcumin was added to the Y79-MDR1 transfected cells and examined after 72 hr. It was found that curcumin treated cells showed decrease in the expression of MDR1 mRNA and protein expression with increase in concentration of curcumin. The P-gp at 170kDa and β-actin (internal control) at 45kda was observed by western blot analysis **(Figure 7.5b).** The MDR1 and GAPDH (house keeping gene) mRNA expression in the Y79-MDR1 cells indicated bands at 193bp and 498bp respectively (**Figure 7.5c**). Values for the expression of MDR1 mRNA by Y79 cells after treatment with 2, 5 and 10µM were decreased by 92%, 77% and 61% respectively, in three independent experiments. Similarly the P-gp protein expression in Y79-MDR1 cells were decreased by 79%, 59% and 38% in curcumin treated cells when compared with the control cells **(Figure 7.5d, e).**

Figure 7.5 b& c

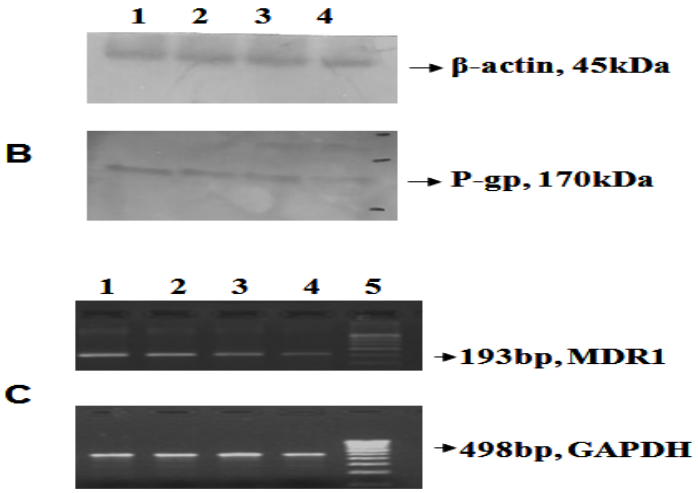

Figure 7.5d&e

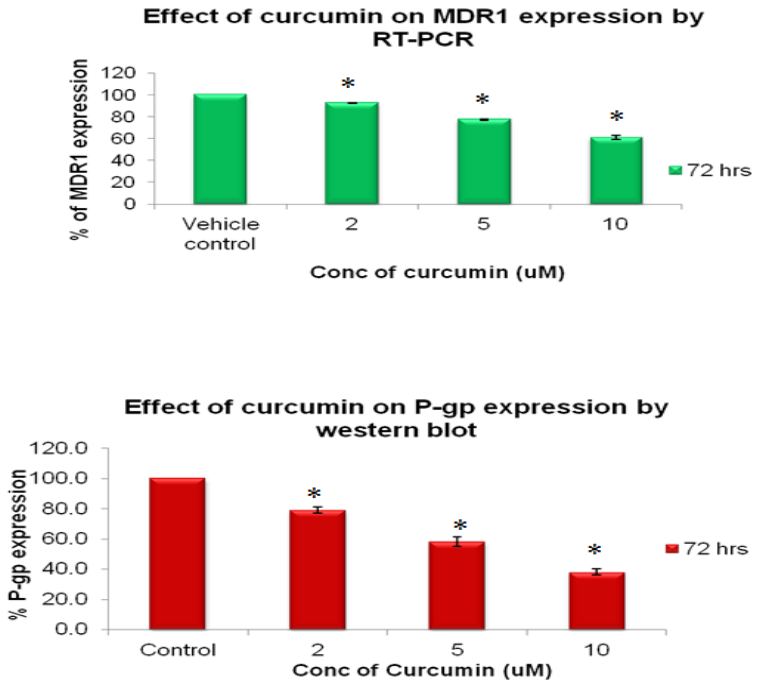

Figure 7.5: Effect of curcumin treatment on MDR1 mRNA and protein expression in RB cell lines: Dose-dependent effect of curcumin (2, 5, 10μM) after 72h on the MDR1 mRNA and protein expression in Y79 RB cells. **b**) MDR1 and GAPDH expression in the Y79 RB cells. **c**) MDR1 and β-actin expression in RB cells. **d&e**) Both mRNA and protein level of MDR1 showed decreased in the expression of MDR1 with increase concentration of curcumin, indicating that curcumin modulated the expression level of MDR1.

7.4.2.2 Effect of curcumin on MDR1 function by flow cytometry

To examine the function of P-gp on curcumin treated Y79-MDR1 cells, Rh123 accumulation and efflux were studied using flow cytometry. It was observed that curcumin treated RB cells showed increase in the accumulation of Rh123 in a concentration dependent manner and also showed a significant decrease in the efflux of Rh 123. The results were statistically significant when compared with the control values $p<0.05$ **(Figure 7.6).**

Figure 7.6: Functional study of P-gp using Rhodamine 123

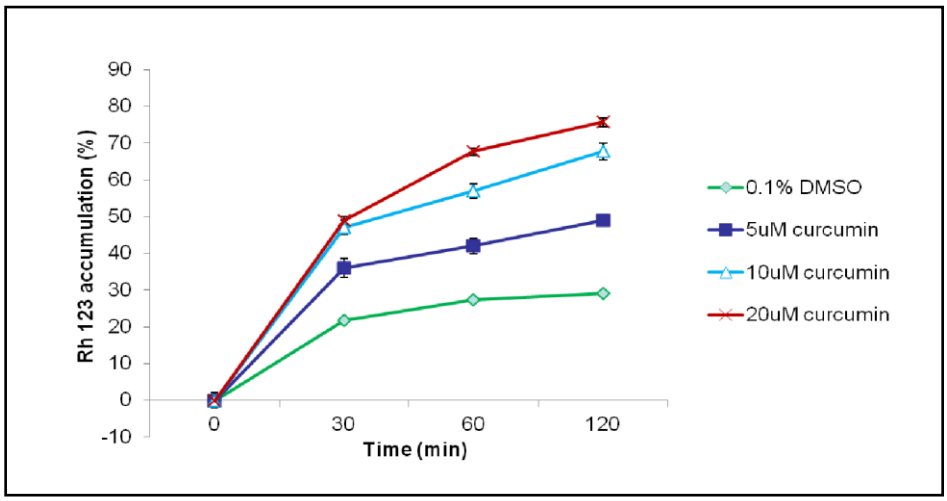

Figure 7.6: MDR1 functional study in Y79 RB cell line: Cells were treated with different concentration of curcumin (5,10 and 20µM) and vehicle control (0.1% DMSO). Rh 123 was added and the cells were incubated for different time intervals at 37^0C in the dark. Cells were then harvested and used immediately to measure Rh 123 fluorescence using flow cytometry. Data are mean ± S.D from three independent experiments.

7.4.2.3 Effect of curcumin on ATPase activity of P-gp

ATPase activity of P-gp was studied to assess the effect of curcumin on this transporter. Our results show that curcumin was able to stimulate the basal ATPase activity of P-gp at very low concentration, but inhibited the activity at higher concentration. This is indicative of curcumin's direct interaction with the P-gp. Moreover, we also observed the inhibition of verapamil stimulated ATP hydrolysis by P-gp, mediated by curcumin in Y79 RB cell lines **(Figure 7.7).**

Figure 7.7: ATPase activity of P-gp

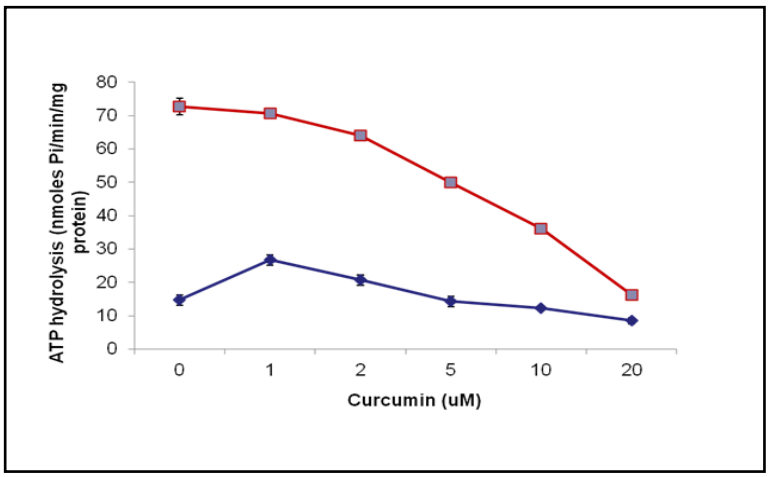

Figure 7.7: Effect of curcumin on basal and verapamil stimulated ATPase activity: Y79-MDR1 cells expressing P-gp (100µg of protein/ml) were incubated with increasing concentration of

curcumin in the presence of verapamil (■) or an equivalent volume of DMSO (♦) in the ATPase assay buffer. Value represents ±SE from at least three independent experiments.

7.4.2.4 Effect of curcumin on photoaffinity labelling of P-gp with 8-azido-ATP-biotin

To determine the interaction sites of P-gp with curcumin, photoaffinity labelling of P-gp was performed using 8-azido-ATP-biotin. Curcumin had no effect on 8-azido-ATP-biotin at 10µM concentration in Y79 RB cell line. The cross linking of 8-azido-ATP was inhibited in the presence of 10mM ATP. This suggests that curcumin produce their effect most likely by interacting at the substrate binding sites rather than at the nucleotide-binding sites of this protein (**Figure 7.8**).

Figure 7.8: Photoaffinity labelling study of P-gp

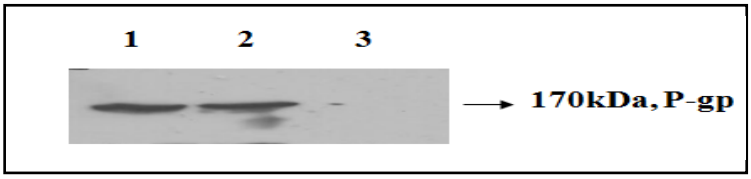

Figure 7.8: Crude membranes of (100µg protein) were incubated with 100µM 8-azido-ATP-biotin in the dark on ice for 5 min in the presence and absence of 10µM curcumin. The protein was electrophoresed, blotted and visualized with streptavidin horseradish peroxidase. The addition of 10mM ATP prevented photolabelling. Lane 1: 8-azido-ATP-bitoin, Lane 2: 10µM curcumin and Lane 3: 10mM ATP.

7.4.2.5 Molecular modelling of P-gp

Among the experimentally determined structures of ABC transporter super family, Multidrug resistance protein 1a (MRP 1a) of *Mus musculus* (PDBID: 3G5U) was found to be an appropriate template for human P-gp. Primary sequence analysis revealed that human P-gp and MRP 1a of *Mus musculus* sharing the sequence identity of 88% and similarity of 94% with an E-value of 0.0 and query coverage of 99% (34-1280) in comparison to other hits. Hence, three dimensional structure of human P-gp was generated with 3G5U as a template using Modeller9v7. The model was further optimized through energy minimization with a potential energy of -1.6654603e+05 kJ/mol. Like 3G5U, the optimized three dimensional structure of human P-gp is predominantly helical in TM domains and β-sheets in the NBDs (**Figure 7.9**).

Figure 7.9

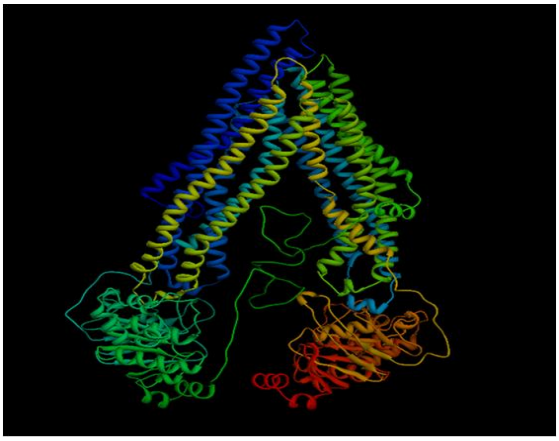

Figure 7.9: Homology based three dimensional structure of P-gp

The overall stereo chemical aspects of the model were assessed through Procheck. Psi-Phi distribution of the amino acids were inspected through Ramchandran plot, in which 88.8% of the residues in the most favoured region,9.3% in allowed region, 1.9% in additionally allowed region and no residues in disallowed region. Moreover, the overall quality of the model was evaluated by comparing the Z-score of generated model to the experimentally determined (**Figure 7.10a**).The interaction energy of each amino acid within the generated model was validated by checking the energetic aspect of the model calculated using ProSA, by plotting the energies as the function of amino acid sequence position. The plot revealed negative energy for maximum of residues with few residues having positive energy (**Figure 7.10b**).

Figure 7.10a&b:

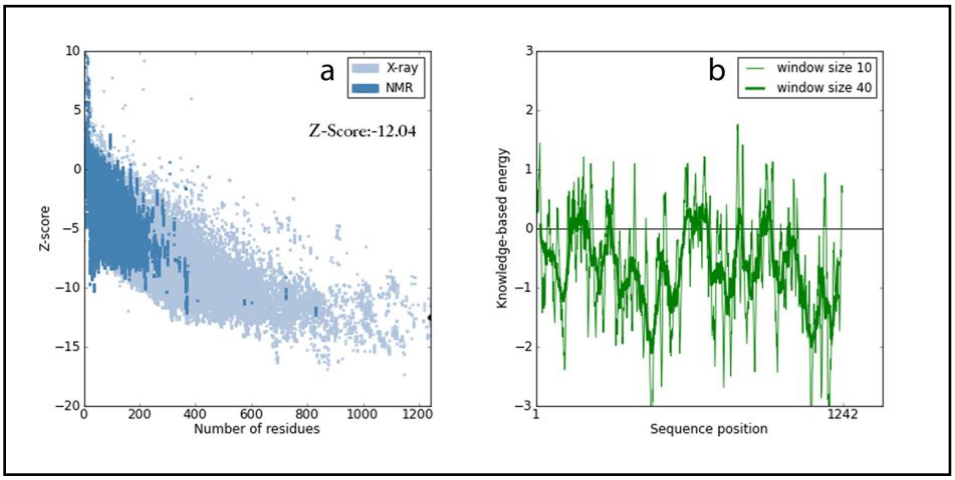

Figure 7.10: (a) Overall quality of the model assessed based on Z-score. Z-score of the generated structure is within the range observed for native set of proteins of same size. **(b)** Local Quality of the P-gp model assessed based on the energy plot calculated using ProSA.

The quality of the structural fold was assessed by comparing predicted model with experimentally determined through structural super positioning. RMSD of 0.47 and TM-score of 0.99830 were calculated using the more sensitive structural alignment algorithm, TM-align for the model/template. These score was suggestive of the generated model to share the same topology with high probability. Hence, the model validated at the geometrical and energetic aspects ensure the plausibility for future analysis. Further, binding site residues of the multi-domain protein P-gp was predicted using DEPTH with a threshold fixed to 0.50 (**Table 7.2**).

Table 7.2: Binding sites residues of P-gp predicted by DEPTH

	Residues spanning the binding site region
DEPTH	MET35,MET36,PHE39,MET42,THR43,PHE46, ALA47,TYR81,TYR274,TYR277,LEU299,PHE303, LEU306,ILE307,PHE310,GLN692,PRO693,PHE695, ALA696,PHE699,ILE703,THR707,ARG708,LEU729, LEU828,PHE924,ALA928,PHE938,GLU939,VAL941, LEU942,PHE945,SER946,ALA947,VAL948,VAL949, PHE950, ALA952 and MET953

7.4.2.6 Molecular Docking of P-gp with curcumin

Molecular docking studies were performed for the optimized three dimensional structures of P-gp with curcumin using LGA, to infer its inhibitory binding mode. Among the 100 conformers generated during the molecular docking analysis for P-gp, potential pose with lowest binding energy and highest binding affinity was selected for further analysis. Curcumin showed increased binding affinity towards P-gp with a binding energy of -7.66 kcal/mol and inhibitory constant of 2.42µM by establishing a network of bonded and non-bonded interactions with Leu32, Met35, Met36, Phe39, Phe161, Leu299, Thr300,Phe303, Ile307, Ser311, Met916 and Phe945 residing the transmembrane region and were proven to have drug interactions (**Figure 7.11a,b**).

Figure 7.11

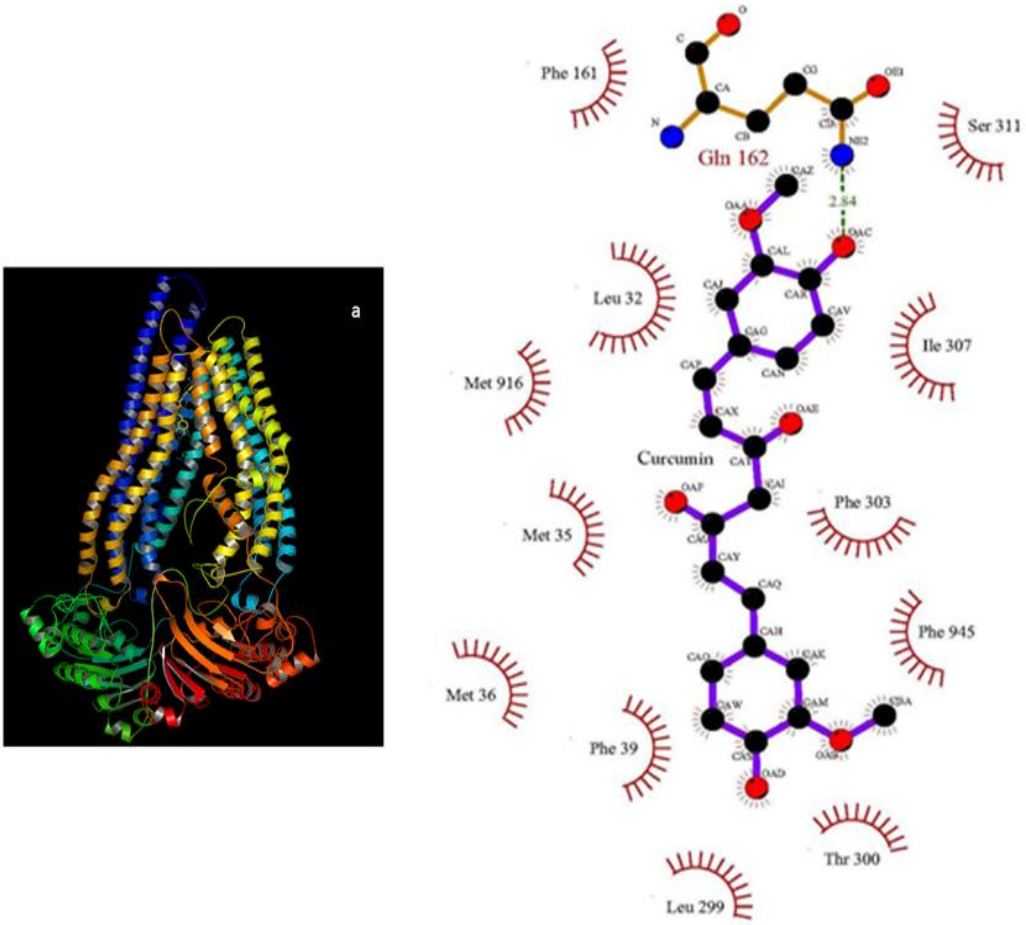

Figure 7.11: Molecular interactions observed between P-gp and Curcumin in 3D (**a**) using PyMOL and 2D (**b**) using LigPlot analysis.

7.4.3 MRP1

7.4.3.1 Effect of curcumin on MRP1 expression in RB cell line:

The Y79 RB cells treated with different concentrations of curcumin (2, 5 and 10µM) for 72 hours were detected by RT-PCR and western blot. It was found that the mRNA and protein level of MRP1 was similar to that of DMSO treated control RB cells, indicating absence of curcumin's effect on the MRP1 expression (**Figure 7.12a,b**).

Figure 7.12a,b: MRP1 expression by RT-PCR and western blot

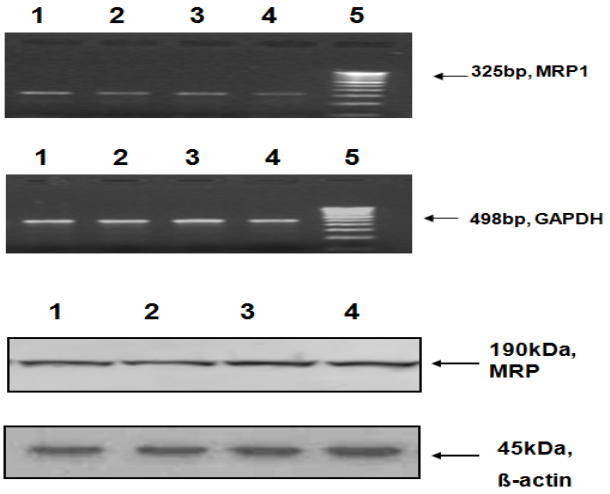

Figure 7.12: Effect of curcumin on MRP1 mRNA and protein expression in RB cell line: Dose-dependent effect of curcumin (2, 5, 10µM) after 72hrs on the MRP1 mRNA and protein expression in Y79 RB cells. **a**) MRP1 and GAPDH expression in the Y79 RB cells. **b**) MRP1 and β-actin expression in RB cells. Lane 1: Control cells, Lane 2: 2µM curcumin, Lane 3: 5µM curcumin, Lane 4: 10µM curcumin and Lane 5: Molecular weight marker. Both mRNA and protein level of MRP1 in curcumin treated was similar to the DMSO treated control, indicating that curcumin did not affect the expression level of MRP1.

7.4.3.2 Effect of curcumin on MRP1 function by flow cytometry:

The effect of curcumin on the MRP1 transport was tested by the accumulation of the fluorescent substrate calcein-AM using flow cytomtery. The Y79 cells were incubated with calcein-AM and the intensity of fluorescence substrate accumulated was measured by FACS. Accumulation of fluorescent substrate was found to be increased (to nearly 50%) in the curcumin treated cells, when compared with the controls **(Figure 7.13a).** Similarly, indomethacin and probenecid (MRP1 inhibitors) caused a significant increase in calcein accumulation at different time intervals in Y79 cell lines, which shows the involvement of MRP1 calcein efflux (**Figure 7.13b**), and the results were also found to be statistically significant with $p<0.05$.

Figure 7.13a

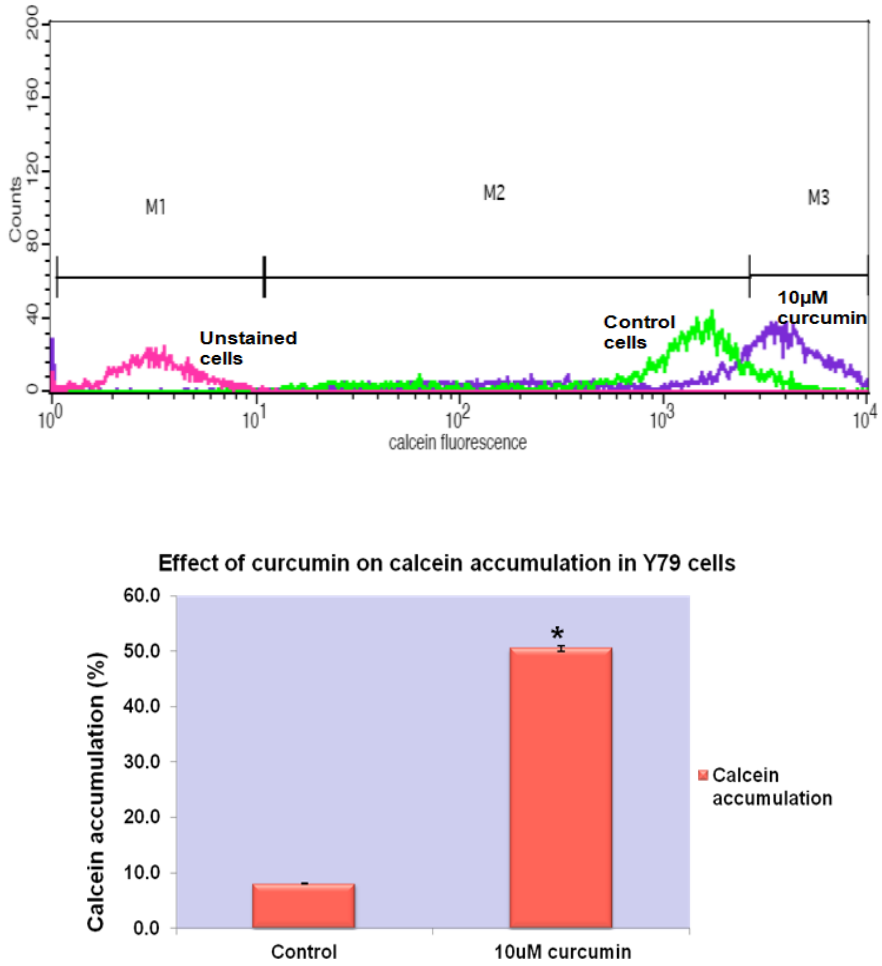

Figure 7.138a: Effect of curcumin on MRP1 function was assessed by measuring the accumulation of fluorescent substrate calcein-AM. Histogram showing peak in pink colour represents (unstained cells), green colour (control cells) and blue colour represents (10µM curcumin treated cells). Calcein accumulation is shown as bar diagram for n=3 experiments and are expressed as the mean ± S.D. * $p<0.05$, significantly different from the control.

Figure 7.13b

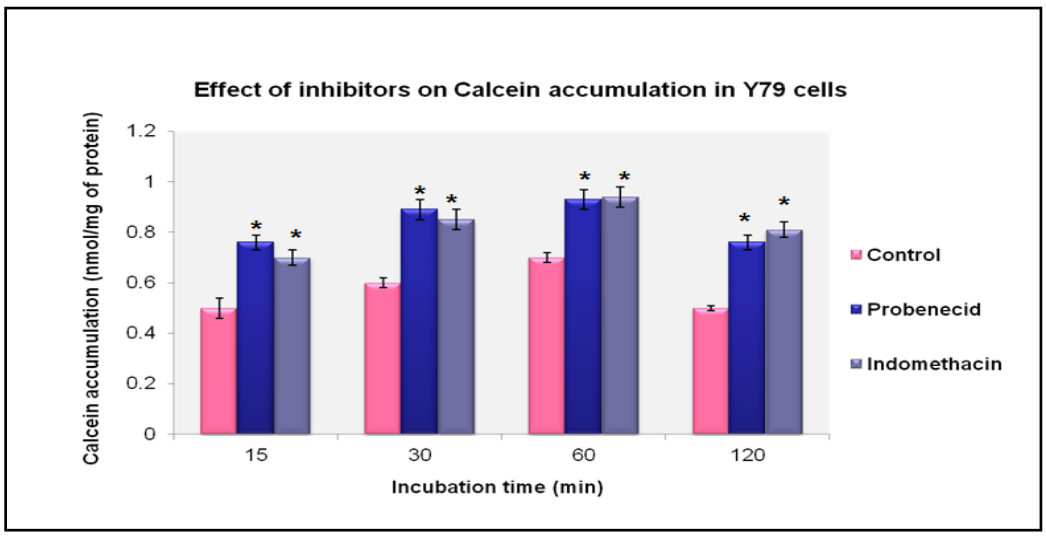

Figure 7.13b: Y79 cells were incubated with and without inhibitors (100µM indomethacin and 1mM probenecid) and the calcein accumulation was observed at different time intervals. Data are expressed as the mean ±S.D for n=3 experiments. ***** $p<0.05$ significantly different from the control.

7.4.3.3 Effect of curcumin on ATPase activity of MRP1:

ATPase activity of MRP1 in the presence of curcumin was studied to assess the effect of curcumin on this transporter. Our results show that curcumin was able to stimulate the basal ATPase activity of MRP1 at very low concentration, but inhibited the activity at higher concentration. This is indicative of curcumin's direct interaction with the MRP1. Moreover, we also observed the inhibition of quercetin stimulated ATP hydrolysis by MRP1, mediated by curcumin in Y79 RB cell lines (**Figure 7.14)**.

Figure 7.14: ATPase activity of MRP1

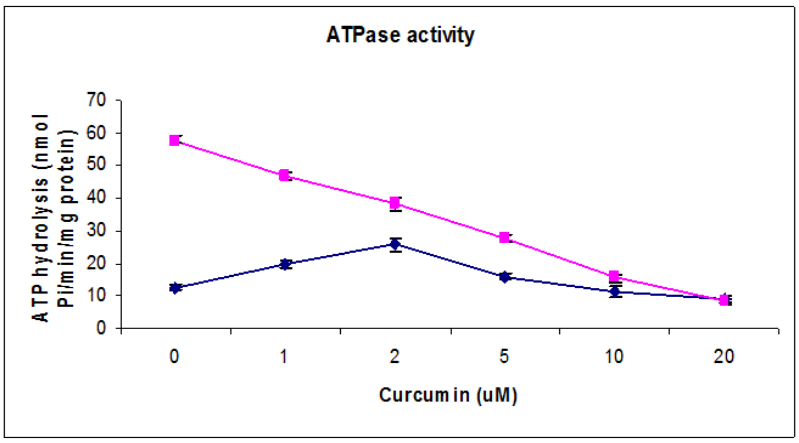

Figure 7.14: Y79 cells expressing MRP1 (100µg of protein/ml) were incubated with increasing concentration of curcumin in the presence and absence of quercetin in the ATPase assay buffer. The reaction was initiated by the addition of 5mM ATP and terminated with 2.5% concentration of SDS after 20 min of incubation; the amount of Pi released was quantitated by colorimeter. (●) MRP1 basal activity; and (■) quercetin-stimulated MRP1 ATPase activity in the presence of different concentration of curcumin. Value represents ±SE from at least three independent experiments.

7.4.3.4 Effect of curcumin on photoaffinity labelling of MRP1 by 8-azido-ATP-biotin:

To determine the interaction sites of MRP1 with curcumin, photoaffinity labelling of MRP1 was performed using 8-azido-ATP-biotin. Curcumin had no effect on 8-azido-ATP-biotin of MRP1 at 10µM concentration in Y79 RB cell line. The cross linking of 8-azido-ATP was inhibited in the presence of 10mM ATP. This suggests that curcumin produce their effect most likely by interacting at the substrate binding sites rather than at the nucleotide-binding sites of the MRP1 protein (**Figure 7.15)**.

Figure 7.15: Photoaffinity labelling study of MRP1

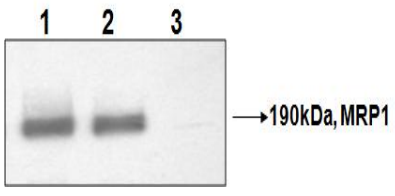

Figure 7.15: Crude membranes of (100µg protein) were incubated with 100µM 8-azido-ATP-biotin in the dark on ice for 5 min in the presence and absence of 10µM curcumin. The proteins were then immunoprecipitated with MRP1 antibody linked to agarose protein A beads. The immunoprecipitated protein was blotted and visualized with streptavidin horseradish peroxidase. The addition of 10mM ATP prevented photolabelling. Lane 1: 8-azido-ATP-bitoin, Lane 2: 10µM curcumin and Lane 3: 10mM ATP.

7.4.3.5 Homology Modelling of MRP1:

Among the experimentally determined structures of ABC transporter super family, SAV1866 (PDBID: **2HYD**) of *Staphylococcus aureus* was found to be an appropriate template for human MRP1 with optimal query coverage (300-1531). Thus, three dimensional structure of human MRP1 was generated based on the molecular modelling protocol implemented by M. K. DeGorter et al (De Gorter et al. 2008**).**The generated structural co-ordinates of human MRP1 was geometry optimized with a potential energy of -1.6761530e+05 kJ/mol. The resultant 3D structure of human MRP1 is predominantly helical in TM domains and β-sheets in the NBDs (**Figure 7.16)**

Figure 7.16

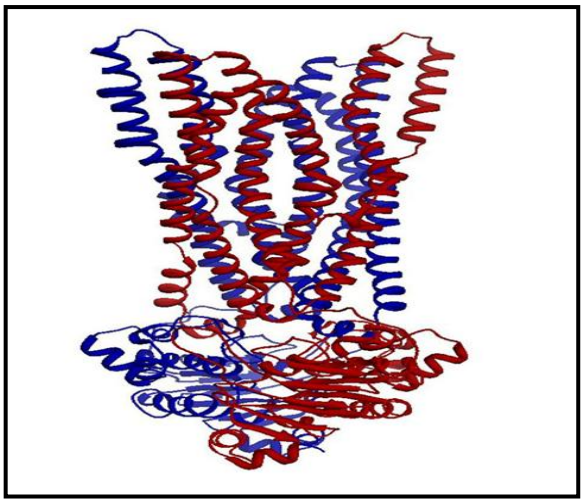

Figure 7.16: Homology based three dimensional structure of MRP1

The overall stereo chemical aspects of MRP1 were inspected through Ramchandran plot, in which 91.0% of the residues in the most favoured region with no residues in disallowed region**.** Moreover, the overall quality of the model was further ascertained to be good with a Z-score of -6.02 as calculated using ProSA. TM-score of 0.93037 was calculated using the more sensitive structural alignment algorithm, TM-align. This score was suggestive of the generated model to share the same topology of the template with high probability. Hence, the model validated at the geometrical and energetic aspects ensure the plausibility for future analysis.

7.4.3.6 Binding cavity analysis:

Binding site residues of MRP1 were predicted using CASTp (**Table 7.3**). For MRP1, the binding cavity of volume and area with 25694 and 9954.7 respectively was considered for the study. The amino acids residing in this cavity were proven to be involved in binding and transport of substrates (Deeley et al. 2006).

Table 7.3: Binding site residue of MRP1 predicted by CAS

Protein	Area (A^2)	Volume (A^3)	Residues spanning in the predicted binding cavity
MRP1	9954.7	25694	W309,K319,G322,P323,Y324,F325,M327,S328,F329,F330,F331,K332,A333,I334,H335,D336,L337,M338,M339,L369,V372,T373,Q377,V380,L381,Y384,F385,C388,F389,V390,S391,G392,M393,K396,V424,N425,S428,V429,Q432,R433,F434,M435,D436,L437,A438,T439,Y440,N442,M443,I444,W445,S446,A447,P448,Q450,L453,A454,V479,N480,M483,T487,Q491,H494,M495,K498,R501,I502,R532,E535,L536,K537,L539,S542,A543,L545,S546,A547,V548,G549,T550,F551,T552,W553,V554,C555,P557,F558,L559,V560,A561,L562,A587,L588,F589,N590,I591,L592,R593,F594,P595,L596,N597,I598,L599,P600,M601,V602,I603,S604,S605,I606,Q608,A609,V611,S612,F982,N985,H986,V987,S988,A989,L990,A991,S992,N993,Y994,W995,L996,S997,W999,G1032,Y1033,S1034,M1035,A1036,V1037,S1038,I1039,G1040,G1041,I1042,L1043,S1045,R1046,C1047,L1048,H1049,V1050,D1051,L1053,H1054,L1057,L1080,V1083,D1084,S1085,M1086,I1087,P1088,E1089,V1090,I1091,K1092,F1094,M1095,G1096,F1099,N1100,V1101,I1102,G1103,A1104,V1107,L1110,S1137,R1138,Q1139,L1140,K1141,E1144,S1145,R1148,Y1152,K1187,Y1190,P1191,I1193,V1194,A1195,R1197,W1198,V1201,R1202,L1203,E1204,C1205,V1206,G1207,N1208,L1212,V1234,S1235,S1237,L1238,Q1239,T1241,T1242,Y1243,L1244,N1245,W1246,L1247,V1248,R1249,M1250,S1251,S1252,E1253, M1254,E1255 and T1256

7.4.3.7 Molecular Docking of MRP1 with curcumin and ATP:

Molecular docking studies were performed for the optimized three dimensional structure of MRP1 with curcumin using LGA, to infer its binding mode. Among the conformers generated, potential pose with lowest binding energy and highest binding affinity was selected for analysis. Curcumin showed bonded and non-bonded interactions with the substrate binding site of MRP1 with the binding energy and inhibitory constant of -7.39 kJ/mol and 3.82µM, respectively. Further, interaction analysis of MRP1 with curcumin showed hydrogen bonding interactions Tyr384, Gln450 and Arg1249 and non bonded interactions with Tyr324, Phe385, Met443, Ser446, Ala447, Ile598, Val1194, Trp1198, Val1248 and Ser1252 (**Figure 7.17**) (**Table. 7.4**).

Figure 7.17: Molecular interaction between curcumin and MRP

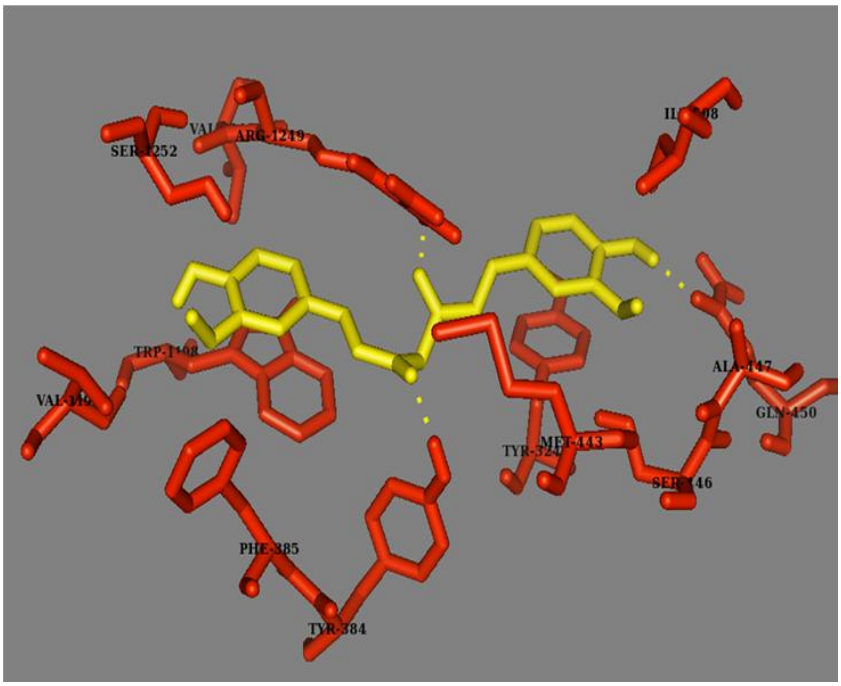

Figure 7.17: Molecular interaction observed between MRP1 with Curcumin. Binding site residues (RED) of MRP1 and Curcumin (Yellow) represented in sticks. The bonded and non-bonded interactions are visualized through PyMOL with H-bonded interaction represented through yellow colour dashed lines.

Table 7.4: Interaction analysis of MRP1 with curcumin

Protein	Predicted Binding Energy (kJ/mol)	Inhibitory constant (Ki)	Interacting Residues (Bonded and Non bonded contacts)
MRP1-Curcumin	-7.39	3.82µM	Tyr324,Tyr384,Phe385,Met443, Ser446,Gln450,Ala447,Ile598,Val1194,Trp1198,Val1248, Arg1249 and Ser1252

7.4.4 LRP

7.3.4.1 Effect of curcumin treatment on LRP expression

In our study, we found that curcumin treatment showed a decrease in the expression of LRP with increase concentration of curcumin in RB cell line by RT-PCR. With the 72hrs curcumin (2, 5 and 10µM) treatment, the LRP mRNA expression was decreased by 19.2%, 30% and 47.6% respectively. Similarly the

expression of LRP at 110kDa and β-actin at 45kda was observed by western blot analysis. LRP protein expression in the immunoblot was decreased 17.7%, 32.3% and 48.7% respectively **(Figure 7.18a&b)**.

Figure 7.18a

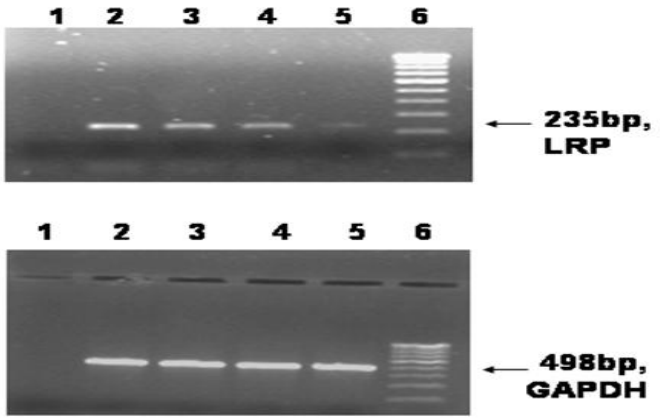

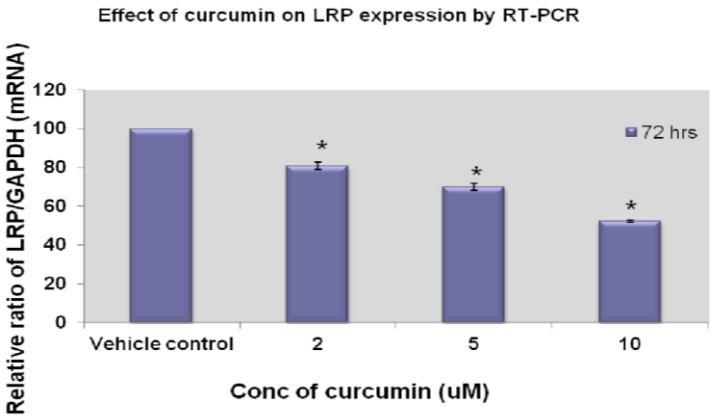

Figure 7.18a: LRP and GAPDH mRNA expression by RT-PCR in Y79 RB cell lines. Lane 1: Negative control, Lane 2: Control, Lane 3: 2µM curcumin, Lane 4: 5µM curcumin, Lane 5: 10µM curcumin and Lane 6: Marker. For LRP mRNA studies, data is expressed as the mean ratio of LRP/GAPDH mRNA band density. Data for LRP mRNA are expressed as the mean ± SEM. for three independent experiments (n=3). * Indicates significant difference.

Figure 7.18b

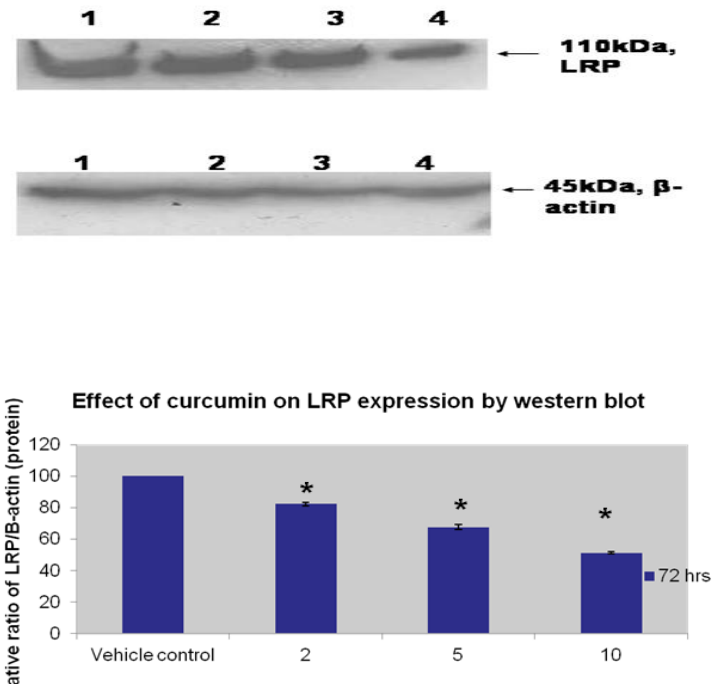

Figure 7.18b: LRP and β-actin protein expression in Y79 RB cell line. Lane 1: Control, Lane 2: 2µM curcumin, Lane 3: 5µM curcumin and Lane 4: 10µM curcumin. Densitometric analysis for the LRP expression. For LRP protein expression, data is expressed as the mean ratio of LRP/β-actin band intensity. Data for LRP mRNA and protein are expressed as the mean ± SEM. for three independent experiments (n=3). * Indicates significant difference.

7.4.4.2 Structural optimization of LRP (*In silico*)

Three dimensional co-ordinates of the LRP functional repeats elucidated through NMR (PDBID: **1Y7X**) was optimized by energy minimization, which resulted the structure with the potential energy of -1.2323199e+05 kJ/mol. Ramachandran plot for the model showed 88.0% of the residues in the most favored region with no residues in the disallowed region . G-factor of -0.23 is indicative of the optimal and plausible three dimensional structures (**Figure 7.19a**).

Figure 7.19a

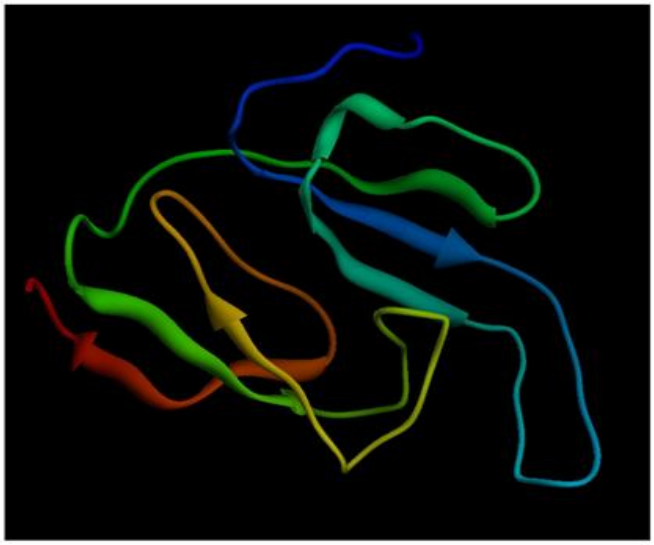

Figure 7.19a: NMR structures of major vault repeats

7.4.4.3 Molecular docking of LRP with curcumin

Molecular docking analysis of LRP-curcumin complex showed binding energy of -5.7 kJ/mol and inhibitory constant of 66.37µM. Curcumin docked complex with LRP showed bonded interactions at Trp35, Ile44 and Arg46; non-bonded interactions at Phe37, Glu38, Gly39, Tyr43, Val49, Arg77 and Asp78, which is the proven vault poly (ADP-ribose) polymerase binding site that mediates drug interaction (**Figure 7.19b, Table 7.5**).

Table 7.5: Molecular interaction observed between LRP and curcumin.

Protein	**Predicted binding energy (KJ/mol)**	**Inhibitory constant (Ki)**	**Interacting residues (polar and non-polar contact)**
LRP	-5.7	66.37µM	Trp 35, Phe 37, Glu 38, Gly 39, Tyr 43, Ile 44, Arg 46, Val 49, Arg 77, Asp 78

Figure 7.21b

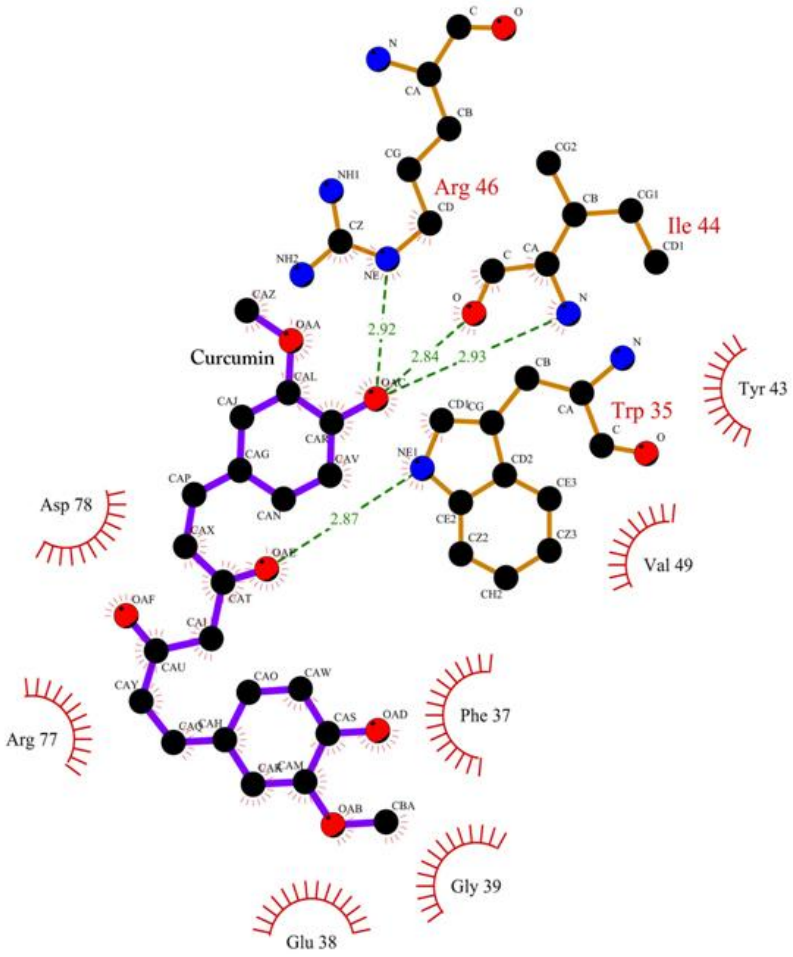

Figure 7.19b: 2D representation of the molecular interaction of LRP with Curcumin through LigPlot analysis

7.5 Discussion:

Our studies showed that curcumin inhibits cell proliferation and induces apoptosis in RB cells, which is indicative of its anti-cancer property. However, anti-cancer drugs may fail to destroy cancer cells due to drug resistance mechanism. **Over-expression of MDR proteins in RB tumours is a major obstacle for successful chemotherapy** (Wilson et al. 2006). Several of the transmembrane drug efflux pumps belong to the ATP-binding cassette (ABC) protein family, such as MDR, MRP, that confers drug resistance by pumping various anti-cancer agents (Lee et al. 2004; Szakacs et al. 2006). Another protein named lung resistance protein (LRP) is also involved in intracellular

redistribution of drugs, thereby reducing concentrations at the target site (Izquierdo et al. 1996). Chemoreduction with carboplatin, vincristine, etoposide (CEV) plus cyclosporin (CSA) is used as a first-line therapy in the clinical management of advanced RB. It has been found that cyclosporine administered as an adjuvant are known to reverse multi-drug resistance and improves long-term response to chemotherapy in RB patients (Chan et al. 1996). However, Eckstein et al have reported that neurotoxicity is associated with CSA therapy. They also showed that CSA is directly cytotoxic to RB cells through inhibition of calcineurin (CN)/ nuclear factor of activated T-cells (NFAT) signalling (Eckstein et al. 2005). Thus, various modulators have been identified to reverse MDR mechanisms and sensitize MDR cancer cells to anti-cancer agents without causing any side effects (Anuchapreeda et al. 2002). It has been studied that **curcumin, a natural phenolic compound serves as an inhibitors of ABC transporters** (Chearwae et al. 2006). The aim of the current study was to determine the expression of MDR (P-gp, MRP1 and LRP) in RB cell line and to further assess whether curcumin modulates the expression of these MDR proteins by *in vitro* and *in silico* studies.

In Y79 RB cells, P-gp was not expressed at the protein level and thus in the present study, P-gp was over-expressed by transfection in RB cells and the effect of curcumin on MDR1 modulation was studied. The effect of curcumin on the MDR1 gene (P-gp) expression was determined by western blotting and RT-PCR in Y79-MDR1 RB cells. The result showed that **curcumin inhibited the MDR1 gene expression at the mRNA and protein level in Y79-MDR1** cells. We also investigated the effect of curcumin on the P-gp function in Y79-MDR1 cells using Rhodamine 123. Curcumin caused an increased in the accumulation of Rh123, and inhibited its efflux in a concentration dependent manner, but had no effect on the untransfected RB cells. These results are quite similar to the work done by Tang et al, where they have shown modulation of P-gp expression and function by curcumin in multi-drug resistant human gastric carcinoma cell line (Tang et al. 2005). An ATPase assay was performed, which clearly demonstrated that curcumin inhibited verapamil stimulated ATPase activity of P-gp at higher concentration. These findings were further supported by the effect of curcumin on the photoaffinity labelling study, which showed that **curcumin had no effect on the binding of 8azido-ATP-biotin**. These results clearly demonstrates that

curcumin interact at the substrate binding site of P-gp and not on the nucleotide binding region. Further, **molecular docking studies also concurrently infer the binding of curcumin into the substrate binding site of P-gp with a binding energy of -7.66 kcal/mol**.

The effect of curcumin on **MRP1 mRNA and protein level did not show any change in the expression in RB cell line**. Cellular accumulation and the efflux studies were performed in Y79 RB cells employing calcein-AM as substrate for MRP1. In an earlier study, it was reported that curcumin inhibited MRP1 transport by increasing the accumulation of fluorescent substrate calcein-AM and fluo4-AM using flow cytometry HEK-293 cells (Chearwae et al. 2006). In our study, we also found that there was a 30% increase in the accumulation of fluorescent substrate calcein-AM on curcumin treated Y79 cells by flow cytometry analysis. Similarly, indomethacin and probenecid (MRP1 inhibitors) caused a significant increase in calcein accumulation at different time intervals in Y79 cell lines, which show that MRP1 is involved in the efflux of calcein.

Similar to P-gp, **curcumin was also able to stimulate the ATPase activity of MRP1 at low concentration**, but there was an inhibition of activity at higher concentration, which can be attributed to curcumin's interaction with MRP1's binding site. Further, our results also showed the inhibitory activity of curcumin on quercetin stimulated ATP hydrolysis by MRP1 in a dose dependent manner. In MDCK II cells, the inhibitory activity of curcumin on both MRP1 and MRP2 mediated transport demonstrated that glutathione dependent metabolism of curcumin play an important role in MRP1 inhibition (Wortelboer et al. 2003). To ascertain the probable curcumin interaction sites on MRP1, photoaffinity labelling of MRP1 was performed. This was done using 8-azido-ATP-biotin, an analog of ATP, which has been already to bind specifically to the nucleotide binding domain of P-gp and MRP (Chearwae et al. 2006). Subsequently, in the post labelling experiments we found the lack of curcumin's effect on 8-azido-ATP-biotin binding to MRP1 at 10μM concentration in Y79 cell lines. This suggests that curcumin produces its effect most likely by interacting at the substrate binding sites rather than at the nucleotide-binding sites of the MRP1 protein to modulate ATP hydrolysis. In the present study, docking interaction analysis of MRP1-curcumin complex showed network of bonded and non bonded interactions with Curcumin interacting to the amino acid residues residing in the

documented substrate binding region. **Docking studies also inferred that oxygen atoms of phenolic and methoxy functional groups spanning terminal phenyl rings of curcumin to play a crucial role for inhibitory action**.

The expression of LRP mRNA and protein level was **decreased with increase concentration of curcumin, indicating that curcumin inhibits LRP in Y79 cells**. Curcumin, a known inhibitor of the signal transducers and activators of transcription protein (STAT) mediated transcription, blocked IFN-γ induced LRP expression in a dose-dependent manner. These phytochemicals are potent antioxidant and an anti-inflammatory agent that suppresses pro-inflammatory cytokines including TNF-α, IL-1β and nitric oxide synthase (NOS) (Steiner et al. 2006). Similarly in our study, we have found that the expression of LRP is modulated by curcumin. **LRP-Curcumin docked complex also showed bonded interactions at Cys73, Lys74 and Thr84 and non-bonded interactions at Ala70, Trp75, Arg82, Val83 and Gly85, which is the proven vault poly (ADP-ribose) polymerase binding site that mediates drug interaction** (Kozlov et al. 2006).

These results show that curcumin reverse MDR in RB cells and further the *in silico* studies also support our experimental data, which indicate curcumin may be used in combination with conventional chemotherapeutic drugs to reverse MDR in RB cells.

7.6. Chapter summary

- The expression of MDR proteins (P-gp, MRP1 and LRP) was observed in Y79 RB cells RT-PCR, wherein the expression of P-gp is absent at the protein level.
- RT-PCR and western blot study showed the inhibitory effect of curcumin on P-gp and LRP protein in Y79 RB cells
- Western blot and RT-PCR analysis did not show any correlation of MRP1 expression with increase in concentration of curcumin. The inhibitory effect of curcumin on MRP1 function was observed as a decrease in the efflux of fluorescent substrate calcein.

- Curcumin did not affect 8-azido-ATP-biotin binding to P-gp and MRP1, which is indicative of curcumin's interaction with the substrate binding site and not on the ATP binding domain.
- *In silico* docking simulation studies of MDR proteins provide deeper insights into the molecular interactions, thereby inferring the potential binding mode of curcumin into the substrate binding site of MDR proteins.

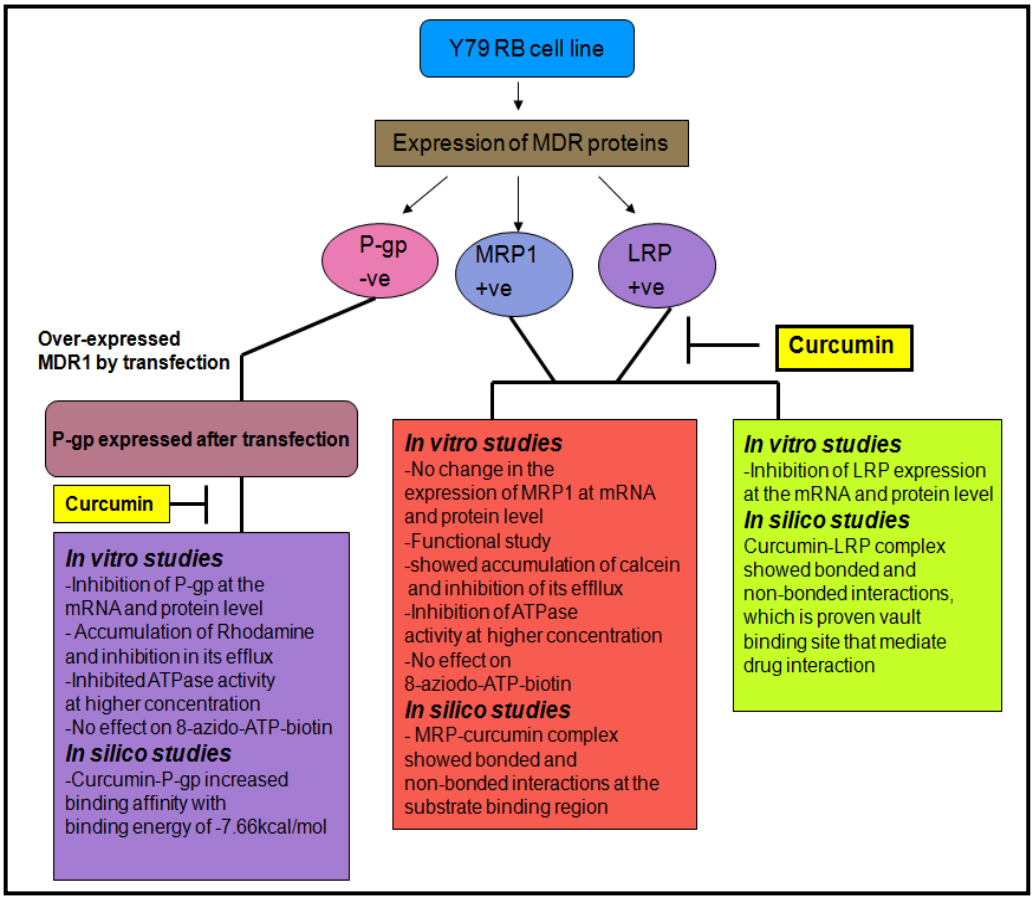

Figure 7.20: Schematic representation of effect of curcumin on the expression of drug resistance protein in RB cell line.

This work has been published in

MRP1: **Bioinformation, 8(1): 013-019, 2012:** *In vitro* and *in silico* studies on inhibitory effects of curcumin on multi-drug resistance associated protein (MRP1) in retinoblastoma cells.

LRP: **Current Eye Research, 34(10): 845-51, 2009:** Effect of curcumin on lung resistance related protein (LRP) in retinoblastoma cells.

P-gp: **Pharmacology and pharmacotherapeutics:** Modulation of MDR1 expression and function in retinoblastoma cells by Curcumin (In press).

CHAPTER 8: SYNERGISTIC EFFECT OF CURCUMIN IN COMBINATION WITH ANTICANCER AGENTS ON HUMAN RB CELL LINES

8.1 Introduction

In cancer treatment it is common to use multiple therapies, usually a combination of chemotherapy, surgery, and/or radiotherapy. Cancer chemotherapy implicates the use of anticancer drugs to treat malignant disease. Today, several cytotoxic compounds are available and from experience it is known which drugs are most suitable for a specific cancer type. However, most anticancer drugs lack tumour specificity and cause damage to normal tissues, leading to side effects. Chemotherapeutic drugs are usually used in combination to give a more effective result. Cytotoxic agents with different mechanisms of action can together contribute to effective tumour killing with fewer side effects, because lower doses of each drug can be used. If possible, solid tumours are often removed by surgery or irradiation and chemotherapeutic drugs can then be used as adjuvants.

8.1.2 Chemotherapy in RB cancer:

Chemotherapy drugs (carboplatin, etoposide and vincristine-CEV) have become an important modality for the treatment of RB in an effort to preserve eye vision and avoid enucleation (Souza Filho et al. 2005). However, the treatment of cancer cells to chemotherapy is often limited due to development of drug resistance. Cancer cells that exhibit multi-drug resistance phenomenon will decrease the intracellular accumulation of drug and enhanced its efflux due to the over-expression of drug resistance proteins like P-glycoprotein (P-gp), multi-drug resistance associated protein (MRP) and lung resistance-related protein (LRP) (Stavrovskaya et al. 2000). In our earlier study we found that, prior to chemotherapy, the expression of P-gp and the LRP in RB tumours (Krishnakumar et al. 2004). It has been reported that in RB patients the use of cyclosporine reverses multi-drug resistance and also increased the intracellular concentration of chemotherapeutic agents (Chan et al. 1996). However, the use of cyclosporine has some drawback due to its neurotoxicities to the cells which may contribute to the morbidity of chemotherapy in these children, who are from a poor socioeconomic background (Eckstein et al. 2005; Chantada et al. 2008).

8.1.3 Use of natural compounds to reduce adverse effect of chemotherapy

Many natural dietary agents present in fruits, vegetables, and spices have drawn much attention from researchers and the general public for their potential in chemoprevention and therapy, and many of them are currently under early phase clinical trials. Natural compounds (ginseng, curcumin, emodin, genistein, apegenin, quercetin) could conceivably increase the efficacy of chemotherapy and radiotherapy through several means. Many animal studies have reported, in fact, that beneficial interactions can be produced between natural compounds and chemotherapy (Boik et al. 2001). Different goals can be envisioned by combining natural compounds with chemotherapy:

1) Natural compounds could diminish the side effects of chemotherapy so that higher, more effective doses could be given with more safety.
2) Natural compounds might overcome cell resistance to chemotherapy or otherwise increase drug accumulation in cancer cells.
3) They produce additive or synergistic cytotoxic effects with chemotherapy.
4) They could modify tumour environment to enhance local delivery of chemotherapy drugs.
5) Immune stimulant drugs could be used to enhance local delivery of chemotherapy drugs.
6) Chemotherapy could be utilized to maximally reduce tumour volume, and then followed by natural compounds to restore immune system and enhance immunologic elimination of any remaining microscopic tumours (Dillmann et al. 1990).

8.1.4 Curcumin as chemosensitizer:

Curcumin is one of the most studied chemopreventive agents. It is a natural compound extracted from rhizome of *Curcuma longa* that allows suppression, retardation or inversion of carcinogenesis. Its particular toxicological profile (8g/day) has allowed the development of a large number of phase II studies. As a chemopreventive agent, curcumin is currently in phase II studies in colorectal cancer patients. Curcumin has shown protective effects in animals in combination with chemotherapy. Curcumin also increased the effectiveness of chemotherapy; 28 mg/kg given orally in combination with cisplatin reduced the progression of

fibrosarcoma in rats (based on analysis of tumour marker enzymes) more effectively than cisplatin alone (Navis et al. 1999).

Curcumin not only acts as a cancer preventive, but also eliminate chemoresistant cancers by sensitizing these tumors to chemotherapy and radiation by increasing the rate of apoptosis. Results from in vivo and in vitro studies have showed the potential chemosensitizing ability of curcumin in multiple cancers and have provided evidence for curcumin's use singly or as an adjunct to current chemotherapeutic drugs.

Thus in the present study, we want to determine whether combining curcumin with chemotherapeutic agents would be a better therapeutic outcome in RB.

8.2 Objective

- To study the sensitivity, apoptosis and cell cycle kinetics to carboplatin, etoposide and vincristine in combination with curcumin were analyzed in RB cell lines.
- To study the drug interactions using median effect/isobologram method and combination index for characterizing the interaction as additive or synergistic.

8.3 Materials and methods:

8.3.1 Reagents

Curcumin was purchased from Sigma Chemical Co. (St. Louis, USA) and dimethyl sulphoxide (DMSO) from Merck Chemicals. RPMI 1640 was purchased from Gibco BRL (Grand Island, USA). Fatal bovine serum and antibiotic-antimycotic solution were purchased from Himedia Laboratories Pvt. Ltd. (Mumbai, India). All other chemicals and reagents were of the highest grade commercially available.

8.3.2 Cell lines and culture conditions

Y79 and Weri RB cell lines were obtained from the Riken Cell Bank (Japan). The cells were maintained in RPMI-1640 medium supplemented with 20% fatal bovine serum, 50ng/mL of streptomycin and 1.25ng/mL of Amphotericin B at 37^0c in a humidified incubator with 95% air and 5% CO_2.

8.3.3 Drugs

Curcumin and etoposide was dissolved in DMSO and stored, protected from light, as a concentration solution at -20^{o}C. Chemotherapy drugs (carboplatin and vincristine) were made in sterile distilled water and stored at -20^{o}C. Each compound was diluted in culture medium on the day of experiment with DMSO concentrations never exceeding 0.1%.

8.3.4 Chemosensitivity assay

RB cell lines were harvested at confluence and plated into 96-well tissue culture plates, at a density of $5x10^3$ cells/well and allowed to incubate overnight. Next day the plating medium was replaced with 0.1ml fresh culture medium containing the vehicle control, curcumin, or a combination of curcumin and CEV. Cells were incubated for additional 3 days. To quantitate cell viability, 5µl of MTT (5mg/ml) was added to each well and the plates were allowed to incubate for 4 hr at 37^0c in a humidified atmosphere of 5% CO_2. Absorbance was read with an ELISA plate reader (Bio-Tek Instruments, VT, USA) at a wavelength of 540nm. Growth inhibition was calculated as the percent difference between drug-treated cells and vehicle control cells. Each experiment was carried out in triplicate.

8.3.5 Isobologram analysis of interactions between curcumin and CEV

Dose-effect retaionships between curcumin and CEV were analyzed with the software program Calcusyn (Biosoft, Cambridge, UK). Data from growth inhibition assays for individual drugs, as well as combinations of the two drugs, were entered into CalcuSyn to produce median-effect plots from which isobologram were constructed.

The combination index (CI) = d1 / D1 + d2 / D2, where *d1* and *d2* represent the doses of chemotherapeutic agents and curcumin used in combination required to produce a fixed level of inhibition IC50, while D1 and D2 are their concentrations able to produce alone the same magnitude of effect (50% inhibition of cell growth). If CI values is less than 1, the effect of combination is synergistic, whereas if CI=**1 or greater than 1 the effect is additive or antagonistic, respectively (**Chou et al. 1984). The dose-reduction index (DRI) is a measure of how much the dose of each drug in a synergistic combination can be

reduced and still produces an effect level comparable to that for each drug alone. The DRIs for two drugs are derived from combination index values such that DRI1 = D1 / d1 and DRI2 = D2 / d2 (Chou et al. 1988).

8.3.6 Curcumin uptake in RB cells

The ability of RB cells to absorb curcumin was quantified using flow cytometry. Cells were treated for 48h with different concentration of curcumin or combination of curcumin and CEV in RB cells. After the incubation period the cells were washed thrice with ice cold PBS. Since curcumin exhibits a green fluorescent signal, the cells were analysed using FACScalibur flow cyotmeter (BD). Fluorescence was detected through a 575nm band filter and quantified using CellQuest Software (Becton Dickinson; Franklin Lakes, NJ). Quantification results are presented as percent increase of mean fluorescence intensity of the curcumin treated samples, compared to untreated cells in triplicate experiments (Chignell et al. 1994; Kunwar et al. 2008).

8.3.7 Cell cycle distribution analysis

RB cell lines were treated with curcumin (5 and 10µM) and different concentration of CEV for 48 hr, then harvested by centrifugation, washed twice with ice-cold PBS, and fixed by 70% ethanol at -20^{o}C overnight. The fixed cells were then washed twice with ice-cold PBS and treated with 10 mg/ml RNAse for 30 min at 37^{o}C. Cells were stained with propidium iodide buffer (0.1 mM EDTA, 0.1% Triton X‑100, 50 mg/ml propidium iodide, PBS pH 7.4) for 15 min in the dark at room temperature. Cell cycle distribution was analyzed on a BD FACSCalibur flow cytometer. Data for 10,000 cells per sample were collected and analyzed using CellQuest software programs (BD Biosciences, San Jose, CA, USA).

8.3.8 Annexin V/Propidium staining assay

RB cell lines ($1x10^5$cells/cm^2) were plated in 12-well plate for overnight at 37^0c. After overnight incubation, the cells were treated with different concentration of curcumin and CEV and incubated for 48 hr. AnnexinV-fluos staining was performed using an AnnexinV-fluos apoptosis detection kit (Roche, Indianapolis)

in accordance with the manufacturer's instructions. In brief, treated cells were centrifuged, re-suspended in 100µl of Annexin-V-Fluos reagent and incubated for 10-15min at RT in the dark. After incubation period, flow cytometry analysis was immediately performed. Data acquisition and analysis were performed by a FACSCalibur flow cytometer using Cell Quest software. Cells that were Annexin V (-) and PI (-) were considered viable cells whereas cells that were Annexin V (+) and PI (-) or Annexin V (+) and PI (+) were considered early stage or late-stage apoptotic cells, respectively.

8.3.9 Measurement of caspase 3 activity

RB cell lines ($1x10^6$cells/cm^2) were plated in 12 well plates and treated with curcumin -CEV combination and incubated for 48 hr. Cells were washed with ice-cold PBS and resuspended in a buffer containing 5mmol/L Tris (pH 8), 20mmol/L ethylenediamine tetraacetate (EDTA) and 0.5% Triton-X 100 on ice for 30 minutes. After incubation, lysates were centrifuged for 5 minutes at 13,000rpm and the clear supernatant was taken for caspase activity. Reactions were carried out with 50µg of protein, 20mmol/L4-(2-hydroxyethyl)-1-piperazineethanesulfonic acid (HEPES) (pH 7), 10% glycerol, 2mmol/L dithiothreitol and 200 µmol/L *N*-acetyl- Asp-Glu-Val-Asp (DEVD)-*p*NA substrate (caspase 3). Reaction mixtures were placed into a flat-bottomed mitrotiter plate and read with a 405 nm filter using a microtiter plate reader. Caspase activities were detected by measuring the proteolytic cleavage of the colored substrates.

8.3.10 Statistical analysis

Data were presented as mean values±standard deviation (SD). Statistical comparisons between groups were performed by one-way analysis variance (ANOVA) followed by Students's test. Value of * $p<0.05$ was considered as statistically significant.

8.4 Results

8.4.1 Dose response of curcumin and chemotherapy drugs in RB cell lines

Cell proliferation assay was performed to determine the ability of curcumin and chemotherapy drugs to inhibit growth of RB cell lines. IC50 were determined for

curcumin and chemotherapy drugs, for both the RB cell lines and presented in **Table 8.1.** The percentage inhibition data indicate that all the compounds possess anti-proliferative effect with varying concentration of the particular drug in RB cell lines.

Table 8.1: IC_{50} values for curcumin and chemotherapy drug effects on RB cell lines

Drugs	**Y79 cell line**	**Weri cell line**
Curcumin	30µM	25µM
Carboplatin	30µg/ml	35µg/ml
Etoposide	2µg/ml	5µg/ml
Vincristine	1nM	50nM

IC_{50} values calculated as mean ± SD concentration required for 50% inhibition of proliferation from triplicate values.

8.4.2 Effect of curcumin in combination with CEV in RB cell lines

As both curcumin and chemotherapy drugs were effective in inhibiting cell growth, we next examined their effects in combination treatment. The RB cell lines were treated with 5 and 10µM doses of curcumin in combination with various concentrations of chemotherapy drugs, to determine if the combination of curcumin+ CEV results in a synergistic effect. The combination of:

a) 5µM curcumin & 0.1-5µg etoposide inhibited cell growth by 47-67% and 25-63% in Y79 and Weri cells, respectively
b) 10µM curcumin and 0.1-5µg etoposide inhibited cell growth by 53-68% and 33-65% in Y79 and Weri cells
c) 5µM curcumin and 5-30µg carboplatin inhibited cell growth in Y79 and Weri cells by 25-65% and 22-61%
d) 10µM curcumin and of 5-30µg carboplatin inhibited cell growth by 39-57% and 27-60% in Y79 and Weri cells
e) 5 and 10µM curcumin with different combination of 0.1-5µM vincristine inhibited cell growth by 46-80% and 58-64% in Y79 cells
f) 5 and 10µM curcumin with different combination of 1-20µM vincristine inhibited cell growth by 37-67% and 31-61% in Weri cells (**Figure 8.1a-f**).

Figure 8.1a

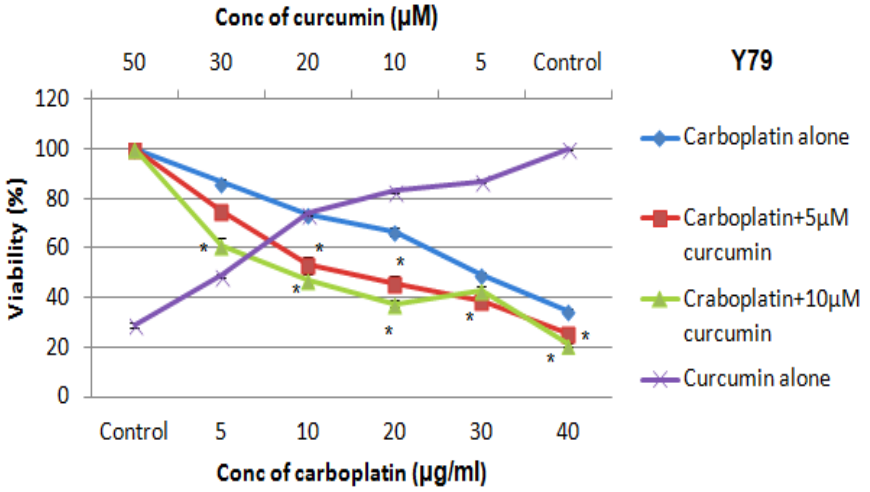

Figure 8.1b

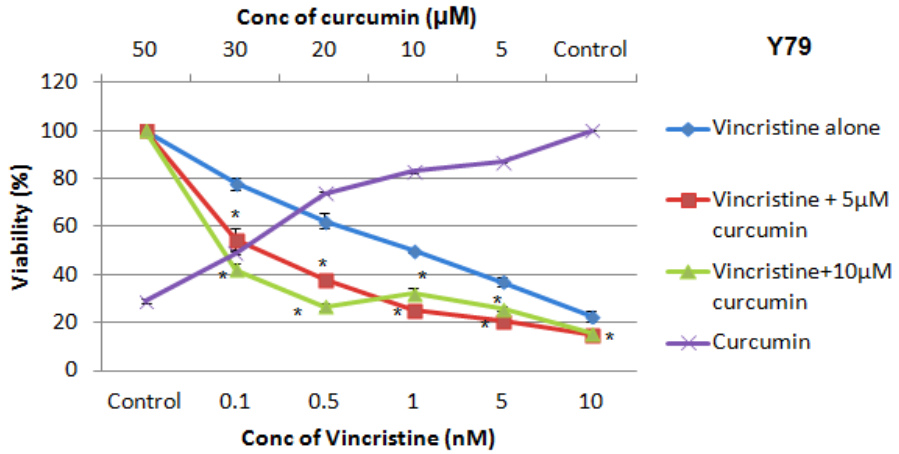

Figure 8.1c

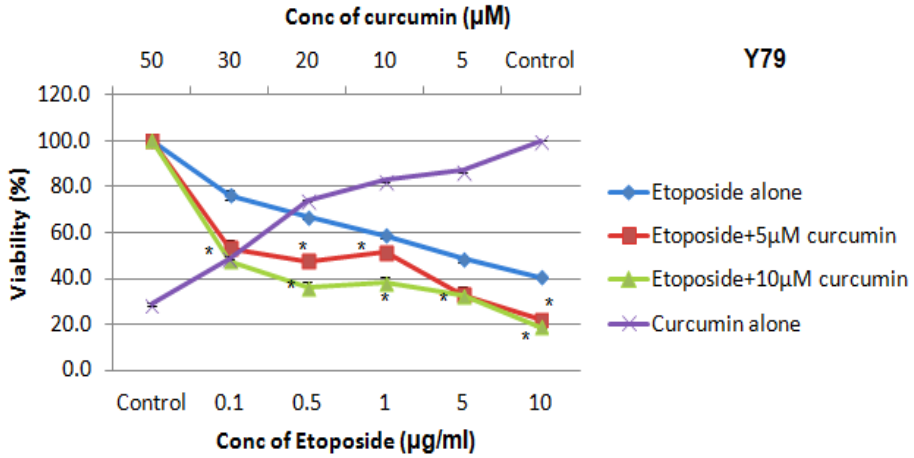

Figure 8.1d

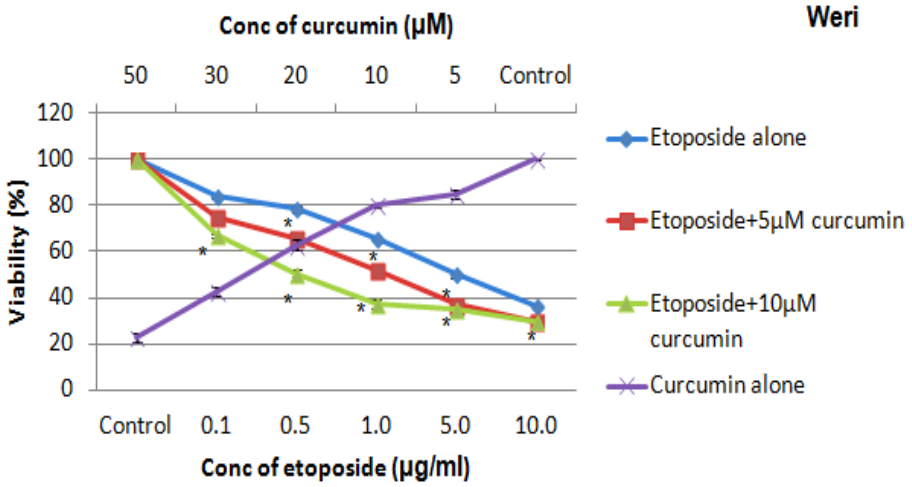

Figure 8.1e

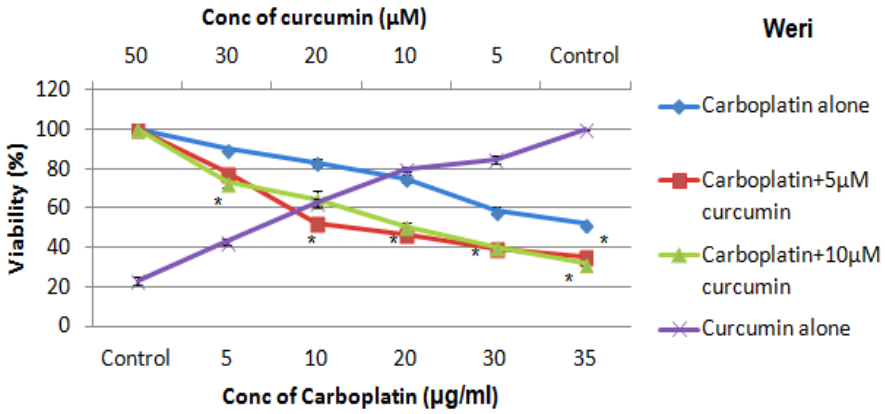

Figure 8.1f

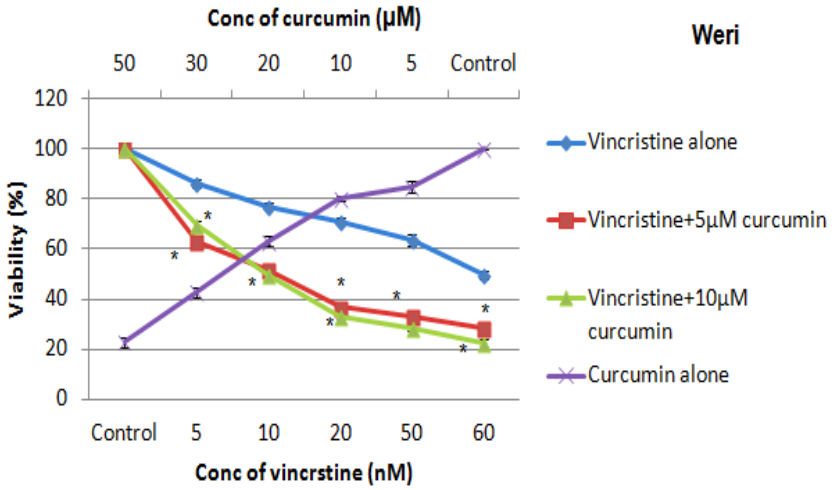

Figure 8.1a-f: Effect of combination of curcumin and chemotherapy drugs (carboplatin, vincristine an etoposide) on growth of RB cell lines (Y79 and Weri). RB cells were treated for 48h with a combination of curcumin (5 and 10µM)) and individual chemotherapy drugs and curcumin as indicated. Cell viability was determined by the MTT assay as described in materials and methods. Each plot represents the mean±SD (n=3); *p<0.05 for comparison with carboplatin, etoposide or vincristine.

8.4.3 Isobolographic analysis of the combination treatment with curcumin and chemotherapeutic agents in Y79 and Weri cells:

Chemotherapeutic agents (carboplatin, etoposide and vincristine) were analyzed in combinations with curcumin in RB cell lines using Calcusyn software in order to study the interaction and to evaluate the possible benefits of combined treatment compared to individual administration. Isobolograms indicated that the interactions between curcumin and CEV are synergistic in both the RB cell lines at certain concentrations. The results from the combination analysis are summarized in **Table 8.2a&b** and selected isobologram are shown in **Figure 8.2a&b**. In Y79 & Weri cells, the combination index for carboplatin, etoposide and vincristine with curcumin was found to be below 1 at certain combination treatment used in this study. Synergism was significant in the Y79 cell line at the inhibition level of 50%, achieving CI values of (0.7 & 0.55 for carboplatin; 0.14 for etoposide), and in the Weri-Rb1 cell line at inhibition levels of 50%, with CI values of (0.5, 0.6 & 0.97 for carboplatin; 0.6 for etoposide). The isobole for ED50 shows that the combination of chemotherapy drug and curcumin used is below the line of additivity indicating synergism.

The DRI quantitate the advantage synergism provides for dose reduction when two drugs are used in combination. For example in table 1, the combination of 5µM curcumin and 0.1µg/ml of etoposide in Y79 cells produced 50% growth inhibition and a CI = 0.3 indicating synergy. The DRI value of 10 for etoposide indicates that this drug would need a 10-fold higher concentration to produce the same inhibition effect in the absence of curcumin. In other words, the addition of 5µM curcumin allowed for a 10- fold reduction in the concentration of etoposide achieving the same inhibition effect. DRI values are listed for all doses of chemotherapy drug and curcumin used in isobologram experiments that identified synergism. Thus the combination of curcumin and chemotherapeutic agent together was more effective than either treatment alone (**Figure 8.2a&b**).

Figure 8.2a

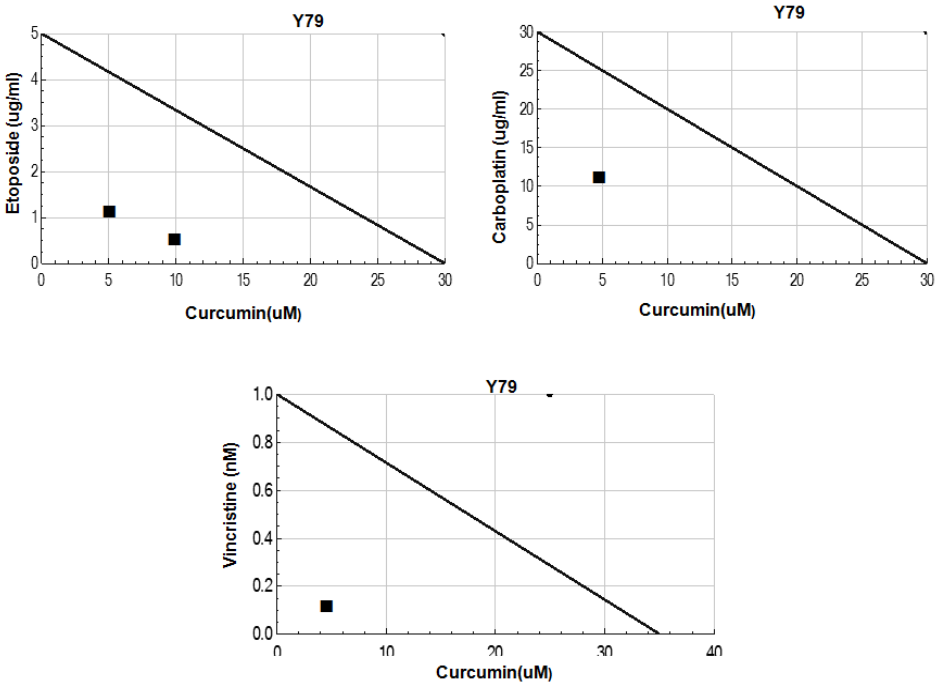

Figure 8.2b

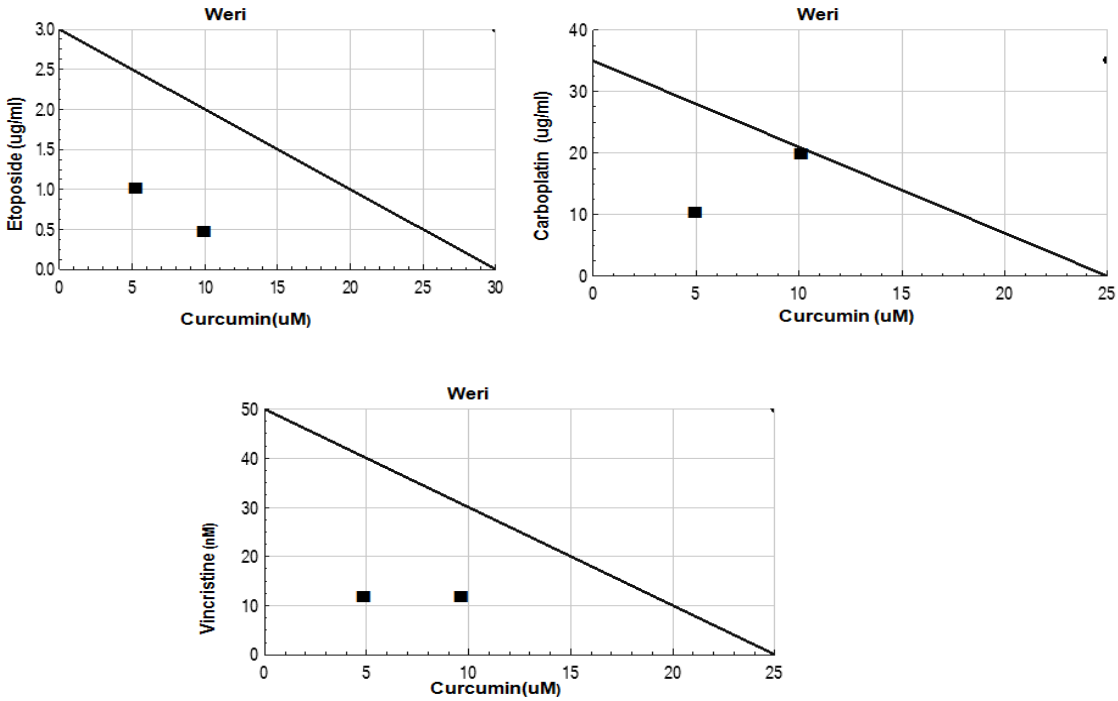

Figure 8.2a&b: Synergistic interactions between carboplatin or vincristine or etoposide and curcumin in a) Y79 and b) Weri cells. Data from the growth inhibition assays for individual drugs, as well as combinations of the three drugs, were entered into the Calcusyn software program to produce normalized isobolograms thus represent equipotent combinations of the compounds at the effective dose of 50% growth inhibition. Individual data points represent the specific dose of carboplatin or vincristine or etoposide to the fixed concentration of curcumin. If a combination data point fall on the diagonal, an additive effect is indicated; on the lower left, synergy is indicated; on the upper right, antagonism is indicated. The data are mean values from three individual experiments.

Table 8.2a: Combination index values and Dose Reduction Index for combined treatments of curcumin and chemotherapy drug in Weri cell line: Chemotherapy drug was dosed in combination with curcumin at several different concentrations. Combination index values were calculated using Calcusyn software and values <1 indicates synergism; CI=1, additivity; and CI>1, antagonism. The dose reduction index for each curcumin and chemotherapy drug is a measure of the extent, i.e, fold, that the dose of each drug in a synergistic combination may be reduced at a given effect level compared with the doses for each drug alone. NA, not applicable to antagonism.

Chemotherapy drug	Curcumin (μM)	Viable cells (%)	CI	Degree of Additve/Syn	DRI	
					Curcumin	Chemo.drug
5μg carboplatin	5	78.0±2.6	**0.75**	**Moderate Synergistic**	2	4
10μg carboplatin	5	52.7±1.5	**0.50**	**Synergistic**	5	3.5
20μg carboplatin	5	46.7±3.2	**0.66**	**Synergistic**	6	2
30μg carboplatin	5	39.3±0.6	**0.67**	**Synergistic**	8	6
5μg carboplatin	10	73.3±2.5	**0.85**	**Slight Synergistic**	1.5	4
10μg carboplatin	10	64.7±4.5	**0.9**	**Slight Synergistic**	2	1.5
20μg carboplatin	10	51.0±2.0	0.97	Nearly additive	2.5	1.75
30μg carboplatin	10	40.3±1.5	1.08	Nearly additive	NA	NA
0.1μg etoposide	5	75.0±2.0	2.0	Antagonistic	NA	NA
0.5μg etoposide	5	66.0±2.6	0.9	Nearly additive	4	2
1μg etoposide	5	51.7±1.5	1.55	Antagonistic	NA	NA
5μg etoposide	5	37.0±1.0	**0.4**	**Synergistic**	8	2
0.1μg etoposide	10	67.0±1.0	**0.6**	**Synergistic**	2	10
0.5μg etoposide	10	50.7±1.5	**0.6**	**Synergistic**	2.5	10
1μg etoposide	10	37.3±2.1	**0.35**	**Synergistic**	4	10
5μg etoposide	10	35.3±2.1	**0.75**	**Synergistic**	4	2
1nM vincristine	5	63.0±2.0	**0.9**	**Slight Synergistic**	4	20
5 nM vincristine	5	52.0±1.0	1.3	Moderate Antagonostic	NA	NA
10 nM vincristine	5	36.7±1.5	**0.75**	**Moderate Synergistic**	8	6
20 nM vincristine	5	33.0±2.0	**0.425**	**Synergistic**	8	3
1 nM vincristine	10	69.7±1.5	1.4	Nearly additive	NA	NA
5 nM vincristine	10	50.0±2.0	1.1	Nearly additive	NA	NA
10 nM vincristine	10	33.2±21.3	**0.53**	**Synergistic**	4	6
20 nM vincristine	10	28.7±1.1	**0.6**	**Synergistic**	5	3.5

Table 8.2b: Combination and Dose Reduction Index for combined treatments of curcumin and chemotherapy drug in Y79 cells: Chemotherapy drug was dosed in combination with curcumin at several different concentrations. Combination index values were calculated using Calcusyn software and values <1 indicates synergism; CI=1, additivity; and CI>1, antagonism. The dose reduction index for each curcumin and chemotherapy drug is a measure of the extent, i.e, fold, that the dose of each drug in a synergistic combination may be reduced at a given effect level compared with the doses for each drug alone. NA, not applicable to antagonism.

Chemotherapy drug	Curcumin (μM)	Viable cells (%)	CI	Degree of Additve/Syn	DRI	
					Curcumin	Chemotherapy drug
5μg carboplatin	5	75.0±2.0	1.5	Antagonistic	NA	NA
10μg carboplatin	5	53.7±3.1	1.25	Moderate Antagonistic	NA	NA
20μg carboplatin	5	45.7±3.1	**0.7**	**Synergistic**	7	1
30μg carboplatin	5	38.7±1.5	**0.87**	**Slight Synergistic**	8	1.1
5μg carboplatin	10	61.0±2.94	**0.65**	**Synergistic**	2.5	4
10μg carboplatin	10	47.3±2.05	**0.55**	**Synergistic**	3	3
20μg carboplatin	10	37.7±1.25	**0.48**	**Synergistic**	4	2
30μg carboplatin	10	43.0±1.63	**0.30**	**Synergistic**	3	1
0.1μg etoposide	5	53.3±3.5	**0.14**	**Strong Synergistic**	6	10
0.5μg etoposide	5	47.7±2.5	1.0	Nearly Additive	NA	NA
1μg etoposide	5	51.3±1.5	2.0	Antagonistic	NA	NA
5μg etoposide	5	33.0±3.6	**0.35**	**Synergistic**	10	4
0.1μg etoposide	10	47.7±2.52	2.0	Antagonostic	NA	NA
0.5μg etoposide	10	36.0±2.65	**0.5**	**Synergistic**	4	40
1μg etoposide	10	38.0±2.65	**0.52**	**Synergistic**	4	10
5μg etoposide	10	32.7±2.08	**0.5**	**Synergistic**	4	4
0.1nM vincristine	5	54.7±4.5	1.25	Moderate Antagonistic	NA	NA
0.5nM vincristine	5	37.7±0.6	1.1	Nearly Additive	NA	NA
1nM vincristine	5	25.3±2.5	1.1	Nearly Additive	NA	NA
5nM vincristine	5	20.7±0.0	**0.56**	**Synergistic**	15	2
0.1nM vincristine	10	42.0±2.6	**0.34**	**Synergistic**	3.5	25
0.5nM vincristine	10	26.7±1.5	**0.25**	**Strong Synergistic**	5	20
1nM vincristine	10	32.0±2.6	**0.4**	**Synergistic**	5	5
5nM vincristine	10	26.0±1.0	**0.7**	**Synergistic**	5	2

8.4.4 Effect of CEV on curcumin uptake

We quantified curcumin uptake by flow cytometry as curcumin is known to fluorescence in the green band. The flow cytometry results showed increase in the absorption of curcumin in RB cells when compared with the control cells, but combining curcumin with CEV showed significant absorption of curcumin in RB cells (**Figure 8.3**).

Figure 8.3

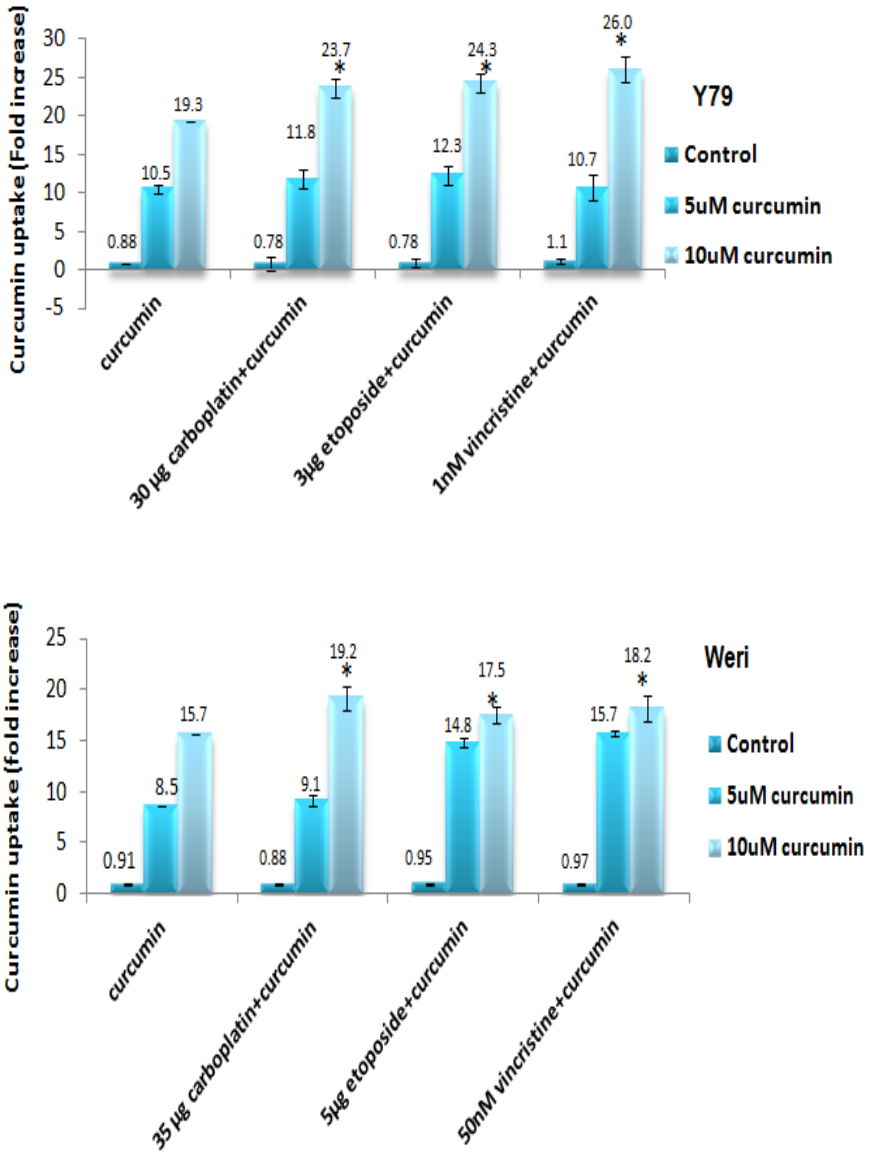

Figure 8.3: Effect of chemotherapeutic agents on curcumin uptake: RB (Y79 & Weri) cells were treated with different concentration of curcumin (5 and 10µM) in the presence and absence of chemotherapy agents and analyzed by flow cytometry. Fold change were compared with control cells. *P<0.05 significant difference compared with the chemotherapeutic agents.

8.4.5 Effect of curcumin and CEV combination treatment on induction of apoptosis

Annexin V/PI staining was performed to assess the induction of apoptosis with combination treatment of curcumin and CEV. The average percentage of apoptotic cells were increased significantly after exposure to CEV and curcumin treatment applied alone when compared with the control. However, the combination produced greatest increase in apoptotic cells when compared with the individual agents when applied alone (**Fig. 8.4**).

Figure 8.4

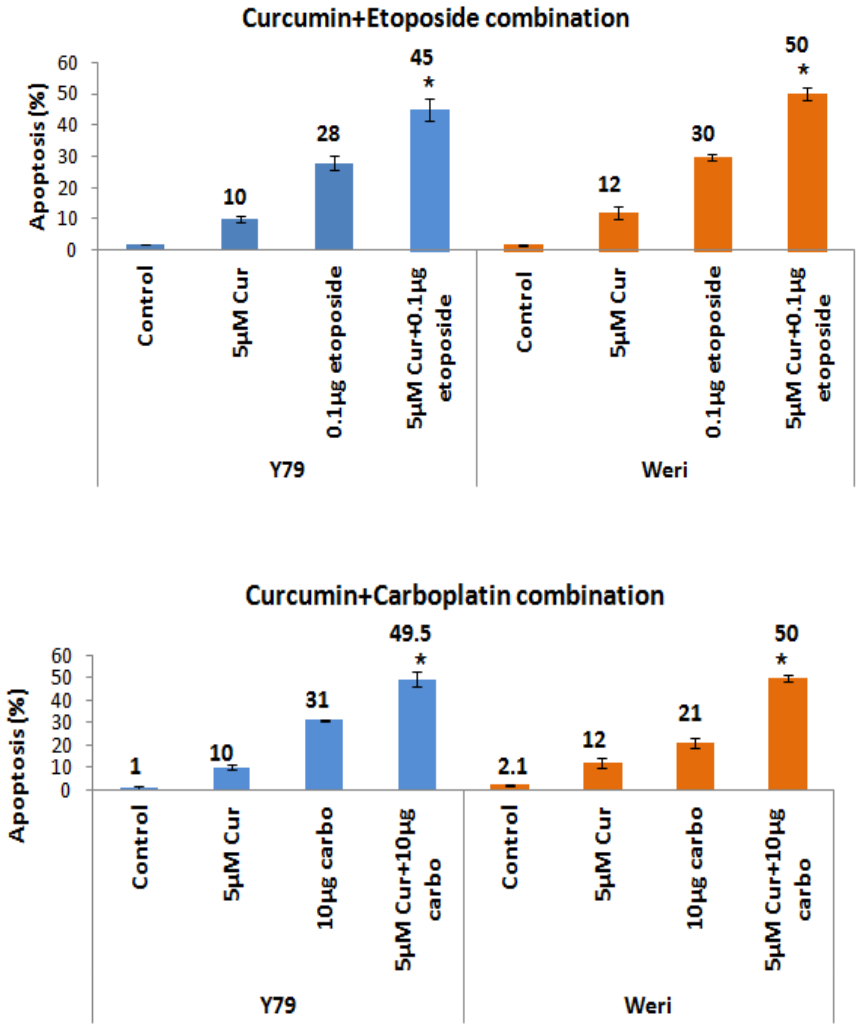

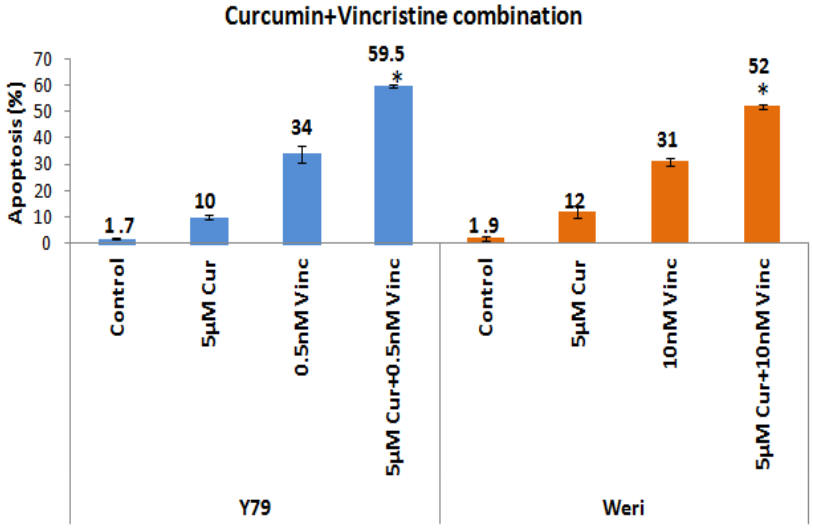

Figure 8.4: Induction of apoptosis by annexin V staining in Y79 and Weri RB cells after 48h treatment with 5µM curcumin alone or in combination with individual treatment of chemotherapy drugs (carboplatin, vincristine and etoposide). Each bar represents the mean±SD (n=3). *P<0.05 significant difference compared with the chemotherapeutic agents.

8.4.6 Effect of combined treatment with curcumin and CEV on cell cycle progression

We examined the effect of curcumin (5µM &10µM) and different concentration of CEV either alone or in combination in the RB cells. The analysis of DNA content in RB cells, revealed that curcumin, significantly increased the percentage of the cells in the S phase and decrease in the percentage of cells in G_0/G_1 phase in RB cells, and this effect was significantly enhanced by combination of curcumin with CEV (**Figure 8.5**).

Figure 8.5

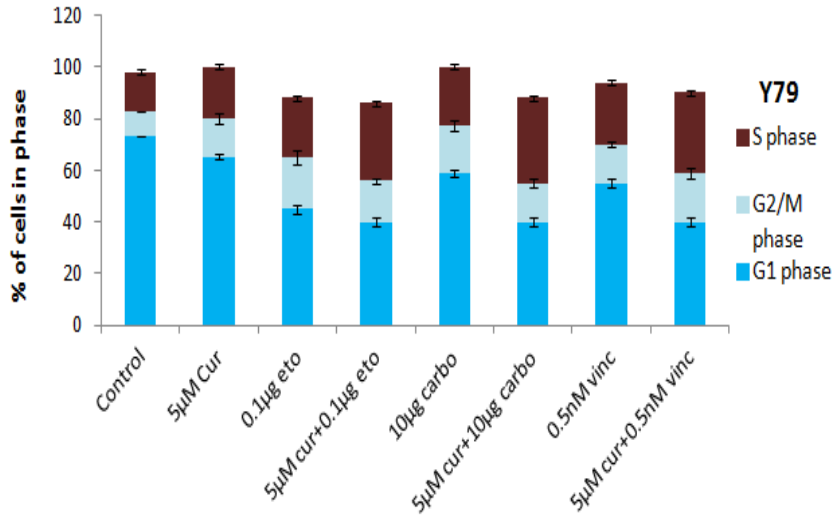

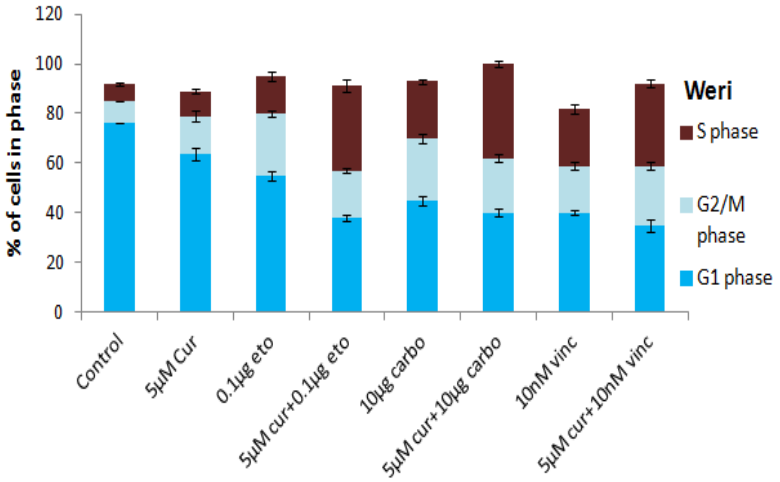

Figure 8.5: Changes in cell cycle distribution by flow cytometry in Y79 and Weri RB cells after 48h treatment with curcumin alone or in combination with chemotherapy drugs. Each bar represents the mean±SD (n=3). The data obtained from FACS were analyzed using Cell Quest software to determine the percentage of cells in each phase of the cell cycle.

8.4.7 Effect of curcumin and CEV combination on caspase 3 activity

Caspase 3 activity was measured to confirm the induction of apoptosis in RB cell lines. The activity of caspase 3 was increased after treatment of RB cell lines with CEV and curcumin alone. This was significantly enhanced upon combination of chemotherapy drugs and curcumin treatment in RB cell lines (**Figure 8.6**).

Figure 8.6

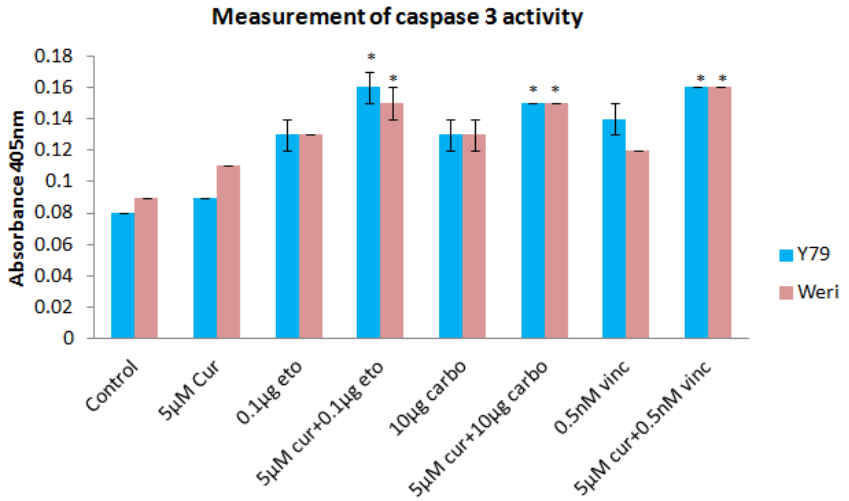

Figure 8.6: Caspase3 activity in RB cell lines after treatment with curcumin and chemotherapy drugs. RB cells were treated with curcumin and CEV combination for 48h to measure the caspase 3 activity calorimetrically. Data represent means ± of at least three independent experiments. *P<0.05 significant difference compared with the chemotherapeutic agents.

8.5 Discussion:

The major drawback involved in chemotherapy treatment is the dose-limiting toxicity and induction of drug resistance (Stavrovskaya et al. 2000). Various molecular mechanism are involved in MDR and many natural compounds have been identified which overcome drug resistance to chemotherapy drugs and thereby increase drug accumulation in cancer cells (Zhao et al. 2004; Dillman et al. 1990). In this study, we investigated the chemosensitizing effect of curcumin alone and in combination with chemotherapy drugs.

Our result found that curcumin inhibits RB cells (Y79 and Weri) **proliferation *in vitro* with IC_{50} value of 30µM and 25µM** respectively. We used RB cells to study the interaction between curcumin and chemotherapy drugs using isobolographic method. Curcumin has been shown to augment the effects of various chemotherapeutic agents like vincristine and doxorubicin, thereby enhancing the cellular accumulation of these drugs onto cancer cells (Harbottle et al. 2001). For example, the combination of curcumin with paclitaxel augments the anticancer effects of paclitaxel against Hela cells via a mechanism involving down-regulation of NF-kB activation and phosphorylation of AKT pathways (Bava et al. 2011). Our study also found that **curcumin enhanced the cytotoxicity of RB cells in combination with CEV** when compared with the individual treatment in a synergism manner.

In order to examine the mechanism of action through which curcumin and CEV exert their growth inhibitory effects, we studied the effects of their combination and individual agent treatment on cell cycle kinetics. Flow cytometric analysis revealed that the **RB cells were arrested in the S-phase after exposure to curcumin and CEV and significant effect was observed on combination treatment**. Andjelkovic et al, showed that combination treatment of curcumin and sulfinosine induced a more pronounced cell cycle arrest in S and G2/M phase in NCI-H4660/R cells **(**Andjelkovic et al. 2008). Several studies have demonstrated that anticancer drugs like cisplatin, etoposide and camptothecin induce tumour cell death via induction of apoptosis. Although various chemotherapeutic agents are in clinical use, the need of identifying a better drug that induces apoptosis in various cancer cells in an efficient manner. Curcumin, a dietary supplement has been reported to induce apoptosis in various cancer cell

lines (Shim et al. 2001). In our study, we investigated the synergistic effect of curcumin and chemotherapeutic agent combination on the growth suppression of RB cells by annexin staining and caspase 3 activities. Our study showed that **combination treatment of curcumin and CEV produced a higher percentage of apoptosis than that caused by either curcumin or CEV alone by annexin staining. Similarly we observed a significant increase in the activity of caspase 3 in combination treatment when compared to a single drug treatment in RB cells**. Our results are similar to the findings of Lev-Ari & Hosseinzadeh et al, where combination treatment of curcumin with celecoxib showed synergistic pro-apoptotic effects in osteoarthritis synovial adherent and cardiomyoblast cells (Lev-Ari et al. 2006; Hosseinzadeh et al. 2010).

Our study shows that the combined treatment of curcumin and chemotherapy drug synergistically augments the inhibition of cell proliferation and also induces apoptosis in RB cells

8.6 Chapter summary

- In both the RB cell lines individual treatment of curcumin and chemotherapy drugs independently inhibited cell proliferation in a concentration dependent manner.
- Combination of curcumin and chemotherapy drugs showed marked synergistic inhibitory effects on cell proliferation, cell cycle and induction of apoptosis than the individual treatment on RB cell lines (**Figure 8.7**).
- Thus combined dosing of curcumin and chemotherapy drugs has potential therapeutic value for the treatment of RB cancer.

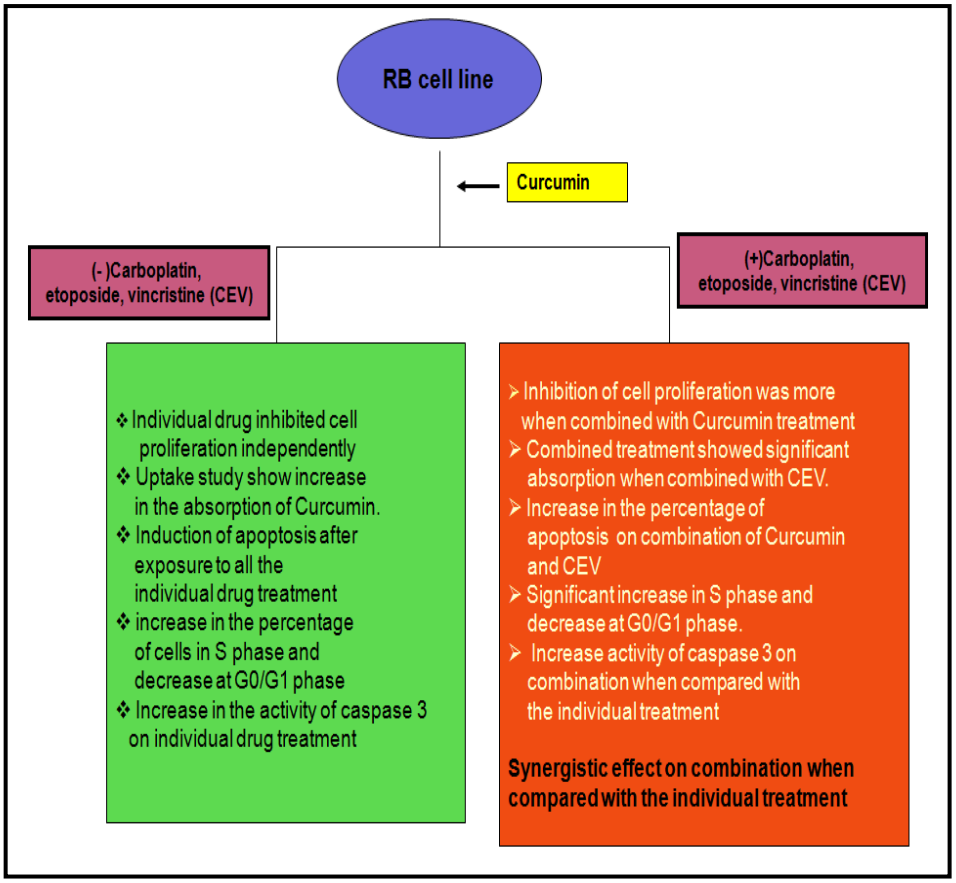

Figure 8.7: Schematic representation of combination treatment (curcmin+chemotherapy) in RB cell lines

CHAPTER 9: SYNTHESIS AND CHARACTERIZATION OF CURCUMIN BIO-CONJUGATES

9.1 INTRODUCTION

Even though curcumin has potential use for various drug delivery applications, it poses certain major challenges. One of them is that the water soluble fraction of curcumin lacks stability. Aqueous solution of curcumin undergoes rapid hydrolysis followed by molecular fragmentation at physiological pH (Manju et al. 2011). Another main challenge of curcumin is its poor aqueous solubility and its lower availability in biological systems. Curcumin is highly hydrophobic and cannot be administered systemically. On intravenous administration, it disappears rapidly from the blood and quickly appears as metabolites in the bile (Singh et al. 2010). Limited bioavailability is the major drawback associated with failure of many naturally occurring chemopreventive agents.

The development of a synthetic methodology to produce curcumin conjugates with water-soluble polymers and targeting proteins or ligands can potentially enhance the therapeutic efficacy of curcumin. An approach that may solve the above problems of the usage of curcumin as an antitumor drug is the use of its conjugate with polyethylene glycol (PEG) or folic acid. Many studies shows that the water soluble polymer based curcumin conjugates exhibited enhanced cytotoxicity as compared to that of the native drug (Manju et al. 2011). A low-molecular-weight drug or compound (such as curcumin) conjugated to higher molecular weight PEG (~20,000) results in high aqueous solubility and lipophilicity of the molecule, sustained release of drug molecule to improve the half-life, slower clearance, reduced systemic toxicity, and efficient accumulation in tumours through enhanced permeability and retention (Singh et al. 2010; Li et al. 2009). Similarly the components of bacterial cell wall, folic acid and other bio-conjugates are known to enhance cellular uptake, lipophilicity of the molecule and sustained release of the drug molecule to improve the half-life and reduce the rate of metabolism of curcumin molecule inside the cell (Singh et al. 2010).

9.1.1 Polyethylene Glycol (PEG)

PEG is a water-soluble amphiphilic polymer showing excellent biocompatibility and is frequently used in biomedical applications. In its most common form

polyethylene glycol, PEG, is a linear or branched polyether terminated with hydroxyl groups and having the general structure:

$$HO–(CH_2CH_2O)_n –CH_2CH_2–OH.$$

To conjugate PEG to a molecule (i.e. polypeptides or organic compounds) it is necessary to activate the PEG by preparing a derivative of the PEG having a functional group at one or both termini. The functional group is chosen based on the type of reactive group on the molecule that will be coupled to the PEG (Roberts et al. 2002). It has been reported that conjugating curcumin with a naturally occurring polymer with intrinsic cell specific binding capacity such as hyaluronic acid could increase curcumin's potential as a target-specific drug carrier. Also, the stability of the conjugate in water was several folds higher compared to free curcumin, thus enhancing the cytotoxicity of the conjugate as compared to curcumin (Manju et al. 2011). Curcumin conjugated to a water-soluble PEG, the new compound sensitized pancreatic cancer cells to gemcitabine-induced apoptosis and cell proliferation inhibitory effects. Collectively, the PEGylated curcumin conjugate has much more potent effects on pancreatic cancer cell growth inhibition than free curcumin (Li et al. 2009). Various modifications have been attempted to conjugate curcumin with gold nanoparticles, PEG, folic acid, and hyaluronic acid in order to challenge the limitations of curcumin (Manju et al. 2012). They state that this conjugate demonstrated enhanced targeting efficacy via hyaluronic acid receptor and folate receptor mediated endocytosis. This aided the effective delivery of Curcumin to the perinuclear or nuclear region of cells (Manju et al. 2011). The role of PEG is crucial in the evolution of drug delivery systems, especially for tumour targeting and treatment. Surface modification of nanoparticulate carriers with PEG has emerged as a strategy to enhance solubility of hydrophobic drugs, prolong circulation time, minimize non-specific uptake, and allow for specific tumour-targeting through the enhanced permeability and retention effect (van Vlerken et al. 2007).

9.1.2 Folic acid:

Even though significant developments have been found in anticancer technology, such as radiotherapy, chemotherapy and hormone therapy, cancer still remains

the second leading cause of cell death all over the world (National Cancer Institute, Cancer Statistics. 2006). Tumor specific treatment is one of the hurdles that need to overcome by current chemotherapy. An ideal solution to current chemotherapy is to deliver anti-cancer agents to the tumour tissues with very high specificity. Tremendous amount of efforts have been performed to develop selective drugs by conjugating anti-cancer agents with hormones, vitamins and antibodies derivatives. Among them, low molecular weight vitamin compound, folic acid, shows a great deal of promise as a tumor-homing agent (Hilgenbrink et al. 2005).

Folic acid is a well-known water soluble vitamin which is present in leafy vegetables. It is required for the healthy functioning of all cells, where cancer cells require much more folate. Folate is necessary for DNA nucleotide synthesis and cell division. It is brought into healthy and cancerous cells by folate receptors. Folic acid binds specifically with the folate receptors which exist on the surface of the tumour cells. It is inexpensive, stable and has high affinity as cell surface receptor.

Folate receptor with molecular weight 38-40 kDa binds folic acid with high affinity (Antony et al. 1996). The presence of folate receptors on the cell surface is regulated by the cell function. Cancer cells express folate receptors (500 times more than healthy cells) because of their vast requirement for folate. As a result, high affinity of folic acid and folate receptors provide a unique opportunity to use this compound as a targeting ligand to deliver anti-cancer compounds into the cancer cells. Because of the lower expression of folate receptors in normal cells and over-expression in tumour cells, folate can be used as a targeting agent for the research purposes (Doucette and Stevens et al. 2001).

Thus in the present study, curcumin is used to conjugate with PEG and folic acid separately in order to enhance its stability and solubility in aqueous solutions and some of the preliminary experiments have been performed to study the characterization of these conjugates.

Apart from this we also received nanoparticle curcumin as a gift from The University of Texas M.D Anderson Cancer Center, Houstan, Texas, USA. This nanoparticle (NP) curcumin was tested for its efficacy in RB cell lines and was also compared with our native curcumin.

9.2 Objective

- To synthesize Cur-PEG and Cur-folic acid conjugate and study its characterization by TLC chromatography, FT-IR analysis and stability testing.
- To compare the efficacy of native and nanoparticle curcumin in RB cell lines.

9.3 Materials & Methods:

Section A

9.3.1 Nanoparticle curcumin:

Co-polymer: PLGA-PEG

PLGA 50:50 mw: 10000

PEG mw: 5000

Surfactant: Pluronic F68

Surface Charge (zeta potential): -40.2mV

Encapsulation efficiency: 90%

Drug Content: 8.2µg/mg NP.

SEM and TEM images of NP curcumin:

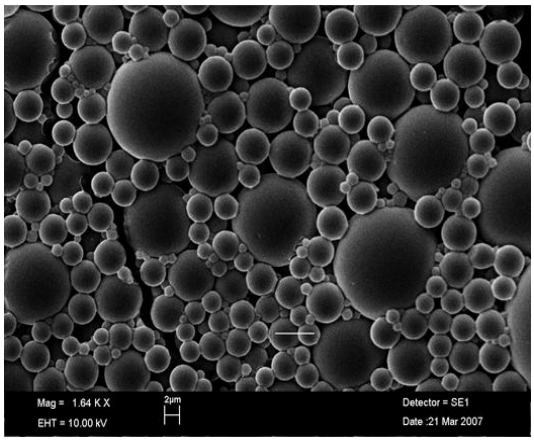

Figure showing **SEM image of Curcumin** nanoparticles before mechanical extrusion to synchronize the size of the particles to 100nm (upper limit).

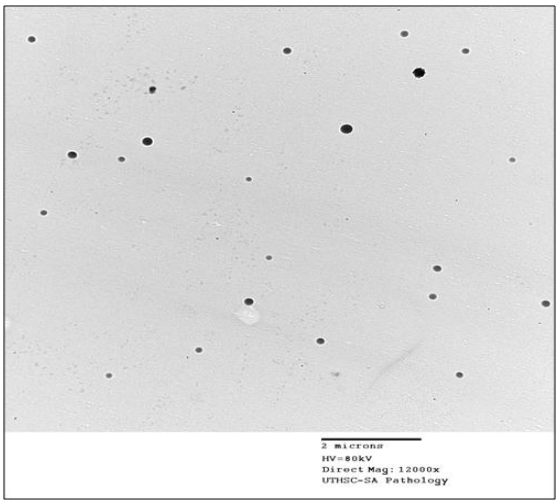

Figure showing **TEM image of curcumin** nanoparticles after mechanical extrusion. Size of the particles is adjusted to 100nm.

The following NP curcumin was used for our study in RB cell lines.

9.3.2 Anti-proliferative assay:

The anti-proliferative effects of native curcumin and NP-curcumin on retinoblastoma cell lines were tested by the MTT (3-(4, 5-dimethyl thiazol-2-yl) - 2, 5 diphenyl tetrazolium bromide) assay as described previously in chapter 4.

9.3.3 Colony forming assay

12-well plates were coated with poly-D-lysine and approximately 10,000 cells/well were plated and incubated at 37^0C for overnight. Next day medium containing 20µM curcumin was added and incubated for 14 days to allow for colony growth. The assay was terminated at day 14, where plates were stained with 0.5% crystal violet and the number of colonies per dish was counted. The assay was performed for at least three independent experiments.

9.3.4 Quantitative cellular uptake study:

Cellular uptake of native and NP curcumin (10 and 20µM) was studied in RB cell lines. Briefly, RB cells were seeded in a 12 well plate at a seeding density of $1x10^4$ cells per well in 1ml growth medium. After 24h of incubation at 37^0C, the cells were treated with different concentration of curcumin and kept in cell culture incubator for 6h. After incubation, the cells were washed twice with PBS and lysed by adding methanol. The cells were centrifuged at 10,000rpm for 10

min at 4^0C. The concentration of curcumin was measured using fluorescence spectrophotometer with excitation of 420nm and emission of 540nm. The assay was performed for at least three independent experiments and the data obtained are mean values of three independent experiments.

9.3.5 Solubility and stability study of curcumin

Equivalent amount of native and NP curcumin (5mg) were dissolved in PBS (0.01M, pH 7.4) to observe the aqueous solubility of the preparation. Further the stability of the compound was estimated by dissolving 30µg/ml of the NP curcumin in PBS and native curcumin was dissolved in PBS in the presence of methanol. At different time points, 100µl of the solutions (either native or NP curcumin) was dissolved in 900µl of methanol to quantify the stability of curcumin with time in PBS (0.01M, pH 7.4) by spectrophotometer.

9.3.6 Plasma integrity assay

To study the effect of native and NP-curcumin on plasma membrane integrity, we determined the intracellular esterase activity and plasma membrane integrity. The cells were treated with native and NP-curcumin (10 and 20µM) for 48h and after incubation the cells were treated with calcein and Ethidium bromide for 30 min at room temperature. Cells were observed under fluorescent microscope by counting live (green) and dead (red) cells.

9.3.7 Statistical analysis

All experiments were done in triplicates and values were compared using one-way ANOVA with a level of significance at $p<0.05$.

9.4 Results

9.4.1 Curcumin inhibits the proliferation of RB cells

RB cells were incubated with different concentration of curcumin or curcumin NP for 48h and then examined for cellular proliferation by MTT assay. The result showed that curcumin and curcumin NP suppressed cell proliferation in both the cell lines. The IC_{50} value of native curcumin is 30 and 25µM in Y79 and Weri-RB cell line, whereas NP curcumin exhibited an IC_{50} value of 15µM and 17µM, respectively. This shows that the inhibition of cell proliferation by NP curcumin

was more effective than the native curcumin in inhibiting the cell growth (**Figure 9.1 a,b**).

Figure 9.1a

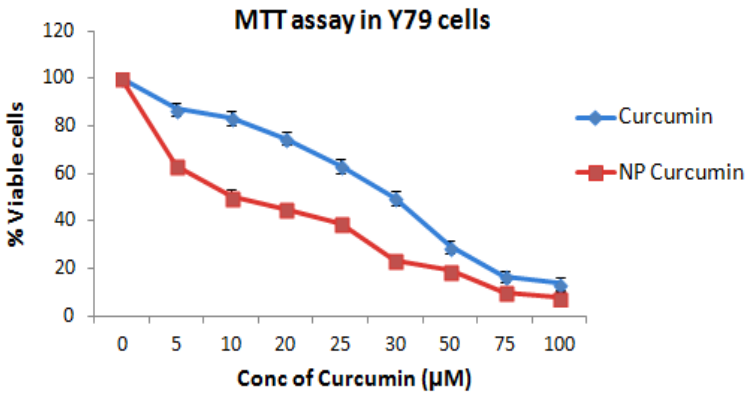

Figure 9.1b

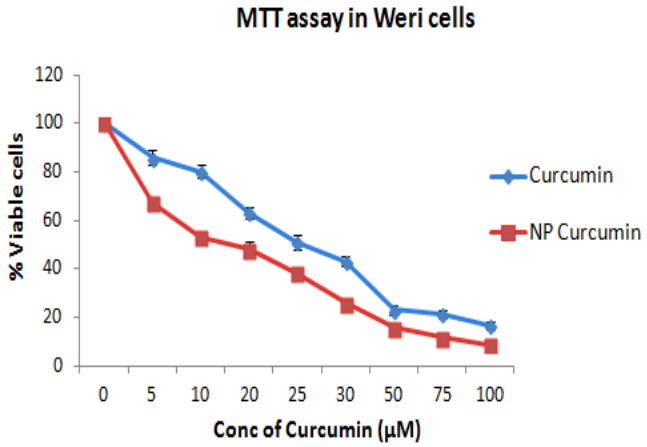

Figure 9.1 a& b: MTT assay for native and NP Curcumin in Weri and Y9 cell lines: Cells were treated with different concentration of native and NP curcumin for 48h and MTT was added after the incubation period and examined spectrophotometrically at 540nm.

9.4.2 Solubility and stability study of curcumin

To compare the solubility of NP curcumin and curcumin, we added curcumin to the PBS solution and found that NP curcumin in aqueous solution was clear, whereas native curcumin was poorly soluble in aqueous media (**Figure 9.2**). In order to study the stability of curcumin, we incubated curcumin in PBS at different time intervals and estimated the percentage stability by spectrophotometer. It was found that NP curcumin was more stable than the native curcumin in PBS by protecting the curcumin against hydrolysis (**Figure 9.2a&b**).

Figure 9.2a

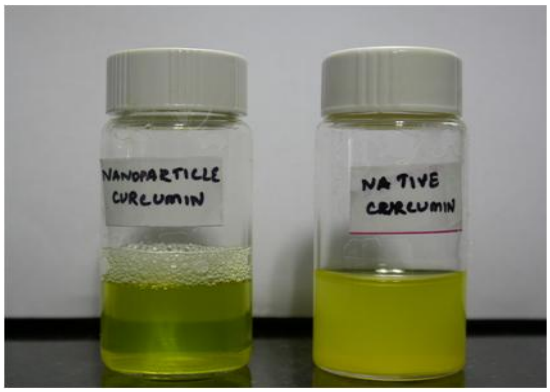

Figure 9.2a: Solubility study of NP curcumin and native curcumin in PBS. 5mg of both the curcumin was dissolved in PBS (0.01M, pH 7.4). Native curcumin was insoluble in aqueous solution and NP curcumin was soluble in aqueous solution.

Figure 9.2b

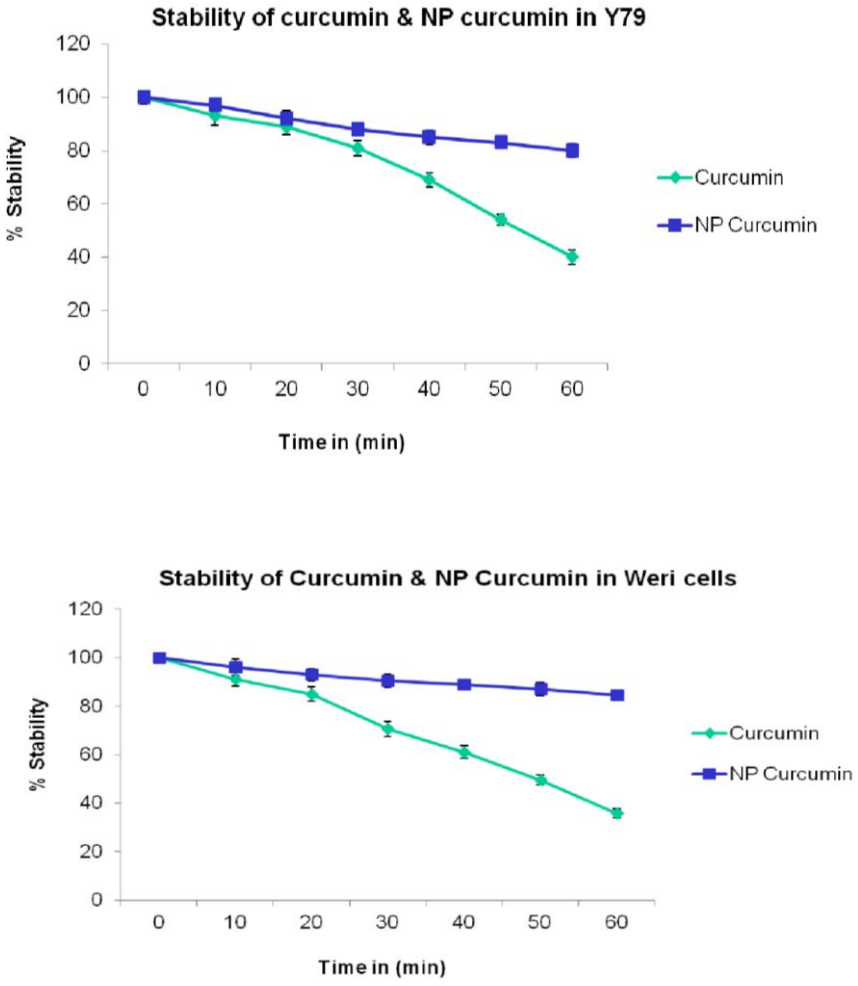

Figure 9.2b: Stability study of native and NP curcumin in Y79 and Weri cells at physiological pH 7.4. Percentage degradation of native and NP curcumin with different time intervals.

9.4.3 Colony soft agar assay

RB cells were treated with curcumin and NP curcumin at a concentration of 20µM for 14 days. The results showed that NP curcumin inhibited the colony formation compared to the colony observed in native curcumin. This shows that NP curcumin show better anti-proliferative activity than the native curcumin, which block the clonogenicity of RB cells greater than when compared with the native curcumin (**Figure 9.3**).

Figure 9.3

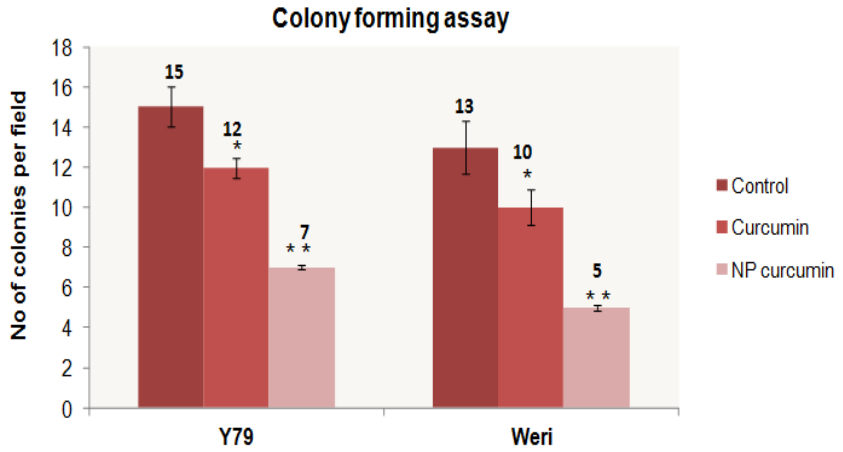

Figure 9.3: Colony forming assay in Y79 and Weri cells. Cells were treated with native and NP curcumin (20µM) and incubated for 14 days. Reaction was terminated after 14 days and stained with crystal violet. Data are mean ± S.D., n=3 experiments.

9.4.4 Cellular uptake studies

The intracellular uptake of NP curcumin was compared with native curcumin by fluorescence spectrophotometer. The results demonstrated that the cellular uptake of NP curcumin was more than the native curcumin in both the RB cell lines (**Figure 9.4a&b**).

Figure 9.4a

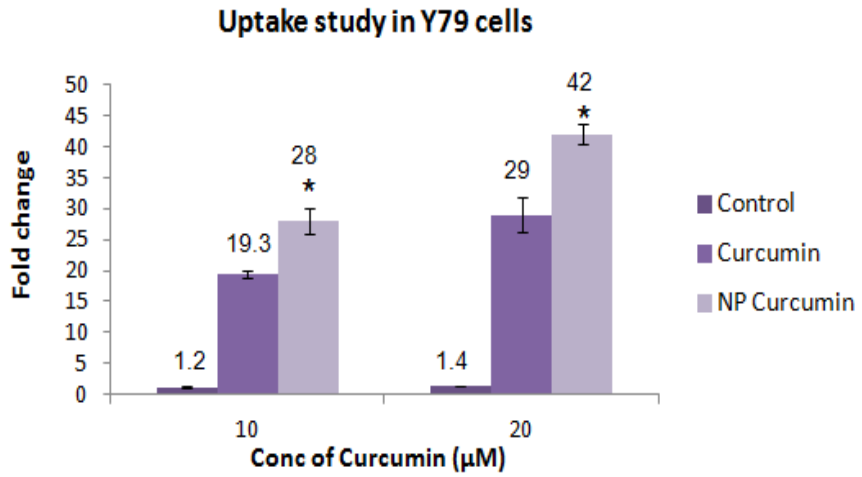

Figure 9.4b

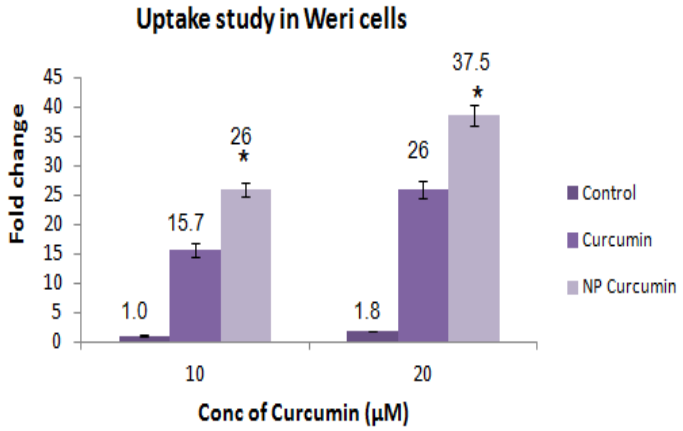

Figure 9.4a&b: Cellular uptake study in Y79 and Weri cells: The cells were treated with 10 and 20µM curcumin for 6h and the uptake study was performed using spectrofluorimeter. Data are mean ± S.D., n=3 experiments.

9.4.5 Plasma membrane integrity assay

To determine the ability of curcumin in inducing apoptosis in RB cells, esterase staining was performed. The result showed that NP curcumin treated cells showed more number of apoptotic cells when compared with the native curcumin. This suggests that NP curcumin treated RB cells showed increased percentage of apoptotic cells (viable cells are green in colour that retain the dye of calcein, red cells are the damaged cells, which take the colour of Ethidium bromide due to the damage of plasma membrane) when compared with the native curcumin (**Figure 9.5a&b**).

Figure 9.5a

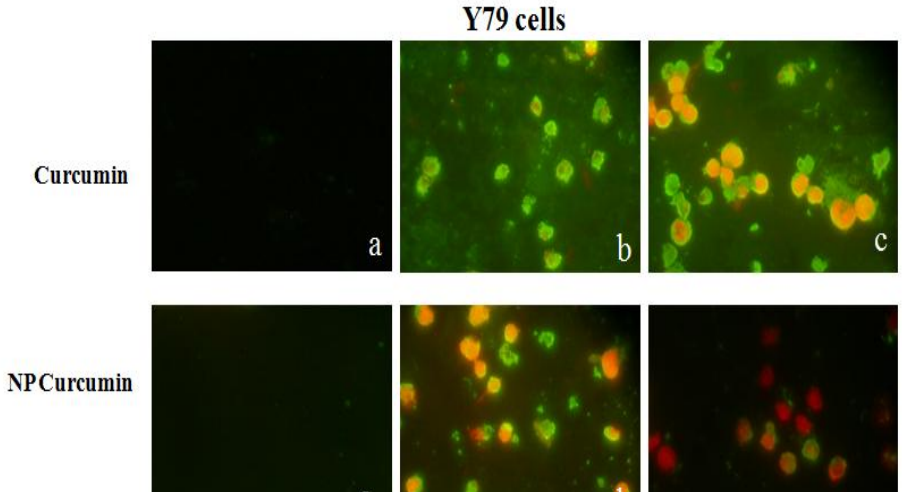

Figure 9.5b

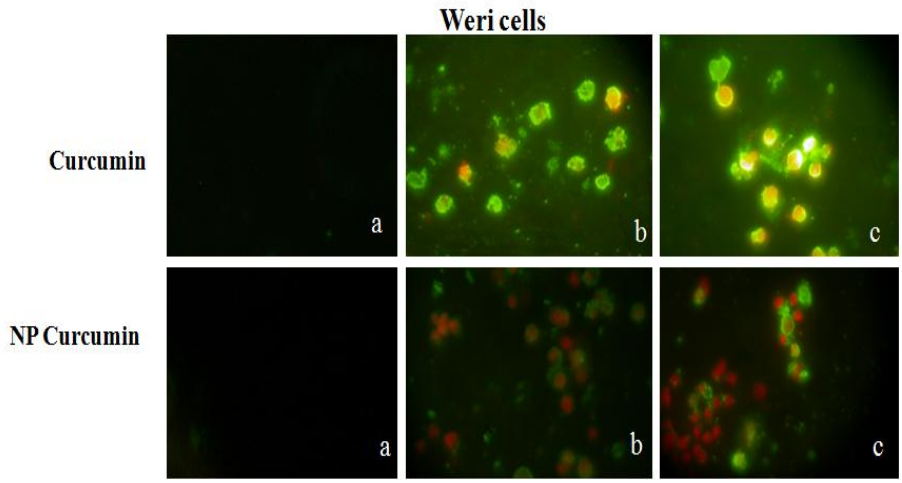

Figure 9.5a&b: Plasma membrane integrity assay in Y79 and Weri cells. Cells were treated with native and NP curcumin (10 and 20µM) for 48h. In both the cell lines the percentage increase in apoptosis is more when compared with the native curcumin (a= Untreated cells, b=10µM curcumin and c= 20µM curcumin). Green cells are the viable cells that retain the dye calcein and the red colour is the Ethidium bromide which easily enters the damaged plasma membrane.

SECTION B

9.5:Cur-PEG and Cur-Folic acid conjugates

9.5.1 Materials: Amine PEG Carboxyl HCl Salt (PEG), MW 2000, was purchased from Jenkem Technology, USA. N, N' – dicyclohexylcarbodiimide 99% (DCC), 4-Dimethylaminopyridine ≥99% (DMAP), Folic acid ≥97%, and 1-

ethyl-3-(3-dimethylaminopropyl) carbodiimide (EDC) were purchased from Sigma-Aldrich, Bangalore, India. Dichloromethane extrapure AR (DCM), Sodium Bicarbonate for molecular biology ($NaHCO_3$), Sodium Chloride extrapure AR (NaCl), and Sodium Sulphate anhydrous extrapure AR (Na_2SO_4) were obtained from Sisco Research Laboratories Pvt. Ltd., Mumbai, India. Sodium dihydrogen phosphate anhydrous GR (NaH_2PO_4), Disodium hydrogen phosphate (Na_2HPO_4), Hydrogen Chloride (HCl), Chloroform GR, Methanol, Acetone, and Ammonia were obtained from Merck Specialities Pvt. Ltd. Mumbai, India. Absolute Alcohol Ethyl alcohol 99.9% v/v (Ethanol) was purchased from Hayman Ltd., Essex, England. Fluka Analytical Silica on TLC Alu foils were obtained from Sigma-Aldrich, Bangalore, India.

9.5.2 Synthesis of Curcumin-PEG conjugates

In this study, we are attempting to conjugate Curcumin (which is a polyphenolic compound) to PEG (which is a polyether compound). For this purpose we are making use of **DCC/DMAP Chemistry**. Hence, the PEG derivative here contains a Carboxyl group (-COOH) on one side and an Amine group ($-NH_2$) on the other side. (The amine group is chosen so that further conjugation studies can be carried out with PEG). The following compounds were dissolved in a beaker containing 15ml DMSO in order, one at a time, stirring until each completely dissolved – PEG (100mg), DMAP (50mg), and Curcumin (100mg), DCC (50mg). Immediately after addition of the last compound, the solution was exposed to nitrogen gas for 10 min. The beaker was then left to stir overnight at 56^oC. 3µl of this extract was loaded on to a Fluka TLC plate. Next to the spot representing the extract, 3µl of Curcumin dissolved in DMSO was loaded on to a separate lane as control. Thin layer chromatography was then carried out using a mobile phase of chloroform: methanol in the ratio of 95:5 and the plate was viewed using a UVP Benchtop 3UV Transilluminator. The remaining extract was dialysed against DMSO for one day, followed by water for 2 days. The dialysed extract was lyophilized, and given for FT-IR analysis.

9.5.3 Curcumin-folic acid conjugate

The following compounds were dissolved in a beaker containing a mixture of Methanol (5ml) and distilled water (15ml), in order, one at a time, stirring until

each completely dissolved – Folic acid (2mg), DMAP (0.2mg), Curcumin (5mg), and DCC (1.1mg). Immediately after addition of the last compound, the beaker was transferred to an ice box kept at 0^oC and stirred continuously for 5min. The beaker was then covered completely with aluminum foil and left to stir overnight at 20^oC. After 24h, 500µl of the reaction mixture was taken and centrifuged. 3µl of the supernatant was loaded on to a Fluka TLC plate, followed by curcumin dissolved in DMSO and 3µl of folic acid dissolved in a mixture of Methanol: distilled water (1:3) was loaded on to two separate lanes as control. Thin layer chromatography was then carried out using a mobile phase of chloroform: ethanol: acetone: ammonia in the ratio of 3: 3: 3: 1 and the plate were viewed using a UVP Benchtop 3UV Transilluminator.

9.5.4: Characterization of two conjugates

1) Retention Factor: Retention Factor (R_f) of each of the conjugates was calculated by the formula

2) FT-IR Analysis: The final extract of the conjugates were sent for FT-IR analysis along with the control compounds to Sophisticated Analytical Instrument Facility (SAIF), Indian Institute of Technology (IIT), Madras.

R_f = (Distance moved by solute / Distance moved by solvent)

3) Absorbance: The wavelength of maximum absorbance for each of the conjugates, as well as the individual control compounds was identified using the Beckman Coulter DU800 Spectrophotometer.

4) Fluorescence: Similarly, the wavelength of maximum fluorescence for each of the conjugates, as well as the individual control compounds was identified using the Molecular Devices Spectra Max Mz^{ρ} Spectrofluorimeter.

5) Stability testing: Each of the conjugates were separately dissolved in Phosphate buffered saline (PBS) solution of pH 7.4 and absorbance at maximum wavelength was recorded every 5 min up to 50 min to test the hydrolytic stability of the conjugates at physiological pH.

9.6: Results

9.6.1 Physical properties of the conjugates:

Table 9.1: Physical properties of the conjugates

Property	Curcumin – PEG	Curcumin – Folic Acid
Solid/Liquid	Liquid	Liquid
Boiling Point	39.6^{o}C	65^{o}C
Smell	Moderately sweet aroma	Sweeter than ethanol
Colour	Dark yellow	Dark yellow
Appearance	Oily	Fluid

9.6.2 Thin layer chromatography:

a) Curcumin-PEG Conjugation: For the solvent system of Chloroform: Methanol in the ratio of 95:5, the following **Retention Factor (R_f)** values were observed for curcumin-PEG conjugate (**Figure 9.6, Table 9.2**).

Figure 9.6

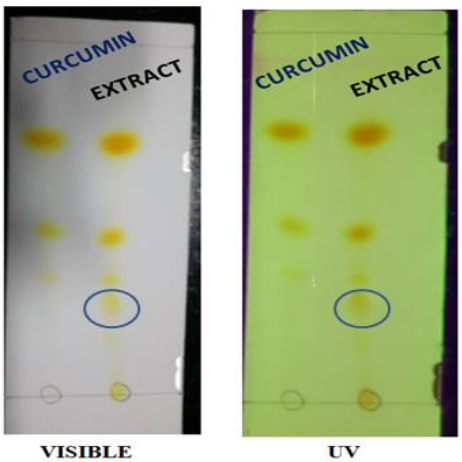

Figure 9.6: TLC plate of Curcumin-PEG conjugate with Lane 1-curcumin, Lane 2- conjugate when viewed under visible and UV light.

Table 9.2

Component	R_f Value
Curcumin	0.69
Demethoxycurcumin	0.35
Bisdemethoxycurcumin	0.2
Curcumin-PEG conjugate	0.13

Table 9.2: R_f values of curcumin, demethoxycurcumin, bisdemethoxycurcumin and Curcumin – PEG conjugate obtained from separation with a mobile phase of chloroform: methanol (95: 5) from the TLC plates.

b) Curcumin-Folic Acid Conjugation: For the solvent system of Chloroform: Ethanol: Acetone: Ammonia in the ratio of 3: 3: 3: 1, the following R_f values were observed (**Figure 9.7**)

Figure 9.7

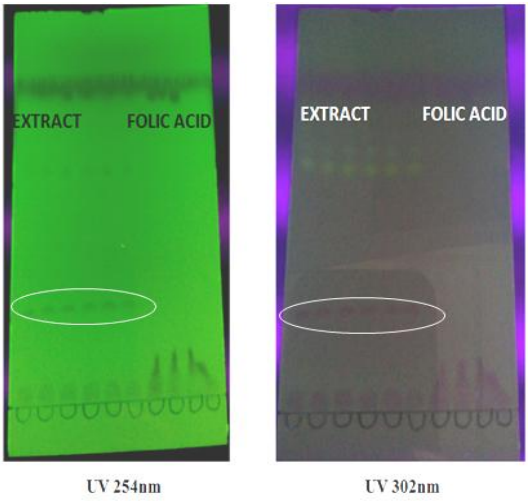

Figure 9.7: TLC plate of curcumin-folic acid conjugate with Lane 1- conjugate, Lane 2- folic acid when viewed under UV light at 254nm and 302nm.

Table 9.3

Component	R_f Value
Curcumin	0.67
Folic Acid	0.12
Curcumin-Folic Acid Conjugate	0.29

Table 9.3: R_f values of curcumin, folic acid and Curcumin – Folic acid conjugate obtained from separation with a mobile phase of chloroform: ethanol: acetone: ammonia (3: 3: 3:1).

9.6.3 FT-IR:

FT-IR analysis was the primary confirmation of successful conjugation. The spectra obtained from shining a beam containing light of many frequencies, provides information on what conformational bonds are present in the sample. Each bond produces a characteristic vibration which finally produces a spectrum. Hence, on the spectrum, if there is a peak at any wave number in a particular range, it indicates the presence of that particular bond.

a) Curcumin-PEG Conjugation: The following figure represents the FT-IR spectrums of the PEG and the curcumin-PEG conjugate obtained via the conjugation extraction procedure. The corresponding tables represent the characteristic IR absorptions of each compound. Every bond in the compound constitutes a particular vibration. If there is a peak at any wave number in this range, it indicates the presence of that particular bond (**Figure 9.8)**

Figure 9.8

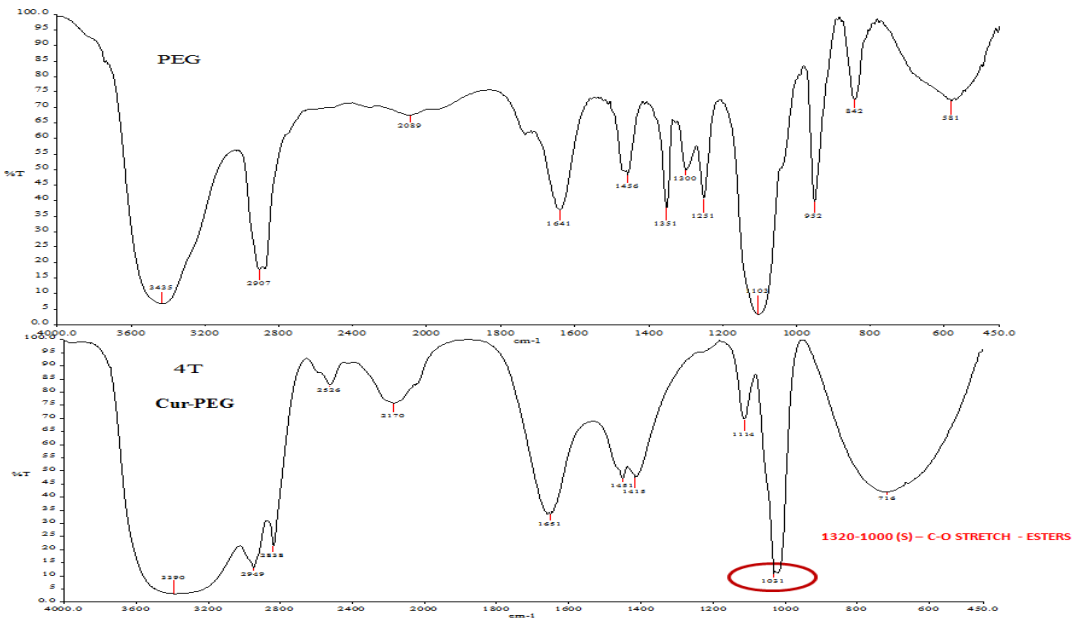

Figure 9.8: FT-IR spectrum of curcumin and Cur-PEG conjugate

In conjugating Curcumin with PEG, an ester bond is formed. A peak at any wave number in the range of 1320 – 1000 cm-1 indicates an ester bond (**Figure 9.8**). In **Table 9.4**, there are two peaks at 1114 cm-1 and 1031 cm-1 indicating that ester

bonds are present in the sample, thus confirming conjugation of Curcumin and PEG.

Table 9.4: Characteristic IR Absorptions for Curcumin – PEG Conjugate

Frequency, cm^{-1}	Bond	Functional Group
1750-1735(s)	C=O Stretch	Esters
1320-1000(s)	C-O Stretch	Esters

b) Curcumin-Folic acid conjugation:

The following figures represent the FT-IR spectrum of the folic acid in powder form and the curcumin-folic acid conjugate obtained via TLC extraction present in methanol. The corresponding table represent the characteristic IR absorption of each compound. Every bond in the compound constitutes a particular vibration.

If there is a peak at any wave number in this range, it indicates the presence of that particular bond. In conjugating curcumin with folic acid, an ester bond is formed. A peak at any wave number in this range of 1320-1000 cm^{-1} indicates an ester bond. In figure, there are two peaks at 1114cm^{-1} and 1022cm^{-1} (**Figure 9.9**) indicating that ester bonds are present, thus confirming the conjugation of curcumin and folic acid (**Table 9.5**).

Figure 9.9

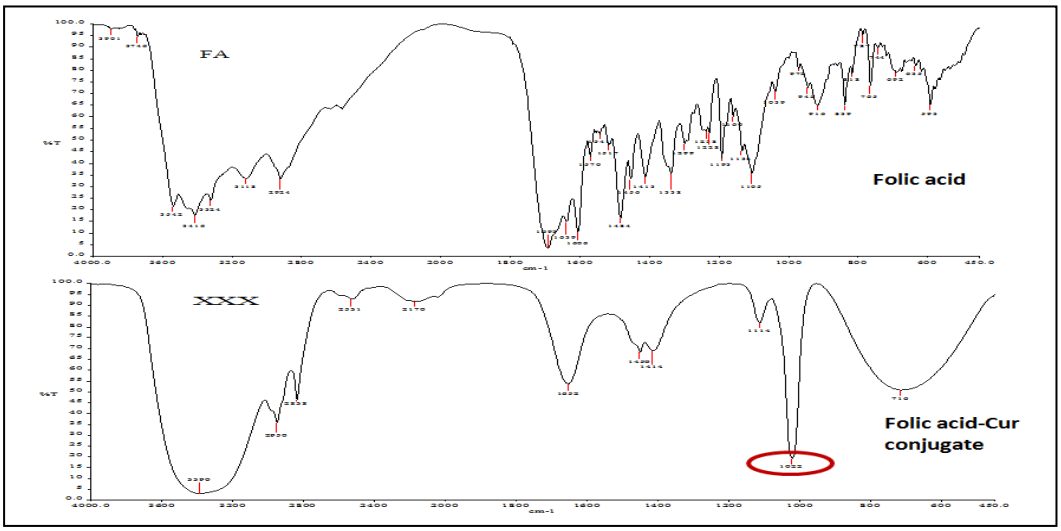

Figure 9.9: FT-IR spectrum of Folic acid and Cur-folic acid conjugate

Table 9.5: Characteristics IR absorption of Curcumin-Folic acid conjugates

Frequency, cm^{-1}	Bond	Functional Group
1750-1735(s)	C=O Stretch	Esters
1320-1000(s)	C-O Stretch	Esters

9.6.4 Absorbance:

a) Curcumin-PEG Conjugation: On carrying out individual wavelength scans for Curcumin, PEG and Curcumin-PEG conjugate, all dissolved in methanol, the wavelength of maximum absorbance were obtained with measurements being carried out against a blank of methanol. Curcumin exhibited an absorption maximum at 422nm while PEG exhibited an absorption maximum at 413nm. The conjugate mimicked PEG's absorption peak at 413nm (**Table 9.6**).

Table 9.6: Maximum wavelength of absorbance of Curcumin – PEG conjugation

Sample	Wavelength of maximum absorbance (nm)
Curcumin	422
PEG	413
Curcumin-PEG Conjugate	413

b) Curcumin-folic acid conjugation:

On carrying out individual wavelength scans for Curcumin, Folic acid and Curcumin-Folic Acid conjugate , all dissolved in methanol, the wavelength of maximum absorbance were obtained with measurements being carried out against a blank of methanol. The conjugate exhibited an absorption maximum of 286nm which was lesser compared to the absorption maximum exhibited by Curcumin and Folic acid at 422nm and 356nm respectively (**Table 9.7**).

Table 9.7: Maximum wavelength of absorbance of Curcumin – Folic acid conjugate

Sample	Wavelength of maximum absorbance (nm)
Curcumin	422
Folic Acid	356
Curcumin-Folic Acid Conjugate	286

9.6.5 Fluorescence:

a) Curcumin-PEG Conjugation: The individual emission spectrums of Curcumin, PEG and Curcumin-PEG conjugate, all dissolved in methanol were recorded using the wavelength of maximum absorbance of each as the excitation wavelength. From the spectrums, the wavelengths of maximum fluorescence were obtained with measurements being carried out against a blank of methanol. Curcumin exhibited a peak of 539nm and PEG exhibited a peak of 453nm. The conjugate exhibited a peak of 528nm which was closer to that of Curcumin than PEG (**Table 9.8**).

Table 9.8: Maximum wavelength of fluorescence of Curcumin – PEG conjugate

Sample	Wavelength of maximum fluorescence (nm)
Curcumin	539
PEG	453
Curcumin-PEG Conjugate	528

b) Curcumin-folic acid conjugation

The individual emission spectrums of Curcumin, Folic Acid and Curcumin-Folic Acid conjugate, all dissolved in methanol were recorded using the wavelength of maximum absorbance of each as the excitation wavelength. From the spectrums, the wavelengths of maximum fluorescence were obtained with measurements being carried out against a blank of methanol. The conjugate exhibited a peak of 550nm which was closer to Curcumin's peak of 539nm than Folic acid's peak of 491nm (**Table 9.9**).

Table 9.9: Maximum wavelength of fluorescence of Curcumin – Folic acid conjugate

Sample	Wavelength of maximum fluorescence (nm)
Curcumin	539
Folic Acid	491
Curcumin-Folic Acid Conjugate	550

9.6.6: Stability testing

One of the main challenges of curcumin is its poor stability in aqueous solutions. At physiological pH, aqueous solution of curcumin undergoes rapid hydrolysis followed by molecular fragmentation. According to the graph below, it was seen that the stability of curcumin decreases from 100% to 54% in 50 minutes. When conjugating curcumin with PEG and folic acid separately, the stability seemed to improve drastically, as can be seen from graphs below (**Figures 9.10**).

Figure 9.10

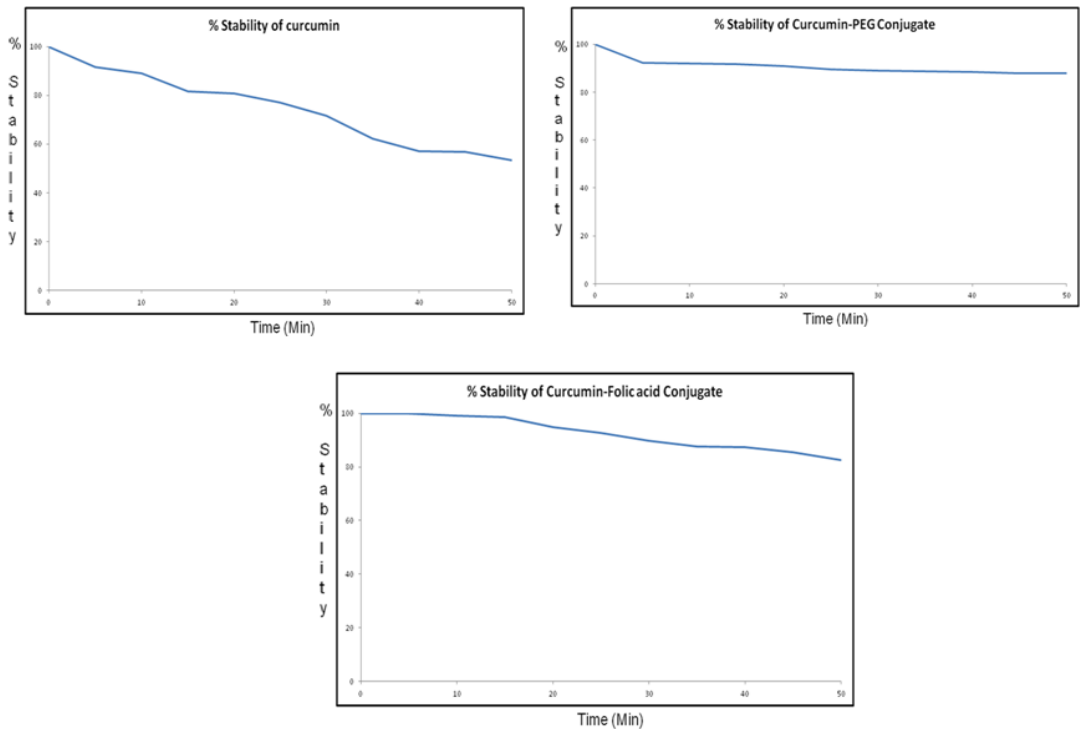

Figure 9.10: Degradation studies of Cur, Cur-PEG and Cur-Folic acid in aqueous solution at physiologic pH7.4. We monitored the absorption spectra of curcumin and respective conjugates for 50min at 5 min intervals to know whether the conjugation has any influence on the stability of curcumin.

9.7 Discussion:

Curcumin possesses various pharmacological properties like anti-inflammatory, anti-oxidant, anti-cancer activities and has been studied as a potential drug for treating many diseases including cancer. Despite the array of biological properties that it possesses, curcumin is highly hydrophobic and has low bioavailability due to its poor aqueous solubility in biological systems (Goel et al. 2008). Various biodegradable polymers have been used has a delivery systems to enhance the effectiveness of food materials and decrease the dosage required. In order to enhance these problems, in our study we developed a Curcumin-PEG (non-targeted) and Curcumin-Folic acid (targeted) conjugates and studied its characterization.

In this study, the amount of curcumin conjugated to PEG or folic acid independently was verified using FT-IR and then measured using UV-Vis spectra. It has already been well studied that the degradation of curcumin in aqueous solution occurs at a pH above neutral (Wang et al. 1997). This indicate that curcumin is deprotonated initially and then fragmentated into Trans-6-(40-hydroxy-30-methoxyphenyl)-2, 4-dioxo-5-hexenal. This is then further degraded into smaller molecules like vanillin, ferulic acid and feruloyl methane (Leung et al. 2008). Therefore, the decrease in the absorption of curcumin signifies the proportional decrease in the concentration of curcumin alone. We monitored the absorption spectrum of curcumin at pH 7.4 and found a minor difference in the absorption spectrum of the Cur-PEG and folic acid conjugates. However, the stability of curcumin decreases about 46% in both the conjugates within 50 min of incubation time. Similarly, Manju et al. also demonstrated 60% degradation of Curcumin-Polyvinylpyrrolidone conjugate within 25 min (Manju et al. 2011). The high stability of the conjugate when compared with the curcumin may be due to the conjugated curcumin exists in the inner core because of its hrdrophobicity and the PEG molecule protrude at the outer core of the micelle. The formed micelle protects the curcumin from deprotonation and subsequent fragmentation in the alkaline media, thereby stabilizes against hydrolysis and enhances its aqueous stability.

These conjugate both Cur-folic acid and Cur-PEG was synthesized by an esterification method using DCC/DMAP reaction. The solubility of the conjugate

in water was several folds higher than the free curcumin, thereby increasing its stability also. However, further studies need to be done to study its cytotoxic effect in RB cell lines.

Apart from this, polymer based NP curcumin (PLGA: PEG) that was gifted from Anderson lab was also tested to study its efficacy in RB cells when compared with the native curcumin. The physiochemical characterization of the drug has been already studied and here the PLGA: PEG NP curcumin was tested for its efficacy on RB cell lines. We investigated the therapeutic potential of NP curcumin and free curcumin in RB cell lines at different concentrations for 48h and measured by using a standard MTT assay. The result showed that NP curcumin exhibited lower IC_{50} value when compared with the native curcumin in the RB cell lines. Similar findings have been observed by Mukerjee et al. where they have shown that curcumin loaded PLGA nanoparticle caused lower IC_{50} value compared with the free curcumin (Mukerjee et al. 2009). Further more, the intracellular uptake of NP and native curcumin were investigated by flow cytometry. We found that the NP curcumin showed high fluorescence due to the more uptake of NP curcumin than the native curcumin by the cancer cells. Other studies have also reported similar uptake characteristics of curcumin nanocarriers in Hela cell lines (Feng et al. 2004).

We found that NP curcumin was more effective in inducing apoptosis than the free curcumin, which may be due to the more cellular uptake of the NP curcumin. Anand et al. also showed that NP curcumin induces more percentage of apoptotic cells than the native curcumin which are similar to our results (Anand et al. 2010). Therefore, based on these results, this NP curcumin formulation can reduce the growth and clonogenicity at lower concentrations than the free curcumin in RB cell lines, which might have a great potential as a therapeutic, for treating RB cancer.

9.8 Chapter summary:

- Two different conjugates Cur-PEG and Cur-Folic acid were synthesized by an esterification step using the DCC/DMAP chemistry.
- Both the conjugates were analysed using various methods which include absorption and fluorescence spectroscopy studies, TLC, FT-IR and stability testing.

- FT-IR results showed difference in the peak range in the conjugates when compared with the native curcumin. Stability testing also showed less degradation of the conjugates over the native curcumin.
- Nanoparticle curcumin showed better efficacy when compared with the native curcumin as analysed from the cell proliferation, colony forming and plasma integrity assay.
- Thus the increased solubility of the conjugates, could potentially improve the medicinal applications of curcumin in the biological systems.

CHAPTER 10: CONCLUSION

- Curcumin was tested for their safety in two non-neoplastic cell lines (3T3 & MIO-M1) and were found to be non-toxic to these normal cell lines, wherein it was toxic to the RB tumour cell lines. Quantitative cellular uptake also confirmed that RB tumour cell lines preferentially take more curcumin than do the normal cell lines.
- Curcumin significantly inhibited cell viability and induced apoptosis in human RB cell lines. We found that curcumin modulates RB cells apoptosis through the mitochondria-mediated pathway subsequent to the disruption of mitochondrial membrane potential, release of cytochrome c, activation of caspase-3 and -9, and the modulation of anti-apoptotic and pro-apoptotic proteins.
- Curcumin treatment altered cell cycle arrest of Y79 RB cells. Whole genome microarray analysis of curcumin treated RB cells revealed differential expression of genes involved in various cellular functions that play an important role in apoptosis, tumour suppressor, transcription, cell adhesion, and cell cycle and differentiation. Curcumin inhibits the proliferation of RB cells by disrupting genes involved in cell cycle check points and cell-cycle progression.
- Curcumin treatment was found to modify the expression of some of the miRNAs in human RB cells, five were up-regulated and sixteen were down-regulated. miR-22 is one of the tumour suppressor miRNA which was up-regulated by curcumin and one of its target genes is confirmed to Erbb3 (oncogene, over-expressed in RB tumour). Transfected miR-22 Y79 cells inhibited the cell proliferation and migration, and suppressed Erbb3 expression which was confirmed to be the target gene of miR-22.
- Our *in vitro* results showed the inhibitory effect of curcumin on P-gp, MRP1 and LRP both in terms of expression and function in RB cell lines. Molecular docking was also carried out with the functional domains of MDR proteins with curcumin and the docking characteristics were studied. *In silico* docking studies also

concurrently infer the binding of curcumin into the nucleotide binding domain (NBD) of P-gp, MRP and LRP functional domain with the binding energy of -7.66 kcal/mol, -7.39kcal/mol and -5.7kcal/mol respectively.

- A synergistic effect was observed in the inhibition of cell growth when the cells were exposed to various concentrations of chemotherapeutic drugs combined with curcumin.
- Synthesis of bio-conjugates of Curcumin-PEG and Curcumin-folic acid showed that the conjugates were soluble and had better stability in aqueous solution than the native curcumin. Similar effect was seen in the nanoparticle (NP) curcumin which showed enhanced cellular uptake and increased bioactivity *in vitro* than the native curcumin in the RB cell lines.
- These studies suggest that curcumin could be a potential chemopreventive agent in the clinical management of retinoblastoma (**Figure 10.1**).

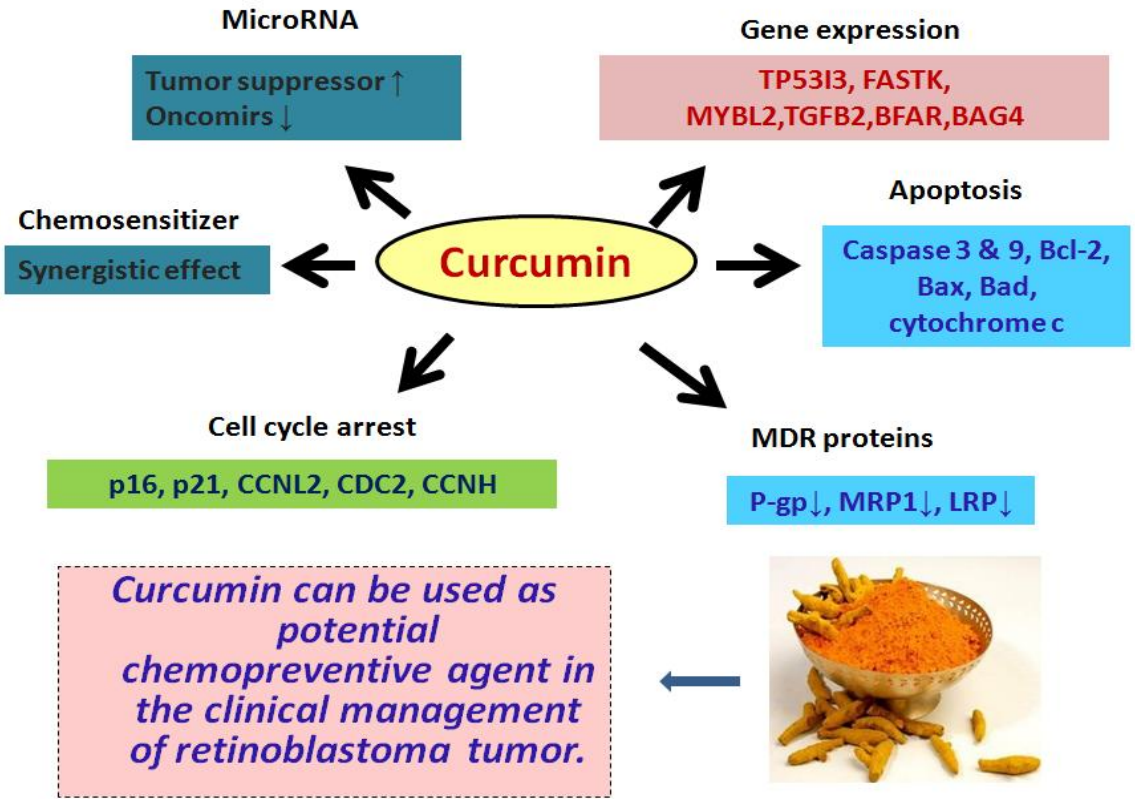

Figure 10.1: Molecular targets shown to be regulated by curcumin in RB cells.

FUTURE SCOPE

- Although the present experiments demonstrate that curcumin is an effective inhibitor of MDR expression and function in vitro, further studies in animal models is required to determine if curcumin has potential as an effective and safe chemosensitizer for treating cells over-expressing MDR proteins.
- Further *in vivo*, studies have to be done for the confirmation of curcumin-miRNA based therapeutics.
- The curcumin-PEG and curcumin-folic acid conjugates need to be purified and tested in the RB cell lines for its cytotoxicity by MTT assay and also performing the uptake studies thereby comparing it with the native curcumin.
- Study the effect of combination therapy (curcumin+chemotherapy drugs) in cultured primary RB tumor cell lines.

APPENDIX I

Cell culture reagents and preparation of media

RPMI 1640 and DMEM Medium:
1 vial of DMEM or RPMI powder dissolved in 900 ml of double sterilized milli Q water and filter sterilized under vacuum. Sterility check-up was done by incubating at room temperature for overnight. After sterility check the growth media was prepared by mixing

DMEM or RPMI 1640 base	90 ml
10%FBS	10 ml
Antibiotic-antimycotic solution	5 drops

Himedia Trypsin: The 0.05g trypsin was weighed and diluted with 100ml of Phosphate Buffered Saline (PBS) (Himedia) and filter sterilized.

Viability count:
0.4 % Trypan Blue (Sigma) dissolved in Phosphate buffered saline (pH 7.4). Count was performed using Neubaeur Chamber (haemocytometer)

Protein estimation:
Reagents

Standard BSA	0.1g/dL
Na_2CO_3	2% in 0.2 N NaOH
$CuSO_4$	0.5% in 1% Trisodium citrate
Alkaline copper reagent	49 ml of Na_2CO_3 + 1 ml of $CuSO_4$
Folin's Ciocalteau Reagent	1:1 dilution

Western blotting Reagents

1. Acrylamide (30%):

Acrylamide-14.6gm
Bis acrylamide-0.4gm
Dissolved in 30ml of water made up to 50ml.

2. Tris-HCl Buffer (pH 8.8):

Tris-9.0gm
Water-25ml
Adjust the pH to 8.8 with1N HCl and made up to 50ml with Distilled water.

3. Tris-HCl Buffer (pH6.8):

Tris-3.0gm
Water-25ml
Adjust the pH to 6.8 with 1N HCl and made up to 50ml with Distilled Water.

4. 10% APS:

Polymerization catalyst required for gel formation. 10% solution used always prepared fresh.

Increasing APS concentration will make the gel set quicker.

Ammonium per sulphate -10gm
Distilled water -100ml.

5. TEMED (readily available):

Polymerization catalyst. Catalyses the formation of persulphate free radicals from the APS, which in turn initiates polymerization. Always the last reagent added to the gel.

6. 10% SDS: Binds proteins so they all become negatively charged, therefore separation is on the basis of size alone and not the intrinsic protein charges.

SDS -10gm
Distilled water-100ml
Stored at room temperature.

Separating gel preparation: Sieves and separates the proteins by size. Percentage gel depends upon the size of target proteins.

Acryl amide %	Range of separation (kDa)
15	12-43
10	16-68
7.5	36-94
5.0	57-212

10%gel:

30% Acrylamide - 4ml
Tris HCl pH 8.8 -2.5ml
10%APS -50µl
TEMED -5µl
10%SDS -100µl
Distilled water -3.344ml

Stacking gel: Large pore size gel with little or no molecular sieving on the sample.

Standard 4% Acrylamide - large enough pore size for most samples.

30% Acrylamide -1.33ml
TrisHCl- (pH 6.8) -2.5ml
10%APS -50µl
TEMED -10µl
10%SDS -100µl
Distilled water -6.01ml.

Western blotting transfer buffer:

Tris -3.3g
Glycine -14.4g

SDS -1.0

The contents were dissolved in 800ml of distilled water. The final volume was then made up to 1000ml with methanol.

Ponseau stain:

Ponseau S -0.5gm
Glacial acetic acid -1ml
Made up to 100ml with distilled water. Prepared just before use.

Electrophoretic buffer (5x):

Tris base -15.1gm
Glycine -72.0gm
SDS -5.0gm

Distilled water made up to 1000ml. Do not adjust the pH of the stock, as the pH will be 8.3 when diluted. Stored at 4^0C until use (up to 1 month).

Radioimmunoprecipitation buffer (RIPA-Lysis buffer)

Tris - 50mM
Nacl - 150mM
SDS - 0.1%
Triiton X-100 - 0.5%
Dissolved in 10 ml dH_2O
Protease inhibitor cocktail (PIC) -1mg/ml
RIPA buffer and PIC solution -10ml HEPES+300µl PIC

Sample loading Buffer (3x):

1M Tris HCl (pH 6.8) -2.4ml
20%SDS -3ml
Glycerol -3ml
β-Mercaptoethanol -1.6ml
Bromophenol Blue -0.006gm

Tris buffered saline (pH:7.6) (TBS):

Sodium chloride -8gm
1M Tris HCl -20ml
Tween-20 -10ml.
Diluted to 1000ml with distilled water.

5% Skimmed milk: 2.5g of skimmed milk powder was dissolved in 50ml of TBS

PCR reagents:

Gene specific primers: The stock was diluted in 100µl of TE buffer and heated at 65^0C for 5 min.

Taq buffer with $MgCl_2$
100mM DNTP mix (Banglore genei)
Taq DNA polymerase 3U/µl (Banglore genei)
Sterile water

Gel Electrophoresis:

Electrophoresis is a method by which the amplification of the gene sequence is confirmed after PCR. DNA, negatively charged moves to the cathode on subjected to electric field and moves according to the molecular weight in a matrix like agarose or polyacrylamide gels. The gels are suitably stained to visualize the product (Fluorescent dyes for agarose gels and silver staining of poly acryl amide gels).

Agarose gel electrophoresis:

Preparation of TBE buffer: 54.1 g of Tris, 27.8g of boric acid and 3.65 g EDTA were added in 500 ml water and pH adjusted to 8.0.The stock solution is diluted 1: 10 for further use.

Tracking dye- Bromophenol blue : 0.1gm BPB+100ml 1X TBE buffer in equal volumes of 40%sucrose solution.

Requirements:
Molecular weight marker, Agarose, 10 X TBE buffer, Ethidium bromide (2mg/ml), BPB.

Preparation of agarose gel: The gel trough was cleaned with ethanol and the ends were sealed with cellophane tape with the combs placed in the respective positions to form wells. Two percentage of agarose gel was prepared by dissolving agarose in 1X TBE buffer and 8µl of ethidium bromide being finally added and mixed thoroughly and poured on to the trough followed by electrophoresis of the amplified products at 100 V for 30 to 45 minutes. The gel was then captured and analysed using ImageJ software.

APPENDIX II

S. No	CONSUMABLES	COMPANY
1	RPMI 1640	Gibco
2	P-glycoprotein, Multi-drug resistance protein antibody	Sigma Aldrich
3	Antibiotic antimycotic solution	Sree venkateshwara scientific suppliers
4	P-gp, MRP1 and LRP, Bax, Bcl-2, cytochrome c primers	Sigma Aldrich
5	LRP antibody	Novacastra
6	Bax, Bcl-2, cytochrome c	Santa cruz
7	Caspase 3 and 9	Santa Cruz
8	Dimethyl sulfoxide	Sigma Aldrich
9	DMEM	Gibco
10	DNTP mix	Sanmar specialty centre
11	Fetal bovine serum	PAA
12	MTT	Sigma Aldrich
13	Ponceau S	Sigma Aldrich
14	RNAse out	Biocorporals
15	Sample buffer for SDS PAGE	Sanmar specialties chemicals
16	Sensiscript reverse transcriptase kit	Qiagen
17	Trypsin (0.01%)	Biocorporals
18	Annexin V-Fluos staining kit	Roche
19	Anti-β actin antibody	Sigma Aldrich
20	Chloroform	Merck
21	Isopropanol	Merck
22	Diethyl pyrocarbonate	Sigma Aldrich
23	Enhanced chemilunescence kit	Pierce
24	LSAB kit	Dako
25	Rabbit anti-mouse antibody	Santa-Cruz
26	Mouse anti-rabbit antibody	Santa-Cruz
27	SYBR green real time RT-PCR master mix	SABiosciences
28	Taqman real time RT-PCR probes	Labindia
29	Triton X 100	HiMedia
30	Trizol	Sigma Aldrich
31	DAPI	Sigma Aldrich
32	Calcein	Sigma Aldrich
33	Rhodamine 123	Sigma Aldrich
34	Ethidium bromide	Sigma Aldrich
35	8-azido ATP-biotin	Affinity labelling technologies
36	Probenecid, indomethacin, Verapamil	Sigma Aldrich

APPENDIX III:

Table 1a: Genes down-regulated at 20µM curcumin concentration in Y79 RB cells

Name	Gene bank accession number	Fold increase	Chromosome location	Gene description
Transcription factor				
SREBF2	NM_004599	-2.56	22q13	sterol regulatory element binding transcription factor 2
POU4F2	NM_004575	-1.77	4q31.2	POU class 4 homeobox 2
RAB26	NM_014353	-2.49	16p13.3	member RAS oncogene family
TFAM	NM_003201	-1.40	10q21	transcription factor A, mitochondrial
MYBL2	NM_002466	-1.19	20q13.12	V-myb myeloblastosis viral oncogene homolog (avian)-like 2
DEK	NM_003472	-1.52	6p22.3	DEK oncogene, DNA binding
IRS1	NM_005544	-2.08	2q36.3	*Insulin receptor substrate 1*
ABL2	NM_007314	-1.22	1q25.2	V-abl Abelson murine leukemia viral oncogene homolog 2
SERBP1	NM_001018067	-1.72	1p31.3	SERPINE1 mRNA binding protein 1
Angiogenesis				
TGFB2	NM_001135599	-2.02	1q41	transforming growth factor, beta 2
EGFL7	NM_201446	-2.30	9q34.3	EGF-like-domain, multiple 7
PGK1	NM_000291	-1.32	Xq21.1	phosphoglycerate kinase 1
IGFBP2	NM_000597	-2.1	2q35	insulin-like growth factor binding protein 2
NTRK1	NM_002529	-2.24	1q23.1	neurotrophic tyrosine kinase, receptor, type 1
Cell cycle and differentiation				
ANAPC7	NM_016238	-1.32	12q24.11	anaphase promoting complex subunit 7
CDC2	NM_001786	-1.66	10q21.1	Cyclin division cycle 2
SKP2	NM_032637	-2.11	5p13	S-phase kinase-associated protein 2
CCNE2	NM_057749	-1.52	8q22.1	cyclin E2
CCNH	NM_001239	-1.04	5q13.3-q14	cyclin H
MYB	NM_005375	-1.64	6q22-q23	v-myb myeloblastosis viral oncogene homolog

MAD2L1	NM_002358	-1.80	4q27	MAD2 mitotic arrest deficient-like 1
MCM7	NM_182776	-2.09	7q21.3-q22.1	minichromosome maintenance complex component 7
CCNF	NM_001761	-1.84	16p13.3	cyclin F
NEK2	NM_002497	-1.44	1q32.2-q41	NIMA (never in mitosis gene a)-related kinase 2
NSL1	NM_015471	-1.29	1q41	NSL1, MIND kinetochore complex component, homolog
KIF20A	NM_005733	-1.36	5q31.2	kinesin family member 20A
KIF14	NM_014875	-1.89	1q32.1	Kinesin family member 14
Cell adhesion				
ICAM5	NM_003259	-1.74	19p13.2	Intercellular adhesion molecule 5
CITED1	NM_004143	-1.01	Xq13.1	Cbp/p300-interacting transactivator, with Glu/Asp-rich carboxy-terminal domain, 1
CRKL	NM_005207	-1.65	22q11.21	v-crk sarcoma virus CT10 oncogene homolog (avian)-like
PPARA	NM_001001928	-1.31	22q13.31	peroxisome proliferator activated receptor
Cell migration				
LAMA1	NM_005559	-1.61	18p11.31	laminin, alpha 1
PPIA	NM_021130	-1.46	7p13	peptidylprolyl isomerase A
YBX1	NM_004559	-1.09	1p34.2	Y box binding protein 1
Anti-apoptosis				
BFAR	NM_016561	-1.49	16p13.12	Bifunctional apoptosis regulator
BAG4	NM_004874	-1.52	8p12	BCL2-associated athanogene 4

Table 1b: Genes up-regulated at 20µM curcumin concentration in Y79 RB cells.

Name	Gene bank accession number	Fold increase	Chromosome location	Gene description
Apoptotic genes				
TRADD	NM_003789	1.29	16q22.1	TNFRSF1A-associated via death domain
FASTK	NM_006712	1.21	7q36.1	Fas-activated serine/threonine kinase
AIFM2	NM_032797	2.42	10q22.1	Apoptosis-inducing factor, mitochondrion-associated, 2
IGFBP6	NM_002178	2.23	12q13	insulin-like growth factor binding protein 6
IRF1	NM_002198	2.27	5q31.1	interferon regulatory factor 1
TP5313	NM_004881	1.50	2p23.3	Tumor protein p53 inducible protein 3
STK17A	NM_004760	3.09	7p13	serine/threonine kinase 17a
TNFSF13B	NM_006573	1.33	13q32-q34	tumor necrosis factor (ligand) superfamily
Tumor suppressor				
LATS1	NM_004690	1.23	6q25.1	Large tumor suppressor, homolog 1
SPRY4	NM_030964	1.39	5q31.3	sprouty homolog 4
ARMETL1	NM_001029954	1.85	10p14	arginine-rich, mutated in early stage tumours-like 1
EXT1	NM_000127	1.44	8q24.11	Exostosin 1
SEMA3B	NM_004636	1.37	3p21.3	sema domain, immunoglobulin domain (Ig), short basic domain, secreted, (semaphorin) 3B
TSPYL2	NM_022117	1.81	Xp11.2	TSPY-like 2
PHLDA2	NM_003311	2.28	11p15.5	Pleckstrin homology-like domain, family A, member 2
CYFIP1	NM_014608	1.42	15q11	cytoplasmic FMR1 interacting protein 1
SLIT2	NM_004787	2.14	4p15.2	slit homolog 2
Cell cycle arrest				
NEK11	NM_145910	1.87	3q22.1	(Never in mitosis gene a)-related kinase 11

CIZ1	NM_012127	1.07	9q34.1	CDKN1A interacting zinc finger protein 1
RHOB	NM_004040	2.30	2p24	ras homolog gene family, member B
OSGIN1	NM_013370	3.08	16q23.3	oxidative stress induced growth inhibitor 1
CDKN2B	NM_078487	1.70	9p21	cyclin-dependent kinase inhibitor 2B
CDKN1A	NM_078467	1.76	6p21.31	cyclin-dependent kinase inhibitor 1A
PAK6	NM_020168	1.95	15q15.1	p21(CDKN1A)-activated kinase 6
CCNL2	NM_001039577	1.11	1p36.33	cyclin L2
EGR1	NM_001964	3.14	5q31.1	early growth response 1
CDCA7	NM_031942	1.45	2q31	Cell division cycle associated 7
Heat shock proteins				
SUHW1	NM_080740	1.58	22q11.22	suppressor of hairy wing homolog 1
HSPB8	NM_014365	3.24	12q24.23	heat shock 22kDa protein 8
HSPA1L	NM_005527	1.49	6p21.33	heat shock 70kDa protein 1-like
HSPA5	NM_005347	1.80	9q33.3	heat shock 70kDa protein 5
HSPA1A	NM_005345	3.13	6p21.33	heat shock 70kDa protein 1A
HSPA6	NM_002155	3.9	1q23.3	heat shock 70kDa protein 6
Phosphatase activity				
PPP1R3C	NM_005398	1.10	10q23.32	protein phosphatase 1, regulatory (inhibitor) subunit 3C
PPP1R15A	NM_014330	2.47	19q13.2	protein phosphatase 1, regulatory (inhibitor) subunit 15A
PPP1R10	NM_002714	1.31	6p21.33	protein phosphatase 1, regulatory (inhibitor) subunit 10
Inactivation of MAPK family kinases				
DUSP10	NM_007207	2.71	1q41	dual specificity phosphatase 10
DUSP18	NM_152511	1.2	22q12.2	dual specificity phosphatase 18
DUSP23	NM_017823	1.4	1q23.2	dual specificity phosphatase 23

DUSP13	NM_001007271	2.78	10q22.2	dual specificity phosphatase 13
DUSP2	NM_004418	1.42	2q11.2	dual specificity phosphatase 2

REFERENCES

(2001). Boik J. Natural compounds in cancer therapy. Quality Books, Inc.

Aggarwal, B. B. and K. B. Harikumar (2009). "Potential therapeutic effects of curcumin, the anti-inflammatory agent, against neurodegenerative, cardiovascular, pulmonary, metabolic, autoimmune and neoplastic diseases." Int J Biochem Cell Biol **41**(1): 40-59.

Aggarwal, B. B. and S. Shishodia (2006). "Molecular targets of dietary agents for prevention and therapy of cancer." Biochem Pharmacol **71**(10): 1397-1421.

Anand, P., H. B. Nair, et al. (2010). "Design of curcumin-loaded PLGA nanoparticles formulation with enhanced cellular uptake, and increased bioactivity in vitro and superior bioavailability in vivo." Biochem Pharmacol **79**(3): 330-338.

Anand, P., C. Sundaram, et al. (2008). "Curcumin and cancer: an "old-age" disease with an "age-old" solution." Cancer Lett **267**(1): 133-164.

Anand, P., S. G. Thomas, et al. (2008). "Biological activities of curcumin and its analogues (Congeners) made by man and Mother Nature." Biochem Pharmacol **76**(11): 1590-1611.

Andjelkovic, T., M. Pesic, et al. (2008). "Synergistic effects of the purine analog sulfinosine and curcumin on the multidrug resistant human non-small cell lung carcinoma cell line (NCI-H460/R)." Cancer Biol Ther **7**(7): 1024-1032.

Antony, A. C. (1996). "Folate receptors." Annu Rev Nutr **16**: 501-521.

Anto, RJ., A.Mukhopadhyay, et al. (2002). "Curcumin (diferuloylmethane) induces apoptosis through activation of caspase-8, BID cleavage and cytochrome c release: Its suppression by ectopic expression of Bcl-2 and Bcl-xl." Carcinogenesis. **23**:143–150.

Anuchapreeda, S., P. Leechanachai, et al. (2002). "Modulation of P-glycoprotein expression and function by curcumin in multidrug-resistant human KB cells." Biochem Pharmacol **64**(4): 573-582.

Arora., RS, Eden., TO, et al. (2009). "Epidemiology of childhood cancer in India". Indian J Cancer **46**(4):264-73. Review.

Bagnyukova, TV., IP. Pogribny, IP, et al. (2006). "MicroRNAs in normal and cancer cells: a new class of gene expression regulators." Exp Oncol **28**:263–269.

Bakhshi, S., Bakhshi, R. (2007). "Genetics and management of Retinoblastoma. " J Indian Assoc Pediatr Surg **12**(3): 109-115.

Bava, S. V., C. N. Sreekanth, et al. (2011). "Akt is upstream and MAPKs are downstream of NF-kappaB in paclitaxel-induced survival signaling events, which are down-regulated by curcumin contributing to their synergism." Int J Biochem Cell Biol **43**(3): 331-341.

Bush, J. A., K. J. Cheung, Jr., et al. (2001). "Curcumin induces apoptosis in human melanoma cells through a Fas receptor/caspase-8 pathway independent of p53." Exp Cell Res **271**(2): 305-314.

Caldon, C. E. and E. A. Musgrove (2010). "Distinct and redundant functions of cyclin E1 and cyclin E2 in development and cancer." Cell Div **5**: 2.

Calogero, A., V. Lombari, et al. (2004). "Inhibition of cell growth by EGR-1 in human primary cultures from malignant glioma." Cancer Cell Int **4**(1): 1.

Campbell, FC., GP, Collett, et al. (2005). “Chemopreventive properties of curcumin.” Future Oncol **1**: 405-414.

Cao, J., Y. Liu, et al. (2007). "Curcumin induces apoptosis through mitochondrial hyperpolarization and mtDNA damage in human hepatoma G2 cells." Free Radic Biol Med **43**(6): 968-975.

Cha, M. C., A. Lin, et al. (2005). "Low dose docosahexaenoic acid protects normal colonic epithelial cells from araC toxicity." BMC Pharmacol **5**: 7.

Chakraborty, S., S. Khare, et al. (2007). "Identification of genes associated with tumorigenesis of retinoblastoma by microarray analysis." Genomics **90**(3): 344-353.

Chakraborty, S., U. Ghosh, et al. (2006). “Inhibition of telomerase activity and induction of apoptosis by curcumin in K-562 cells.” Mutat Res **596**: 81–90.

Chan, H. S., Y. Lu, et al. (1997). "Multidrug resistance protein (MRP) expression in retinoblastoma correlates with the rare failure of chemotherapy despite cyclosporine for reversal of P-glycoprotein." Cancer Res **57**(12): 2325-2330.

Chang, T. C., D. Yu, et al. (2008). "Widespread microRNA repression by Myc contributes to tumorigenesis." Nat Genet **40**(1): 43-50.

Chantada, GL., F. Doz, et al. (2008). "International Retinoblastoma Staging Working Group. World disparities in risk definition and management of retinoblastoma: a report from the International Retinoblastoma Staging Working Group. " Pediatr Blood Cancer **50**:692-4.

Chainani-Wu N et al. (2003). “Safety and anti-inflammatory activity of curcumin: a component of turmeric (Curcuma longa).” J Altern Complement Med. **9**:161-168.

Chattopadhyay, I., Biswas, K, et al. (2004). “Turmeric and curcumin: Biological and medicinal applications.” Current Science 87: 44-53.

Chearwae, W., C. P. Wu, et al. (2006). "Curcuminoids purified from turmeric powder modulate the function of human multidrug resistance protein 1 (ABCC1)." Cancer Chemother Pharmacol **57**(3): 376-388.

Chen, HW., HC.Huang et al. (2000). “ Effetc of curcumin on cell cycle progression and apoptosis in vascular smooth cells. Br. J. Pharmacol **124**:1029-40.

Chen, H. W., S. L. Yu, et al. (2004). "Anti-invasive gene expression profile of curcumin in lung adenocarcinoma based on a high throughput microarray analysis." Mol Pharmacol **65**(1): 99-110.

Chen, A., J, Xu, et al. (2006). “Curcumin inhibits human colon cancer cell growth by suppressing gene expression of epidermal growth factor receptor through reducing the activity of the transcription factor Egr-1.” Oncogene. **25**:278–287.

Chignell, C. F., P. Bilski, et al. (1994). "Spectral and photochemical properties of curcumin." Photochem Photobiol **59**(3): 295-302.

Chintagumpala, M., P. Chevez-Barrios, et al. (2007). "Retinoblastoma: review of current management." Oncologist **12**(10): 1237-1246.

Cho, J. W., K. S. Lee, et al. (2007). "Curcumin attenuates the expression of IL-1beta, IL-6, and TNF-alpha as well as cyclin E in TNF-alpha-treated HaCaT cells; NF-kappaB and MAPKs as potential upstream targets." Int J Mol Med **19**(3): 469-474.

Chou, T. C. and P. Talalay (1984). "Quantitative analysis of dose-effect relationships: the combined effects of multiple drugs or enzyme inhibitors." Adv Enzyme Regul **22**: 27-55.

Chou., JH, and Chou., TC. (1988)."Computerized simulation of dose reduction index (DRI) in synergistic drug combinations." Pharmacologist **30:** A231.

Choudhuri, T., S. Pal, et al. (2002). " Curcumin induces apoptosis in human breast cancer cells through p53-dependent Bax induction." FEBS Lett **512**:334-340.

Chuang, SE., ML. Kuo et al. (2000). " Curcumin containing diet inhibits diethyl nitrosamine and induced murine hepatocarcinogenesis. Carcinogenesis 21: 331-335.

Cohen, G. M. (1997). "Caspases: the executioners of apoptosis." Biochem J **326 (Pt 1)**: 1-16.

Conkrite, K., M. Sundby, et al. (2011). "miR-17~92 cooperates with RB pathway mutations to promote retinoblastoma." Genes Dev **25**(16): 1734-1745.

Conseil, G., H. Baubichon-Cortay, et al. (1998). "Flavonoids: a class of modulators with bifunctional interactions at vicinal ATP- and steroid-binding sites on mouse P-glycoprotein." Proc Natl Acad Sci U S A **95**(17): 9831-9836.

Corbeil, C. R., P. Englebienne, et al. (2007). "Docking ligands into flexible and solvated macromolecules. 1. Development and validation of FITTED 1.0." J Chem Inf Model **47**(2): 435-449.

Dawson, R. J. and K. P. Locher (2006). "Structure of a bacterial multidrug ABC transporter." Nature **443**(7108): 180-18

Debatin, KM., et al. (2004). "Apoptosis pathways in cancer and cancer therapy." Cancer Immunol Immunother **53**:153-159.

Dillman, R. O. (1990). "Rationales for combining chemotherapy and biotherapy in the treatment of cancer." Mol Biother **2**(4): 201-207.

Dimaras, H., K. Kimani, et al. (2012). "Retinoblastoma." Lancet **379**(9824): 1436-1446.

Doe JM, et al. (2008). "MicroRNA: Cancer and future treatment applications. Basic Biotech eJournal." 36–42.

Doucette, M. M. and V. L. Stevens (2001). "Folate receptor function is regulated in response to different cellular growth rates in cultured mammalian cells." J Nutr **131**(11): 2819-2825.

Dorai, T., YC, Cao, et al. (2001). "Therapeutic potential of curcumin in human prostate cancer. III. Curcumin inhibits proliferation, induces apoptosis, and inhibits angiogenesis of LNCaP prostate cancer cells in vivo." Prostate **47**: 293–303.

Dunn, JM., RA. Phillips, et al. (1988). "Identification of germline and somatic mutations affecting the retinoblastoma gene." Science **241**,1797–1800.

Eckstein, L. A., K. R. Van Quill, et al. (2005). "Cyclosporin a inhibits calcineurin/nuclear factor of activated T-cells signaling and induces apoptosis in retinoblastoma cells." Invest Ophthalmol Vis Sci **46**(3): 782-790.

Eswar, N., D. Eramian, et al. (2008). "Protein structure modeling with MODELLER." Methods Mol Biol **426**: 145-159.

Feng, S. S. (2004). "Nanoparticles of biodegradable polymers for new-concept chemotherapy." Expert Rev Med Devices **1**(1): 115-125.

Filho, J. P., Z. M. Correa, et al. (2005). "Histopathological features and P-glycoprotein expression in retinoblastoma." Invest Ophthalmol Vis Sci **46**(10): 3478-3483.

Fuchs, J. R., B. Pandit, et al. (2009). "Structure-activity relationship studies of curcumin analogues." Bioorg Med Chem Lett **19**(7): 2065-2069.

Fulda, S., KM. Debatin, et al. (2004). "Apoptosis Signaling in Tumor Therapy." Ann N Y Acad Sci. **1028**:150–156.

Gallie, B. L., A. Budning, et al. (1996). "Chemotherapy with focal therapy can cure intraocular retinoblastoma without radiotherapy." Arch Ophthalmol **114**(11): 1321-1328.

Goel, A., S. Jhurani, et al. (2008). "Multi-targeted therapy by curcumin: how spicy is it?" Mol Nutr Food Res **52**(9): 1010-1030.

Goel, A., CR. Boland et al. (2001). " Specific inhibition of cyclooxygenase-2 (COX-2) expression by dietary curcumin in HT-29 human colon cancder cells." Cancer Lett 172: 111-118.

Goodsell, D. S., G. M. Morris, et al. (1996). "Automated docking of flexible ligands: applications of AutoDock." J Mol Recognit **9**(1): 1-5.

Gupta, S. C., S. Prasad, et al. (2011). "Multitargeting by curcumin as revealed by molecular interaction studies." Nat Prod Rep **28**(12): 1937-1955.

Gupta., SC, Patchva., S et al. (2012). Discovery of curcumin, a component of golden spice, and its miraculous biological activities. Clin Exp Pharmacol Physiol **39**(3):283-99.

Harbottle, A., A. K. Daly, et al. (2001). "Role of glutathione S-transferase P1, P-glycoprotein and multidrug resistance-associated protein 1 in acquired doxorubicin resistance." Int J Cancer **92**(6): 777-783.

He, H., K. Jazdzewski, et al. (2005). "The role of microRNA genes in papillary thyroid carcinoma."Proc Natl Acad Sci US*A*.**102**:19075–19080.

Hilgenbrink, A. R. and P. S. Low (2005). "Folate receptor-mediated drug targeting: from therapeutics to diagnostics." J Pharm Sci **94**(10): 2135-2146.

Hosseinzadeh, L., Behravan, J et al. (2010). "Effect of curcumin on doxorubicin-induced cytotoxicity in H9c2 cardiomyoblast cells." Iran J of Basic Medi Scienc **14**: 49-56.

Huang, MT., RC. Smart et al. (1988). " Inhibitory effect of curcumin, chlorogenic acid, caffeic acid and ferulic acidon tumour promotion in mouse skin by 12-O-tetradecanoylphorbol-13-acetate." Cancer Res 48: 5941-46.

Huang, MT., T. Lysz et al. (1991). "Inhibitiry effects of curcumin on in vitro lipoxygenase and cycloxygenase activities in mouse epidermis." Cancer Res 51: 813-819.

Huang, J. C., T. Babak, et al. (2007). "Using expression profiling data to identify human microRNA targets." Nat Methods **4**(12): 1045-1049.

Hungerford, J. L., N. M. Toma, et al. (1995). "External beam radiotherapy for retinoblastoma: I. Whole eye technique." Br J Ophthalmol **79**(2): 109-111.

Ioriof., MV, Ferracin., M, et al. (2005). "MicroRNA gene expression deregulation in human breast cancer." Cancer Res **65**(16):7065-70.

Ireson, C., S. Orr, et al. (2001). "Characterization of metabolites of the chemopreventive agent curcumin in human and rat hepatocytes and in the rat in vivo, and evaluation of their ability to inhibit phorbol ester-induced prostaglandin E2 production." Cancer Res **61**(3): 1058-1064.

Izquierdo, M. A., R. H. Shoemaker, et al. (1996). "Overlapping phenotypes of multidrug resistance among panels of human cancer-cell lines." Int J Cancer **65**(2): 230-237.

Jana, N. R., P. Dikshit, et al. (2004). "Inhibition of proteasomal function by curcumin induces apoptosis through mitochondrial pathway." J Biol Chem **279**(12): 11680-11685.

Jaruga, E., A. Sokal, et al. (1998). "Apoptosis-independent alterations in membrane dynamics induced by curcumin." Exp Cell Res **245**(2): 303-312.

Joe, B., M. Vijaykumar, et al. (2004). "Biological properties of curcumin-cellular and molecular mechanisms of action." Crit Rev Food Sci Nutr **44**(2): 97-111.

Jones, EA., A. Shahed et al. (2000). " Modulation of apoptotic and inflammatory genes by bioflavonoids and angiotensin II inhibition in ureteral obstruction." Urology **56**(2): 346-51.

Kabore, AF., JB. Johnston, et al. (2004). "Changes in the Apoptotic and Survival Signaling in Cancer Cells and Their Potential Therapeutic Implications." Curr Cancer Drug Targets. **4:**147-163.

Kayaselcuk, F., S. Erkanli, et al. (2006). "Expression of cyclin H in normal and cancerous endometrium, its correlation with other cyclins, and association with clinicopathologic parameters." Int J Gynecol Cancer **16**(1): 402-408.

Kelloff, CJ., Boone, CW, et al. (1994). " Mechanistic considerations in chemopreventive drug development. " J. Cell Biochemistry Supplement **20**:1-24.

Khar, A., A. M. Ali, et al. (1999). "Antitumor activity of curcumin is mediated through the induction of apoptosis in AK-5 tumor cells." FEBS Lett **445**(1): 165-168.

Khopde, SM., KI. Priyadrashini et al. (1999). " Free radical scavenging ability and antioxidant efficiency of curcumin and its substituted analogue. Biophysical chemistry **80**:83-89.

Kim, HY., EJ. Park, et al. (2003). " Curcumin suppresses JAN-STAT inflammatory signalling through activation of Src homology 2 domain-containing tyrosine phosphatase 2 in brain microglia." J. Immuno 171: 6072-79.

Kim, R., M. Emi, et al. (2006). "The role of apoptosis in cancer cell survival and therapeutic outcome." Cancer Biol Ther **5**(11): 1429-1442.

Kitagawa, S., T. Nabekura, et al. (2004). "Inhibition of P-glycoprotein function by tea catechins in KB-C2 cells." J Pharm Pharmacol **56**(8): 1001-1005.

Kohli, J. Ali, et al. (2005). " Curcumin: A natural anti-inflammatory agent." Indian J Pharmacol 37: 141-47.

Kozlov, G., O. Vavelyuk, et al. (2006). "Solution structure of a two-repeat fragment of major vault protein." J Mol Biol **356**(2): 444-452.

Krishnakumar, S., K. Mallikarjuna, et al. (2004). "Multidrug resistant proteins: P-glycoprotein and lung resistance protein expression in retinoblastoma." Br J Ophthalmol **88**(12): 1521-1526.

Kunwar, A., A. Barik, et al. (2008). "Quantitative cellular uptake, localization and cytotoxicity of curcumin in normal and tumor cells." Biochim Biophys Acta **1780**(4): 673-679.

Kunwar, A., A. Barik, et al. (2006). "Transport of liposomal and albumin loaded curcumin to living cells: an absorption and fluorescence spectroscopic study." Biochim Biophys Acta **1760**(10): 1513-1520.

Kuo, M. L., T. S. Huang, et al. (1996). "Curcumin, an antioxidant and anti-tumor promoter, induces apoptosis in human leukemia cells." Biochim Biophys Acta **1317**(2): 95-100.

Kuttan, R., PC. Sudheeran et al. (1987). " Turmeric and curcumin as topical agents in cancer therapy. Tumori 73: 29-31.

Laskowski, R.A., MacArthur, M.W et al. (1993). PROCHECK: a program to check the stereochemical quality of protein structures. J. Appl. Crystallogr **26**, 283-291.

Lee, EJ., Y. Gusev, et al. (2007). "Expression profiling identifies microRNA signature in pancreatic cancer." Int J Cancer **120**:1046–1054.

Lee, C. H. (2004). "Reversing agents for ATP-binding cassette (ABC) transporters: application in modulating multidrug resistance (MDR)." Curr Med Chem Anticancer Agents **4**(1): 43-52.

Leung, M. H., H. Colangelo, et al. (2008). "Encapsulation of curcumin in cationic micelles suppresses alkaline hydrolysis." Langmuir **24**(11): 5672-5675.

Lev-Ari, S., L. Strier, et al. (2006). "Curcumin synergistically potentiates the growth-inhibitory and pro-apoptotic effects of celecoxib in osteoarthritis synovial adherent cells." Rheumatology (Oxford) **45**(2): 171-177.

Lewis, B. P., I. H. Shih, et al. (2003). "Prediction of mammalian microRNA targets." Cell **115**(7): 787-798.

Li, J., S. Liang, et al. (2010). "An inhibitory effect of miR-22 on cell migration and invasion in ovarian cancer." Gynecol Oncol **119**(3): 543-548.

Li, N., J. Alam et al. (2004). " Nrf2 is a key transcription factor that regulates antioxidant defense in macrophages and epithelial cells: protecting against proinflammatory and oxidizing effects of diesel exhaust chemicals. J. Immunol 173:3467-481.

Li, J., Y. Wang, et al. (2009). "Polyethylene glycosylated curcumin conjugate inhibits pancreatic cancer cell growth through inactivation of Jab1." Mol Pharmacol **76**(1): 81-90.

Li, M., Z. Zhang, et al. (2007). "Curcumin, a dietary component, has anticancer, chemosensitization, and radiosensitization effects by down-regulating the MDM2 oncogene through the PI3K/mTOR/ETS2 pathway." Cancer Res **67**(5): 1988-1996.

Liang, J., H. Edelsbrunner, et al. (1998). "Anatomy of protein pockets and cavities: measurement of binding site geometry and implications for ligand design." Protein Sci 7(9): 1884-1897.

Lin, H. I., Y. J. Lee, et al. (2005). "Involvement of Bcl-2 family, cytochrome c and caspase 3 in induction of apoptosis by beauvericin in human non-small cell lung cancer cells." Cancer Lett **230**(2): 248-259.

Lin, J. K., M. H. Pan, et al. (2000). "Recent studies on the biofunctions and biotransformations of curcumin." Biofactors **13**(1-4): 153-158.

Lin, L., S. Deangelis, et al. (2010). "A novel small molecule inhibits STAT3 phosphorylation and DNA binding activity and exhibits potent growth suppressive activity in human cancer cells." Mol Cancer **9**: 217.

Liu, Z., A. Sall, et al. (2008). "MicroRNA: An emerging therapeutic target and intervention tool." Int J Mol Sci **9**(6): 978-999.

Livak., KJ, Schmittgen., TD. (2001). "Analysis of relative gene expression data using real-time quantitative PCR and the 2(-Delta Delta C(T)) Method." Methods **25**(4):402-8.

Lowry, O. H., N. J. Rosebrough, et al. (1951). "Protein measurement with the Folin phenol reagent." J Biol Chem **193**(1): 265-275.

Lu, C., E. Song, et al. (2010). "Curcumin induces cell death in human uveal melanoma cells through mitochondrial pathway." Curr Eye Res **35**(4): 352-360.

Lu, H. F., K. C. Lai, et al. (2009). "Curcumin induces apoptosis through FAS and FADD, in caspase-3-dependent and -independent pathways in the N18 mouse-rat hybrid retina ganglion cells." Oncol Rep **22**(1): 97-104.

Lu, J., G. Getz, et al. (2005). "MicroRNA expression profiles classify human cancers." Nature **435**(7043): 834-838.

Manju, S. and K. Sreenivasan (2011). "Synthesis and characterization of a cytotoxic cationic polyvinylpyrrolidone-curcumin conjugate." J Pharm Sci **100**(2): 504-511.

Manju, S. and K. Sreenivasan (2012). "Gold nanoparticles generated and stabilized by water soluble curcumin-polymer conjugate: blood compatibility evaluation and targeted drug delivery onto cancer cells." J Colloid Interface Sci **368**(1): 144-151.

Martin-Cordero, C., M.Lopez-Lazaro et al. (2003). "Curcumin and a DNA topoisomerase II poison." J. Enzyme Inhib.Med.Chem **18**:505-509.

Melkamu, T., X. Zhang, et al. (2010). "Alteration of microRNA expression in vinyl carbamate-induced mouse lung tumors and modulation by the chemopreventive agent indole-3-carbinol." Carcinogenesis **31**:252–258.

Mimeault, M. and S. K. Batra (2011). "Potential applications of curcumin and its novel synthetic analogs and nanotechnology-based formulations in cancer prevention and therapy." Chin Med **6**: 31.

Miyashita, T., S. Krajewski, et al. (1994). "Tumor suppressor p53 is a regulator of bcl-2 and bax gene expression in vitro and in vivo." Oncogene **9**(6): 1799-1805.

Mohanty, C., S. Acharya, et al. (2010). "Curcumin-encapsulated MePEG/PCL diblock copolymeric micelles: a novel controlled delivery vehicle for cancer therapy." Nanomedicine (Lond) **5**(3): 433-449.

Mohanty, C. and S. K. Sahoo (2010). "The in vitro stability and in vivo pharmacokinetics of curcumin prepared as an aqueous nanoparticulate formulation." Biomaterials **31**(25): 6597-6611.

Mohney, B. G., D. M. Robertson, et al. (1998). "Second nonocular tumors in survivors of heritable retinoblastoma and prior radiation therapy." Am J Ophthalmol **126**(2): 269-277.

Moragoda L, Jaszewski R, et al. (2001). "Curcumin induced modulation of cell cycle and apoptosis in gastric and colon cancer cells." Anticancer Res **21**:873–878.

Mukerjee, A. and J. K. Vishwanatha (2009). "Formulation, characterization and evaluation of curcumin-loaded PLGA nanospheres for cancer therapy." Anticancer Res **29**(10): 3867-3875.

Mukhopadhyay, A., C. Bueso-Ramos, et al. (2001). "Curcumin downregulates cell survival mechanisms in human prostate cancer cell lines." Oncogene **20**:7597–7609.

Munoz, M., M. Henderson, et al. (2007). "Role of the MRP1/ABCC1 multidrug transporter protein in cancer." IUBMB Life **59**(12): 752-757.

Nabekura, T., S. Kamiyama, et al. (2005). "Effects of dietary chemopreventive phytochemicals on P-glycoprotein function." Biochem Biophys Res Commun **327**(3): 866-870.

Narayanan, N. K., D. Nargi, et al. (2009). "Liposome encapsulation of curcumin and resveratrol in combination reduces prostate cancer incidence in PTEN knockout mice." Int J Cancer **125**(1): 1-8.

Navis, I., P. Sriganth, et al. (1999). "Dietary curcumin with cisplatin administration modulates tumour marker indices in experimental fibrosarcoma." Pharmacol Res **39**(3): 175-179.

Newman, DJ., GM. Cragg et al. (2003). "Natural products as sources of new drugs over the period 1981-2002." J. Nat. Prod. **66**:1022-1037.

Padua, M. B. and P. J. Hansen (2009). "Changes in expression of cell-cycle-related genes in PC-3 prostate cancer cells caused by ovine uterine serpin." J Cell Biochem **107**(6): 1182-1188.

Pal, S., T. Choudhuri, et al. (2001). "Mechanisms of curcumin-induced apoptosis of Ehrlich's ascites carcinoma cells." Biochem Biophys Res Commun **288**(3): 658-665.

Pan, M. H., T. M. Huang, et al. (1999). "Biotransformation of curcumin through reduction and glucuronidation in mice." Drug Metab Dispos **27**(4): 486-494.

Pandey, D. P. and D. Picard (2009). "miR-22 inhibits estrogen signaling by directly targeting the estrogen receptor alpha mRNA." Mol Cell Biol **29**(13): 3783-3790.

Park, K. and J. H. Lee (2007). "Photosensitizer effect of curcumin on UVB-irradiated HaCaT cells through activation of caspase pathways." Oncol Rep **17**(3): 537-540.

Patel, J. B., H. N. Appaiah, et al. (2011). "Control of EVI-1 oncogene expression in metastatic breast cancer cells through microRNA miR-22." Oncogene **30**(11): 1290-1301.

Pattnaik., N, Ahmed Khan., M, et al. (2012). "Pediatric malignancies." J of Clinical & Diagnostic Research **6**(4); 674-677.

Ramachandran, C., S. Rodriguez, et al. (2005). "Expression profiles of apoptotic genes induced by curcumin in human breast cancer and mammary epithelial cell lines." Anticancer Res **25**(5): 3293-3302.

Ramani, P. and H. Dewchand (1995). "Expression of mdr1/P-glycoprotein and p110 in neuroblastoma." J Pathol **175**(1): 13-22.

Rashmi, R., T. R. Santhosh Kumar, et al. (2003). "Human colon cancer cells differ in their sensitivity to curcumin-induced apoptosis and heat shock protects them by inhibiting the release of apoptosis-inducing factor and caspases." FEBS Lett **538**(1-3): 19-24.

Ren, B., G. Yu, et al. (2006). "MCM7 amplification and overexpression are associated with prostate cancer progression." Oncogene **25**(7): 1090-1098.

Roberts, M. J., M. D. Bentley, et al. (2002). "Chemistry for peptide and protein PEGylation." Adv Drug Deliv Rev **54**(4): 459-476.

Sa, G., Das, T., et al. (2010). "*Curcumin: From exotic spice to modern anticancer drug*. " A A J Med Sci 3: 21-37.

Saini, S., S. Majid, et al. (2010). "Diet, microRNAs and prostate cancer." Pharm Res **27**(6): 1014-1026.

Sarkar, FH., Y. Li, et al. (2004). "Cell signaling pathways altered by natural chemopreventive agents." Mutat Res **555**:53–64.

Sarkar, FH., Y. Li, et al. (2006). "Using Chemopreventive Agents to Enhance the Efficacy of Cancer Therapy." Cancer Res **66**, 3347-50.

Sastre., X, Chantada., GL et al. (2009). International Retinoblastoma Staging Working Group. Proceedings of the consensus meetings from the International Retinoblastoma Staging Working Group on the pathology guidelines for the examination of enucleated eyes and evaluation of prognostic risk factors in retinoblastoma. Arch Pathol Lab Med **133**(8):1199-202.

Scheper, R. J., H. J. Broxterman, et al. (1993). "Overexpression of a M(r) 110,000 vesicular protein in non-P-glycoprotein-mediated multidrug resistance." Cancer Res **53**(7): 1475-1479.

Schuttelkopf, A. W. and D. M. van Aalten (2004). "PRODRG: a tool for high-throughput crystallography of protein-ligand complexes." Acta Crystallogr D Biol Crystallogr **60**(Pt 8): 1355-1363.

Sen, S., H. Sharma, et al. (2005). "Curcumin enhances Vinorelbine mediated apoptosis in NSCLC cells by the mitochondrial pathway." Biochem Biophys Res Commun **331**(4): 1245-1252.

Sharma, RA., AJ. Gescher et al. (2005). " Curcumin: the story so far. " Eur J. Cancer 41: 1955-68.

Shen, M. Y. and A. Sali (2006). "Statistical potential for assessment and prediction of protein structures." Protein Sci **15**(11): 2507-2524.

Shi, M., Q. Cai, et al. (2006). "Antiproliferation and apoptosis induced by curcumin in human ovarian cancer cells." Cell Biol Int **30**(3): 2f21-226.

Shibata, H., H. Yamakoshi, et al. (2009). "Newly synthesized curcumin analog has improved potential to prevent colorectal carcinogenesis in vivo." Cancer Sci **100**(5): 956-960.

Shields, C. L., C. G. Bianciotto, et al. (2011). "Intra-arterial chemotherapy for retinoblastoma: report No. 1, control of retinal tumors, subretinal seeds, and vitreous seeds." Arch Ophthalmol **129**(11): 1399-1406.

Shields, C. L., A. Mashayekhi, et al. (2004). "Practical approach to management of retinoblastoma." Arch Ophthalmol **122**(5): 729-735.

Shields, J. A., C. L. Shields, et al. (1992). "Enucleation technique for children with retinoblastoma." J Pediatr Ophthalmol Strabismus **29**(4): 213-215.

Shim, JS., Lee, HJ., et al. (2001). "Curcumin-Induced Apoptosis of A-431 Cells Involves Caspase-3 Activation." J of Biochemistry and Molecular Biology **34**: 189-193.

Singh, S., BB. Aggarwal, et al. (2005). " Activation of transcription factorNF-kappaB is suppressed by curcumin." J. Biol. Chem 270: 24995-25000.

Singh, R. K., D. Rai, et al. (2010). "Synthesis, antibacterial and antiviral properties of curcumin bioconjugates bearing dipeptide, fatty acids and folic acid." Eur J Med Chem **45**(3): 1078-1086.

Singh, S. and B. B. Aggarwal (1995). "Activation of transcription factor NF-kappa B is suppressed by curcumin (diferuloylmethane) [corrected]." J Biol Chem **270**(42): 24995-25000.

Souza Filho, J. P., M. C. Martins, et al. (2005). "Relationship between histopathological features of chemotherapy treated retinoblastoma and P-glycoprotein expression." Clin Experiment Ophthalmol **33**(3): 279-284.

Sporn, M. B. and N. Suh (2002). "Chemoprevention: an essential approach to controlling cancer." Nat Rev Cancer **2**(7): 537-543.

Stavrovskaya, A. A. (2000). "Cellular mechanisms of multidrug resistance of tumor cells." Biochemistry (Mosc) **65**(1): 95-106.

Steiner, E., K. Holzmann, et al. (2006). "The major vault protein is responsive to and interferes with interferon-gamma-mediated STAT1 signals." J Cell Sci **119**(Pt 3): 459-469.

Summa, C. M. and M. Levitt (2007). "Near-native structure refinement using in vacuo energy minimization." Proc Natl Acad Sci U S A **104**(9): 3177-3182.

Sun, M., Z. Estrov, et al. (2008). "Curcumin (diferuloylmethane) alters the expression profiles of microRNAs in human pancreatic cancer cells." Mol Cancer Ther 7(3): 464-473.

Suprenant, K. A. (2002). "Vault ribonucleoprotein particles: sarcophagi, gondolas, or safety deposit boxes?" Biochemistry **41**(49): 14447-14454.

Surh, Y. J. (2003). "Cancer chemoprevention with dietary phytochemicals." Nat Rev Cancer **3**(10): 768-780.

Surh, Y.J. (1999). " Molecular mechanism of chemopreventive effects of selected dietary and medicinal phenolic substances. " Mutations Research **428**: 305-327.

Syng-Ai, C., A. L. Kumari, et al. (2004). "Effect of curcumin on normal and tumor cells: role of glutathione and bcl-2." Mol Cancer Ther **3**(9): 1101-1108.

Szakacs, G., J. K. Paterson, et al. (2006). "Targeting multidrug resistance in cancer." Nat Rev Drug Discov **5**(3): 219-234.

Takamizawa., J, Konishi., H, et al. (2004). "Reduced expression of the let-7 microRNAs in human lung cancers in association with shortened postoperative survival." Cancer Res 64(11):3753-6.

Tamvakopoulos, C., K. Dimas, et al. (2007). "Metabolism and anticancer activity of the curcumin analogue, dimethoxycurcumin." Clin Cancer Res **13**(4): 1269-1277.

Tan, K. P., R. Varadarajan, et al. (2011). "DEPTH: a web server to compute depth and predict small-molecule binding cavities in proteins." Nucleic Acids Res **39**(Web Server issue): W242-248.

Tang, X. Q., H. Bi, et al. (2005). "Effect of curcumin on multidrug resistance in resistant human gastric carcinoma cell line SGC7901/VCR." Acta Pharmacol Sin **26**(8): 1009-1016.

Thiyagarajan, S., K. Thirumalai, et al. (2009). "Effect of curcumin on lung resistance-related protein (LRP) in retinoblastoma cells." Curr Eye Rese **34**:37–43.

Tolomeo, M., D. Simoni, et al. (2002). "Drug resistance and apoptosis in cancer treatment: development of new apoptosis-inducing agents active in drug resistant malignancies." Curr Med Chem Anticancer Agents **2**(3): 387-401.

Tsang, WP., TT. Kwok, et al. (2010). "Epigallocatechin gallate up-regulation of miR-16 and induction of apoptosis in human cancer cells." J Nutr Biochem.**21**:140–146.

Tsang, WP., TT. Kwok, et al. (2010). "Regulation of microRNAs by natural agents: an emerging field in chemoprevention and chemotherapy research." Pharm Res. **27**:1027–1041.

Unnikrishnan, MK., MN. Rao. (1995). " Curcumin inhibits nitrogen dioxide induced oxidation of haemoglobin." Molecular and Cellular Biochemistry **146**: 35-37.

Van Der Spoel, D., E. Lindahl, et al. (2005). "GROMACS: fast, flexible, and free." J Comput Chem **26**(16): 1701-1718.

van Vlerken, L. E., T. K. Vyas, et al. (2007). "Poly(ethylene glycol)-modified nanocarriers for tumor-targeted and intracellular delivery." Pharm Res **24**(8): 1405-1414.

Vetrivel, U. and K. Pilla (2008). "Open discovery: An integrated live Linux platform of Bioinformatics tools." Bioinformation **3**(4): 144-146.

Vetrivel, U., N. Subramanian, et al. (2009). "InPACdb--Indian plant anticancer compounds database." Bioinformation **4**(2): 71-74.

Vial, T., J. Descotes (2003). "Immunosuppressive drugs and cancer." Toxicology **185**:229-240.

Vogel F. (1979). "Genetics of retinoblastoma." Hum Genet. **52**: 1–54.

Volinia, S., GA. Calin, et al. (2006). "A microRNA expression signature of human solid tumors defines cancer gene targets." Proc Natl Acad Sci USA **103**:2257–2261.

Walker, MC., JR. Masters et al. (1986). "Intravesical chemotherapy: in vitro studies on the relationship between dose and cytotoxicity." Urol. Res. **14**: 137–140.

Wang, Y. J., M. H. Pan, et al. (1997). "Stability of curcumin in buffer solutions and characterization of its degradation products." J Pharm Biomed Anal **15**(12): 1867-1876.

Wiederstein, M. and M. J. Sippl (2007). "ProSA-web: interactive web service for the recognition of errors in three-dimensional structures of proteins." Nucleic Acids Res **35**(Web Server issue): W407-410.

Wilson, M. W., C. H. Fraga, et al. (2006). "Immunohistochemical detection of multidrug-resistant protein expression in retinoblastoma treated by primary enucleation." Invest Ophthalmol Vis Sci **47**(4): 1269-1273.

Wortelboer, H. M., M. Usta, et al. (2003). "Interplay between MRP inhibition and metabolism of MRP inhibitors: the case of curcumin." Chem Res Toxicol **16**(12): 1642-1651.

Xiang, CC., Y. Chen, et al. (2000). "cDNA microarray technology and its applications." Biotechnol. Adv **18**: 35-46.

Xiong, J., D. Yu, et al. (2010). "An estrogen receptor alpha suppressor, microRNA-22, is downregulated in estrogen receptor alpha-positive human breast cancer cell lines and clinical samples." FEBS J **277**(7): 1684-1694.

Xu, J. and Y. Zhang (2010). "How significant is a protein structure similarity with TM-score = 0.5?" Bioinformatics **26**(7): 889-895.

Yan, C., M. S. Jamaluddin, et al. (2005). "Gene expression profiling identifies activating transcription factor 3 as a novel contributor to the proapoptotic effect of curcumin." Mol Cancer Ther **4**(2): 233-241.

Yang, G., G. Ayala, et al. (2002). "Elevated Skp2 protein expression in human prostate cancer: association with loss of the cyclin-dependent kinase inhibitor p27 and PTEN and with reduced recurrence-free survival." Clin Cancer Res **8**(11): 3419-3426.

Zhang, L., S. Volinia, et al. (2008). "Genomic and epigenetic alterations deregulate microRNA expression in human epithelial ovarian cancer." Proc Natl Acad Sci U S A **105**(19): 7004-7009.

Zhao, J. J., J. Yang, et al. (2009). "Identification of miRNAs associated with tumorigenesis of retinoblastoma by miRNA microarray analysis." Childs Nerv Syst **25**(1): 13-20.

Zhao, L., M. G. Wientjes, et al. (2004). "Evaluation of combination chemotherapy: integration of nonlinear regression, curve shift, isobologram, and combination index analyses." Clin Cancer Res **10**(23): 7994-8004.

LIST OF PUBLICATIONS

Articles published:

- **Seethalakshmi T**, Karthiyayani thirumalai, Nirmala, Jyotirmay Biswas, Krishnakumar Subramanian. Effect of curcumin on lung resistance protein in retinoblastoma cells. Curr Eye Res, 2009: 34, 10, 37-43.

- **Seetha lakshmi Sreenivasan,** Thirumalai K, Danda R, Krishnakumar S. Effect of curcumin on miRNA expression in human Y79 RB cells. Curr Eye Res, 2012; 37(5):421-8.

- **Seethalakshmi Sreenivasan**, Thirumalai K, Krishnakumar S. Expression profile of genes regulated by curcumin in Y79 RB cell. Nutr Cancer, 2012; 64(4), 607-16.

- **Seethalakshmi Sreenivasan**, Ravichandran S, Vetrivel U, Krishnakumar S. In vitro and in silico studies on inhibitory effects of curcumin on multi-drug resistance associated protein (MRP1) in retinoblastoma cells. Bioinformation. 2012; 8(1):13-9.

- **Seethalakshmi Sreenivasan**, Sathya baarathi Ravichandran, Umashankar Vetrivel, Subramanian Krishnakumar. Modulation of MDR1 expression and function in retinoblastoma cells by curcumin. Journal of pharmacology and pharmacotherapeutics **(provisionally accepted).**

- Angayarkanni N, Barathi S, **Seethalakshmi T**, Punitham R, Sivaramakrishna R, Suganeswari G, Tarun S. Serum PON1 Arylesterase activity in relation to hyperhomocysteinaemia and oxidative stress in young adult central retinal venous occlusion patients. Eye, 2007.

- Selvi R, Angayarkanni N, Asma B, **Seethalakshmi T**, Vidhya S. Amino acids influence the glucose uptake through GLUT4 in CHO-K1 cells under high glucose conditions. Mol Cell Biochem, 2010.

Articles under Preparation:

1. Induction of apoptosis by curcumin in RB cells through mitochondrial mediated pathway.

2. Chemosensitizing effect of curcumin in combination with anticancer agent in RB cells.

3. LRP docking analysis using Curcumin analogues.

LIST OF PAPERS PRESENTED IN CONFERENCES & AWARDS

NATIONAL:

1. Expression of Multi-drug resistance proteins and anti-tumor effect of Curcumin in Y79 retinoblastoma cell line **IERG conference, July 2007 at Hyderabad.**
2. Modulation of Multi-drug resistance associated proteins (MRP1) by Curcumin Longa Derivative in Y79 retinoblastoma cell line **IERG conference, July 2008, Madurai**.
3. Modulation of MRP1 by curcumin longa derivative in Y79 retinoblastoma cell line **KNBIRVO symposium 2008**, **Sankara Nethralaya, Chennai.**
4. Induction of apoptosis by curcumin in Y79 RB cells. Emerging trends in Life Sciences Research, **March 2009, BITS pilani**.
5. Expression profile of genes regulated by curcumin in Y79 retinoblastoma cells, **IERG conference, July 2010, Hyderabad.**

INTERNATIONAL:

1. Effect of curcumin on lung resistance protein in retinoblastoma cells **ASIA ARVO, 2009 Conference, Hyderabad.**

AWARDS

- Endowment award in biochemistry for best performance in the Biochemistry internship.
- Endowment award for best performance in the examination of Clinical Genetics.
- Awarded second prize for poster presentation at **KNBIRVO Symposium** 2008 Conference.
- Travel fellowship award for attending IERG conference, 2010.

BRIEF BIOGRAPHY OF THE SUPERVISOR

Dr. S.KRISHNAKUMAR is currently faculty at Vision Research Foundation, Sankara Nethralaya, Chennai, India and Ocular Pathologist and Professor in Ophthalmology in the Larsen and Turbo Department of Ocular Pathology. He has undergone six months research fellowship in ophthalmic pathology at Doheny Eye Institute, University of Southern California, USA. He has been selected as DBT Associate and awarded short-term Overseas Fellowship Award in nanotechnology at University of Missouri-Columbia and ICMR Fellowship for training in nanotechnology and drug delivery at University of Nebraska Medical Center, Omaha. Also has been selected for "Sir Sriram Travel Fellowship Award" for training in proteomics for the year 2006-2007 by National Academy of Medical Sciences. His total publications are 70 in number in all international journals. His area of interests range from retinoblastoma tumor biology, corneal and retinal stem cells and nanomedicine. (Recent paper accepted in drug discovery today on nanotechnology and ocular drug delivery). His lab currently has collaborative Research grants in proteomics, siRNA, Nanotechnology, RNA aptamer, Novel Recombinant molecules, nanofiber scaffolds, gene expression, retinal stem cells. His collaborators are from IIT madras, ILS Orissa, CCMB, Deakin University Melbourne, University of Missouri, Columbia, NASA etc. Currently there are 15 PhD students, 23 SRF and 2 JRF in the lab.

BRIEF BIOGRAPHY OF THE CANDIDATE

MS. T.SEETHALAKSHMI obtained her B.Sc Biochemistry degree from Ethiraj College, University of Madras, Chennai in 2003. She obtained her M.S. (Medical Laboratory Technology) degree of Birla Institute of Technology and Science, Pilani in 2006 with course work at Medical Research Foundation, Chennai. Then she joined the Microbiology department, Sankara Nethralaya as Junior Scientist and worked as a junior scientist in Sankara Nethralaya for 1 month and was recruited into project in 2007 funded by Indian council of medical research in Ocular Pathology Department. She registered for Ph. D in Jan 2007 in Birla Institute of technology & Science, Pilani. She has made presentations in 5 national and 1 international conferences, comprising 4 poster presentations and 2 oral presentations. She has 6 publications. 1 paper is in review related to thesis and 3 more papers are under preparation. She is also involved in teaching, doing routine work with related to histopathological techniques. She has received "Second prize" for poster "Modulation of MRP1 by C*urcuma longa* derivative in RB cells" (KNBIRVO Symposium Conference) 2008. She has received the travel grant for IERG (Hyderabad, 2010). Her research interests are in ocular cancer diseases like Retinoblastoma.